

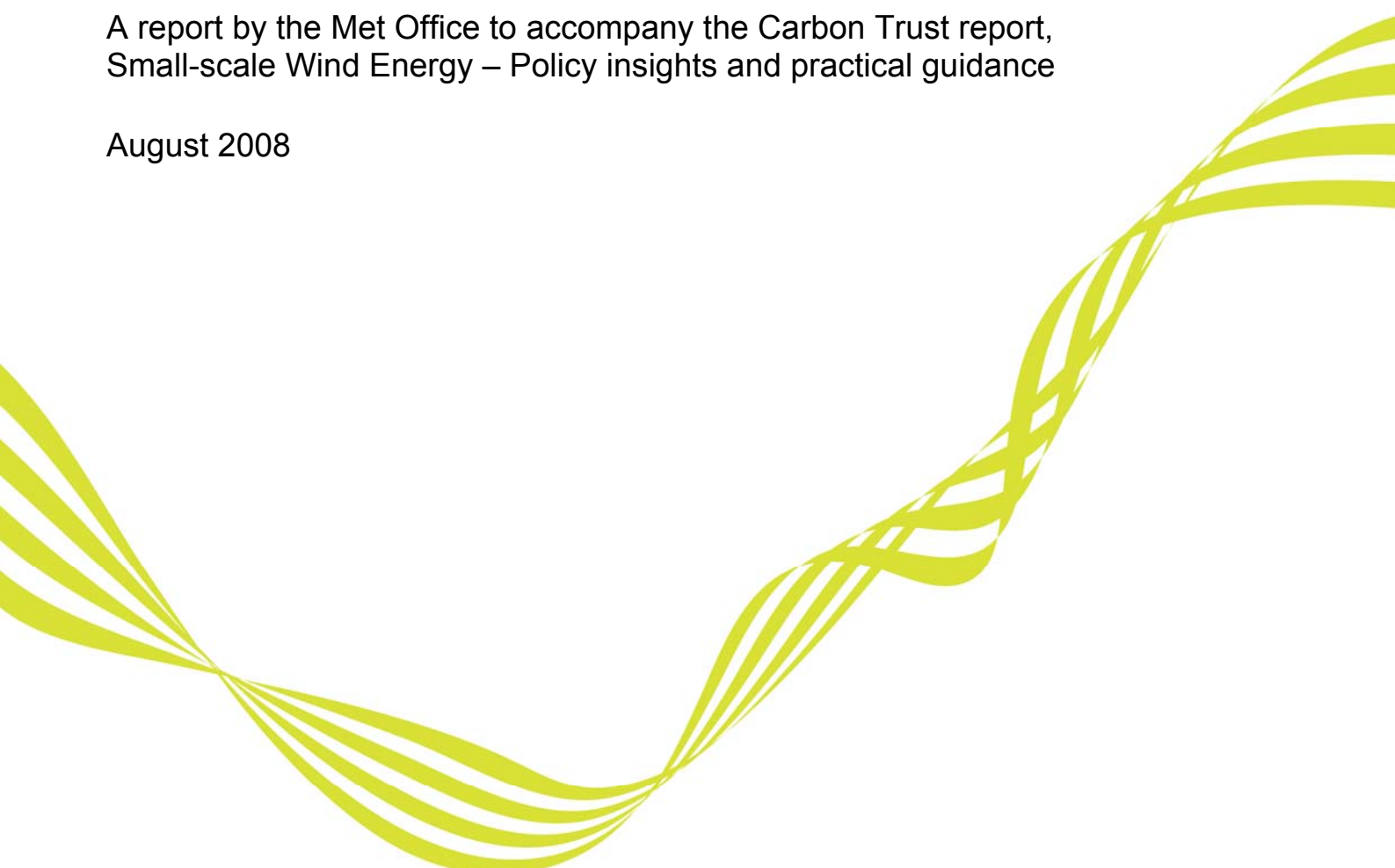


Met Office

Small-scale wind energy Technical Report

A report by the Met Office to accompany the Carbon Trust report,
Small-scale Wind Energy – Policy insights and practical guidance

August 2008





Preface

This work was commissioned by the Carbon Trust as part of research into the potential for small-scale wind energy to help reduce UK carbon emissions.

It is principally intended for engineers and scientists working in the field of small-scale wind energy, and to be read alongside the Carbon Trust report "Small-scale Wind Energy – Policy insights and practical guidance" (CTC738), published in August 2008.

For more information about the work of the Carbon Trust, call 0800 085 2005 or visit www.carbontrust.co.uk

For further information about the work of the Met Office call our 24-hour customer centre on 0870 900 0100, email consulting@metoffice.gov.uk or visit www.metoffice.gov.uk



Small-scale Wind Energy – Technical Report

Urban Wind Energy Research Project

Part 1 – A Review of Existing Knowledge

Prepared for the Carbon Trust

by

Martin Best, Andy Brown, Pete Clark,
Dan Hollis, Doug Middleton, Gabriel Rooney,
Dave Thomson and Clive Wilson

Reviewed by: Brian Golding

Authorised for issue by: Ross Lothingland

August 2008

The information in this report is provided in good faith and is believed to be correct, but the Met. Office can accept no responsibility for any consequential loss or damage arising from any use that is made of it.

Met Office FitzRoy Road Exeter Devon EX1 3PB
Tel: 0870 900 0100 consulting@metoffice.gov.uk

www.metoffice.gov.uk

© Crown Copyright 2008

Contents

1	Introduction.....	5
2	Observations	6
2.1	Met Office Anemometer Network	6
2.2	Summary Statistics.....	11
2.2.1	Long-term Averages.....	11
2.2.2	Wind Speed Frequency Distributions	13
3	Atmospheric Modelling	14
3.1	Large-scale spatial variations.....	14
3.1.1	The wind above the boundary layer and the geostrophic wind	14
3.1.2	The effects of the boundary layer.....	14
3.2	Numerical Weather Prediction (NWP) Models	16
3.2.1	NWP and large-scale climatologies.....	16
3.2.2	Downscaled climatologies from NWP data	17
3.2.3	Dynamical downscaled climatologies.....	19
4	Boundary Layer Modelling.....	21
4.1	Wind profile near the surface	21
4.2	Internal Boundary Layers and Fetch Effects	29
4.2.1	Overview	29
4.2.2	Canopy and roughness sublayers.....	29
4.2.3	Inertial sublayer.....	30
4.2.4	Heterogeneity, blending methods and source areas.....	35
4.2.5	Boundary layer	38
4.2.6	Mesoscale	40
4.2.7	Implications for urban wind energy.....	42
4.3	Urban Surface Energy Balance.....	43
4.3.1	The urban surface	43
4.3.2	Radiation.....	44
4.3.3	Turbulent heat flux.	44
4.3.4	Turbulent moisture flux.....	45
4.3.5	Heat storage flux.....	45
4.3.6	Anthropogenic heat source	46
4.3.7	Impact of surface energy balance on urban wind.....	46
4.4	Orographic Flow Models	47
4.4.1	Introduction	47
4.4.2	Linear analytic models	47
4.4.3	Linear numerical models.....	48
4.4.4	Validity of linear models	48
4.4.5	Non-linear models.....	49
4.4.6	Mass-consistent models.....	49
5	Urban Wind Modelling.....	51
5.1	Effects of streets/buildings	51
5.1.1	Average flow in the urban roughness sublayer	51
5.1.2	Street Canyons	55
5.1.3	Individual buildings and other obstacles.....	56
5.1.4	Flow at Particular Locations within Collections of Buildings.....	58
5.1.5	Research in COST 715.....	60

5.2	Field Experiments.....	65
5.2.1	Birmingham and Salford Urban Meteorology Experiments	65
5.2.2	DAPPLE.....	70
5.2.3	The Mock Urban Setting Test (MUST) experiment	72
5.3	Wind Tunnel Experiments	74
5.4	Computational Fluid Dynamics (CFD).....	75
6	Tools.....	78
6.1	Geostatistical Interpolation and Gridded Averages	78
6.2	Measure-Correlate-Predict.....	81
6.2.1	MCP Techniques.....	81
6.2.2	Comparisons of different MCP techniques	82
6.2.3	Limitations of MCP and Applicability to Urban Locations	83
6.3	WAsP	87
6.3.1	Background.....	87
6.3.2	Methodology.....	88
6.3.3	Published Literature	89
6.3.4	Applicability of WAsP to Urban Environments.....	90
6.4	Other Wind Farm Applications Software	91
6.4.1	WindFarmer	91
6.4.2	WindFarm.....	91
6.4.3	WindPRO	92
6.5	NOABL and the DTI Wind Speed Database.....	92
6.6	ADMS.....	94
6.7	Intercomparisons.....	97
7	Siting Guidelines	99
8	Summary	108
9	Conclusions.....	112
10	Glossary.....	114
11	List of Symbols	115
12	References	118

1 Introduction

For several decades now the wind energy industry has focussed on the generation of electricity from large wind turbines located in exposed locations with high mean wind speeds, such as hill tops and coastal waters. In recent years an increasing number of manufacturers have produced small turbines suitable for use by individual householders or small businesses. Although the definition of 'small wind systems' is generally accepted to include any devices up to a rated power of 50kW (typically 16m diameter), turbines for domestic applications are generally less than a few metres in diameter and generate 2-3 kW of power. They can be mounted on roof-tops or free-standing poles and are usually connected to the user's distribution board (fuse box). The electricity that is generated can be used directly on site, with any surplus being fed into the electricity grid.

With the possibility for widespread adoption of small turbine technology, two key questions arise:

- a) What is the total potential wind energy resource in the UK from small-scale turbines?
- b) What is the potential wind energy resource at any given location?

Given that small wind systems are inevitably installed close to where people live, and the majority of people live in towns and cities, the answers to these questions depend on an understanding of the wind climatology of urban areas. As well as the overall mean wind speed, knowledge is also required of the wind speed distribution (due to the non-linear relationship between wind speed and wind power) and the wind direction distribution (for optimum turbine siting). Short-duration fluctuations in both speed and direction are also of interest as these can affect the efficiency of the turbine.

This report is the result of the first phase of a project to address these questions. It describes a review of existing knowledge that is of relevance to the estimation of wind climatologies in urban areas. The scope of the review encompasses three strands: published literature, data sets and analysis techniques.

The measurement of wind, in particular using conventional anemometers and wind vanes, and the creation of long-term averages from such data, are considered in §2. Surface winds are driven by what is happening aloft in the free atmosphere. The use of numerical models to describe large-scale variations in the wind climatology throughout the atmosphere, and the possibilities for predicting the surface wind from that higher up in the atmosphere using down-scaling techniques, are described in §3. The effects of the underlying surface on the wind flow near the ground, and the ways in which they can be modelled, are covered in §4. The theory, experimental findings and modelling techniques relating to wind flow close to streets and individual buildings are described in §5. Finally, a number of existing tools for estimating the local wind climatology are described in §6.

2 Observations

Measurements of wind speed and direction can be made in a variety of ways:

- Cup anemometers and wind vanes – These are generally mounted on a mast or tower and are used to measure directly the wind close to the surface.
- Radiosondes – Radiosondes can be tracked by radar, radio direction finding, or navigation systems (such as the satellite Global Positioning System) to obtain wind data.
- AMDAR (Aircraft Meteorological Data Reporting) systems – Aircraft carrying appropriate sensors and software can calculate wind speed and direction from measurements of air speed, aircraft position, acceleration and orientation.
- Weather radar – Doppler weather radars can be used to measure the wind speed along the direction of the radar beam ('radial' winds) at intervals of a few hundred metres out to a maximum range of about 100km. Data are normally only obtained within areas of rain, but some 'clear-air' winds are possible where concentrations of insects are high.
- Vertical wind profilers – These use near vertical-pointing Doppler radar to derive the vertical profile of wind speed and direction from echoes of the transmitted radio waves produced by turbulence in the clear air. Sodar and lidar technology can also be used for wind profiling.
- Atmospheric motion vectors (satellite winds) – Wind speeds and directions can be calculated by tracking clouds or gradients in water vapour through successive satellite images.

Of these, only anemometers produce measurements of the wind speed close to the surface i.e. within a few tens of metres above ground level. The Met Office anemometer network is described in the following section and field experiments in which data have been gathered using surface anemometry are covered in section 5.2.

The other data types relate to winds at higher levels in the atmosphere e.g. cloud height or aircraft cruising altitude. Weather radars have beams that are angled between 0.5 and 4 degrees above the horizontal, so even these do not measure the wind very close to the surface. The incomplete or irregular spatial and temporal coverage of these data types (e.g. due to being restricted to areas of rain or cloud, or to aircraft flight paths and flight times) and often short record lengths of these data types make them difficult to use for climatological applications. Instead their primary use is within numerical models of the atmosphere, from which climatologies of the wind at various levels in the atmosphere may be obtained – see section 3.

2.1 *Met Office Anemometer Network*

The Met Office operates a network of wind observing sites spanning the whole of the UK. Currently there are approximately 180 stations in operation. Due to changes in the network over the years, historical records exist for a total of nearly 670 different sites. The earliest digitised data are from 1949 but the large majority of the archive covers the period from 1969 onwards. Although other organisations collect wind data, it is believed that the Met Office holds the largest and most comprehensive archive of surface wind observations in the UK.

The bulk of the data comprises hourly values of mean speed, mean wind direction and maximum gust speed. In the early part of the archive (generally prior to 1969) many stations only reported



one gust value per day (rather than one for each hour). The archive also contains a large volume of 10-minute means of speed and direction – these ‘spot’ values are recorded once per hour. There is also a small amount of daily ‘run of wind’ data (obtained by counting the total number of revolutions of the anemometer during a 24-hour period) – these are effectively daily mean speeds.

Data sets of sub-hourly data are less extensive. During the late 1980s and early 1990s a digital logging system was used to collect 1-minute wind data from around 80 stations, although a proper climatological archive was never created. None of the stations was in an urban area. In recent years the Met Office has again begun collecting sub-hourly wind data on a routine basis. Complete 10-minute data (i.e. six observations per hour, rather than just one spot value) are now available for around 75 sites, and since September 2006 raw 1-minute data have been collected from approximately 30 stations. Data sets such as these will continue to increase in both number and record length, and eventually will form a useful source of information for examining wind speed variability at sites across the UK.

Wind data are collected by the Met Office primarily for the purposes of weather forecasting and monitoring the climate of the UK. They are also used internally for a variety of other applications, such as dispersion modelling, and the data are also licensed for use by a wide range of other organisations including some in the wind energy sector.

The aim has always been to ensure, where practical, that the observations are made in a uniform way across the entire network. Wind speed and direction are measured using a cup anemometer and wind vane. The standard exposure is at 10m above the ground on a mast or tower in open, level terrain i.e. above short grass and away from obstacles such as buildings and trees (the exception being run of wind measurements which have typically been made on 2m masts). This standard exposure complies with the advice given by the World Meteorological Organization on good practice in making measurements of surface wind (WMO, 1996).

In practice the archive is not entirely homogeneous. Much of the data has been collected using anemometers with a start-up speed of 5 knots (~2.5 m/s). However some of the older data will have been measured using equipment with a start-up speed of 7 knots (~3.5 m/s). Conversely, in recent years the network has been upgraded to use modern, lightweight anemometers with a start-up speed of less than 1 knot (~0.5 m/s). These changes in low wind speed performance should not be of great significance to wind energy calculations (where the focus is on higher wind speeds and power is related to the cube of the wind speed) but they nevertheless highlight the difficulties of balancing consistency and quality in an archive that has been built up over many years.

With regard to the sites themselves, most are well exposed. However some sites have moved short distances during their lifetime (e.g. from one side of an airfield to another) while others will have been affected by gradual changes (e.g. changes in the land use of the surrounding area, such as increasing urbanisation).

More importantly, for small-scale wind energy, some stations have been located in, or adjacent to, urban areas. This has happened either because there was ready access to urban sites (such as the Met Office’s network of regional Weather Centres), or because of the lack of more suitable sites in a particular area, or because of the need to collect wind data in certain areas to meet a particular business need.

There are currently 373 distinct locations for which the Met Office holds some hourly mean wind data. The basic character of each site has been assessed using 1:50,000 scale mapping and a total of 68 stations have been identified that could be considered ‘urban’ to a greater or lesser degree. This assessment is summarised in Table 1.

Table 1: Numbers of Met Office anemometers in different built-up environments

CATEGORY	NUMBER OF SITES
City centre sites	16
Town centre sites	5
Suburban sites	13
Villages	1
Park locations within a built-up area	6
Coastal locations adjacent to a built-up area	17
Sites on the fringe between rural and built-up areas	4
Unclassified	6

Note that this is a subjective classification i.e. the distinction between different categories is not exactly defined and ultimately each site has a unique exposure. This is reflected by the fact that several sites did not fall clearly into one category and so remain unclassified.

The locations of these sites are shown in Figure 1 and they are listed in Table 2.

Table 2: List of Met Office anemometer stations in or adjacent to built-up environments

CLASSIFICATION	STATION NAME
City centre	BRISTOL WEATHER CENTRE
	CARDIFF WEATHER CENTRE
	KIRKLEES COUNCIL
	LEEDS COUNCIL
	LEEDS WEATHER CENTRE
	LIVERPOOL MUSEUM
	LONDON WEATHER CENTRE
	MANCHESTER WEATHER CENTRE
	MANCHESTER, HULME LIBRARY
	MIDDLESBROUGH, LONGLANDS COLLEGE
	NEWCASTLE WEATHER CENTRE
	NORWICH WEATHER CENTRE
	POST OFFICE TOWER (LONDON)
	PRESTON BOROUGH TOWN HALL
	SOUTHAMPTON
	WOLVERHAMPTON
Town centre	CAMBRIDGE GUILDHALL
	MILTON KEYNES
	OXFORD
	PAISLEY
	RUGBY

Table 2 (cont.): List of Met Office anemometer stations in or adjacent to built-up environments

CLASSIFICATION	STATION NAME
Suburban	BELFAST DANESFORT
	CHANNEL TUNNEL
	CLEETHORPES, HAVERSTOE PARK
	COVENTRY, COUNDON
	DEPTFORD
	EAST KILBRIDE NO 2
	EDGBASTON
	ENFIELD
	HERNE BAY NO 2
	RENFREW
	ROSS-ON-WYE
	SHEFFIELD
	SHEFFIELD UNIVERSITY
Village	MANBY
Park	BIDSTON
	LEICESTER UNIVERSITY
	MIDDLESBROUGH, COULBY NEWTON SCHOOL
	SHINFIELD PARK
	SOUTHWARK
	ST JAMES'S PARK
Coastal	BELFAST HARBOUR
	BELFAST HARBOUR DOCK
	DEAL
	FLEETWOOD
	FRASERBURGH
	GORLESTON
	GRAVESEND NO 2
	GREENOCK PORT
	KILKEEL
	MILFORD HAVEN CONSERVANCY BOARD
	PETERHEAD HARBOUR
	PLYMOUTH, MOUNTBATTEN
	SHOREHAM-BY-SEA
	SOLENT
	SOUTH SHIELDS
SOUTHAMPTON, OCEANOGRAPHY CENTRE	
SOUTHSEA	
Rural fringe	NOTTINGHAM, WATNALL
	PORTADOWN S WKS
	SHEPSHED
	SOUTHPORT
Unclassified	CUMBERNAULD
	INNSWORTH
	LONGBRIDGE
	MILDENHALL
	ROCHDALE
WALTON-ON-THE-NAZE	

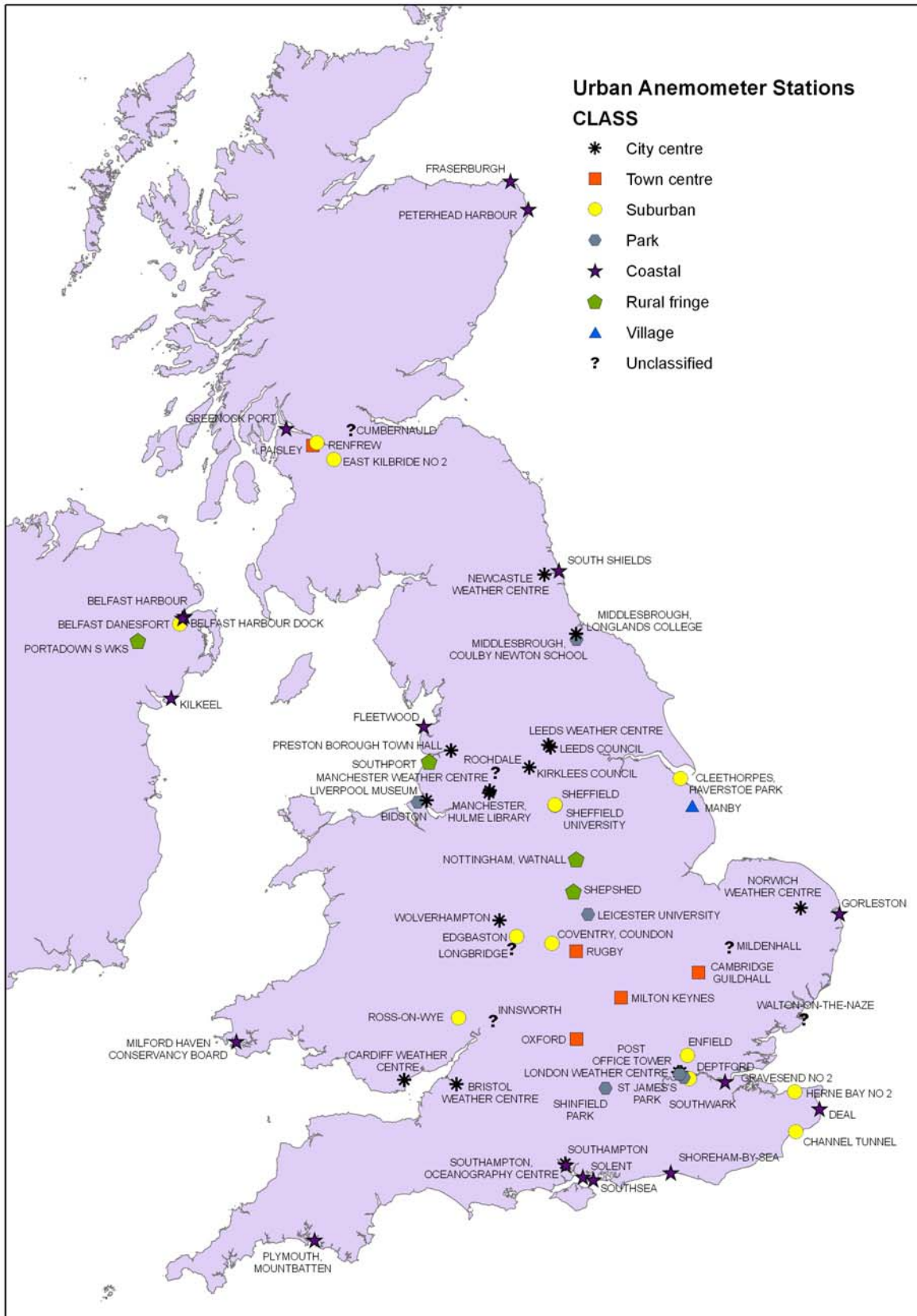


Figure 1: Map of Met Office anemometer stations located in or adjacent to built-up environments

Even for stations in or near to built-up areas the aim is still to locate the anemometer so that it is well exposed e.g. on a mast fixed to the top of a building without neighbouring obstructions. Figure 2 shows two typical examples in London and Newcastle.



Figure 2: Photographs of the anemometers at London Weather Centre (left) and Newcastle Weather Centre (right)

Recent guidance on the siting of meteorological instruments in urban areas (Oke, 2006) recommends that wind sensors should be mounted on a tall tower above the level at which the effects of individual buildings are discernable. This 'blending height' is estimated to be anywhere between 1.5 and 5 times the mean building height, depending on the building density and the height variations of the surrounding buildings (see §5).

In practice few of the Met Office stations in urban areas are high enough to ensure that the observations are unaffected by the local micro-climate i.e. such stations are unlikely to be truly representative of the wider urban area in which the station is located. Conversely few, if any, of these anemometers will be in positions that might be regarded as typical of the sort of environment in which an urban wind turbine would be located.

2.2 Summary Statistics

2.2.1 Long-term Averages

Climatological averages are conventionally calculated for periods of 30 years e.g. 1961-1990, 1971-2000. This is long enough to produce a robust average but short enough to produce a value that is representative of 'current' conditions. In recent decades the climate has been changing more rapidly than previously, making it more difficult to characterise the current climate from historical data. This is a particular problem for averages of temperature as the trends are strongest for this variable. The possible impacts of climate change on the wind climatology of the UK will be examined in the second phase of this project.

To calculate a 30-year average for a station that has a complete set of observations covering the entire period is a straightforward exercise. In practice there are few stations that have operated continuously for 30 years. Even during the period that a station has been reporting there are invariably issues affecting the quality of the data record. For example:

- there may be gaps in the record due to equipment failure or malfunction, data transmission problems etc
- the location of the anemometer mast may have changed during the history of the site e.g. from one side of an airfield to the other
- the equipment may have changed e.g. from an anemometer with a start-up speed of 5 knots to a lightweight device with a start-up speed of 1 knot
- the exposure of the site may have changed e.g. due to urbanisation of the surrounding area
- the processes used to check the quality of the observations have changed over the years

Such factors can have a complex effect on the data and sophisticated analysis techniques are required to correct for them.

The Met Office has calculated 30-year averages of mean wind speed for 1961-1990 and 1971-2000 for the stations in its observing network. The starting point is the archive of hourly mean speeds. These data have been subject to basic quality control tests to eliminate values that are clearly in error but no attempt has been made to adjust the data for inhomogeneities or trends. The hourly data are used to create a time series of monthly mean values for the whole observing record of each site. Some monthly values are based on an incomplete set of hourly data – only months with less than 2 days (i.e. 48 hours, or 6-7%) of missing data are used to generate the 30-year averages.

As noted above, few stations have data for every month of a 30-year period. In order to produce unbiased estimates of the true long-term average it is necessary to fill in the gaps using an appropriate estimation technique. This infilling procedure is carried out separately for each month i.e. all Januarys are analysed separately from all Februarys etc. It involves using linear regression to model the relationship between the monthly mean wind speed at a target station and at a neighbouring station. For each station with gaps in its record, the six best neighbours are chosen based on their correlation with the target station. A linear regression equation is calculated for each neighbour, using data for the years of overlap with the target station, and this equation is used to calculate an estimate for the target station. A weighted average (based on the correlation coefficient) of the estimates from all six neighbours is taken to arrive at the final estimate for the missing monthly value. See Perry and Hollis (2005a) for a more detailed description.

Once the gaps in the monthly data have been filled, the 30-year averages can be calculated from the complete set of data for each calendar month. The annual average is obtained by taking a weighted average (to reflect month length) of the 12 monthly long-term averages.

In a few instances, the estimation process is unable to fill every gap in a station's record. This is most likely to occur for stations with small amounts of original data, for which there can be insufficient well-correlated neighbours to produce a robust estimate. The actual number of years of data used is stored alongside the average itself in the Met Office's climate statistics database.

Note that these averages are therefore not corrected for changes in the character of the observation, but only for gaps in the record.

2.2.2 Wind Speed Frequency Distributions

To accurately determine the annual output from a turbine it is necessary to know more than just the long-term mean wind speed. This is because the amount of power that can be generated is, both theoretically and in practice, a non-linear function of wind speed. As well as the theoretical dependency of wind power on the cube of the wind speed, the majority of turbines only generate power between a minimum 'cut in' speed and a maximum 'cut out' speed, so knowing the proportion of time that the wind speed is outside this range is clearly important. An understanding of the frequency distribution of wind speed is therefore essential when estimating energy production.

Small turbines can respond to quite rapid changes in wind speed, and fluctuations around the cut-in and cut-out speeds are particularly significant as these can cause the turbine to become disconnected from the electricity distribution network. Ideally the frequency distribution would be constructed from short-duration (e.g. 1-minute) mean values but in practice hourly mean values are often used due to the much longer records of hourly data that are available.

For locations with long records of on-site wind speed measurements the frequency distribution can be obtained directly from the observations. However in most cases the wind climatology is estimated from data from another location e.g. a nearby reference station, or from winds higher up in the atmosphere. In such situations it is convenient to describe the frequency distribution using a statistical model, thus reducing large volumes of wind speed data to a small number of parameters.

For many years the 2-parameter version of the Weibull distribution (Weibull, 1951) has been the de facto industry standard for modelling wind speed distributions. It is the only distribution to be utilised in the popular WAsP wind atlas software package (see §6.3). The cumulative distribution function is given by:

$$\Pr(U \leq V) = F(V) = 1 - \exp\left[-\left(\frac{V}{A}\right)^k\right]$$

where U is wind speed and A and k are the scale and shape parameters of the distribution respectively. Various methods for calculating the parameters have been used – see Basumatary et al (2005) for a recent comparison of five alternatives.

Chadee and Sharma (2001) give a comprehensive summary of the history of the Weibull distribution from its first application to wind speed data over 50 years ago. They note that in comparative tests the Weibull distribution was found to be preferable to alternatives such as the Rayleigh and 2-parameter log-normal distributions, and that its flexibility and general applicability has led to its widespread adoption by the wind energy community. However they also note that no single distribution could be expected to give good results in all situations, given that wind patterns vary from station to station due to differing topography. They assert that the acceptance of the 2-parameter Weibull as the only distribution to use is questionable and go on to describe five 3-parameter distributions that they believe merit further investigation as possible alternatives.

3 Atmospheric Modelling

3.1 Large-scale spatial variations

3.1.1 The wind above the boundary layer and the geostrophic wind

In the free atmosphere there is very little friction and, at mid-latitudes, the wind may be approximated by the geostrophic wind. This is the wind for which the effects of the pressure gradient and the rotation of the Earth are in balance. It flows parallel to the isobars (lines of constant pressure on a weather map), with high pressure on the right in the Northern Hemisphere. The strength of this wind, G (in ms^{-1}), is given by

$$G = P_x / (\rho f)$$

Here P_x is the magnitude of the pressure gradient (in Pa m^{-1}), ρ is the density, and f is the Coriolis parameter ($= 2\Omega\sin\Phi$, where $\Omega = 7.3 \times 10^{-5} \text{ s}^{-1}$ is the rate of rotation of the Earth and Φ is the latitude in degrees). At 50 degrees N (as in parts of the UK), this gives $G \cong 7500P_x$.

The pressure gradient varies as weather systems move through (e.g. being large in the vicinity of a deep Atlantic cyclone and much smaller in the middle of a large anticyclone). Climatologies can be obtained from observations of surface pressure corrected to sea level (e.g. Borresen (1987) for the North Sea; Palutikof et al. (1992) for the UK). It is also possible to directly construct a climatology of winds at a level chosen to be above the boundary layer (e.g. 850 hPa) from radiosonde data. This has been done by a number of authors, sometimes over a limited area as part of a statistical-dynamical downscaling exercise (e.g. Hinneburg and Tetzlaff 1996; Mengelkamp et al. 1997), but also over much of Europe (e.g. Szepesi et al., 2000). One difficulty is in obtaining a sufficiently long and homogeneous dataset with spatial resolution adequate to resolve mesoscale features.

Near-surface wind observations can also be used in the construction of regional wind climatologies. This was done in the construction of the European Wind Atlas (Troen and Petersen, 1989). The main difficulty with this approach is that near-surface winds are strongly influenced by local effects (land-use, orography etc), and it is necessary to disentangle the effects of local variations from larger-scale effects. This may be particularly difficult where local circulations are set up (Lyons 1989; Mengelkamp et al., 1997)

3.1.2 The effects of the boundary layer

To leading order, the near surface winds will vary with the geostrophic wind (as the pressure gradient provides the driving force). However, drag at the surface slows the near surface winds and turbulent eddies mix low momentum air upwards. The result is that the mean wind within the boundary layer is slowed relative to the geostrophic wind. In turn this means that the pressure gradient and Coriolis forces are no longer in balance, and the wind within the boundary layer rotates so that it has a component in the direction from high to low pressure (i.e. flow is no longer parallel to the isobars).

The details of the wind profile within the boundary layer depend on the strength of the turbulent mixing. In near-neutral conditions (when heating or cooling of the atmosphere from the surface is not significant) the turbulence is largely mechanically driven. The resulting wind profile has a logarithmic form and boundary layer depths over the United Kingdom are typically around 500-1000 m. Heating at the surface (e.g. in the afternoon) leads to the formation of thermals which give stronger mixing, producing a convective boundary layer which typically shows a mean wind that is roughly constant through most of its depth, with strong shear close to the surface. Conversely, cooling at the surface (e.g. at night) damps the turbulence, producing a stable boundary layer which is typically shallower (tens to a few hundred metres deep) and shows significant wind shear throughout its depth.

This picture is extremely well-established, both from observations (e.g. Garratt, 1992) and large-eddy model simulations (e.g. Brown, 1996). The result is that there is typically a pronounced diurnal cycle in near-surface winds. As an example, Figure 3 shows monthly time-series of observed 10m wind at 00, 06, 12 and 18UTC averaged over the United Kingdom. The day time winds are systematically stronger than the night time ones, particularly in summer when the daytime heating is strongest. In winter the winds are stronger at all times of day, and show a rather weaker diurnal cycle. This highlights the general point that the windiest conditions of most interest for wind power are likely to have near-neutral boundary layers. Indeed, it is commonly assumed in wind power applications that the boundary layer can be assumed to be neutrally stratified (or, as in WASP, that stability effects can be assumed to be a small perturbation about a neutral basic state). It is not clear that the errors associated with these assumptions have been fully quantified, although they may be expected to be smaller over urban areas than rural ones due to increased mechanical mixing and a reduced tendency to form stable boundary layers by night.

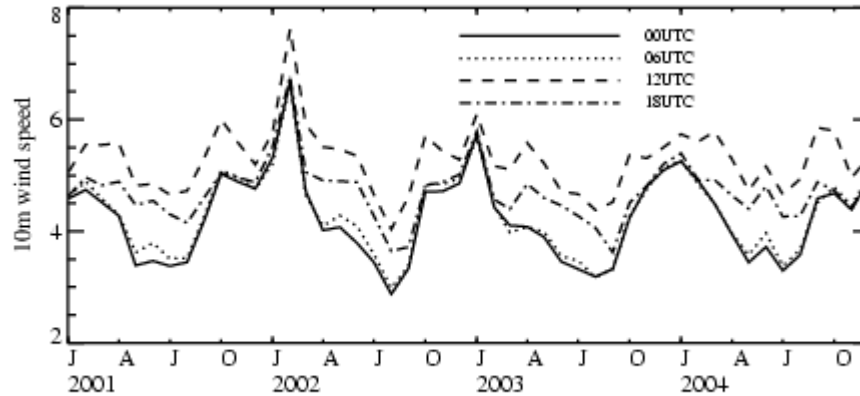


Figure 3: Time series of 10m wind observations averaged over the United Kingdom at 00, 06, 12 and 18 UTC.

Although the qualitative understanding of the behaviour of the boundary layer is good, quantifying the relationship between the geostrophic wind and low-level winds is rather more problematic. A number of observational studies (e.g. Grant and Whiteford, 1987 and references therein) have attempted to relate, in the framework known as Rossby Similarity theory, the geostrophic wind either directly to the 10m wind, or, more commonly to the surface stress (from which low-level winds can be obtained as described in Section 4). The relationship between the surface stress and geostrophic wind is commonly referred to as a geostrophic drag law.

Typically the results for stress or low-level wind are quite scattered, with, for example, the values quoted in Grant and Whiteford implying a range of 10 m winds in neutral conditions from 4.3 to 5.2 m s⁻¹ for a geostrophic wind of 10 m s⁻¹ and a roughness length (see Section 4) of 0.1 m. It is

likely that some of the uncertainty arises from the impossibility of finding truly equilibrium, neutral conditions in which to make measurements (e.g. Arya and Wyngaard, 1975). Idealized modelling studies (e.g. Brown, 1994) provide a possible cleaner alternative, but the models themselves have uncertainties in their formulation, and even in neutral conditions an uncertainty in 10m wind speed of 5-10% must be accepted. Application of these idealized results will in any event be difficult as, for example, the real atmosphere will not be exactly neutral and in equilibrium. It may be the most promising way forward is to use NWP models. These predict surface stress and low level wind routinely, taking into account stability and non-equilibrium conditions. Although these models rely on simple representations of turbulence (and indeed are sensitive to them), they have been implicitly tuned over many years through the requirement to give accurate predictions of 10 m wind when compared with surface anemometer observations (which will be primarily in rural areas).

3.2 Numerical Weather Prediction (NWP) Models

3.2.1 NWP and large-scale climatologies

Weather forecasts are produced by numerical models which solve the fluid equations of motion describing the atmospheric flow and include relevant physical processes and boundary conditions such as orographic height, and surface sea temperatures. The model forecasts are initialised from a blend of recent forecasts and observations which have been used to modify the model variables through a process of data assimilation. The total set of model values, or state, is then self consistent and consistent with the dynamical equations and atmospheric balanced motions. This initial state is called a numerical analysis. The process of ingesting observations and then making predictions by solving the equations for future times is called Numerical Weather Prediction (NWP).

To produce operational forecasts in a timely way powerful supercomputers and reliable communications to collect the observations are needed. There are relatively few centres that run global models. Leading centres in terms of global coverage, model sophistication and accuracy include the European Centre for Medium Range Weather forecasts (ECMWF), the US National Centres for Environmental Prediction (NCEP), the Met Office, and the Japanese Met Agency.

Despite the powerful supercomputers the mesh of points that represents the atmosphere is still limited in both horizontal and vertical extents by processing time constraints. For global models the grid size is typically around 40-50km and 40-90 vertical levels. This limits the fine-scale detail that may be represented, so that, for example the height of orographic features is smoothed to average values for 50x50km areas. Many models use the hydrostatic equations which are a very good approximation for larger scales down to around 5km but exclude smaller scale motions and vertical accelerations. Local effects are therefore inadequately captured by these models. To improve the resolution smaller limited area (LAM) domains are used. These may be regional models covering an area such as Europe, or mesoscale models such as the Met Office UK area model with 4km grid mesh. Typically, limited area models have grid sizes from 12km down to a few km. Vertical levels are usually around 40-70.

Operational forecasts are usually run twice or 4 times each day with new initial states based on the inclusion of the latest observations. Since the NWP systems synthesise the observations and the information carried forward by the model from past observations they represent the best comprehensive data sources for meteorological variables, such as winds, at arbitrary locations within their domains. Complete time series for individual sites and climatologies may be derived

from the archived NWP analyses and forecasts. Besides mean wind speeds and wind direction roses it is potentially possible to investigate seasonal and diurnal variations and make estimates of both mean wind and gusts. NWP data is most useful for the larger scales and captures well the geostrophic (or synoptic) wind variations. Because it is limited by spatial resolution it does not represent local effects and small scale influences due to the details of land use, buildings etc. For this the data need to be further processed or downscaled in a sensible way. This may be by microscale models with finer specification of the local influences.

A possible disadvantage of past NWP data is that the forecast systems have been steadily improved and so the accuracy and errors are not constant over longer periods. In recent years global reanalysis data has become available from both ECWMF and NCEP/NCAR. These have been produced by running the most up-to-date NWP systems with historical weather observations so that the improved NWP systems are able to treat consistently the observations over an extended period of typically 40+ years. A limitation of these reanalyses is the degraded horizontal resolution. The NCEP/NCAR reanalysis (Kalnay et al, 1996, Kistler et al, 2001) is around 200km and ECMWF's ERA-40 (Uppala et al, 2005) is 125km, whilst the earlier ECMWF ERA-15 (Gibson et al, 1997) was also 125km but with a less accurate representation of the orography. Currently at ECMWF an interim reanalysis is being made (Simmons et al, 2007). This is at a slightly higher resolution (80km) and uses improved model formulation and data analysis methods. The period starts from 1989 and the data will be available when the reanalysis reaches the end of the ERA-40 period (end of 2002). Another global reanalysis, JRA-25 has recently been made available (March 2006) by the Japanese Meteorological Agency (JMA) and Central Research Institute of Electric Power Industry (CRIEPI) (<http://www.jreap.org>). The resolution is again 125km. It should be noted that these reanalyses are still not completely homogeneous due to the evolution of the observing network and the greater use of satellite data in the modern period.

3.2.2 Downscaled climatologies from NWP data

Estimates of possible wind power resources require representative wind statistics over a reasonable period, at least several years, to capture the full range of variation. Mean values or climatologies are employed. The problem is to describe local scale details from large-scale NWP or general circulation climate models. A downscaling procedure has to be used. The most obvious, but computationally intensive way, is taking the coarse resolution data and performing progressively higher resolution model simulations to produce data with a horizontal (and vertical) resolution much higher than the resolution of the original data. The computing resources (power and storage) have generally been prohibitive for this approach. A number of statistically based alternatives have been used to construct climatologies economically.

The simplest approach is statistical downscaling. Observations at a location are related to the large-scale NWP grid values of one or more model parameters by regression for a shorter but sufficiently long period for the relationships to be statistically stable. These may then be applied for the full NWP data to derive climate values. The drawback of this method is that it assumes the relationships hold for all times and that it can only be applied where there are sufficient observations to establish the relationships. Finer scale variations to establish climatologies on a higher resolution grid or at arbitrary locations are not possible. Therefore a combined statistical-dynamical approach, sometimes called regionalisation, (Mengelkamp et al, 1997, Frey-Buness et al, 1995, Frank and Landberg, 1997, Heimann, 2001) is used, Figure 4.

The main steps are performing a cluster or class analysis (e.g. by weather type) of the large-scale atmospheric parameters from either observations or a long time series of NWP analyses. It is assumed that the climate of a region is described by the classification of an appropriate (small) set of parameters, such as wind speed and direction at 850hPa and vertical temperature

gradient (Mengelkamp et al, 1997) or geostrophic wind (Frank and Landberg, 1997). The frequency in each class is determined from the NWP analyses. For each member of the classification a mesoscale model is run to quasi-equilibrium and the wind fields obtained are weighted by the frequency to provide a climatology. The mesoscale model is forced by a prescribed profile of geostrophic wind and background temperature. Different approaches to the classification have been used. Frank and Landberg (1997) analysed the wind climate over Ireland using 65 classes of geostrophic wind in 30° wind sectors and equal frequency wind speed bins from the 850hPa wind observed at Valencia. Frey-Buness et al (1995) used a total of 48 classes using 12 wind direction intervals, 2 seasons and 2 cloud/rain divisions. Nineteen years of relatively coarse ECHAM climate model simulations over the Alpine region were analysed and downscaled to produce a regional wind and temperature climatology. The major advantage is a much smaller number of higher resolution simulations are required to produce a climatology. Rather than predefined classes an optimum clustering method can be employed (e.g. Cutler et al, 2006).

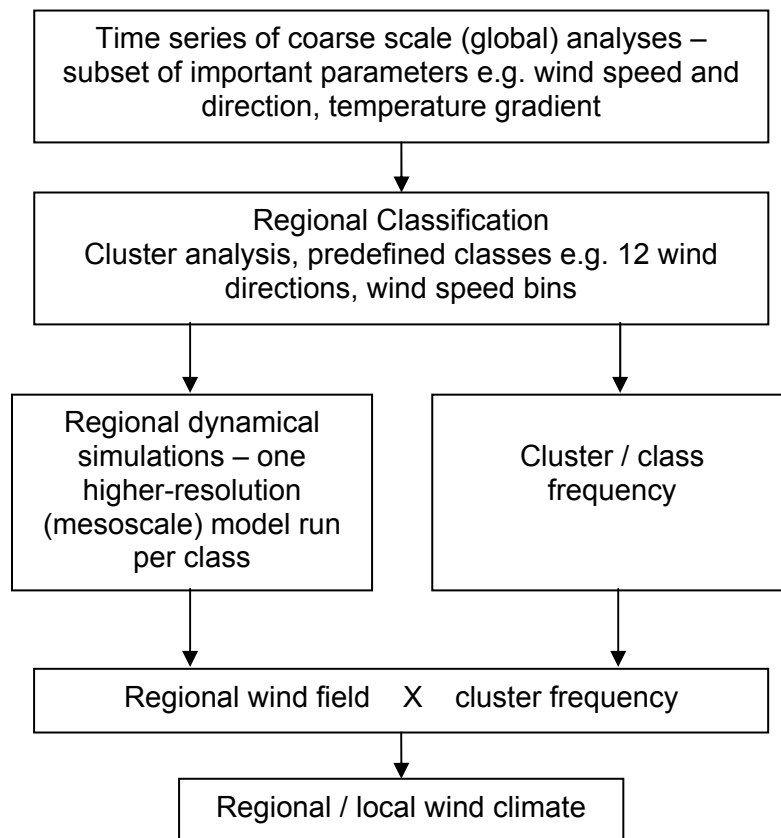


Figure 4: Statistical-dynamical approach (after Mengelkamp et al, 1997)

A similar statistical-downscaling approach has been developed at the Meteorological Service of Canada to produce a wind atlas for Canada (<http://www.windatlas.ca/en/index.php>, Glazer et al, 2005), which forms part of the Wind Energy Simulation Toolkit (WEST), (Yu et al, 2006). NCEP/NCAR reanalyses at 2.5° resolution were classified for each of 65 overlapping tiles. Geostrophic wind was classified into 16 directions and 14 speed intervals, along with the sign of the vertical wind shear between 1500m and 0m to produce 432 possible classes. No wind shear split was applied to the lightest winds. For each tile domain the musicale MC2 model (Girard et al, 2005) was initialised using a single atmospheric profile for each class. The model was run

with constant lateral boundaries for each domain, gradually growing the mountains and with a dry atmosphere. Surface temperatures were fixed and radioactive effects were excluded so that sea/lake-breezes and mountain/valley circulations are not possible. The model was run to establish a dynamical equilibrium and climate statistics obtained by weighting by the frequency of each of the classes.

Fuentes and Heimann (2000) suggested an improved statistical-dynamical downscaling method based on the assumption that the *“evolution of the large-scale circulation can be described as a sequence of large-scale weather types prevailing for several days (episodes). During the prevalence of a certain weather type, the dominant circulation pattern does not change significantly. The transition from one weather type to the next occurs within the order of one day which is rather quick in comparison to the duration of each type.”* The idea is related to the notion of large-scale weather types over Europe. Instead of defining weather types by single horizontal averaged parameters over a domain, large-scale fields of several meteorological parameters are classified in combination using multivariate statistical methods. The mesoscale model is then run using the most typical episode in each class. Time-varying large-scale flow is imposed through the lateral boundaries, so that the temporal evolution of mesoscale features is modelled for the full duration of the multi-day episodes. The method was applied to ERA-15 data at 12 hourly intervals to derive the winter precipitation climate over the Alps. A 20km resolution wind climatology of the eastern Adriatic coast was obtained by this approach (Heimann, 2001), again using ERA-15 reanalyses and 22 weather types.

An objective method for classification of synoptic weather regimes over Europe and the north east Atlantic has recently been developed (James, 2007) using both ERA40 and NCEP/NCAR reanalyses. The classification could be applied to future statistical-dynamical downscaling applications.

3.2.3 Dynamical downscaled climatologies

The statistical-dynamical approaches whilst being economical have the drawback that extremes and transient behaviour are excluded by the weather type classification. Potentially these may be better captured by a more direct dynamical downscaling. A limited area mesoscale model is run with large-scale analyses used as initial and lateral boundary data for a long representative period which should sample these. This has been attempted with the ALADIN model (Agar et al, 2005). The ERA-40 analyses for 1992-2000 were interpolated to a 30km grid and run for every other day of the 10 year period for 60h. Smaller multiple nested ALADIN models with 10 and 2.5km were run within this. Disregarding the first 12h spin-up period as the mesoscale models adjusted from the larger-scales the subsequent model fields were averaged to form a surface wind climatology over Slovenia. Validation against surface observations showed the 10km model results to be reasonable in coastal and flat land area whilst the 2.5km results were an improvement at mountain stations. A similar downscaling approach with the ALADIN model downscaling from ERA-40 to 10km has been validated for the special observing period of the Mesoscale Alpine Program (MAP-SOP) (Agar et al, 2006). A Fourier analysis showed the model simulated the low level winds well at mountain stations where 80% of the spectral power was due to motions longer than diurnal periods. However the majority of stations, which were at lower elevations, had over 40% of the power in the sub-diurnal range. For these the model significantly underestimated the spectral power (at only 10%) indicating that the downscaling is predominantly a dynamical adjustment to the new (finer-scale) terrain.

A similar dynamical adaptation approach has been applied to NCEP/NCAR reanalyses from 1995 to make digital wind atlases for Poland and Sardinia on a 6km horizontal grid (Sander and Chun, 2004).



A wind atlas for Ireland has been made by downscaling NCEP/NCAR reanalyses with the MASS (Mesoscale Atmospheric Simulation System) model (Brower et al, 2003). A stratified random sampling of 15 years of reanalysis data was used to simulate 366 days with nested mesoscale domains of 30, 8, and 2km. The sampling ensured each month and season were represented equally. The output from the finest resolution was then coupled to Wind Map, a mass consistent wind flow model to derive a 200m resolution climatology.

Rather than perform special model simulations from reanalyses it is possible to extract data from the operational archives of NWP forecast models and form means over a number of years. Although the modelling systems gradually evolve and improve over the extended period of study, the major variations due to the weather are well captured by modern NWP systems and dominate the generally smaller changes in accuracy of the forecasts and analyses. An offshore UK marine renewable atlas (Cooper et al, 2006) includes a wind climatology, at 19.5m above sea-level, derived from the Met Office operational mesoscale model winds at 12km horizontal resolution. The atlas is formed from moaned model winds over the period June 2000 to September 2003.

A similar atlas is in preparation at the Met Office for the UK including land and near coastal regions from both 12km models and a more recent 4km grid model. There is an archive of 12km data since June 1998, whilst the 4km data are available from the beginning of 2006. The advantage of this method is that similar computing resources are needed as are used in analysing the climate of the reanalyses in the statistical-downscaling approach, but the models have already been run for all the cases at a much higher resolution with full parameterisations of the important physics. Potentially this enables a much better sampling of smaller scale mesoscale circulations and fuller analysis of the wind characteristics.

Table 3 NWP data sources

Data	NWP system	Resolution/area	Period
NCEP/NCAR Reanalyses	Global NCEP forecasting system as at 1995	200km global	Jan1948 - onwards
ECMWF ERA-15 ERA-40	IFS as at 1995 IFS as at 2001	125km global 125km global	Dec1978 - Feb1994 Sep1957 - Aug 2002
JMA/CRIEPI JRA-25	Jam's operational system in April 2004	125km global	Jan 1979 - Dec 2004
Met Office 12km LAM analyses	Intermittent improved (approximately 2-3/year)	12km UK & surrounds	June 1998 - onwards
Met Office 4km UK analyses	Intermittent improved (approximately 2-3/year)	4km UK & surrounds	Jan 2006 - onwards
Links			
NCEP/NCAR Reanalyses	dss.ucar.edu/pub/reanalysis/ www.cpc.ncep.noaa.gov/products/wesley/reanalysis.html		
ECMWF ERA-15 ERA-40	http://www.ecmwf.int/research/era/ERA-15/index.html http://www.ecmwf.int/research/era/index.html		
JMA/CRIEPI JRA-25	http://www.jreap.org		

4 Boundary Layer Modelling

4.1 Wind profile near the surface

Near the ground, the speed of the wind is reduced because of the drag of the ground surface. The size of the drag depends on the texture of the surface, so that it is greater when the surface is composed of trees and buildings than when it is composed of blades of grass, for example. Such components of the surface are generally referred to as *roughness elements* and together they form the *canopy*. The roughness elements interact with the wind directly through the pressure exerted on them by the wind. The drag thus caused is transmitted to the wind at higher levels by the action of turbulent stresses, resulting in a gradual reduction of wind speed with decreasing height.

The region of the atmospheric boundary layer in which the height scale is much less than the boundary layer depth, but much greater than the (mean) height of the canopy, h , is called the *inertial sublayer*. The region below this layer, up to a few times the canopy height, is called the *roughness layer* (or *roughness sublayer*). These layers are illustrated in Figure 5. [The inertial sublayer is often also called the *surface layer*, and indeed the latter term is more common in the meteorological community as a whole. However it seems inappropriate when the roughness elements are large (as in urban areas) and the layer does not extend close to the surface. As a result, urban meteorologists tend to use the term “surface layer” to include both the inertial and roughness sublayers. To avoid confusion we will not use the term “surface layer” in this report.]

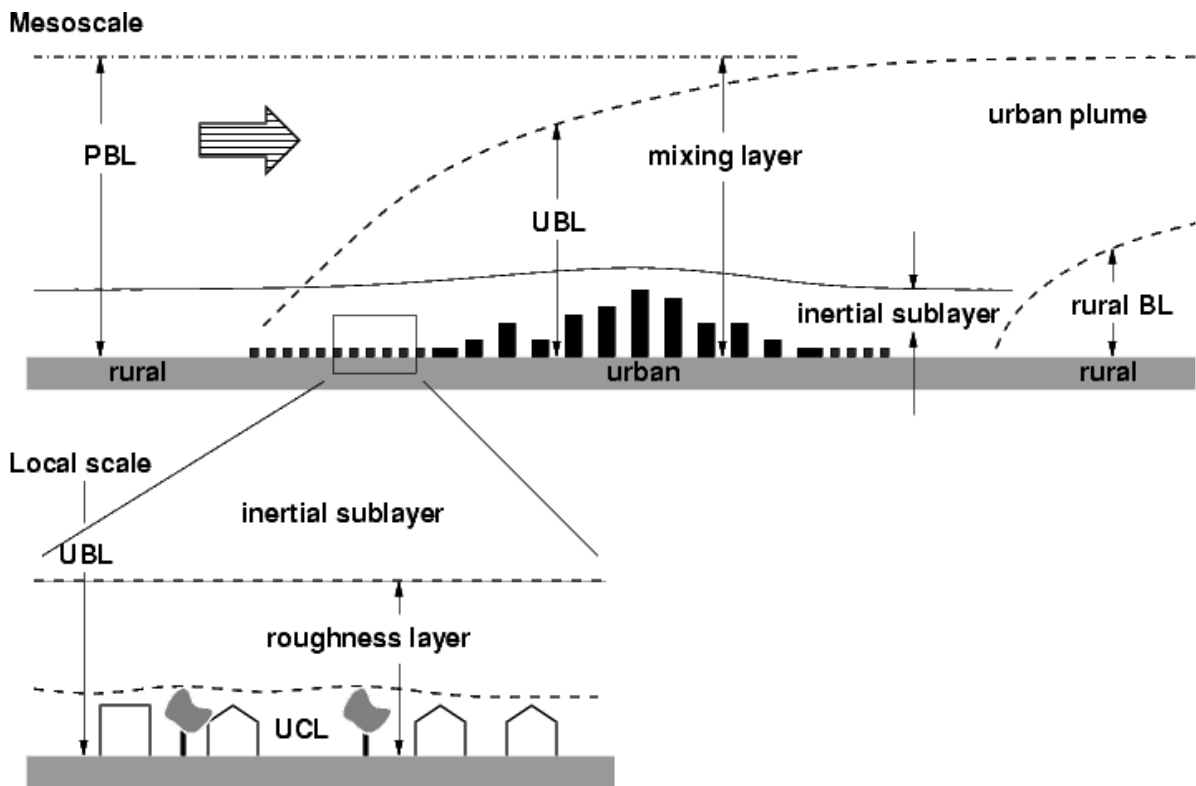


Figure 5: The layers of the atmosphere and the urban plume,
PBL = planetary boundary layer,
UBL = urban boundary layer,
UCL = urban canopy layer

In the inertial sublayer, the magnitude of the turbulent shear stress, τ , is approximately constant, and the height-gradient of wind, or *wind shear*, may be related to the shear stress, the height, and the density of air by a dimensional argument,

$$du/dz \propto u_* / z \quad (1)$$

where u is the wind speed, z is the height and $u_* = \sqrt{\tau/\rho}$ is a quantity called the *friction velocity*, obtained from τ and the air density ρ . Since τ is approximately constant in the inertial sublayer, so is u_* . Thus the expression for the wind shear may be integrated to yield the logarithmic wind profile near the ground,

$$u(z) = \frac{u_*}{\kappa} \ln \left(\frac{z-d}{z_0} \right) \quad (2)$$

Here, the proportionality constant (called *Von Karman's constant*) is $\kappa \approx 0.4$, and z_0 and d are called the *roughness length* and *displacement height* (or zero-plane displacement), respectively. It can be seen that varying the value of d changes the effective origin from which height is measured (moving the wind profile 'up' or 'down'), whereas varying the value of z_0 changes the value of the wind speed by the same amount at all heights. The roughness length is a measure of the drag exerted on the wind by the underlying surface – higher values indicate more drag. The displacement height quantifies flow-blocking effects. The sizes of these lengthscales depend on the properties and arrangement of the roughness elements.

When the ground (or canopy) becomes warmer or colder than the air above, turbulent eddies will transport a buoyancy flux B_T as well as a momentum flux through the boundary layer. From the buoyancy flux, a new dimensionless group called the *stability parameter* (z/L) may be formed, where the *Obukhov length* $L = -u_*^3 / \kappa B_T$. Note that for a neutral boundary layer,

$B_T = 0 \Rightarrow \frac{z}{L} = 0$, for a stable boundary layer (cold ground) $\frac{z}{L} > 0$, and for an unstable boundary

layer (warm ground) $\frac{z}{L} < 0$. It is assumed that the dimensionless wind shear must depend on this parameter, so that the equation for the wind shear now becomes

$$\frac{\kappa z}{u_*} \frac{du}{dz} = \Phi_m \left(\frac{z}{L} \right)$$

where Φ_m is an unknown function, known as the *Monin-Obukhov stability function* for momentum. To recover the neutral case, it is expected that $\Phi_m(0) = 1$. Since stably stratified air resists vertical mixing more than neutral air, it is expected that wind shear will be greater in the stable case, and so $\Phi_m(z/L) > 1$ when $z/L > 0$, and vice versa for unstable stratification. The effect of buoyancy is often incorporated as a perturbation to the logarithmic wind profile, e.g. by writing $\Phi_m(z/L) = 1 + A(z/L)$.

For urban canopies, the height of the roughness elements may be so large that there is no clear separation of height scales that allows for the presence of an inertial sublayer (Schmid *et al.* 1991). In this case there is some evidence, however, that inertial-sublayer predictions such as the logarithmic velocity profile continue to be approximately satisfied in the roughness sublayer (Rotach, 1993; Rooney, 2001).

Power law wind speed profiles are often used in engineering calculations. Although power laws are not theoretically correct, they often perform not too badly in practice. If u_i is the wind speed at height z_i , $i = 1, 2$, then

$$\frac{u_1}{u_2} = \left(\frac{z_1}{z_2} \right)^p.$$

A commonly used value for the exponent p is $1/7$ (see e.g. Monin and Yaglom, (1971, pages 310 and 663), Mikhail and Justus (1988), Gipe (2004, pages 40-44)). For neutral conditions, where we expect a log profile in the inertial sublayer, the power law profile can be regarded as a reasonable approximation to the log profile over a limited range of $(z-d)/z_0$. The power law gives the same value of the “wind shear exponent” $(z/u)du/dz$ as the log law when $p \approx [\ln((z-d)/z_0)]^{-1}$. For $p = 1/7$ this corresponds to $(z-d)/z_0 \approx 1000$. If we are estimating winds at heights with $z-d$ of order 10m, then $p = 1/7$ should give good results over open plains (where z_0 is of order 0.01 m). However in urban situations we would expect a larger value of p to be appropriate. Gipe (2004, page 41) gives a table of values for the exponent p . Values range from 0.07 over ice, to 0.14 ($\approx 1/7$) over cut grass, to 0.24 over scattered trees and hedges, to 0.31 in suburbs and 0.43 over woodlands. The value of p measured in experiments conducted in Birmingham (see Section 5.2.1) was approximately 0.35, which falls nicely between suburbs and woodlands in Gipe’s table. Gipe (2004) remarks to the effect that because rough surfaces slow the wind more than smooth ones, there is more to be gained by building a tower to gain height when installing a wind power device over a rough surface. This is clear from the variation of p with roughness or of course from the logarithmic inertial sublayer wind profile.

The simple power law (with $p = 1/7$) is examined along with more complicated power laws (p depending on z_2 , u_2 and z_0 with $z_2 < z_1$), Monin-Obukhov similarity profiles, and the logarithmic profile, by Mikhail and Justus (1988). They compared the models with measurements from the point of view of using the models to extrapolate measurements at around 10 m to higher heights. No one model was superior at all the sites used.

Garratt (1992) summarises much early work on the calculation of z_0 and d , particularly over natural surfaces. He assesses the often-quoted rule of thumb that $z_0 = 0.1h$, and concludes that for a variety of natural surfaces this is consistent with experimental values, which were found to lie mainly in the range $0.02 < z_0/h < 0.2$. For crops and forests he finds that the simple relationship $d = 2h/3$ is fairly representative.

However, he also discusses the importance of roughness-element distribution, or *packing*, and the flow regimes resulting from different packing densities. The packing of roughness elements may be quantified by a number of measures, and two which are widely used are the plan-area density and the frontal-area density, respectively denoted λ_p and λ_f (Raupach et al., 1991; Grimmond & Oke, 1999). These are defined as the ratio of the total plan area of the roughness elements to the total plan area (λ_p), and the ratio of total frontal area of the roughness elements, in the direction facing the wind, to the total plan area (λ_f). They may be illustrated with reference to Figure 6, which shows a simple square array of identical cuboid roughness elements. In this case $\lambda_p = A_p/A_T$ and $\lambda_f = A_F/A_T$. Note that λ_f is dependent on the wind direction, and $\lambda_p < 1$.

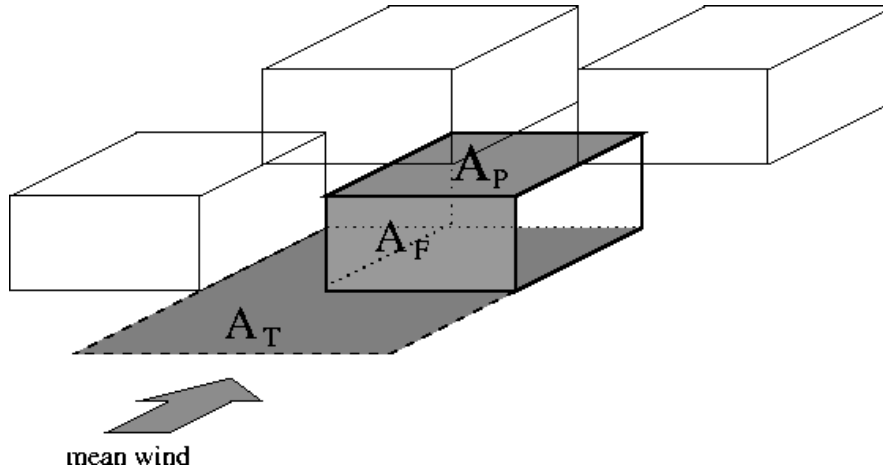


Figure 6: Illustration of the areas considered when calculating different area densities, after Grimmond & Oke (1999).

With this simple surface geometry in mind, it may be envisaged that for values of λ_p approaching 1, the canopy begins to resemble a flat surface which is merely the true surface raised a height h . That is, we expect $d/h \approx 1$ when $\lambda_p \approx 1$. Similarly, within certain limits, the increased drag from taller buildings may translate into z_0 increasing as λ_f increases. Macdonald *et al.* (1998) have derived analytical forms for the dependences of d/h and z_0/h on λ_p and λ_f for a canopy composed of cuboids, based on the assumption that a logarithmic wind profile exists for $z \geq h$. These are

$$\begin{aligned} d/h &= 1 + A^{-\lambda_p} (\lambda_p - 1) \\ z_0/h &= (1 - d/h) \exp \left[- \left(0.5 \beta \frac{C_d}{\kappa^2} (1 - d/h) \lambda_f \right)^{-0.5} \right] \end{aligned} \quad (3)$$

where C_d is the *drag coefficient* of a *single obstacle*, A is a tuning parameter controlling the curvature of the d/h graph, and β is a parameter which in effect modifies the drag coefficient to a value more appropriate to a particular configuration of an *array* of obstacles. For cubical roughness elements, if it is assumed that $\lambda_p = \lambda_f = \lambda_{eq}$, equations (3) may be plotted as shown in Figure 7. In these plots $C_d = 1.2$, a nominal value for a cube, and with the appropriate tuning parameters Macdonald *et al.* (1998) show that the curves agree with experimental data from a wind-tunnel study by Hall *et al.* (1996). The curve for the square array was also found to agree with the results of an urban canopy model formulated by Coceal & Belcher (2004).

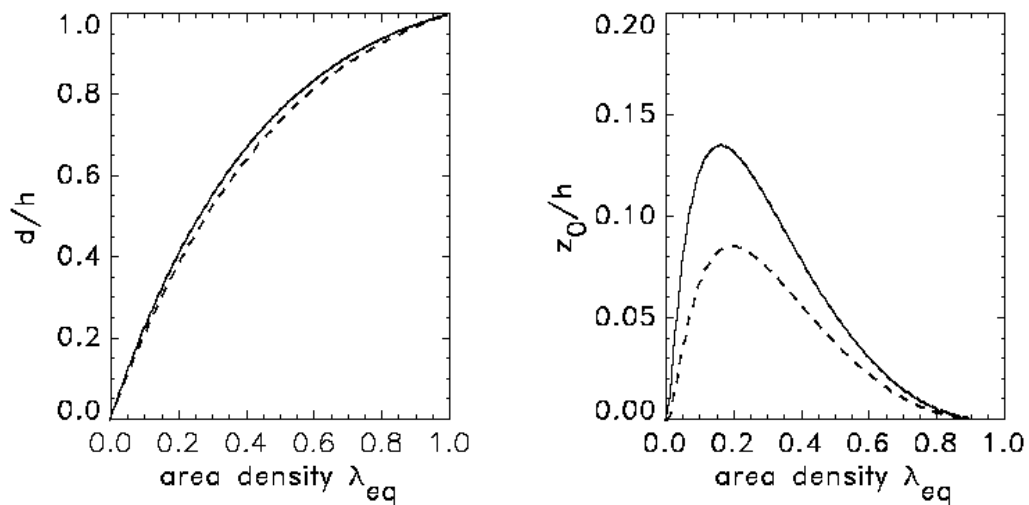


Figure 7: Relationships between normalised displacement height, roughness length and area density for canopies of cubical obstacles, derived by Macdonald et al. (1998), see equations (3). The dashed lines are for square arrays aligned along the wind direction, for which the tuning parameters take values of $A = 3.59$ and $\beta = 0.55$, and the solid lines are for staggered arrays, for which $A = 4.43$ and $\beta = 1$.

The plots indicate that, in this model, d/h increases monotonically with increasing λ , whereas z_0/h peaks at an intermediate value of λ . This behaviour has been linked (see e.g. Garratt (1992) and Grimmond & Oke (1999)) to different flow regimes of the air around the canopy. When roughness-element density is low ($\lambda_p \approx 0.1$), the roughness elements are *isolated*, in the sense that each is outside the main wake area of the element upwind. At intermediate densities ($0.1 < \lambda_p < 0.4$) there is *wake interference*, so that the wind does not have space to recover its undisturbed profile between one roughness element and the next. At the highest densities ($\lambda_p > 0.4$), *skimming* flow occurs, in which the roughness elements block the wind at canopy level, and the effective origin of the wind profile is displaced upward to near the canopy top. These regimes are illustrated qualitatively in Figure 8.

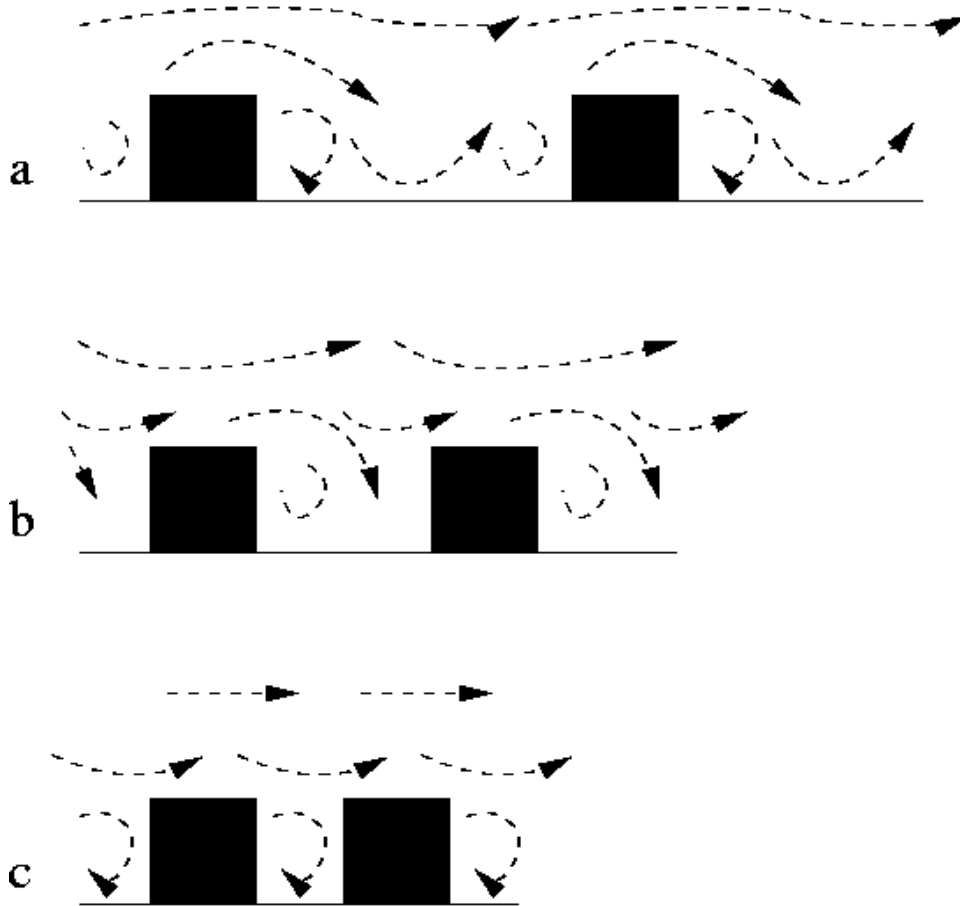


Figure 8: Flow regimes for different roughness element densities: (a) isolated elements, (b) wake interference, (c) skimming.

An alternative to Macdonald *et al.*'s (1998) formulae, is a proposal made by Raupach (1994, 1995). This was originally developed for vegetation canopies but has been subsequently applied to urban canopies by Grimmond and Oke (1999). Raupach's approach can be written in the form:

$$\frac{d}{h} = 1 - \frac{1 - \exp(-\sqrt{15\lambda_f})}{\sqrt{15\lambda_f}}$$

and

$$\frac{z_0}{h} = \left(1 - \frac{d}{h}\right) \exp\left(-\frac{\kappa}{\min(\sqrt{0.003 + 0.3\lambda_f}, 0.3)} + 0.193\right).$$

Here we have inserted Raupach's recommended values of the various constants in the equations. These results give a qualitatively similar behaviour to Macdonald *et al.*'s approach, although z_0/h does not approach zero as λ_f tends to zero (there is some allowance for the roughness of the ground itself). Also, since λ_f , unlike λ_p , is not constrained to be less than unity, the large λ_f behaviour is only reached asymptotically as λ_f tends to infinity. The formulae are plotted in Figure 9.

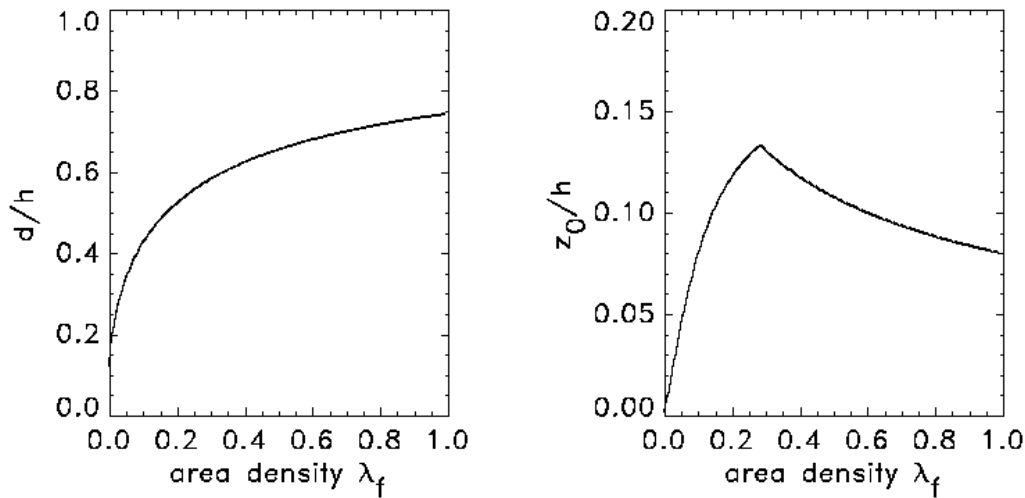


Figure 9 : Relationships between normalised displacement height, roughness length and frontal area density as represented by Raupach (1994, 1995). κ is taken to be 0.4.

Grimmond & Oke (1999) estimate that real urban environments usually lie in the range $0.1 < \lambda_p < 0.6$. In their comprehensive review of morphometric calculations of z_0 and d , they find that measured values of these parameters can generally be grouped within broad bands which follow curves such as those in Figure 7. In comparison with measured values of z_0 and d (from both full scale and wind tunnel experiments), they conclude that the approaches of Macdonald *et al.* (1998) and Raupach (1994, 1995) are to be preferred to the other approaches which they tested, with the exception of approaches which require much more information on building shape statistics. Of the two, they prefer Raupach to Macdonald *et al.* The Macdonald *et al.* approach tends to underestimate z_0 in real conditions with $\lambda_p > 0.4$ (a common urban situation), possibly because real situations tend to have $\lambda_f < \lambda_p$ while the approach was developed mainly for cubes. Also, while it is theoretically appropriate that z_0/h becomes small as λ_p tends to unity for the case of identical cubes (this is the “roof tops become a new flat surface” case discussed above), in reality buildings have different heights and so this limit does not apply.

Grimmond and Oke (1999) conclude that values of these aerodynamic parameters are difficult to estimate accurately either from field measurements of wind and turbulence or from morphometric analysis. However they give values of first-order estimates for different categories of cityscape, based on a combination of previous measurements and informed speculation, as shown in Table 4.

Hanna & Britter (2002) reproduce the data in Table 4 as part of their long review of methods for characterising the effects of surface roughness on flow. They also present a similar classification by Davenport *et al.* (2000), which has values of z_0 varying logarithmically in the range 0.1m–2.0m as built-environment roughness increases over a 5-category scale.

Table 4: Typical aerodynamic properties of homogenous zones in urban areas, ordered by height and density, after Grimmond & Oke (1999)

Urban surface form	h (m)	z_0 (m)	d (m)
Low height and density Residential—one- or two-storey single houses, gardens, small trees. Mixed houses and small shops. Warehouse, light industrial, few trees.	5–8	0.3–0.8	2–4
Medium height and density Residential—two- and three-storey large or closely spaced, semi-detached and row houses, large trees. Less than five-storey blocks of flats with open surroundings. Mixed—houses with shops, light industry, churches, schools.	7–14	0.7–1.5	3.5–8
Tall and high density Residential—closely spaced, less than six-storey row and block buildings or major facilities (factory, university, etc.), town centre.	11–20	0.8–1.5	7–15
High-rise Urban core or suburban nodes with multi-storey tower blocks in dense urban surroundings. Major institutional complexes.	>20	>2.0	>12

Cheng and Castro (2002) found, in a wind tunnel study of flow over cuboidal obstacles, that the roughness of an array of identical obstacles was less than the roughness of an array of obstacles with varying heights (with the same mean height). This accords with the ideas of Grimmond and Oke (1999). By considering the limit $\lambda_p = 1$ (see discussion of this limit above) it is clear that height variability must play some role in determining the roughness length. Also studies by Pavageau *et al.* (1997) and Rafailidis (1997) involving an array of parallel street canyons in a wind tunnel suggest that roughness lengths are increased for pitched roof buildings. This is discussed further in section 5.1.2 below.

For modelling wind flow at scales larger than the neighbourhood scale, the roughness length is still a useful concept when considering flow near the ground. However, for a numerical model with a spatial resolution of several kilometres, it is often the case that surface inhomogeneities are also included in the parametrization of z_0 . An *effective* roughness length may parametrize the presence of orography (Wood & Mason, 1993), or a surface composed of patches of terrain with different roughness lengths (Mason, 1988), when these are below the model resolution, such that the model yields the correct spatial average of shear stress or wind speed at heights of order the hill height or above.

In the case of a heterogeneous surface, studies suggest that the effective roughness length will take a value between the roughness lengths characteristic of each patch, the exact value of which will depend on the distribution of the patches, e.g. Goode & Belcher (1999). In the absence of detailed morphometric data or in an inhomogeneous canopy, one may attempt to infer the effective roughness length based on the distribution of patches of different surface cover and their typical values of z_0 , e.g. Rooney *et al.* (2005).

For resolved orography, it has been shown that increasing the value of z_0 on the hill surface reduces the critical hill slope at which recirculation of flow (often called *separation*) behind the hill occurs (Wood 1995).

4.2 Internal Boundary Layers and Fetch Effects

4.2.1 Overview

As discussed above, many of the concepts which are used when discussing the impact of a surface on the atmospheric flow are based on the idea of equilibrium flow over a 'horizontally uniform' surface. This assumes that surface heterogeneity is confined to small scales within the canopy, i.e. buildings in urban areas, and that the general characteristics of the canopy elements are uniform for a long distance upstream (a long 'fetch') once one averages over a number of elements. When the atmospheric flow encounters a change in surface, it has to adjust to the new surface characteristics, and this takes time (which translates to a distance along the flow).

For example, when the wind flows from a rural area to an urban area, the first few buildings see a stronger wind than would exist further towards the centre of the town. The forces exerted by the buildings slow down the general flow at building level. This lower momentum air is mixed upwards through the inertial sublayer into the boundary layer as a whole. Thus, the impact of the surface gradually makes its way upwards through the previous boundary layer. A new boundary layer effectively starts to grow from the surface within the original boundary layer. This is called an internal boundary layer (IBL). However, it is often the case (especially in the smooth to rough transition from rural to urban) that the eventual depth of the new boundary layer exceeds that of the upstream boundary layer.

As a result of the pressure forces exerted at (primarily) the leading edge of the roughness change, and continuity (i.e. horizontal slowing leading to vertical acceleration), there is also an upward deflection of the mean flow over the roughness change. However, this is generally so small that it can be neglected.

Apart from this small flow deflection, it is important to note that the flow some way away from the surface initially 'knows' nothing of the change in surface below it – standard methods to estimate the near-surface wind from, say, the 950 hPa wind, will fail close to the roughness change. Eventually, the IBL reaches elevated levels, though initially the wind will not show the equilibrium behaviour that is eventually reached after a long fetch.

Garratt (1990) comprehensively reviewed the IBL and much of what follows is covered by this review. Garratt's review itself states that by far the most work that has been done is confined to IBL development within the inertial sublayer. This is best understood and also probably of most importance, especially since our understanding has allowed us to produce fairly rigorous approaches to heterogeneity of surface characteristics on scales large enough that roughness concepts apply but small enough that the impact can be thought of as the interaction of IBL growth within inertial sublayers. Furthermore, many of the simpler results are derived for neutral boundary layers. More recent work has been done on the impact within the canopy itself. Perhaps inevitably, because of the inherent variability within the canopy, less progress has been made on simple, general theories, but nevertheless some simple results have emerged.

4.2.2 Canopy and roughness sublayers

Most work on the general properties of canopy and roughness sublayers has concentrated on equilibrium flow in horizontally homogeneous canopies. One reason for this is the difficulty of defining meaningful 'average' parameters if such parameters vary substantially. However, recent approaches to urban canopy modelling, building on ideas derived from vegetation canopies, have made some progress in bridging the gap between the area-average roughness concept and the building scale. Work based largely on wind-tunnel measurements and very high

resolution numerical modelling has shown that real arrays of buildings can, for many purposes, be treated as arrays of simply-interacting, fairly simple geometrical bodies. Given this approach, relatively simple models can be constructed. Recent ideas are very well summarised by MacDonald, 2000. These ideas do not explicitly, however, cover large changes in canopy properties (or edge effects). Canopy-based parametrization schemes designed for mesoscale models, such as that of Martilli *et al.* (2002), include these effects naturally but require the full mesoscale model to be run to make predictions. As such, they do not lead to general predictions (though they could certainly be used in this context).

Belcher *et al.* (2003) introduce a canopy drag length scale, L_c , which relates the canopy drag, D_i , to the in-canopy mean wind speed U_i :

$$D_i = U_i^2 / L_c \quad (4)$$

and show that this length scale can be expressed as

$$L_c = \frac{2h}{C_d(z)} \frac{(1 - \beta_v)}{\lambda_f} \quad (5)$$

where h is the mean building height, $(1 - \beta_v)$ the fractional volume occupied by air in the canopy, λ_f is the roughness density, or total frontal area of buildings per unit ground area, and C_d is the drag coefficient of the building elements (which, in general, depends on their shape). For buildings which are uniform with height, $\beta_v = \lambda_p$, the plan area density.

This length scale defines a distance over which the canopy flow adjusts to changes in canopy structure (and hence defines a scale over which averaging is meaningful). Specifically, the adjustment distance is $3L_c \ln K$ where $\ln K$ depends on upwind conditions and varies between 0.5 and 2 in typical urban conditions (Coceal and Belcher, 2004). Coceal and Belcher (2005) adopt a drag coefficient of 2, suitable for cuboid buildings, and introduce an adjustment number,

$$N_c = \frac{2}{C_d(z)} \left[\frac{1 - \lambda_p}{\lambda_f / \lambda_s + \lambda_p} \right] \quad (6)$$

where λ_s is the mean building height to street width aspect ratio. This is essentially the adjustment distance expressed in units of horizontal building spacing. They show that, for a wide variety of morphologies, the adjustment length scale is about three rows of buildings.

4.2.3 Inertial sublayer

Ideas based on the inertial sublayer are associated with a 'roughness length' description of the surface, so that the transition from, say, rural to urban corresponds to a jump in surface roughness length. The roughness length itself only has meaning for a uniform surface, so here it is defined as the roughness length the surface would have if extended over a long fetch. The concept of an IBL immediately leads to the idea of a depth δ , the *internal boundary layer depth*, over which the flow differs from the upstream flow. Different precise definitions exist, leading to different results, since the rate at which different variables change with height depends on the variable. For example, the stress profile shows a different shape to the mean wind profile. Within the IBL, it is usually assumed that a growing layer exists closer to the surface within which the flow is in equilibrium with the new surface. Kaimal and Finnigan (1994) point out that, while this layer exhibits equilibrium profiles, it may not quantitatively exhibit the equilibrium eventually attained after a long fetch. Furthermore, they point out that this layer only exists after a finite distance from the roughness change, though, in practice, assuming it grows from the surface at

the roughness change does not lead to major problems. Between the new equilibrium layer and the top of the IBL lies the *transition zone*.

We are generally interested in how the depth of the IBL and the profile of variables such as wind speed and turbulence intensity varies with height and distance from the roughness change. Most simple theories start from ideas based on diffusion: with constant diffusivity, ν , a sudden change at a point diffuses with a depth scale, z , which varies with time since the change, t , as $z = (\nu t)^{\frac{1}{2}}$. While this idea leads to considerable insight into the problem, it is complicated by two issues:

1. Insofar as the concept of eddy diffusivity applies, the diffusivity is not constant. In a homogeneous, equilibrium inertial sublayer, the eddy diffusivity increases linearly with height, so the rate of diffusion increases as the depth of the IBL increases.
2. The concept of eddy diffusivity relies upon a local balance between production and dissipation of turbulence, with negligible transport. This cannot be the case in an IBL where local homogeneity does not apply. Consequently, results based on eddy diffusivities have some systematic errors, but it would appear that they remain approximately applicable. The alternative requires use of much more complex treatments of turbulence which almost invariably require numerical solution.

A number of empirical power-law relationships for δ have been proposed. In addition, more complex relationships based upon integral relationships derived from the equation of motion and closure assumptions have been derived. Most are summarised by Garratt (1990). Savelyev and Taylor (2005) summarise a variety of formulae for 'short fetch IBL height', meaning IBLs with a short enough fetch that inertial sublayer concepts still apply, and it is clear from their list that all arise either from simple power-law fits or similar analyses of the dynamical equations. They also propose a stability-dependent form. However, their paper does not address either the wind profile or surface stress in the IBL, both of which are of far more interest.

Walmsley (1989) compared a number of relationships with available atmospheric data. Overall, he found that the (implicit) formula of Panofsky and Dutton (1984) gave best agreement with data. The form used by Walmsley (1989) is (in our notation):

$$\left\{ \frac{\delta}{z_{02}} \left[\ln \left(\frac{\delta}{z_{02}} \right) - 1 \right] + 1 \right\} = B\kappa \frac{x}{z_{02}} \quad (7)$$

where x is the distance downstream of the change in roughness, $B=1.25$ and z_{02} is the downstream roughness length. This is easily solved iteratively. This fitted data better than Elliott's (1958) formula:

$$\frac{\delta}{z_{02}} = A \left(\frac{x}{z_{02}} \right)^{0.8} ; A = 0.75 - 0.03M \quad (8)$$

where

$$M = \ln \left(\frac{z_{02}}{z_{01}} \right) \quad (9)$$

is a measure of the roughness change. The shapes of the two growth curves are, however, very similar and the main problem with Elliott's curve, eq.(8), is a general over-estimate. Much closer agreement can be achieved by adjusting A , using a value of about 0.6 to 0.65 rather than 0.75 and, in practice, this may be easier to use. Savelyev and Taylor (2001) revisited Panofsky and Dutton's formula and derived a slightly different form:

$$\left\{ \frac{\delta}{z_{01}} \left[\ln \left(\frac{\delta}{z_{01}} \right) - 1 \right] + 1 \right\} = 1.25 A_N \kappa \frac{x}{z_{01}} \quad (10)$$

with

$$A_N = 1.0 + 0.1M \quad (11)$$

Note the use of upstream roughness length in eq. (10) compared with downstream in eq. (7).

The vertical profile of variables within the IBL is governed by the adjustment between the new surface (and equilibrium layer, if it exists) and the upstream profile. A very simple approach is to assume a standard neutral logarithmic profile in equilibrium with the surface roughness up to the IBL depth, i.e.

$$\begin{aligned} u(z) &= \frac{u_{*2}}{\kappa} \ln(z/z_{02}) \\ &= u(\delta) \frac{\ln(z/z_{02})}{\ln(\delta/z_{02})} \end{aligned} \quad (12)$$

where the second expression arises from forcing the wind speed to be continuous at the top of the IBL ($z = \delta$).

This may give useful estimates but cannot be entirely accurate as it introduces a discontinuity in wind shear at $z = \delta$, which would introduce additional turbulent stress rather than the required decay. Mulhearn (1977) used eddy diffusivity ideas and a self-preserving assumption to derive a similar relationship for IBL depth to Panofsky and Dutton (1984) together with formulae for various profiles, including the velocity and shear stress profiles in the IBL. The self-preserving idea is powerful, in that it assumes that the shape of vertical profiles is independent of fetch – profiles scale in height with a single length scale l_0 which is a function of fetch only, and the amplitude of the flow perturbation depends upon a single velocity scale, also a function of fetch only. Under conditions typical of rural to urban transition, Mulhearn (1977) found an implicit relation for the length scale, wind-speed change and stress change given, respectively, by:

$$l_0 \{ \ln(l_0/z_{01}) - 1 \} = 2\kappa^2 \{ (\tau(0) - \tau_1) / (u_0 u_{*1}) \} (x - x_0) \quad (13)$$

$$(U - U_1) / u_0 = -E_1(z/l_0) \quad (14)$$

$$(\tau - \tau_1) / (\tau(0) - \tau_1) = e^{-z/l_0} \quad (15)$$

Here, U_1 and τ_1 are the upstream velocity and kinematic shear stress profiles, x_0 is a small offset which recognises the IBL does not necessarily grow exactly from the roughness change, and E_1 is the first E_n function (the exponential integral, see Abramowitz and Stegun, 1972). The velocity scale is given by:

$$u_0 = \tau^{0.5}(0) - u_{*1} \quad (16)$$

If the upstream profile is a logarithmic wind profile with constant shear stress, $z_1 = z_{01}$ and $u_{*1} = \tau_1^{0.5}$. For large fetches, Mulhearn (1977) found simplified forms:

$$l_0 \{ \ln(l_0/z_{01}) - 1 \} = 2\kappa^2 x \quad (17)$$

$$u_0 / u_{*1} = M / (\ln(l_0/z_{02}) - \gamma) \quad (18)$$

where γ is Euler's constant, 0.577216.

The depth scale is not exactly the same as the IBL depth; eq. (14) suggests the velocity deficit reaches 1% of u_0 when $E_1(z/l_0) = 0.01$, which occurs when $z/l_0 \approx 3.2$, so we may take

$\delta \approx 3.2l_0$. Note the similarity in form of the depth scale, eq. (17), to the Panofsky and Dutton (1984) formula for δ , eq.(7), but it should also be noted that the upstream roughness appears in eq. (17).

The mean wind speed and surface stress near the surface are clearly of greatest interest for urban wind applications – the surface stress, in particular, characterises the turbulence levels and mean wind within the canopy and roughness sublayers. As suggested above, the surface stress is greatest close behind the roughness change as the surface ‘sees’ the stronger flow over the smooth upwind surface. The simplistic idea suggested above, that the IBL exhibits an equilibrium profile up to the IBL height (eq. (12)) actually produces reasonably good estimates of the change in surface stress. Note that the equilibrium profile is not the same as the long distance equilibrium profile because it is ‘driven’ by the upstream wind at δ , which is stronger than the long-fetch equilibrium wind over the rough surface. Assuming that the upstream profile is in equilibrium with the upstream surface, eq. (12) can be written:

$$u(z, x) = \frac{u_{*1}}{\kappa} \ln(z/z_{02}) \frac{\ln(\delta(x)/z_{01})}{\ln(\delta(x)/z_{02})} \quad (19)$$

which implies the surface friction velocity is given by:

$$u_{*2} = u_{*1} \frac{\ln(\delta(x)/z_{01})}{\ln(\delta(x)/z_{02})} \quad (20)$$

This can also be written:

$$u_{*2} = u_{*1} \left(1 + \frac{M}{\ln(\delta/z_{02})} \right) \quad (21)$$

The accuracy of this depends upon the accuracy of δ (as well as the basic assumption behind it).

Panofsky and Townsend (1964) derive the following:

$$u_{*2} = u_{*1} \left(1 + \frac{M}{\ln(\delta/z_{02}) - 1} \right) \quad (22)$$

which is extremely similar and yields very similar results in practice since $\delta \gg z_{02}$.

The solution of Mulhearn (1977) for large fetches (eq. (18)) may also be rewritten to give the surface friction velocity

$$u_{*2} = u_{*1} \left(1 + M / (\ln(l_0/z_{02}) - \gamma) \right) \quad (23)$$

which again is very similar (though note comments above regarding the difference between δ and l_0 - this leads to an additive constant of about 1 in the denominator of the fraction in this expression).

The agreement between these expressions arises because of the desire to asymptote to an equilibrium profile at long fetch. However, they do lead to very different values at short fetch, especially in the region where stress changes very rapidly as the near-surface wind adjusts to the new roughness (which we shall call the *transition region*). According to Garratt (1990), the ‘self-similar’ forms over-estimate the surface stress in the transition region (and over-estimate the distance taken for the surface stress to adjust) when compared with results from higher order closure models and, fortuitously, the simple formula of Elliott provides better estimates.

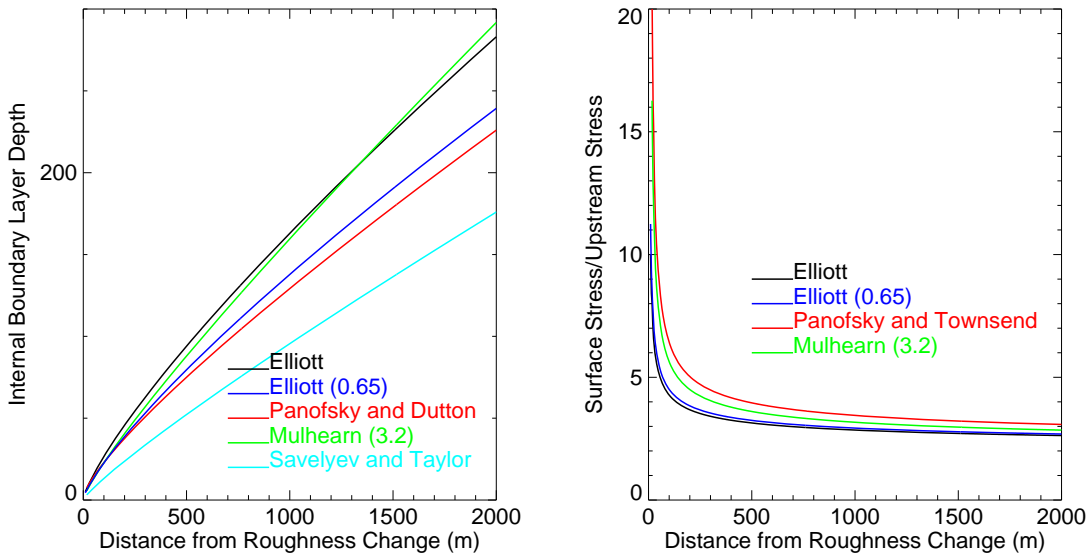


Figure 10 Neutral internal boundary-layer heights and surface stresses for a roughness change from 0.03 m to 1 m computed according to various formulae.

The formulae above are compared for a typical rural to urban roughness change in Figure 10. There is clearly significant uncertainty in IBL depth but the Panofsky and Dutton formula, as recommended by Walmsley, is reasonably central. Though the intensity and length scale of the transition region clearly varies from formula to formula, all agree that major deviations from the long-fetch stress only occur within 100-200 m of the roughness change. This seems very consistent with the canopy adjustment length-scale discussed above – the idea that the canopy flow adjusts within about 3 building spacings (or street spacings) is very consistent if we take typical street spacings to be 30-60 m, which seems quite reasonable.

In practice, the concepts above may be used to adapt a given wind speed, U_A , at a given height, z_A , in the inertial sublayer, taken as in equilibrium over a long fetch of constant roughness length z_{0A} (i.e. a ‘rural’ roughness) to give an urban inertial sublayer wind profile as a function of fetch from the edge of a roughness change. The key is to use an expression such as eq. (21), (22) or (23) to derive the surface friction velocity over the urban area, together with an expression for the IBL depth, such as eq. (7) or (8) and the neutral wind profile to derive the upstream surface friction velocity in terms of U_A , z_A , and z_{0A} . This is precisely the approach taken by Heath *et al*, 2007. They adopt the simplest choices for the neutral inertial sublayer. The upstream wind profile is taken to be

$$u(z) = \frac{u_{*1}}{\kappa} \ln(z/z_{0A}) \quad (24)$$

so that the upstream surface friction velocity is given by

$$u_{*1} = \frac{\kappa U_A(z_A)}{\ln(z_A/z_{0A})} \quad (25)$$

The wind profile over the urban area is taken as eq. (2), including the displacement height (which has been ignored in the IBL discussions above), and a simple matching at the IBL height, δ , assumed (as eq. (20) but including the displacement height), i.e.

$$\begin{aligned}
 u(z) &= \frac{u_{*2}}{\kappa} \ln\left(\frac{z-d}{z_0}\right) \\
 &= u(\delta) \frac{\ln\left(\frac{z-d}{z_0}\right)}{\ln\left(\frac{\delta-d}{z_0}\right)} \\
 &= U_A(z_A) \frac{\ln\left(\frac{\delta}{z_{0A}}\right) \ln\left(\frac{z-d}{z_0}\right)}{\ln\left(\frac{z_A}{z_{0A}}\right) \ln\left(\frac{\delta-d}{z_0}\right)}
 \end{aligned} \tag{26}$$

The IBL height is taken from eq. (8) but ignoring the M factor.

The discussion above suggests that this approach is likely to yield reasonably accurate results in near neutral conditions – other neutral formulae might give somewhat different results, especially over the rapid transition region. However, the transition region occupies only a small area of most significant urban areas, and the most important parameter is the asymptotic wind speed (or friction velocity) at long fetch. Care needs to be taken with this and the approach taken by Heath *et al* is likely to have some difficulties at long fetch once the IBL depth significantly exceeds the upstream inertial sublayer depth (which will happen with fetches longer than a few km). This is discussed further below (in section 4.2.5), and possible improvements to this approach to deal with this problem are available. However, it is likely that the main limitations of the method are:

- The quality of the input wind data (Heath *et al* use NOABL – see section 6.5).
- The assumption of neutrality – urban boundary layers are probably more likely to be unstable (and less sheared) and rural may be quite stable, especially at night.
- Derivation of basic urban parameters such as roughness length.

4.2.4 Heterogeneity, blending methods and source areas

Though urban surfaces are very different from surrounding countryside, they are rarely internally uniform. More typically, neighbourhoods may exhibit reasonably uniform characteristics, either through having been developed at a similar time, or because of common use (e.g. suburban housing, light industry, warehousing, high-rise residential). Often the scale of variation is such that the boundary layer as a whole does not have time to respond to each change separately, but, instead, sees a mixture of impacts from the upstream surface. Conceptually, we anticipate that the further away from the surface one looks, the more the flow is directly influenced by the surface further upstream. For relatively small-scale surface variations, it is anticipated that the boundary layer as a whole responds to an overall ‘effective surface’ with uniform characteristics.

These ideas can be quantified, to some extent, as discussed by Mason (1988). Consider a sinusoidal variation in surface roughness with wavenumber k , wavelength λ . We might assume that, near the surface, the flow perturbation is also sinusoidal. The amplitude of this variation gradually decreases away from the surface as turbulence mixes across horizontal gradients. At some height, called the diffusion height, ℓ_d , the variation becomes negligible. We can define an advective timescale at height z

$$\tau_{adv} = \lambda / u(z) \tag{27}$$

Considering the diffusion equation, the depth scale of the solution varies as $z = (\nu\tau_{adv})^{\frac{1}{2}}$, where ν is the kinematic turbulent viscosity, given by $u_*\ell$ where ℓ is the turbulent lengthscale and u_* the friction velocity over the effectively uniform surface. We can estimate a height scale over which the sinusoidal perturbation decays, ℓ_d :

$$\ell_d^2 = u_*\ell\lambda / U(\ell_d) \quad (28)$$

In the neutral case, with $\ell = \kappa z$ this gives us

$$\ell_d \ln(\ell_d / z_0) = \kappa^2\lambda \quad (29)$$

For a given roughness length and roughness wavelength, this may easily be solved iteratively.

The diffusion height is the height at which flow perturbations tend to zero. The area averaged profile exhibits an equilibrium profile (logarithmic in neutral conditions) in a region above a height known as the blending height (Wieringa, 1986). Essentially, this is the height at which the stress divergence equals the advection of perturbations. Above this, the stress divergence term becomes the dominant term and the wind profile is in equilibrium with the overall surface. The blending, ℓ_b , height can be estimated from

$$\ell_b = \frac{2}{k} \left(\frac{u_*}{u(\ell_b)} \right)^2 \quad (30)$$

In neutral flow in equilibrium this may be rewritten

$$k\ell_b (\ln(\ell_b / z_0))^2 = 2\kappa^2 \quad (31)$$

Mason (1988) gives an alternative argument which is a little more intuitive. Suppose the overall surface is made up of alternating patches of two roughnesses each with length $\lambda/2$. The essential idea is that, after a transition from one surface to the other an IBL grows; the blending height is (roughly) the depth of this IBL at the end of the patch. The detailed argument shall not be repeated here. Note, however, that it does not rely on the IBL growth law, only on the idea that the surface stress is given by an equilibrium profile matching the wind at the IBL depth. The idea is therefore very consistent with those expressed above for IBL growth.

The concept of the blending height leads to a precise derivation of the effective roughness length. At height ℓ_b the wind profile is in equilibrium with both the overall stress and the stress separately over each surface. Given equal areas of each surface, the total stress is

$$u_*^2 = 0.5(u_{*1}^2 + u_{*2}^2) \quad (32)$$

therefore

$$\begin{aligned} \kappa^2 u(\ell_b)^2 (\ln(\ell_b / z_{0eff}))^{-2} = \\ 0.5 \left(\kappa^2 u(\ell_b)^2 (\ln(\ell_b / z_{01}))^{-2} + \kappa^2 u(\ell_b)^2 (\ln(\ell_b / z_{02}))^{-2} \right) \end{aligned} \quad (33)$$

i.e.

$$(\ln(\ell_b / z_{0eff}))^{-2} = 0.5 \left((\ln(\ell_b / z_{01}))^{-2} + (\ln(\ell_b / z_{02}))^{-2} \right) \quad (34)$$

Note that the blending height should strictly be derived by iteration of eq. (31) (in neutral conditions) with eq. (34) (to provide the overall stress). However, Mason (1988) shows that a good approximation is

$$\ell_b \approx L_R / 200 \quad (35)$$

where L_R is the length scale of each region of roughness (i.e. $\lambda/2$ in the case of alternating patches of equal size).

In practice, land-use may not have a single characteristic length scale, and it is often not obvious how to define the blending height. Fortunately, Mason and others have shown that the precise choice of blending height is not critical – it is a height scale, not a fixed height. The primary requirement is that inertial-sublayer scaling is applicable at this height both for individual surfaces and for the aggregated surface.

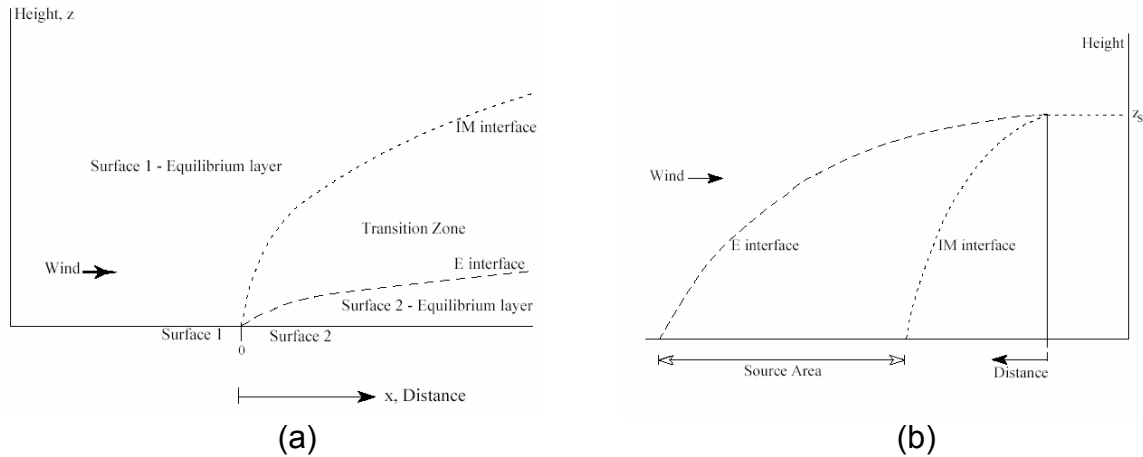


Figure 11 (a) Internal boundary layer interfaces for a 1D discontinuity (b) The diagnosis of the source area for 1D patchiness. From Hopwood, 1988.

A complementary view point introduces the concept of *source areas*. As discussed above, it is anticipated that, as one goes further away from the surface, the more upstream surface properties have an impact on the local flow characteristics. In effect, one is considering the IBL in reverse (Schmid and Oke, 1990).

If we consider each patch of surface as initiating its own IBL, then, for a reference observation point located at some height z_s , upstream patches fall into one of three categories (see Figure 11). Those close to the reference position will have an IBL depth too shallow to influence the observation point. Points a long way away will have an IBL for which the equilibrium inertial sublayer is deeper than z_s . These points may be thought of as contributing to the overall flow but not to local perturbations of it. Only points between these two extremes (for which z_s is above the equilibrium layer but still within the IBL) contribute to the source area. In practice, the wind direction also varies through turbulence, so points away from the mean upstream direction also contribute, the less so the further away from the mean wind direction.

The relative contribution of different surface elements to the flow is the source weight distribution (SWD), and those surface elements with a significant contribution are considered part of the source area. Note that the distribution is smooth. Attempts to compute the source weight distribution are based on solutions of the advection diffusion equation. If one imagines a tracer emitted from a surface element, the relative contribution to the source weight distribution is given by the probability that the tracer reaches the observation point. This may be addressed by solving the advection diffusion equation for tracers emitted from the surface. In practice, it is helpful to exploit the symmetry (reciprocity) of the advection diffusion equation; the probability that a tracer observed at the observation point was emitted from a surface element is precisely the same as the probability that a tracer emitted at the observation point reaches a surface element given the opposite wind direction. This enables the use of point source dispersion models to estimate the SWD.

Schmid and Oke (1990) take this approach, and a similar approach is used in the Met Office's 'Site Specific Forecast Model' (Clark, 1997), in which a Source Area Model (SAM) was

implemented in a 1D boundary layer model to derive the effective land-use contributing to surface exchange in the model (Hopwood, 1998). We shall not reproduce the detail here as it is quite complex. The basic principle, however, is that the concentration distribution from a unit source is given by

$$C(x, y, z) = \frac{D_y(x, y)D_z(x, z)}{U(x)} \quad (36)$$

where D_y and D_z are crosswind and vertical source weight distributions and $U(x)$ is the effective plume advection speed. The crosswind source weight distribution is assumed to be a Gaussian plume in common with conventional dispersion models:

$$D_y(x, y) = \frac{1}{\sqrt{2\pi}\sigma_y} \exp\left\{-\frac{y^2}{2\sigma_y^2}\right\} \quad (37)$$

The lateral plume spread, σ_y , is assumed to be a function of travel time downwind, with the rate of spread determined by estimates of horizontal turbulence intensity at source height.

The vertical distribution is more complex due to the vertical variation in diffusivity:

$$D_z(x, z) = \frac{A}{\bar{z}(x)} \exp\left\{-\left(\frac{Bz}{\bar{z}(x)}\right)^s\right\} \quad (38)$$

A and B are functions of s, and s depends upon stability and the mean plume depth, \bar{z} , but a value of 1.5 serves as a reasonable approximation. The mean plume depth, \bar{z} , is derived from numerical solution of an ordinary differential equation:

$$\frac{d\bar{z}}{dx} = \frac{\kappa^2}{\left[\ln(p\bar{z}/z_0) - \Psi(p\bar{z}/L)\right]\Phi_h(p\bar{z}/L)} \quad (39)$$

where p is a constant depending on s, L is the Obukhov length and Ψ and Φ_h are standard Monin-Obukhov stability functions.

Strictly, the solution to these equations depends upon turbulence levels, which depend on the source area characteristics, so an iterative approach should be adopted. However, in practice the concept only applies well for relatively small perturbations in surface characteristics, for which iteration does not yield significant changes.

It should be noted that all of the work on blending heights and source areas has neglected the zero-plane displacement height. This is probably of secondary importance for source areas, but does introduce some conceptual problems for derivation of effective surface parameters. Some allowance can be made within the computation of fluxes over individual surfaces (i.e. the blending height could be corrected for displacement), but a problem remains as we have no means of deriving an 'effective' zero plane displacement.

4.2.5 Boundary layer

Most of the above has applied to the inertial sublayer or below. Furthermore, most results concerning the IBL have been derived (and calibrated) for neutral conditions, though Savelyev and Taylor (2005) show that stability can be introduced in a fairly straightforward way. In practice, where urban wind is concerned, neutral results are probably reasonably applicable in the inertial sublayer and below in most cases with reasonably strong winds.

The problem becomes much more complex above the inertial sublayer. First, the well-known Monin-Obukhov similarity profiles no longer apply even in equilibrium. Over sufficiently long

fetches, Rossby similarity theory can be applied (see Section 3.1.2), which effectively allows one to derive a surface friction velocity from the wind at the top of the boundary layer, or geostrophic wind if that is all that is available. The logarithmic profile can be applied to the lower 10-20% of the neutral boundary layer. It is possible to extend the ideas used in modelling the IBL in the inertial sublayer by introducing upstream profiles of wind and vertical turbulence intensity based on Rossby similarity theory. An example is the model of Sempreviva et al (1990). In practice the wind above the inertial sublayer is of little interest for wind energy applications, and the main value of extending the neutral theory is to reconcile the surface stress predictions above with the asymptotic prediction from Rossby similarity theory; Sempreviva et al (1990) propose, for smooth to rough changes

$$\frac{u_{*2}}{u_{*1}} = \frac{\ln(\delta(x)/z_{01}) - 2\delta(x)/H_1}{\ln(\delta(x)/z_{02}) - 2\delta(x)/H_2} \quad ; \delta(x)/H_1 \leq 1$$

$$\frac{u_{*2}}{u_{*1}} = \frac{\cos \alpha \frac{\ln(H_1/z_{01}) - 2}{\cos \alpha_1 \ln(\delta(x)/z_{02}) - 2\delta(x)/H_2}}{\cos \alpha_1 \ln(\delta(x)/z_{02}) - 2\delta(x)/H_2} \quad ; \delta(x)/H_1 > 1$$
(40)

where subscript 1 refers to the upstream conditions, α is the angle between the top-of-boundary-layer wind and surface stress and H is the equilibrium boundary layer depth according to Rossby similarity theory. The height of the IBL is given by

$$\left\{ \left(\frac{1}{1 - (\delta/H)} \right) \frac{\delta}{z_{02}} \left[\ln \left(\frac{\delta}{z_{02}} \right) - 1 - y \left(\frac{\delta}{H} \right) \right] + 1 \right\} = c \frac{x}{z_{02}}$$
(41)

with $y \left(\frac{\delta}{H} \right) \sim \frac{\delta}{H}$ and c a constant $O(1)$, taken to be 0.9.

The relationship between these equations and eq. (22) and (7), valid when $\delta \ll H$, is obvious, and, apart from the treatment of the turning of wind with height which leads to a discontinuity between the $\delta > H_1$ and $\delta \leq H_1$ cases, form a consistent analytic approach to dealing with neutral boundary layer development over a city. However, it is questionable how applicable they are to the real world since

- a) The upstream flow is often not neutrally stratified. Even if the rural boundary layer is neutral, it often forms beneath a stably stratified layer into which the deeper urban boundary layer will penetrate.
- b) The rural/urban transition is often accompanied by a change in surface heat flux as well as a change in roughness.

During the daytime, neutral results may be useful for much of the time as the roughness change dominates, though it may be necessary to use stability corrected estimates of IBL depth.

Bigger problems are likely to arise at night, where a stable rural boundary layer encounters a neutral or even unstable urban surface. The above, turbulent diffusion-based, arguments are unlikely to be useful. Instead, the IBL growth is dominated by buoyancy effects; the surface heat flux gradually erodes the stable boundary layer, producing a steadily deepening, well mixed layer. This situation is similar, in many ways, to the cold sea or lake to warm land transition typical of daytime, summertime, onshore flows which has been studied a great deal in the literature. Knowledge of the potential temperature gradient of the upstream flow, the surface heat flux (H_s) and momentum flux plus a parametrization of the entrainment heat flux at the top of the internal boundary layer (H_δ) enables an equation for the rate of change of IBL height to be derived (along with an equation for the IBL potential temperature). A typical example is that of Gryning and Batchvarova (1990):

$$\frac{Bu_*^2 T}{Cg\delta} \frac{d\delta}{dt} = A \frac{H_s}{\rho C_p} - \frac{H_\delta}{\rho C_p} + \frac{Bu_*^3 T}{g\delta} \quad (42)$$

where A, B and C are constants (0.2, 2.5, 1.3) and T is the temperature of the stable layer at the interface. They derive an implicit analytic expression for the IBL height. However, the driving term, the surface heat flux, is specified (as is the friction velocity). In practice, this is not fixed and not known, so additional parametrization of the surface heat flux is required. The discussion of the neutral IBL above suggests that the ‘transition region’ is of minor importance, so it may be acceptable to assume a uniform urban heat flux in spite of the dynamically varying IBL.

It is not unusual for a stable rural boundary layer to encounter an urban area with surface heat flux close to zero at night, so perhaps the most useful application of analytical results may be in situations of zero urban heat flux. Beyond this, it is the job of complex mesoscale models to compute the evolution of the boundary layer in situations with strong coupling between the surface and the atmosphere and unknown and variable upstream conditions. To compute the transition behaviour between urban and rural requires sufficient resolution to treat the growing IBL.

4.2.6 Mesoscale

The term ‘mesoscale’ covers an enormous range of phenomena – it is usually regarded as including atmospheric phenomena with characteristic scales from 1 to 1000 km. The range is so great that a sub-division is often employed, defining 1000-100 km, 100-10 km and 10-1 km as meso- α , β and γ respectively. Meso- γ phenomena are often restricted to the boundary layer, though at the large end may include deep convective clouds. In the context of urban areas, boundary layer impacts essentially mean the complex response to variable surface forcing discussed above. In practice, even the upstream surface is rarely uniform, and the urban surface itself often shows substantial variability on the city scale (e.g. suburban vs city centre). In this case, a great deal may be achievable using the general, idealized results discussed above provided a certain amount of idealization of the surface is acceptable. Where the surface is too complex for this approach (as it often is), the only viable approach is to use a detailed, non-linear flow model with a reasonably sophisticated treatment of the surface. This is a typical application of mesoscale models, though such models are actually designed to deal with a much wider range of phenomena than boundary-layer adjustment.

A good example of mesoscale model use to study urban boundary layer (UBL) development is given by Martilli (2002a), who uses a mesoscale model with a sophisticated urban canopy parametrization to study the idealised (2D) development of the UBL over a small, uniform, city, 10 km across, using a horizontal grid length of 1 km. The paper goes on to investigate sensitivity to factors such as wind speed, urban morphology and upstream soil moisture (and, hence, heat flux). Findings may be summarised thus:

- The model used can reproduce the elevated nocturnal inversion that has been observed over some cities, and the vertical structure of turbulent heat fluxes. The ‘traditional’ rough concrete approach to surface exchange fails to do so. The reasons for this are discussed below in discussions of the urban surface energy budget; the central feature is that the methods discussed above for estimating the IBL depth in non-neutral conditions require a good estimate of the surface heat flux, which requires a fairly sophisticated approach to the urban surface.
- Both thermal and mechanical factors generate vertical mixing in the nocturnal UBL; thermal factors are more important in the lower part (reduction of cooling because of trapping of LW radiation in street canyons), mechanical factors are more important in the upper part (controlling inversion strength).

- Model results show increases in daytime UBL height compared with rural that are similar to those observed. Differences are strongly controlled by rural soil moisture values (which control rural sensible heat flux).
- Weak winds favour a greater rural/urban difference in daytime UBL height.
- The daytime UBL is dominated by thermal factors until the evening when mechanical factors control the evening transition.

These results primarily serve to illustrate that, to predict rural/urban differences in boundary layer structure requires information on both mechanical impacts (i.e. building drag) and thermal impacts (surface heat flux, including the upwind conditions) that renders quantitative generalisation very difficult.

Beyond these mesoscale boundary layer impacts, many authors have discussed meso- β scale impacts of urban areas, where the urban area as a whole has an impact on the atmospheric dynamics. Perhaps the most common phenomenon alluded to might be described as the 'urban breeze', by analogy with the sea breeze (though since the sea breeze comes from the sea, perhaps 'rural breeze' would be better terminology). In very weak mean flows, a sufficiently strong urban heat island (UHI) may form to induce a thermally forced circulation – essentially the UHI produces a pressure drop over the city which, initially, at least, forces a low level flow from the outskirts to the city centre. Around the centre of the city the convergent low level wind causes lifting and an outflow at elevated levels (probably a few 100 m). Though the daytime UHI is often weaker than the nocturnal UHI, the overall temperature anomaly, given the depth of the boundary layer, may be stronger, and, as a result, the daytime urban breeze may be stronger.

A good example of the 'urban breeze' is reported by Lemonsu and Masson (2002), who use a mesoscale model nested down to 1 km grid length to study an anti-cyclonic event over Paris. The event is characterised by extremely weak large scale (geostrophic) flow in mid-summer (mid-July). They find a daytime convergent flow into the city peaking at 5-7 m s⁻¹ at 200 m, with compensating outflow at the top of the boundary layer at about 2000 m. Similar events have previously been studied over other cities, notably St Louis (e.g. Wong and Dirks, 1978) though the Paris study is probably more relevant to UK conditions. It should be remembered, however, that Paris is probably more likely to experience an urban breeze than many UK cities; much of the urban surface in England occurs in the Midlands conurbation and is much more distributed (in the sense that a sharp urban/rural distinction is harder to make). London is quite distinct, but also strongly influenced by the Thames estuary – on days where an urban circulation might occur, a sea breeze is also very likely to penetrate far inland. The same may be true of Liverpool, while Manchester is likely to be affected by local hills.

The overriding message is that, in the absence of strong flow induced by large scale meteorological systems, the perturbation caused by an urban area can cause very significant local flows. However, the same can be said of many other changes in surface, such as land/sea contrast and topography, and the urban area has to compete with these effects. As a result, it is extremely difficult to generalise for real cities unless they can genuinely be identified as the only surface variation over quite a wide area.

It is in these complex, surface-forced situations that the mesoscale numerical model comes into its own. There are many documented studies of mesoscale interactions between cities and coastal flow (e.g. for New York), and it would appear that, provided the model surface exchange scheme can do a reasonable job of predicting urban (and rural) fluxes and temperatures, the resulting flows can be predicted quite well.

It would appear that only a small mean flow is required to disrupt the urban breeze. Studying other cases, Lemonsu and Masson (2002) show that a mean flow of only 2.5 m s⁻¹ (presumably 5 kt, the lightest wind category above calm actually reported by routine observations) is enough to

displace the warm urban air downstream, so that, instead of an urban breeze an urban thermal plume develops. This may be thought of in terms of the IBL discussed above. Downstream of the urban area a cold rural IBL forms, so the urban plume is elevated. While this thermal plume undoubtedly has some impact on mesoscale dynamics, it is small since the ventilation of the city prevents a large temperature anomaly building up (i.e. it is spread downwind).

Though clearly not exactly the same, it may be worth considering the sea breeze as an analogy. A number of indices have been developed to predict the onset of a sea breeze. Simpson (1994) discusses using an index based upon $U^2 / \Delta T$, where U is the 'mean flow' (e.g. geostrophic wind) and ΔT the temperature contrast. A critical value of 7 separating sea-breeze and non-sea-breeze days is suggested based on Thorney Island data. For a temperature difference of 3 K, this would suggest a critical wind speed of about $4\text{--}5 \text{ m s}^{-1}$. Though certainly plausible (Lemonsu and Masson (2002) found an urban breeze for a mean flow of less than 5 m s^{-1} and no urban breeze for a mean flow of 7.5 m s^{-1} for example), the complication is that the temperature contrast will interact strongly with the flow; this is less of a problem for sea-breeze estimation as it is possible to use an inland temperature.

Other authors, (e.g. Bornstein and Lin, 2000, studying three Atlanta cases) have studied the urban breeze and claimed a connection between the lifting associated with the urban breeze convergence (and the heat source associated with it) and triggering of thunderstorms. It is certainly the case that some storms are very sensitive to perturbations in the atmosphere (and so very small changes indeed may promote or prevent their formation). However there is little or no evidence of a strong systematic effect over UK cities (or, probably, anywhere else).

4.2.7 Implications for urban wind energy

The above discussion of IBL and fetch effects enables a few general statements to be made concerning estimation of urban wind energy resource.

1. Within the urban canopy, changes in canopy characteristics lead to 'transition effects' over a distance of about three streets (or typical building spacings). Conversely, in defining 'neighbourhood' characteristics, it may be sensible to average over about six streets (three in each direction).
2. The surface friction velocity, which determines the wind profile in the inertial sublayer and has a major influence on that in the canopy and roughness sublayers, adjusts rapidly at the edge of a major roughness change (e.g. the edge of a city), so that major edge effects are confined to one or two hundreds of metres. However, slower changes occur as the boundary layer adjusts to the new surface.
3. In neutral conditions, which probably pertain to most strong-wind conditions, simple analytic models can do a reasonable job of predicting the change in wind profile and, most importantly, the change in surface friction velocity (as a function of distance from the edge of the city due to a change in surface roughness) given the upstream wind profile or, equivalently, the 'free stream' (top of boundary-layer) wind and surface roughness.
4. The depth of the internal boundary layer over an urban area is very roughly 10% of the distance from the upwind edge of the urban area – this means that the whole boundary layer is affected by any urban area larger than about 10 km across, and even a small village 1 km across affects the wind at 100 m. This means that any rural wind data must be used with careful adjustments to urban conditions.

5. Blending height methods enable the overall impact of heterogeneity of the surface on scales of a few hundred metres to be taken account of in estimating an effective urban roughness provided the urban area is relatively uniform on smaller scales.
6. In non-neutral conditions, primarily where an urban area produces a major change in surface heat flux, predictions can be made by considering the energetics of the IBL. However, it is much more difficult to generalise because a) more information is needed about the upwind temperature structure of the atmosphere and b) the estimation of the urban heat flux requires knowledge of the wind field, so simple solutions are difficult to obtain. A more comprehensive calculation on a case-by-case basis using a comprehensive boundary-layer or mesoscale model is required. This is especially true of light wind conditions at night.
7. In light wind conditions a local 'urban breeze' may be set up, driven by the urban heat island. In extreme conditions (i.e. high summer, no mean wind), this may reach as much as $5-7 \text{ m s}^{-1}$ at 200 m. 'Light wind' probably means when the wind at the top of the boundary layer is less than about 5 m s^{-1} . While it may be possible to diagnose conditions where this may occur, the resulting flow is a complex interaction of between the mean flow and the thermally forced flow, which requires a full mesoscale model to estimate in all but the simplest cases. This is especially true where other mesoscale effects such as sea or mountain breezes can occur. It is likely that conditions favourable for urban breezes strong enough to provide a significant wind power resource are quite rare over the UK (i.e. a few days per year at most), so it is likely to be a reasonable approximation to neglect this effect.

4.3 Urban Surface Energy Balance

The structure of the urban surface is very complex and as such, it alters each of the terms in the surface energy balance compared to most natural types of surface. Despite these complexities, it is not yet clear how complex a model of the urban surface energy balance has to be. There are a number of physically-based models within the literature that vary in their complexity, from simple bulk representations, to detailed energy balances on many parts of each facet of the urban structure. Before looking at the various ways in which the urban surface energy balance is modelled for each of the components, namely radiation, heat flux, moisture flux and the heat storage flux, we must define what the urban surface is.

4.3.1 The urban surface

For the simplest urban surface energy balance models, the surface is defined as a single area with bulk characteristics (e.g. Best, 2005; Dupont and Mestayer, 2006). With this type of model the surface is modelled in a similar way to natural surfaces, with certain model parameters taken to be an aggregate of the surfaces that exist in the urban structure. The next stage of complexity is to resolve the differences between the roofs of buildings and the street canyons below. It has been shown that this type of approach gives an improvement compared to the simple single surface (Best et al., 2006). However, the urban canyon is still represented with aggregate parameters which are difficult to define and hence difficult to measure.

The majority of urban surface energy balance models take a street canyon as the building block for the urban surface. Within these street canyons the models distinguish between the roofs of buildings, the walls of the buildings and the road (gardens are generally not included), and are largely based upon the work of Masson (2000), for example Kondo et al. (2005). Some models make a further distinction between walls which are sunlit and walls which are shaded (Kondo et

al., 2005; Martilli et al., 2002) with some going further by having different orientations for the street canyons (e.g. Martilli et al., 2002). Some go even further and split each wall into vertical sections, each of which has its own energy balance (Krayenhoff and Voogt, 2007). This enables the time evolution of the wall to have a profile of sunlit and shaded areas.

Whilst the model of multiple energy balances for walls is at the most complex end of the spectrum of models, there are other models that have complexity in a different form. Whilst most use the street canyon as a building block, some also include the intersections of these street canyons, enabling the model to distinguish between the radiation and turbulence effects within the canyon compared to those in the more open space of the intersection.

There is a still further classification of complexity for surface energy balance models that effectively do not have a single surface for energy and moisture exchange with the atmosphere. These models distribute the impact of the urban area within the boundary layer of an atmospheric model (e.g. Martilli et al., 2002; Ca et al., 2002; Otte et al., 2004; Dupont et al., 2004). As well as introducing elevated sources of heat and moisture into the atmosphere, this type of model can also represent the bluff body drag on the atmosphere due to the solid surface of the buildings themselves.

4.3.2 Radiation

For most surfaces, the balance of radiation at the surface is straightforward and consists of incoming and outgoing fluxes of short and long wave radiation (i.e. radiation in the visible and infra-red parts of the spectrum) at the surface boundary. The complex geometry of an urban area means that there is no simple surface on which you can consider these fluxes. Therefore you obtain multiple reflections of both the short and long wave radiation throughout the street canyons of an urban area.

In the simplest models these multiple reflections are basically ignored (e.g. Best, 2005), or the parameters such as albedo or emissivity are changed to give effective values which have the correct behaviour in general. However, it is not possible to select a single value for the albedo which gives accurate results compared to observations (Best et al., 2006).

In the more complex models the multiple reflections are taken into account in varying degrees. In some only a single reflection is calculated (e.g. Masson, 2000; Kondo et al., 2005). This represents what is likely to be the dominant impact of the reflections, but does not capture the whole effect. It is possible to construct a model to describe an infinite number of reflections (Harman et al., 2004), although this requires detailed information about the site. However, it is still possible to parameterise an effective albedo that varies in time (Harman, 2003), although an effective emissivity is more difficult to obtain due to the dependence of the emitted long wave radiation on the temperature of the surface.

The models that take account of sunlit and shaded walls also need to resolve the direct and diffuse components of the short wave radiation. However, this is not generally an increase on the complexity of the energy balance of natural surfaces, as the ratio of direct and diffuse radiation is also important for vegetation.

4.3.3 Turbulent heat flux.

The basic principle for the turbulent heat flux is the same in all of the models of the urban surface energy balance. The flux is determined by the gradient of temperature between the surface and a reference point in the atmosphere and the level of turbulence which is the

mechanism for transporting this energy. The differences between the models come from the way in which the turbulence is modelled. In simple models such as Best (2005), there is no enhancement for the urban area and the turbulence is represented using standard surface theories based upon “effective” roughness lengths. Despite resolving the energy balance of the walls and road within the urban canopy, the model of Masson (2000) still uses this same approach of a roughness length with the stability coefficients of Mascart et al. (1995). A parameterisation of the turbulence within a street canyon based upon wind tunnel measurements has been proposed by Barlow (Barlow and Belcher, 2002; Barlow et al., 2004). This distinguishes the difference in turbulence felt by the road and the various walls within a street canyon.

4.3.4 Turbulent moisture flux

Due to the complex nature of the urban surface, most research has concentrated upon the radiation, heat flux and heat storage components of the energy balance. Whilst the moisture flux is similar in nature to the heat flux in that it is transported by the same turbulence, the availability of moisture at the surface make this flux more difficult to model.

Many urban energy balance models have been designed to be dry (i.e. they do not take account of the moisture fluxes within the urban area and assume that these are zero), e.g. Masson (2000). Hence they do not include the turbulent moisture flux.

The simple model of Best (2005) does allow for a moisture flux because it represents the urban surface within the same framework as the energy balance for natural surfaces (in which the moisture flux plays a dominant role). However, such a simple approach to the moisture flux is not adequate to describe the complexity of the moisture fluxes within urban areas (Best et al., 2006).

Little research effort has been undertaken into the impact of vegetation and other natural surfaces within an urban area on the moisture fluxes. Most research has concentrated upon the impact of parks within a city, but there is little on the impact of trees along roads, or gardens in residential areas. So it is not known at present if vegetation within urban areas has a different moisture flux compared to the same vegetation in rural areas.

4.3.5 Heat storage flux.

For most natural surfaces, the heat storage flux is represented by the flux of heat into the soil. This is generally modelled using the diffusion equations.

For urban areas, there is a similar flux of heat into the soil under a road, but this is only a small component of the total heat storage within the urban surface. Heat is also stored within the fabric of the walls and to a lesser extent the roof. It is the large heat storage capacity of an urban area that enables it to release heat long into the night and maintain a near neutral boundary layer structure, unlike other surfaces that tend to have stable nocturnal boundary layers.

In the simple model of Best (2005) the heat storage is modelled using a single block to represent the surface with a high thermal capacity. This has been shown to capture the general nocturnal behaviour of urban areas, which is not possible using the thermal properties of concrete within the basic model of a soil (Best, 2005).

For the models that represent the various facets of a street canyon, the heat storage under the road is represented by a soil model, whereas the heat storage in both the roofs and the walls are also represented by the diffusion equation using an appropriate depth and appropriate thermal properties (e.g. Masson, 2000; Martilli et al., 2002; Kondo et al., 2005; Dupont and Mestayer, 2006).

4.3.6 Anthropogenic heat source

In addition to the standard components of the surface energy balance, the urban surface has a source term which is due to human factors, such as energy consumption, traffic emissions, etc. The magnitude of this term is significant and can be 30 Wm^{-2} even for small cities such as Lodz in Poland (Offerle et al., 2005)

The energy consumption part of the anthropogenic heat source is generally modelled by assuming a fixed temperature inside of the buildings (e.g. Masson 2000, Kondo et al. 2005, Dupont and Mestayer, 2006) or a fixed temperature at the base of the walls and roof (e.g. Martilli, 2002; Kondo et al., 2005; Dupont and Mestayer, 2006). This fixed temperature supplies energy to the atmosphere by diffusing through the walls of the building and then impacting on the energy balance of the walls, leading to an increase heat flux.

This approach can not be taken for the simple models such as that of Best (2005), so in this case the anthropogenic heat source can be applied in two ways, either by adding a source term to the energy balance (equivalent to increasing the net radiation), or by adding the heat source directly to the turbulent heat flux. The first of these represents the heat source due to energy consumption and the second represents the contribution from traffic emissions (e.g. Masson, 2000). Other heat sources, such as power stations, tend not to be of significance for urban areas and are generally not included.

4.3.7 Impact of surface energy balance on urban wind

Urban areas have their largest impact on the structure of the nocturnal boundary layer. Although in the UK, the nocturnal boundary layer is often dominated by the synoptic situation (e.g. neutral due to the high windshear in stormy conditions), in calm conditions urban areas have a boundary layer which is unusual compared to that over natural surfaces.

The physical impact on the turbulent heat flux of the large heat storage capacity of urban areas, along with the significant anthropogenic heat source and the turbulence due to the large irregular buildings, is to maintain an upward flux into the night (e.g. see Best, 2005). This means that the surface remains warmer (or at least only slightly cooler) than the atmosphere, despite the absence of the solar heating at the surface. The resultant boundary layer is one which remains well mixed and near to neutral. This is in contrast to the nocturnal boundary layer over a rural area which is usually stable in nature, i.e. the surface is cooler than the atmosphere and hence air is buoyantly stable and can not mix as effectively.

For a stable nocturnal boundary layer, there are often low wind speeds close to the surface. The wind speed then increases with height until a level where a nocturnal jet forms. However, with a well mixed boundary layer, the wind speed at night will remain at a higher value near the surface during the night with no nocturnal jet forming aloft, due to the higher turbulence and the neutral buoyancy of the air. Hence urban areas are likely to have higher wind speeds during the night close to the surface than their surrounding rural areas.

This lack of stable conditions, the higher roughness in urban areas, and the fact that light wind situations are not of great interest for wind energy, means that, for the purpose of urban wind power generation predictions, it is likely to be a reasonable first approximation to assume neutral conditions.

4.4 Orographic Flow Models

4.4.1 Introduction

While large ranges of hills and mountains are known to have large effects on the wind, even relatively small hills within the boundary layer can have a significant impact on the wind field. Typically there is flow speed-up relative to the undisturbed flow at the crest, and deceleration at the upstream and downstream base. For example, a sinusoidal ridge of wavelength 2 km and 50m high (base to crest) will give a flow speed up above the crest of around 15% (and an increase in power of over 50%). Steeper hills have still larger impact, with increased speed-up at the crest and, beyond a critical threshold (e.g. Wood, 1995), the formation of separated region of weak or reversed flow behind the hill.

Much of the work on understanding and modelling the effects of hills on the wind has used a linear approach to the problem. In this method, the wind $u(z)$ is decomposed into an undisturbed or upstream part ($u_{ref}(z)$) and a perturbation induced by the hill ($u'(z)$). The perturbation quantities are then assumed to be small so that terms in the equations of motion which involve products of perturbation quantities can be neglected. Once this simplification (the validity of which will be discussed later) has been made, predicting hill-induced wind perturbations becomes more tractable analytically and also cheaper numerically.

4.4.2 Linear analytic models

These models all build on the original work of Jackson and Hunt (1975) in which flow over a hill is broadly divided into two layers – an inner region close to the surface in which turbulence effects are important, and an outer region in which the flow is essentially inviscid. The result is a prediction of streamwise velocity perturbations which scale on

$$\frac{H_h u_{ref}^2(L_h)}{L_h u_{ref}(l_i)}$$

Here H_h is the height of the hill and L_h is the half width at half height (and so the perturbations increase linearly with increasing hill steepness). l_i is the depth of the inner region, which itself depends on L_h and the surface roughness. Various heuristic modifications to the theory which led to improved agreement with observations were made in the development of the MS3DJH model (Taylor et al, 1983; Walmsley et al, 1986) and separately by Mason and King (1985). These include allowing for the decay of pressure perturbations with height, making various modifications to the chosen velocity scales for each region, and also treating each Fourier mode of the orography independently, each using its own appropriate length scales (rather than using a single bulk length scale). Hunt et al (1988a) completed a more formally exact linear solution for neutral flow over a hill, properly matching the different regions and including the (previously

neglected) impact of shear in the upstream solution. Hunt et al (1988b) further extended this analysis to include stability effects.

WAsP uses an orographic flow model closely related to MS3DJH (and, for computational efficiency, uses a polar numerical grid to enable concentration of resolution close to the point of interest). Flowstar is effectively an implementation of Hunt et al (1988a,b), although it does not use separate wavenumber-dependent scales for each Fourier mode.

4.4.3 Linear numerical models

A parallel series of developments has used numerical models to solve the linearized equations of motion (rather than using asymptotic matching). For example Beljaars et al. (1987) introduced the mixed spectral finite-difference (MSFD) approach, using spectral methods in the horizontal combined with the finite-difference method in the vertical. This combined the simplicity and efficiency of linear methods with the flexibility of being able to use different turbulence closure schemes. With a mixing length closure the results for the mean velocity over a hill were found to be similar to those previously obtained by Taylor et al. (1983) using asymptotic matching. Switching to a higher-order E-epsilon turbulence closure led to some increase in velocity speed-up at the crest in the inner region (improving agreement with observations) but had little impact higher up.

The MSFD model was further developed by Ayotte et al (1994) who tested the effects of a series of different turbulent parametrizations. Consistent with the earlier studies, these were found to have a large impact on the turbulence statistics, but only affected the mean fields in the inner region (where up to 20% variations in predicted fractional speed-up for a given hill could be obtained). Ayotte et al. (1996) further extended the model, allowing a more realistic range of upstream profiles (effectively generated by a one-dimensional boundary layer model) rather than assuming a logarithmic profile. This is potentially important when modelling flow over hills whose length is sufficient that the inner region becomes comparable to the inertial sublayer depth. A similar approach has been taken in the 3d-VOM model (Vosper, 2003; King et al, 2004) used operationally at the Met Office to predict orographically-induced wind perturbations (and in particular lee waves).

4.4.4 Validity of linear models

These linear models (both analytic and numerical) have been extensively tested against observations of flow over small-scale hills in the boundary layer e.g. Blashaval (Mason and King, 1986), Askervein (Taylor and Teunissen, 1987), and in the wind tunnel (e.g. Rushil (Khurshudyan et al, 1981)). Encouragingly the limitations of the model due to the assumption of linearity have been found to be less restrictive than might be assumed from theory e.g. Taylor et al. (1987) and Finardi et al (1993) both report good results from linear models on the upslope and crest for H/L as large as around 0.35 (or equivalently slopes of around 20 degrees), although as the flow in reality approaches the point at which it separates behind the hill, linear models tend to underestimate slowing of the winds in this region. Even for H/L=0.58, Finardi et al found speedup errors of less than 20% except in the wake region behind the hill. Similar results have been obtained comparing solutions from linear and fully non-linear models.

Linear approaches will also fail if the height of the hill becomes comparable to the buoyancy scale (U_0/N , where N is the buoyancy frequency, given by $N^2 = (g/\theta)\partial\theta/\partial z$, where θ is the potential temperature). In reality, in these conditions the effects of stability lead to flow splitting around the hill rather than going over it. For short wavelength hills this will only occur on calm, stable nights (when drainage currents will also be an issue). Fortunately these cases will contribute little to the overall wind resource, and so the errors are probably of no great

consequence. However, for larger hill and mountain ranges such as the Pennines the effects may be more significant.

4.4.5 Non-linear models

Some attempts have been made to extend linear models to include non-linear effects (e.g. the iterative approach of Xu et al, 1996). However, it is more common to use fully non-linear models. These are much more expensive to run than linear models, but obviously do not suffer from the limitations imposed through the linear assumption (although some aspects of the results remain sensitive to the turbulence closure, particularly for hills steep enough to cause separation e.g. Ying and Canuto, 1996). Examples of such models include global and regional NWP models, and also a number of research models (e.g. BLASIUS (Wood and Mason, 1993)).

NWP models will only represent the effects of resolved hills. While it is always possible in principle to run nested non-linear model simulations with finer and finer resolution, an alternative is to use a hybrid approach in which the larger scale hills and mountains are represented in a non-linear NWP model, and linear techniques are then used to estimate the small unresolved scales (e.g. Howard and Clark, 2007). This is a potentially attractive approach for UK wind resource modelling where the effects of small-scale hills (wavelengths of up to a few kilometres) in the vicinity of major towns and cities can be expected to be well represented by linear models.

4.4.6 Mass-consistent models

Mass-consistent models have a long history in the literature; the earliest proposed model is probably Sasaki (1958), though many models can be traced back to the MATHEW model of Sherman (1978). Mass-consistent models are not dynamical models, *per-se*, but are better described as objective analysis tools. The wind field is assumed to be in steady-state and the only other physical basis is the constraint of producing a non-divergent (in 3D) wind-field with zero flow through material surfaces (i.e. the ground, in practice) as well as an upper surface (usually taken to be the boundary layer depth). This guarantees conservation of mass (hence the name). This is insufficient, in itself, to determine the flow, and some additional information is required. In practice, this is usually the observed wind at one or more locations.

Though a number of solution approaches have been used, the most common is through the calculus of variations (as proposed by Sasaki (1958)). A 'first guess' wind-field is supplied, usually using some interpolation technique to generate a 3D wind-field from input point measurements, and a 3D wind field is output which minimises the difference (error) between the input and output subject to the constraint of non-divergence. Different weightings are applied to each wind component error, supposedly based upon *a priori* information about the statistics of error in the input first guess.

The technique has much in common, in principle, with (3D) variational approaches to data assimilation in NWP models. However, much depends on the nature of the first guess and knowledge of the error statistics of the first guess. In the NWP 3DVAR system, the first guess is a short forecast using a fully non-linear dynamical model started from the previous analysis, and error statistics are based upon a combination of knowledge of dynamical constraints (which influence the covariance of errors between locations and different variables) and past history of a long-running system. On the other hand, the mass consistent model first guess is usually based on some form of interpolation in the horizontal (perhaps on terrain-following coordinate surfaces) and a simple representation of the vertical wind profile (usually a power law in the vertical). Error statistics are largely based upon specification of a variance for each component (ignoring any spatial covariance), possibly changing with stability. Improvements of mass-consistent models are largely focussed upon (largely heuristic) modifications of the initial wind-field estimation to

allow for some stability effects, and it may be better to think of the ‘mass consistent’ aspect of these models as a post-processing method to force conservation properties on a simple, intelligent interpolation system rather than as a model in its own right.

The approach gained popularity in the 1980s for a number of reasons:

- Primarily, it is simple and relatively cheap, involving, in the variational approach, the solution of a linear 3D Poisson equation for which numerous, efficient codes exist. It was therefore practicable to implement on desktop computers even during the 1980s. Application has been largely to wind power resource estimation and atmospheric dispersion. In the latter case, mass-conservation is regarded as essential as predictions of concentration of material from a release of a given size would not be regarded as credible if some material were lost.
- The results are plausible in complex terrain, as some speedup over hills and channelling around is almost inevitable.
- The technique is observation based, and so maintains credibility by being guaranteed to agree (to an acceptable level) with the observations used. However, this is also a failing, especially where very few observations are used, since the accuracy of prediction away from the observation is limited by the accuracy of the model at the observation; in many cases the approach is used with only one observation. In effect, in this case, the method produces a flow pattern which is then calibrated by the observation.

Given the steady state assumption, the method can only be applied to relatively small areas (a similar limitation to most linear models), which tends to be the reason for only a few observations being available when applied using routine meteorological observations.

A number of comparisons have been made between different wind diagnosis methods – usually between mass-consistent approaches and linear approaches. However, these comparisons have usually concentrated on small scale hills where a number of observations are available. For example, Finardi *et al* (1993) compared predictions from two diagnostic (MATHEW and MINERVE) and two linear (MS3DJH/3R and FLOWSTAR III) models against two-dimensional wind tunnel data for neutrally-stable flow. In his review of mass-consistent and linear flow models, Homicz (2002) concludes: “*If the interpolated wind field has not been sampled at points sufficiently representative of the underlying terrain, there is little hope that the final winds will faithfully reflect its influence.*”

Thus, it is reasonable to say that mass-consistent models can do reasonably well (with lots of caveats) if several profiles of input data are available over a hill. They should not be used if only limited data are available, e.g. upstream profile. Linear models, on the other hand, require limited input data, representative of the large-scale or upstream flow and, perhaps, are more difficult to use so effectively with substantial amounts of observation data. Mass-consistent models therefore cannot take the place of linear models to represent effects of a small-scale hills that input observations do not resolve.

It has been argued (Homicz, 2002) that linear models which rely on a spectral solution in the horizontal based on Fast Fourier Transforms have difficulty with truly complex terrain that does not tend to zero at the domain boundaries as the solution technique relies on periodic lateral boundaries. However, the mass consistent approach also has boundary issues (as the component of flow along the lateral boundaries remains the same as the first guess). In both cases, solutions are usually sought for an area larger than that of interest, and only data in the interior (for example, 100x100 km of a 120x120 km domain) used. In either case extending the domain to cover much wider areas so as to avoid edge effects introduces the problem that, in practice, the large-scale wind is rarely, if ever, uniform over large areas. In extending the domain one effectively replaces a slightly inaccurate solution to a realistic problem with an accurate solution to an unrealistic problem.

5 Urban Wind Modelling

5.1 Effects of streets/buildings

As we have seen above, the presence of buildings in urban areas has a significant effect on the flow in the atmospheric boundary layer. In the bulk of the boundary layer above a few building heights the effect can be represented adequately by describing the surface in terms of a roughness length and displacement height. [Strictly this assumes that building heights are much less than the boundary layer depth, but this is likely to be the case in general, except perhaps in the high rise part of city centres, due to the rarity of very stable flows in urban areas. It is especially likely to be the case in the stronger wind cases of most interest in this report.] However, at heights comparable to the roughness elements (buildings), the flow is more complicated. In section 5.1.1 we consider the flow within the canopy as a whole, with the aim of describing the horizontally average flow as a function of height. Sections 5.1.2 and 5.1.3 discuss particular canonical building configurations, namely street canyons and isolated single buildings. Section 5.1.4 discusses the more complex problem of understanding the details of the flow through collections of buildings (i.e. understanding more than just the horizontally averaged flow). Finally section 5.1.5 summarises the research into urban flows conducted under COST Action 715.

5.1.1 Average flow in the urban roughness sublayer

Although the flow around individual buildings and in individual streets can be complex and specific to the particular building geometry, the horizontally-averaged flow in the roughness sublayer is easier to estimate. Here the horizontal average is taken over a 'neighbourhood'. This can be thought of as a region large enough to average the effect of many buildings but small enough that the general character of the buildings does not change significantly. For example, in a neighbourhood one would want statistical parameters describing the buildings – such as the plan-area density, λ_p , the frontal-area density, λ_f , and the mean (plan-area weighted) building height, h – to be insensitive to the averaging scale. We expect such a neighbourhood scale to exist in most parts of UK cities where the character of the buildings and their spacing is not changing very rapidly. This is especially likely to be so in regions dominated by residential housing. It may be less valid however in the central business district of some cities, where a few particularly tall buildings may have a disproportionate effect and can't be regarded as part of a reasonably homogeneous neighbourhood. To quantify the extent to which the concept of a neighbourhood is valid would require computation of building statistics over different averaging scales to look for a range of insensitivity to averaging scales.

Most of the theoretical approaches for describing the neighbourhood average wind profile $u(z)$ are based on methods previously developed for plant canopies (see Finnigan (2000) for a review of the plant canopy work). In particular models have been developed by Macdonald (2000) and Coceal and Belcher (2004, 2005) based on a mixing length model of the turbulent stress within the canopy and a drag force distributed in the vertical over the height of the canopy. When the flow within the canopy is in equilibrium, we can equate the stress divergence to the drag force. This leads to $u(z)$ being the solution of

$$\frac{d}{dz} \left(l_c \frac{du}{dz} \right)^2 = \frac{u^2}{L_c}.$$

Here l_c is the mixing length and L_c is the canopy drag length scale. When l_c and L_c are constant with height this leads to an exponential form for the wind within the canopy given by

$$u(z) = u(h) \exp\left(-a \frac{h-z}{h}\right)$$

where $a^3 = h^3 / 2l_c^2 L_c$. This exponential decay of wind speed with height is a commonly used profile within plant canopies where a is generally much greater than 1 and so the flow becomes very small at the ground. However, as pointed out by Coceal and Belcher (2004), a is not generally so large for urban building canopies. This means that the profile can represent the initial decay of wind with height realistically but is not accurate near the ground; it predicts a non-zero wind at ground level whereas in reality we expect the wind speed to approach zero at the ground. We note that Macdonald (2000) also gave the empirical estimate $a = 9.6\lambda_f$ for the coefficient of the exponential decay, based on evidence from arrays of cubes in wind tunnel experiments. This is based on experimental wind tunnel data for aligned and staggered cube arrays with λ_f covering the range 0.05 to 0.33.

Various forms for l_c and L_c have been proposed. Macdonald (2000) gives $l_c = 0.18(h-d)$ within the canopy as a fit to wind tunnel measurements of flow through arrays of identical cubic buildings. Above the canopy l_c is linearly interpolated between the canopy value and the inertial sublayer value $\kappa(z_w - d)$ at height z_w , where κ is the von Karman constant and z_w is chosen so that the flow matches smoothly to the usual log profile (with displacement height d) above z_w . Coceal and Belcher (2004) choose l_c within the canopy to be given by

$$\frac{1}{l_c} = \frac{1}{\kappa z} + \frac{1}{l_{c0}}$$

where l_{c0} is chosen so that l_c matches to the expression $\kappa(z-d)$ which is used above the canopy. For L_c , Macdonald uses

$$L_c = \frac{2h}{c_d(z)} \frac{1}{\lambda_f}$$

where $c_d(z)$ is the 'sectional drag coefficient' of the buildings. This is defined so that the drag force on a building over a layer of thickness dz is $0.5c_d(z)\rho u(z)^2 dA_F$ where dA_F is the frontal area of the building over the height range dz . Coceal and Belcher (2004) add an extra factor of $1 - \lambda_p$ to account for the fact that the volume of air that the drag acts on does not include the building volume. Both studies make the approximation that $c_d(z)$ is independent of height and Coceal and Belcher estimate $c_d(z)$ as 2, using data from Cheng and Castro (2002). The drag term is of course zero above the canopy (i.e. $L_c = \infty$ there). Note these models can be easily adapted to take some account of building height variability by making λ_f a function of height (see e.g. Solazzo et al, 2007b).

With both these parametrizations of l_c and L_c , the wind speed profile shows satisfactory agreement with the results of the wind tunnel studies of Hall et al (1998) and Macdonald et al (1998b) for arrays of cubic buildings. However we would caution that the experiments did not measure $u(z)$ at enough points to obtain a truly accurate horizontal average. Also the direct numerical simulations of Coceal *et al.* (2006) show a mixing length profile within the canopy which is rather different to the above parametrizations. Coceal *et al.* found a sharp local

minimum in l_c at the canopy top and a local maximum at about half the height of the canopy. All these mixing length models show a maximum in the wind shear du/dz at the top of the canopy which is caused by the sharp change in the drag term. This means that small changes in the location/extent of the shear layer or in the height of interest could lead to significant changes in wind speed and suggests that one should not expect high accuracy in wind speed prediction around the canopy top. This is a significant issue from the perspective of predicting the wind energy resource from small wind turbines mounted close to roof level.

An advantage of Macdonald's approach is that the profile can be calculated analytically. However the profile within the canopy is exponential which, as noted above, is not appropriate near the ground and the method requires estimates of d and z_0 which ideally would be outputs from the canopy flow model. The Coceal and Belcher approach requires numerical solution, but allows a no-slip condition to be imposed at the ground (at $z = z_0$ where z_0 here is the roughness length of the ground, not including building effects) and also allows the roughness length of the surface (including building effects) to be calculated. The displacement height d needs to be specified however. Note that, in the Coceal and Belcher approach, the inertial sublayer log profile (with displacement height d) holds (for the horizontally averaged flow) right down to the top of the buildings. This is despite the fact that the log profile is only theoretically well founded well above the buildings. This extended validity of the log law is supported by wind tunnel measurements conducted by Cheng and Castro (2002). These measurements involved both canopies of identical cubes and also canopies made from obstacles based on cubes but with their heights randomly perturbed following a Gaussian distribution with standard deviation equal to 30% of the mean height. The extended validity of the log law is also supported by the direct numerical simulations of flow over arrays of cubic obstacles by Coceal *et al.* (2006) and by the field measurements of Rooney (2001) conducted in Birmingham.

Bentham and Britter (2003) proposed a simpler approach to estimate a velocity scale U_c which is representative of winds within the canopy. They assume that the total drag of the surface on the atmosphere is known and that the total drag is dominated by the building drag, with the surface friction of the ground between the buildings being negligible. The total drag per unit area ρu_*^2 is simply equated to the total building drag per unit area estimated as $0.5C_d\rho U_c^2\lambda_f$. Here C_d is the bulk drag coefficient of the buildings which Bentham and Britter take to be 1. Note however that, with the assumption of a single velocity scale U_c , the distinction between bulk and sectional drag coefficients is not treatable within this approach. This yields $U_c = u_*\sqrt{2/\lambda_f}$. This formula is shown to give good agreement with a range of wind tunnel and water channel experiments, with U_c interpreted as the mean in-canopy velocity. Bentham and Britter also consider Lettau's (1969) simple estimate for z_0 given by $z_0 = 0.5\lambda_f h$. They interpret the 0.5 as a drag coefficient (see discussion in Lettau (1969) and Macdonald *et al.* (1998)), replace it with 1 and then substitute in their expression for U_c to obtain $U_c = u_*\sqrt{2h/z_0}$. This performs better than $U_c = u_*\sqrt{2/\lambda_f}$ for small λ_f cases, presumably because z_0 contains information on aspects of the building drag which can't be represented through λ_f as well as information on the surface friction which may be significant for small λ_f . However it does not work well for large λ_f . Here the relation $z_0 = 0.5\lambda_f h$ breaks down because of the onset of the 'skimming' flow regime (see discussion in section 4.1) with z_0 decreasing while λ_f increases. Bentham and

Britter recommend the z_0 formula for $\lambda_f < 0.2$ and the λ_f formula for larger values. Note most urban areas have $\lambda_f > 0.2$.

The physics used by Bentham and Britter (2003) applies to the models of Macdonald (2000) and Coceal and Belcher (2004, 2005), at least when one can neglect the surface friction and, in the case of Coceal and Belcher, the volume factor $1 - \lambda_p$. Hence these models will give results consistent with $U_c = u_* \sqrt{2/\lambda_f}$, subject to issues connected with the interpretation of the velocity scale U_c and the definitions and values of drag coefficients. Note that the condition of negligible surface friction does have significance for the Macdonald approach because, although surface friction is not explicitly included, there is some implicit treatment of it because $l_c du/dz$ does not tend to zero at the ground.

The above equilibrium profile results should be a valid approximation when the urban building statistics are changing slowly compared to the distance required for the wind to adjust to the building statistics. As discussed in section 4.2.2 above, the results of Coceal and Belcher (2004, 2005) show that in general the wind should adjust within a few building lengths, so the use of equilibrium profiles is appropriate. Exceptions are where the canopy is rather sparse or where the change in the character of the canopy is very abrupt. The nature of the adjustment at sharp transitions has been investigated by Coceal and Belcher (2004, 2005) by using the drag and turbulent stress parametrizations within a full non-linear (but 2-D) flow model. The results show good agreement with the experiments on the adjustment in field trials with cubic obstacles (Davidson et al, 1995, 1996) and also show the possibility of over- and under-shoots in the near surface wind in the transition region (including reversed flow). Asymptotic methods for obtaining approximate solutions to these equations are given by Belcher et al (2003).

Most of the experimental data underpinning the above theory is based on wind tunnel experiments of flow through arrays of cubes. The extent to which the results are the same for arrays of buildings with pitched roofs, typical of residential housing, is therefore of considerable interest. Heath et al (2007) conducted numerical simulations of flow through a staggered array of pitched roof buildings. The buildings had a 10m by 10m plan area with a height of 5m to the start of the roof and 10m to the roof peak. The frontal and plan area densities of the array were $\lambda_f = \lambda_p = 0.22$, the frontal area density being here evaluated for the case of a wind which is aligned with the orientation of the buildings. The computational fluid dynamics model ANSYS CFX 10 (see section 5.4) was used with a $k-\epsilon$ turbulence model. Heath et al reported detailed information on the flow around the building which will be considered in section 5.1.3 below. However here we are interested in the 'neighbourhood average' flow. They used an inflow profile constructed from a log profile above the canopy with $z_0 = 0.8\text{m}$ and $d = 4.3\text{m}$ (based on Macdonald's (1998) formulae – see section 4.1 above – with $A = 4.4$, $\beta = 0.55$ and $C_D = 1.2$), and an exponentially decaying profile within the canopy with decay constant $a = 2.1$ (based on Macdonald's (2000) estimate $a = 9.6\lambda_f$). They followed the flow through four rows of buildings and found that the flow below about twice the building height was slowed relative to that above. This suggests that the assumed inflow profile was not an appropriate equilibrium profile for the building array and that the correct profile should have a slower flow below $2h$ relative to that above. If we assume that equilibrium has been reached by the fourth row, the equilibrium wind speed at building height is about 70% of that in the inflow profile. We note however that $\beta = 1$ gives a better fit to Macdonald's data for staggered arrays and that using this value would increase z_0 and hence decrease the lower level winds. Hence we cannot without further evidence conclude that the effect of pitched roof buildings is different from cubes. In fact

intuitively one might expect the effective height (or “equivalent cube height”) for a pitched roof building to be less than the peak height, which would lead to smaller z_0 and faster flow at lower levels. However we note that the reduced flow is consistent with the wind tunnel results of Pavageau *et al.* (1997) and Rafailidis (1997) on the effect of pitched roofs on the flow above street canyons. This is discussed further in section 5.1.2 below.

Above we have been concerned with the wind profile averaged over the neighbourhood scale. It is appropriate to comment briefly on the variability within a neighbourhood. Within the canopy itself we expect great variability, including instances of reversed flow in street canyons and in the wake of buildings (see sections 5.1.2 and 5.1.3). However above the building roofs the variability is not as great. Cheng and Castro (2002) measured the “dispersive stresses” (i.e. the spatial variances and covariances of the time averaged velocity components) at heights above the buildings in wind tunnel experiments. The spatial standard deviation of the along-wind component (which should be a good estimate of the wind speed standard deviation) was small compared to the mean wind (less than one tenth of the mean wind) down to the lowest height measured. This was about $1.2h$ for the cubic obstacles and $2h$ for the random height obstacles (where h here is the mean obstacle height).

5.1.2 Street Canyons

The street canyon – two rows of buildings on either side of a street – is a common feature of urban areas. In its idealised form, it consists of two parallel identical buildings which are infinitely long and of square cross section. Real street canyons are of course more complex with gaps between adjacent buildings and various shapes and sizes of building. When the canyon aspect ratio is not too different from 1 and the wind is across the street this leads to a recirculating flow within the street as shown in Figure 12. When the wind is at an angle to the street, an along-street component is added to the recirculating flow to produce a helical motion along the street. This pattern is seen, for example, in the field experiment of Nakamura and Oke (1988). For this experiment the street cross section was very close to being square. Nakamura and Oke discuss the magnitude of the in-street wind from a range of field experiments. They conclude that, if the roof-top and street measurements are at heights of about $1.2H_B$ and $0.06H_B$ respectively, where H_B is the building height, then the street wind speed is about $2/3$ of the roof-top speed.

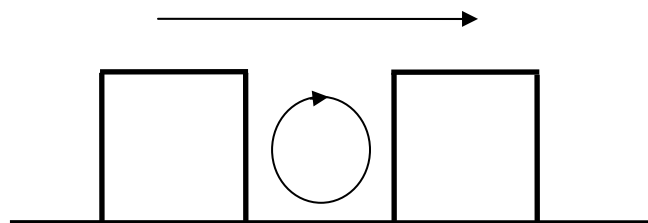


Figure 12: Illustration of flow in a street canyon

Sini *et al* (1996) use a numerical $k-\epsilon$ model (see section 5.4) to simulate flow in an idealised street canyon. They systematically investigated the effect of W_S/H_B , where W_S is the street width. For $W_S/H_B > 5$ the vortex core starts to split into two with two local centres of circulation in the flow, one behind the upwind building and one ahead of the downwind building. For $W_S/H_B > 9$ these two vortices are completely separate, with the region of separated flow behind the upwind building reattaching before the downwind building is reached. At large W_S/H_B , the effects of the two buildings will cease to interact, with the flow returning to equilibrium before the second building has an effect. However this is not observed at realistic values of W_S/H_B , with the flow between the two buildings not reaching equilibrium even at $W_S/H_B = 15$. For narrow streets,

$W_s/H_B < 0.6$, the vortex doesn't reach down to the ground and a weak secondary counter-rotating vortex forms below the main vortex. This is supported by the results of Pavageau *et al.* (1997). For $W_s/H_B = 0.33$, two such vortices are observed above one another. However, here the flow near the ground is so weak that, in real situations, imperfections in the geometry, thermal influences and traffic induced turbulence are likely to alter the flow, making this idealised multi-vortex structure of academic interest only.

The effect of changes in geometry that go beyond simple changes in aspect ratio is explored in wind tunnel experiments with cross-wind orientated street canyons by Pavageau *et al.* (1997) and Rafailidis (1997). Pavageau *et al.* varied the heights of the buildings on either side of the canyon, both with respect to each other and with respect to a sequence of canyons upwind and downwind of the canyon selected for detailed study. They also investigated the effect of adding pitched roofs on the upwind and/or downwind sides of the canyon in question. Rafailidis considered a long sequence of canyons and compared the case where they all had pitched roofs with the flat roof case. The focus of these studies is mainly on pollution dispersion and flow measurements are only available above the canopy. Close to the canopy top, the pitched roof results show a significant slowing of the wind and an increase in turbulence intensity (turbulent velocity standard deviation divided by the mean velocity) relative to the flat roof case. When the velocity is compared at the same height (and with the same velocity at heights high above the canyons) the reduction is substantial. However the pitched roofs are added to the top of the flat roof buildings and so the greater total height of the pitched roof buildings may explain some of the effect. Rafailidis (1997) estimates an increase in z_0 of 4.5 and 12.5 times for canyon aspect ratios W_s/H_B of 1 and $\frac{1}{2}$ respectively. This is of course much larger than the increase in peak building height and is also larger than the increase implied by the formula of Macdonald *et al.* (1998) (see section 4.1, equation (3)). The displacement height d also increases, although by a smaller factor which is comparable to the increase in peak building height. However the interpretation of the z_0 and d values is complicated by the fact that it is not completely clear how they are calculated and by the large vertical gradients in the stress measured above the canopy. These gradients suggest that either the stress is not adjusted to the canopy over a reasonably deep layer or that the values measured are not representative of the horizontally averaged stress or that a significant momentum flux is carried by the 'dispersive' stress (i.e. the vertical momentum flux due to horizontal fluctuations in the time averaged flow).

For an example of a real street canyon with irregular building heights, side streets etc, which has been extensively studied using field, wind tunnel and computational fluid dynamics approaches, see Ketzel *et al.* (2005) and Schatzmann *et al.* (2005). This shows that real street canyons often depart significantly from the idealised two-dimensional flow patterns described above.

In reality we expect the flow to be complicated by thermal effects (e.g. one canyon wall may be in sunshine and the other in shade) and by traffic generated turbulence, although these effects are unlikely to play a dominant role except in light wind conditions. Thermal effects involving differing temperatures for the various canyon surfaces have been investigated by, for example, Sini *et al.* (1996), Louka *et al.* (2002) and Xie *et al.* (2006), while the effect of stable stratification in the flow as a whole has been considered by Rafailidis (2001). Traffic effects have been explored by, for example, Vachon *et al.* (2002) and Solazzo *et al.* (2007). However the main interest of these studies is the dispersion of pollution. Given the lack of interest in light winds for wind energy purposes, these effects will not be considered further here.

5.1.3 Individual buildings and other obstacles

Flow around a single isolated building has been extensively studied. The general characteristics of such flow are described by Hunt *et al.* (1978), Meroney (1982) and Hosker (1984). The most

important features of the flow are illustrated in a somewhat simplified way in Figure 13 for the idealised case of a cuboid building. The most obvious feature is the recirculation region in the wake of the building. The flow separates off the leading edge of the roof and sides to form a recirculation region. If the building is long enough (in the along wind direction) the flow may reattach with the flow separating again from the rear edge. The turbulence in the recirculation region is large with the recirculation region itself fluctuating in size and position. Figure 13 is a somewhat simplified picture of the recirculation region. It is most appropriate for wide two-dimensional obstacles. However for three-dimensional cases there is no reason why the streamline leaving the separation point has to be the same as that reaching the reattachment point. As a result it is possible for material to enter and leave the recirculation region by advection with the mean flow (Hunt et al, 1978). A complicated diagram consistent with this can be found in Hunt et al (1978) and Hosker (1984).

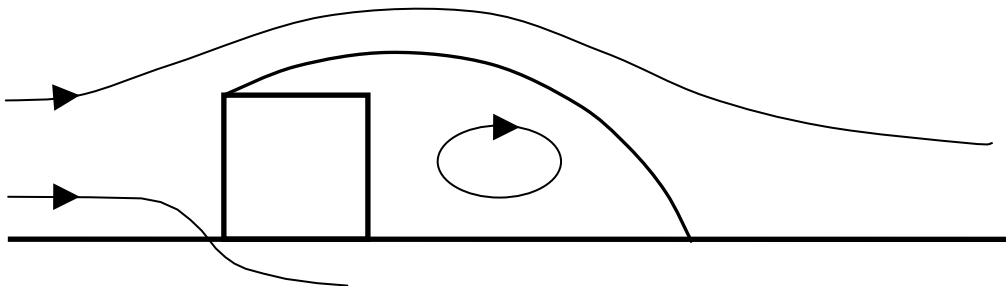


Figure 13: Illustration of the main features of flow around a cubic building

Beyond the recirculation region is a longer wake region where the flow velocity gradually recovers to its upwind value, accompanied by downwash. Turbulence is generally greater than in the upwind flow but gradually returns to its upwind value. Above the recirculation region and wake the flow velocity can be mildly enhanced. For cuboid buildings aligned at 45° to the wind, a pair of vortices forms as the flow separates off the leading edge of the roof. These vortices increase the downwash behind the building and tend to reduce the velocity deficit in the main wake or even cause a velocity excess. If the recirculation region on the roof reattaches, then there is a similar wake region on the roof behind the roof top recirculation region.

In the front of the obstacle there is generally another recirculation region, although this is much smaller than that behind the obstacle (it is not shown in the figure). This is a consequence of the shear in the upwind flow combined with the increased pressure in front of the building, with the effect of the adverse pressure gradient on the slow moving air near the ground causing the flow to separate. This recirculation forms part of a so-called horseshoe vortex which wraps around the front of the building and trails off down the sides.

The dimensions of the various regions have been observed in a wide range of experiments, mainly in wind tunnels. The results show significant variation between different studies, especially for realistic non-cuboid buildings. Meroney (1982) gives the size of the recirculation region behind the building as being $1.5H_B$ high and $2.5H_B$ to $3H_B$ long for the case of a cubical building of height H_B aligned with the flow. Wider buildings obstruct the flow more and tend to have deeper and longer recirculation regions, the length being up to $12H_B$. Hosker (1984) provides expressions to fit experimental data on the recirculation region. Suppose the along wind length of the building is L_B , the cross wind width is W_B , and the height is H_B . Then the length of the main recirculation region (measured from the rear of the building) is

$$\frac{AW_B}{1 + BW_B / H_B}$$

Here $A = 3.7(H_B / L_B)^{1/3} - 2$ and $B = 0.305(H_B / L_B)^{1/3} - 0.15$ for short buildings with $L_B < 2H_B$ where we do not expect the roof top separation region to reattach on the roof, and $A = 1.75$ and $B = 0.25$ for long buildings with $L_B > 2H_B$ where we do expect roof top reattachment. The maximum width of the region is

$$1.1W_B + 1.7W_B \exp(-0.55W_B / H_B)$$

(the data supporting this are all from short buildings with $L_B < H_B$) while the maximum height is

$$H_B + 1.6H_B \exp(-1.3L_B / H_B).$$

The data used come from experiments with low levels of shear in the approach flow and Hosker cautions that they may not be as applicable to more realistic flows. However comparisons for the length of the recirculation region show good agreement with other experiments with more realistic boundary layer wind profiles.

Wilson (1979) examined the roof top recirculation for flat roofed buildings using experiments conducted in a water channel. He found the maximum height of the recirculation occurred when the upwind face of the building was perpendicular to the wind. For this case, the maximum height of the recirculation region was $0.22R$ above the roof at a distance of $R/2$ from the leading edge, where $R^3 = W_B H_B \min(W_B, H_B)$. Reattachment occurred at $0.9R$ from the leading edge. Beyond the maximum height there was a roof top wake region with height given approximately by $0.22R(2x/R)^{1/3}$, x being distance from the leading edge.

For the main wake region, the main theoretical understanding comes from various modifications of the theory of Counihan et al (1974) for the wake behind a wide two-dimensional obstacle. A modification for three-dimensional buildings is used in ADMS to predict the decay of the velocity deficit with downwind distance. This is described further in section 6.6. When vorticity shed from the roof is important the wake becomes very complicated, with the downwash induced by the vortices reducing the velocity deficit or even causing a velocity excess at certain heights (see discussion in Hosker (1984)). The wake perturbations then die out rather more slowly than they otherwise would. Meroney (1982) gives an estimate of the length of the region with significant wake effects as between $5H_B$ and $30H_B$, although strong roof top induced vortices can persist to $80H_B$.

We will comment briefly on the effect on the flow of isolated obstacles other than buildings. Isolated trees or groups of trees and hedges are likely to have effects on the flow which are similar to but somewhat smaller than buildings of the same size. They are porous to the wind and so should not produce such significant vertical motions or levels of turbulence as buildings. It seems possible that the reduced downwash on the downstream side of the obstacle means that the wind speed takes a greater distance to recover to its unperturbed value. This is most likely to be the case in comparison with buildings which generate roof top vortices which enhance the downwash. The evidence from the literature on windbreaks (e.g. Gandemer (1979), Perera (1981) and Wilson (1985, 1987)) is inconclusive as to whether solid or porous obstacles have the greatest effect on the mean flow at large distances downwind, although of course solid fence-like wind breaks are not like typical buildings and will not produce roof top vortices. (There is a consensus that the most effective wind breaks have some level of porosity, but this is more because of a reduction in turbulence levels than a reduction in mean wind velocity.)

5.1.4 Flow at Particular Locations within Collections of Buildings

Above we have considered the general flow through the roughness sublayer (the “neighbourhood averaged” flow) and flow for particular canonical arrangements of buildings – a

street canyon and an individual isolated building. The understanding of the detailed flow at particular locations within a complex array of buildings is less well developed. When the buildings are far apart, the results for isolated buildings can be applied. However, as the building separation reduces there is a transition first to a wake-interference regime where the approach flow to each building is significantly perturbed by the upwind buildings, and then to a skimming flow regime where the majority of the flow “skims” over the tops of the buildings with a much reduced flow within the canopy (see discussion in section 4.1).

To some extent each situation is different and needs to be addressed separately, e.g. through numerical simulations, wind tunnel experiments or full scale measurements. In this regard we note that the DAPPLE project has investigated a particular location within London in detail – this is discussed in section 5.2.2 below. However the detailed study of the flow through regular arrays of buildings can shed some light on winds at particular locations. Of course real urban or suburban areas are not regular and we would expect the irregularities to be more important in studying wind at particular locations than in studying the neighbourhood average flow. None-the-less it seems likely that the flow through regular arrays can be used to give guidance for real situations.

The work by Heath et al (2007) is an example of a study which includes information on the flow at particular locations within an array of identical buildings. The buildings are pitched roof buildings which are typical of a suburban residential area. The results were obtained from CFD calculations and were aimed specifically at assessing the potential for small scale wind energy generation. We have already discussed this work in sections 4.2.3 and 5.1.1 above in connection with the effect of roughness changes and the neighbourhood averaged flow through the roughness sublayer, and we refer the reader to section 5.1.1 for further details of the upwind flow, the building layout, and the larger scale aspects of the flow. The shape and dimensions of the buildings are indicated in Figure 14.

The flow over each house is very different from that over an isolated house (Heath et al also simulate flow over an isolated building with the same shape for comparison), with the flow skimming over the roof peak with much less speed up than for an isolated building and with far less happening below roof level. This is primarily because the wind below roof height is already slowed down by the upwind buildings. Vertical profiles of wind speed were obtained at four potential wind turbine mounting points (see Figure 14) for a variety of wind directions. The mounting points (other than the “centre” location) were located 0.5 m away from walls to allow for mounting brackets etc and also to allow wind speed results to be obtained below roof height (although of course here any turbine would actually have to be mounted further away and the wind speed might be expected to vary with distance from the wall). The results show strong shear at all mounting points around roof height as expected. Also all mounting locations show significant variations in wind speed with wind direction (for the same upwind wind speed profile).

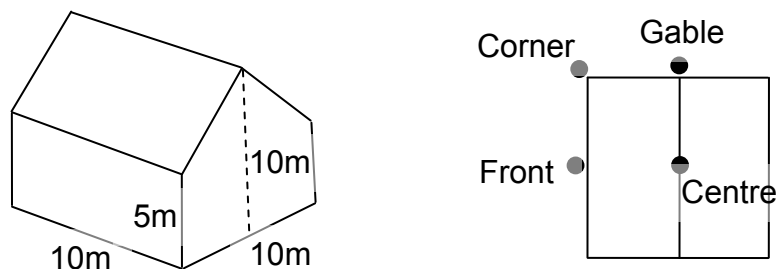


Figure 14: Shape and dimensions of buildings and locations of possible wind turbine mounting points (perspective and plan views) in the study by Heath et al (2007)

The wind speeds are compared with the upwind speed at 10 m. Preferred mounting locations were obtained for various wind directions and for mounting (a) at 8 m, (b) at 10 m, (c) at 13 m, (d) on a mast no longer than 3 m, and (e) below 9 m with a mast no longer than 3 m. These last two conditions are intended to represent various possible planning permission restrictions. Only rarely was the centre location preferred over other locations, and then only for certain wind directions for height condition (d). The preferred locations and the mean wind speeds at these locations for a uniform distribution of wind directions and for the various mounting heights are given in Table 5.

Table 5: Preferred locations for different turbine mounting heights (from Heath et al, 2007)

Height	Preferred location	Mean wind speed / Upwind speed at 10 m
(a) 8 m	Corner	0.5
(b) 10 m	Corner	0.6
(c) 13 m	Front	1.0
(d) Mast < 3 m	Gable or centre	0.9
(e) < 9 m & mast < 3 m	Corner	0.5

Interpretation of the mean wind speed is not completely straightforward because it is expressed relative to the upwind speed at 10 m and the upwind profile does not match the equilibrium flow within the array (see 5.1.1). It is likely that the wind speed ratios would be larger if the equilibrium upwind profile was used. However the relative performance of different height turbines is more straightforward. Table 5 shows a factor of 1.7 between the speed at the best location at 13m and that at the best location at 10m, which, assuming maximum efficiency of energy extraction, translates into a factor of 4 to 5 difference in power.

5.1.5 Research in COST 715

5.1.5.1 Overview of COST 715

COST or Co-operation in Science and Technology, is a European activity which supports scientific exchange and networking. COST 715 was entitled 'Meteorology Applied to Air Pollution Problems'. It brought together scientists and meteorologists from 20 countries. It addressed the latest scientific approaches to describing the urban boundary layer, which has a complex structure involving wide variations in time and space. Whilst COST 715 addressed the urban boundary layer from an air pollution perspective, the work is equally relevant for wind power, especially the studies of the urban wind flow by COST 715 Working Group 1, or WG1. The Final Report from COST 715, by Fisher et al. (2005), includes several chapters that are directly relevant to the wind speed over an urban area.

5.1.5.2 COST 715 Working Group 1 – Reviewing the Urban Flow Field

Working Group 1 was chaired by Matthias Rotach. In the COST 715 final report (Fisher et al, 2005), Chapter 2 considered the structure of the urban boundary layer. A convenient conceptual model is the urban roughness sublayer, a layer near the city where the flow is directly influenced by the buildings and other structures, and is therefore essentially three-dimensional. The urban canopy layer, by analogy with forests and plant canopies, is conceptually the lower part of the

urban roughness sublayer, and extends from the ground up to approximately the heights of buildings. However cities are not uniform in space and therefore Chapter 2 of Fisher et al. (2005) suggests that several internal boundary layers may form over a city, each associated with some noticeable change in the underlying geometry of the city. If wind power devices are to be placed within the urban roughness sublayer, then we suggest that the flow properties of this sublayer will have to be taken into account. This means the height of the urban roughness sublayer z^* , which is linked to the average height of buildings and other roughness elements, is of prime consideration for urban wind power design calculations. Fisher et al. (2005) quote Raupach (1991) as giving $z^* = az_H$ with a between 2 and 5 for plant canopies, or Rotach (2001) and Kastner-Klein and Rotach (2004) as giving $z^* = az_H$ with a about 2 or slightly less for cities. In other words, for wind power devices placed upon buildings, we conclude that it seems fairly likely that they will be within the urban roughness sublayer, unless placed well above twice mean building height z_H .

In which sublayer the wind power device sits is important, in that it indicates what assumptions or formulae might be used to model the wind speed and the turbulence where the device is placed. The definitions of the various layers should therefore be carefully distinguished. In Chapter 2 of Fisher et al. (2005), Rotach defines the following terms: urban canopy layer which forms the bottom of the urban roughness sublayer; and above these is the inertial sublayer, which in idealised conditions will correspond to the true matching layer over ideal surfaces and wherein Monin-Obukhov similarity theory may apply. In practise Rotach (ibid) suggests that the inertial sublayer over a city may be 'squeezed' between other layers and consequently shallow compared to the urban roughness sublayer. In such a flow regime, Rotach (ibid) cautions against the somewhat confusing use of the terms 'surface layer' and 'surface layer scaling'. In urban areas the urban roughness sublayer is so important that it is preferred by Rotach (and hence COST 715 as a whole) to refrain from using these terms invoking surface layer, and to use the terms 'inertial sublayer' and 'urban roughness sublayer' instead.

5.1.5.3 Modifying the Conceptual Approach for the Urban Roughness Sublayer

Modifications to the wind and to the turbulence associated with the urban area are discussed in COST 715 Final Report, Chapter 3. From these arise some valuable lessons with relevance for assessing the potential wind power over urban areas. In Chapter 3 of Fisher et al. (2005), Rotach and Working Group 1 state that the roughness sublayer "is key to understanding the flow structure over an urban surface". When modelling at the mesoscale, when individual roughness elements cannot be resolved, bulk surface properties determine exchange processes. Presence of the urban roughness sublayer means that these exchanges differ from those over a reasonably smooth surface. In high resolution mesoscale models, when down to 1 km scales or less, the lower level or levels may be within the urban roughness sublayer. Such models may still adopt some kind of similarity scaling, but is this still appropriate for the urban roughness sublayer?

Within the urban roughness sublayer, COST 715 WG1 concluded that "turbulent fluxes are not constant with height", following Kastner-Klein (2002), Rotach (2001) and Kastner-Klein and Rotach (2004). Urban parameterisations exist which use the height of the maximum Reynolds stress and a zero plane displacement height as length scales, and with the magnitude of the maximum Reynolds stress as the basis for a velocity scale. It follows that Rotach and WG1 concluded that the usual similarity based inertial sublayer scaling cannot be used within the urban roughness sublayer. They also suggested that local scaling applies within the upper parts of the urban roughness sublayer – and cite Roth (2000) for supporting review and data sets.

Wind tunnel data were presented to COST 715 WG1 by Kastner-Klein, as published in Kastner-Klein and Rotach (2004) and shown as Figure 3.1 in Fisher et al. (2005). This figure is important for understanding the significance of the urban roughness sublayer, and is reproduced below (Figure 15). It shows that the turbulence increases with height quite steeply to a maximum, and then decreases at heights above this. The height of the maximum Reynolds stress is an important quantity – being generally 1.5 to 5 times average building height, but also depending upon the variability of building heights about their mean. If the variability in heights is large, then the maximum Reynolds stress in Figure 15 is shifted to a higher value, nearer 5 times mean building height. The magnitude of the maximum value of the Reynolds stress is representative of the total drag on the wind by the city, according to Fisher et al. (2005). It determines in effect the overall frictional drag on the flow – and can be used to define a friction velocity for use above the urban roughness sublayer, i.e. in the inertial sublayer above the height of maximum Reynolds stress. To parameterise and hence use these data in Figure 15 an algebraic or other description of the profile below the maximum (i.e. within the roughness sublayer) is also required (see Kastner-Klein and Rotach, 2004). The local Reynolds stress τ at any height of interest within the roughness sublayer can be used (once known) to derive a local friction velocity $u_* = \sqrt{|\tau/\rho|}$.

Finally WG1 reported in Fisher et al. (2005) that in the lower region below the zero plane displacement height the Reynolds stress becomes very small and local scaling is not useful.

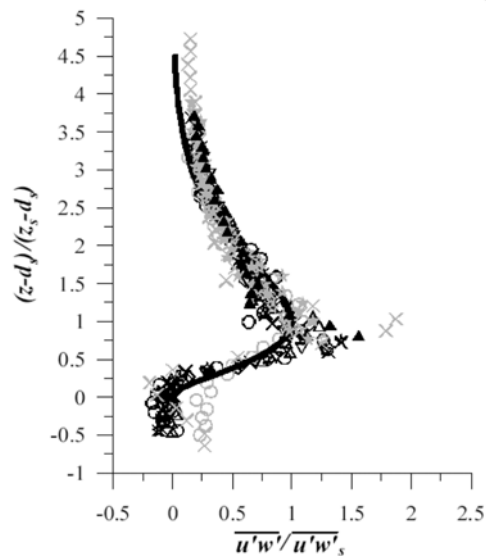


Figure 15: Profiles of suitably scaled momentum flux at 11 different urban sites from a wind tunnel study using a model of the city of Nantes (Kastner-Klein and Rotach, 2004). The diagram plots the non-dimensional height vertically and non-dimensional Reynolds stress horizontally.

d_s is displacement height and z_s and $u'w'_s$ are the height and magnitude of the peak of a curve $a(z - d_s)^2 \exp(-b(z - d_s))$ fitted to each stress profile. (Acknowledgement: Figure 3.1 from COST 715 Final Report by Fisher et al. (2005).)

In conclusion, we see that WG1 of COST 715 found that it is important to recognise the large vertical extent of the urban roughness sublayer, the fact that in this layer Monin-Obukhov similarity theory is not appropriate, and to recognise that the Reynolds stress varies with height.

WG1 argue that local scaling (using the local value of u_* at the height of interest) may be a useful replacement for Monin-Obukhov similarity theory within the upper parts of the roughness sublayer, although there is no strong theoretical reason why local scaling should hold. Wind tunnel data rather than urban field experiments currently provide the most reproducible insights into the vertical stress profile, and highlight the presence of a point of maximum Reynolds stress. WG1 also concluded that if a mesoscale model is used to calculate the wind over a city, but the model does not explicitly take into account the urban roughness sublayer (i.e. does not parametrise or model the change in stress with height through this sublayer) then the lowest model level should be at a height greater than z^* , the height of this sublayer. Finally, in this Chapter 3, WG1 also report that wind speed varies most rapidly with height just above roof level, and this we note might be a likely height where smaller wind power devices might be placed in urban areas.

5.1.5.4 'Recipe' for Obtaining an Urban Wind Speed in the Urban Roughness Sublayer

Rotach, Christen and WG1 in Chapter 8 of the COST 715 Final Report by Fisher et al. (2005) produce their method or "recipe" for obtaining the wind speed profile in the urban roughness sublayer. This was intended primarily for dispersion modellers. However the work should be of value to the wind power community as well. The method or "recipe" is now summarised.

Step 1: Estimate basic quantities.

1. Estimate average building or roughness element height, z_H , from geometry of city buildings.
2. Estimate height of urban roughness sublayer, z^* , from $z^* = az_H$ with a about 2.
3. Estimate height of zero plane displacement, d , possibly from independent measurements (wind profile), or more likely in practice from morphometric parameters λ_p & λ_F after Grimmond and Oke (1999), or by using $d = 0.7z_H$ as a first estimate.
4. Estimate value of friction velocity to use in the inertial sublayer, and at the top of the urban roughness sublayer, u_{*IS} . This can be done using e.g. a direct measurement, by using a measurement in the roughness sublayer and using the profile described in step 2 below, or by adapting a rural measurement of friction velocity.

Step 2: Estimate the profile of local friction velocity, u_{*l} .

Above z^* (although not too far above) we have $u_{*l} = u_{*IS}$. Below z^* we allow for variation of friction velocity with height within the urban roughness sublayer as follows. Using non-dimensional height $Z = \frac{(z-d)}{(z^*-d)}$, the height dependence is approximated by

$\left(\frac{u_{*l}}{u_{*IS}}\right)^b = \sin\left(\frac{\pi}{2}Z^a\right)$ when $0 \leq Z \leq 1$. This is plotted below (Figure 16). The values of the parameters a and b are taken to be $a = 1.28$ and $b = 3.0$. Note the formula actually given in the reference has $\sin\left(\frac{\pi}{2}Z\right)^a$ on the right hand side. However, unlike the formula given above,

neither $\sin\left(\left(\frac{\pi}{2}Z\right)^a\right)$ nor $\left(\sin\left(\frac{\pi}{2}Z\right)\right)^a$ agrees with the curve plotted in the reference, although the latter is very close.

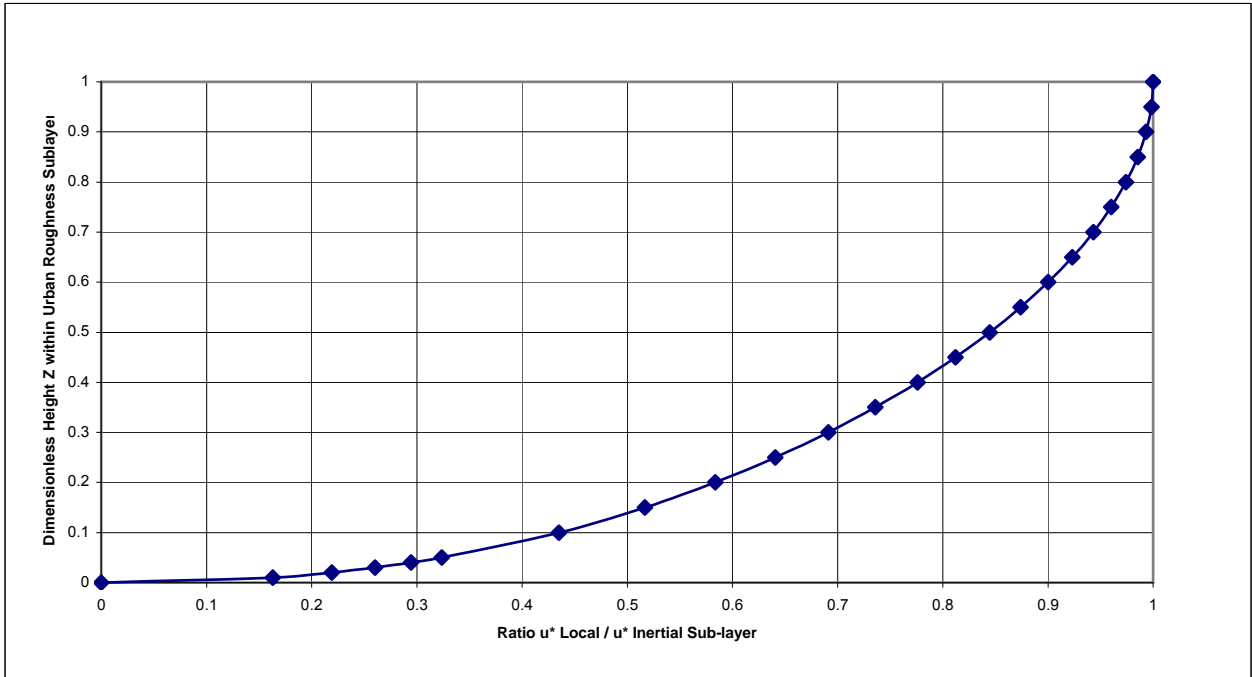


Figure 16: Graph showing the variation of friction velocity with height, within the urban roughness sublayer, using $\left(\frac{u_{*l}}{u_{*IS}}\right)^b = \sin\left(\frac{\pi}{2}Z^a\right)$ (COST 715 Final Report, Fisher *et al.*, (2005))

Step 3: Calculate the urban wind speed at the required height.

COST 715 WG1 led by Rotach concluded from his earlier work that the velocity gradient can be parametrized in terms of the local friction velocity. Stability effects are represented using a local Monin-Obukhov length L_l defined using the net sensible heat flux from the surface (i.e. a single value independent of height which can be obtained from the energy balance) and the local friction velocity. The equation

$$\frac{du}{dz} = \frac{u_{*l}}{\kappa(z-d)} \phi\left(\frac{z-d}{L_l}\right)$$

can then be integrated numerically to relate the wind at one height to another.

In Chapter 8 of COST 715 Final Report, Fisher *et al.* (2005), WG1 point out that the procedure suggested has only been incompletely validated. There is also discussion of some of the uncertainties involved in estimating the various values of parameters used in the procedure. Of these, it is the value of z^* that is thought to be most uncertain. Towards the end of Chapter 3 in Fisher *et al.* (2005) there is a summary by WG1 of some attempted validation of this scheme to estimate urban wind speeds.

5.2 Field Experiments

In this section we describe some urban field experiments on flow and dispersion conducted in the UK. We also describe the Mock Urban Setting test (MUST) experiment as an example of a field experiment involving an idealised artificial urban-like environment. For a list of a wider range of urban field experiments conducted around the world, see Karppinen and Robins (2005).

5.2.1 Birmingham and Salford Urban Meteorology Experiments

5.2.1.1 Birmingham experiments

The Birmingham urban meteorology experiments (Ellis and Middleton, 2000, 2001) were carried out by the Met Office's Met Research Unit (Cardington) over the three years 1998-2000, as detailed in Table 6. The aim of the experiments was to improve the understanding of how a city modifies the local meteorology. Specifically, the aim was to measure the wind speeds and turbulence at several heights, to measure the heat flux, and to study the atmospheric stability. These data from the experiments were obtained for the verification of dispersion models that were being developed for air quality forecasting and Local Air Quality Management. The experiments were also used to provide data for the analysis of urban meteorology more generally. Thus studies were included to look at the roughness length and to see how it varied with the urban fetch over which the wind was flowing. The amount of instrumentation deployed increased over the course of the experimental series.

The experiments took place at the Dunlop tyre factory near Junction 5 of the M6 motorway (Fort Dunlop), the instruments being deployed on a small grassed area within the factory complex (see Figure 17), British National Grid reference SP126906. In 2000, one remote rural site was also instrumented. The Dunlop tyre factory was in a belt of factory and retail complexes aligned roughly east-west along the motorway, with areas of housing to the north and south, see the OS map, Figure 18, and satellite-derived land use categories, Figure 19. (Comparing these figures shows which areas of green space have been built over between 1990 and the present day.)



Figure 17: Photographs of the Birmingham instrumentation site, taken in summer 2000. The photographs show the 15m mast from different viewpoints. Other masts are also visible on the right-hand photo.

5.2.1.2 Salford experiment

The Salford experiment (SALFEX) took place in spring 2002, and was a joint effort by several university groups, with input from the Met Office. The details of instrument deployment are again given in Table 6. The instrumentation was spread over 3 sites, with anemometry within and above a *street canyon* (Thursfield Street, BNG ref. SD816003), SODAR wind profiling and radiosonde launches at a nearby open space on the other side of the River Irwell, and LIDAR wind field measurements made from a ridge approximately 1.5km to the north.

Table 6: Dates and instrumentation of Birmingham and Salford experiments

year	dates	instrumentation	notes
1998	2 April-11 May	<ul style="list-style-type: none"> sonic anemometers at 30 and 15m thermometers at 30, 15, 1.5m and surface upward and downward facing solarimeters net radiometer 1m subsoil thermometer 	<p>Birmingham. Both anemometers operational between 8 April-30 April only.</p>
1999	15 January-16 February	<ul style="list-style-type: none"> sonic anemometers at 45, 30, 15m thermometers at 45, 30, 15, 1.5m and surface upward and downward facing solarimeters net radiometer barometer screen-level hygrometer raingauge 1m subsoil thermometer 	<p>Birmingham. Problems with 30m anemometer.</p>
2000	29 June-7 August	<ul style="list-style-type: none"> sonic anemometers at 45, 30, 15m thermometers at 45, 30, 15, 1.5m and grass and concrete surfaces hygrometers at 45, 30, 15m upward and downward facing solarimeters net radiometer barometer screen-level hygrometer raingauge infra-red surface thermometer 10cm, 50cm, 1m subsoil thermometers concrete-slab body temperature near-surface soil moisture probe remote sonic anemometer at rural site (Coleshill) 	<p>Birmingham. Problems with net radiometer.</p>
2002	22 April-9 May	<ul style="list-style-type: none"> sonic anemometers in street canyon at 2, 3, 6, 8 and 20m (Reading and Manchester universities) LIDAR measurements of wind field (Salford university) SODAR measurements of wind profile (Salford university) radiosonde wind and temperature profiles (Met Office) 	<p>Salford.</p> <ul style="list-style-type: none"> Data collected on 11 separate days. 11 days with measurements of turbulence in and above a street canyon 3 days with lidar measurements of wind field 4 days with sodar measurements of vertical wind profile 4 days with radiosonde ascents (hourly intervals)

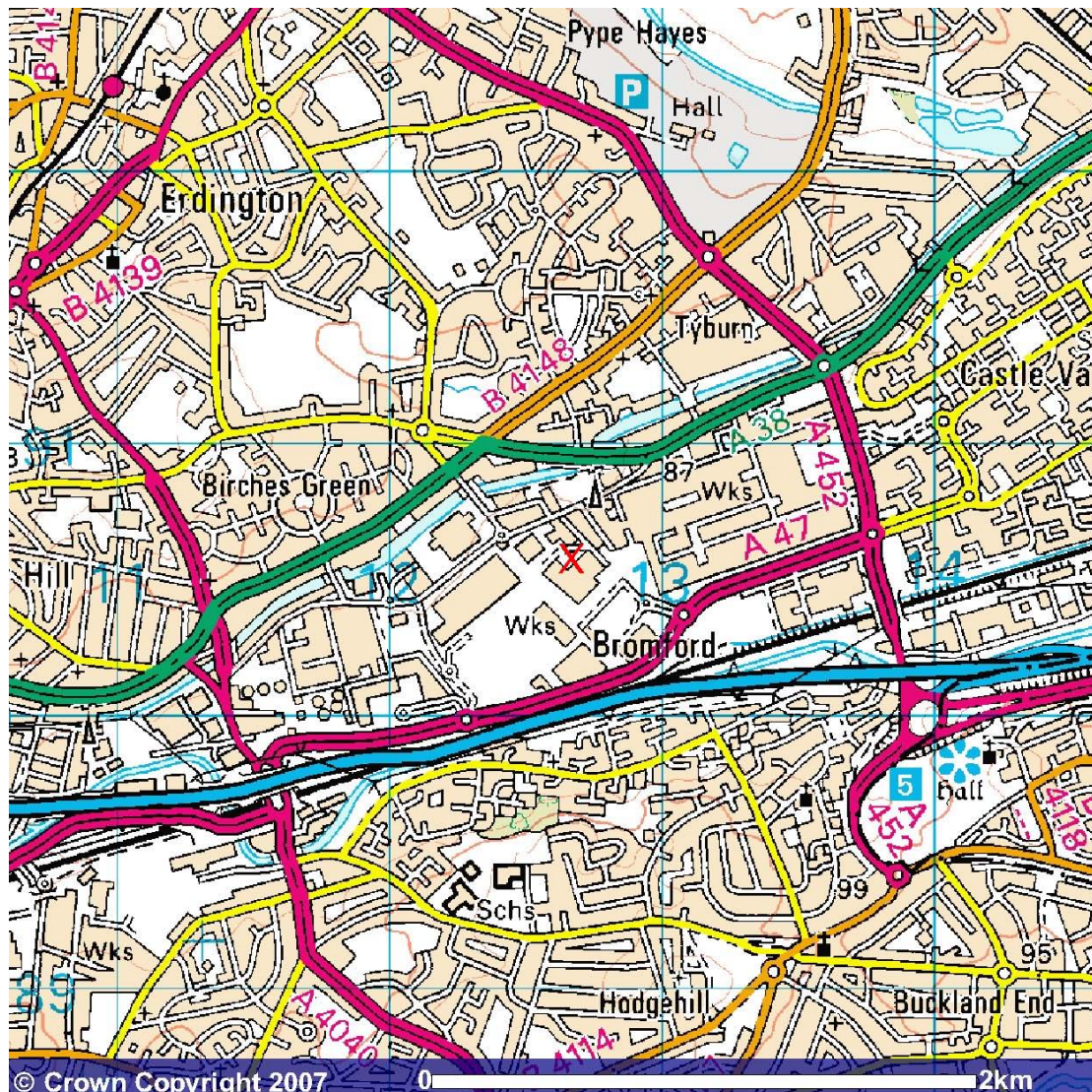


Figure 18: Recent OS map of the area around the Birmingham experimental site, which is marked with a red X.

5.2.1.3 Scientific outcomes

In terms of wind power, a very useful rule of thumb was noticed from the graphs. We plotted the urban wind speed (Dunlop Tyres Ltd factory site) versus the rural (Coleshill synoptic station) wind speed. The data from the three separate trials were thus able to be combined, showing that the 15 metre urban wind speed was slower than the 10 m rural speed, the 30 metre urban speed was approximately similar in magnitude to the 10 m rural speed, and the 45 metre urban speed was faster than the 10 m rural speed. This is of interest because it shows in a graphical way the slowing of the wind by the city. These simple but useful observations are summarised below. Also, as a rule of thumb, the observations of the urban wind profile were approximated by a simple power law with velocity proportional to height to the power $p=0.35$. Such simple rules should be regarded as illustrative in giving a feel for the effects of the city, for the height range studied here (15 – 45 m).

$$\frac{u_1}{u_2} = \left(\frac{z_1}{z_2} \right)^p$$

Ellis and Middleton (2000) found that for the Birmingham data:

- Dunlop 15 m wind speeds (D_{15}) were slower than Coleshill (C_{10}) synoptic 10 m wind speeds by approximately 20%:
 $C_{10} \sim 1.18 \times D_{15}$ (1998 data)
 $C_{10} \sim 1.24 \times D_{15}$ (1999 data)
- Dunlop 30 m wind speeds (D_{30}) were comparable to Coleshill (C_{10}) synoptic 10 m wind speeds within approximately 5%:
 $C_{10} \sim 0.95 \times D_{30}$ (1998 data)
- Dunlop 45 m wind speeds (D_{45}) were faster than Coleshill (C_{10}) synoptic 10 m wind speeds by approximately 20%:
 $C_{10} \sim 0.82 \times D_{45}$ (1999 data)

Morrison and Webster (2005) conducted a study of turbulence profiles over an urban area (using the same Birmingham data) and over a flat rural area (using turbulence data from Met Research Unit, Cardington Airfield). They found that with good meteorological inputs of local friction velocity and of sensible heat flux, formulae for turbulent velocity variances originally developed for rural conditions were equally well suited to the urban case.

One of the main scientific outcomes has been a prolonged study of the usefulness of land-cover data as a means of deriving the surface parameters required by numerical models, in particular roughness length, z_0 .

The sonic anemometry deployed in all the experiments measures the components of the wind velocity in all 3 spatial directions, at high sampling frequencies. These measurements can be used to directly calculate turbulent quantities such as the turbulent shear stress (or momentum flux), as well as the mean wind velocity. Sonic anemometers also yield measurements of the air temperature as part of their operation, thus the sensible heat flux may be obtained, and the thermal stability of the air may then be computed. The availability of such data (particularly at multiple heights) allows the direct computation of z_0 and d (see section 4.1).

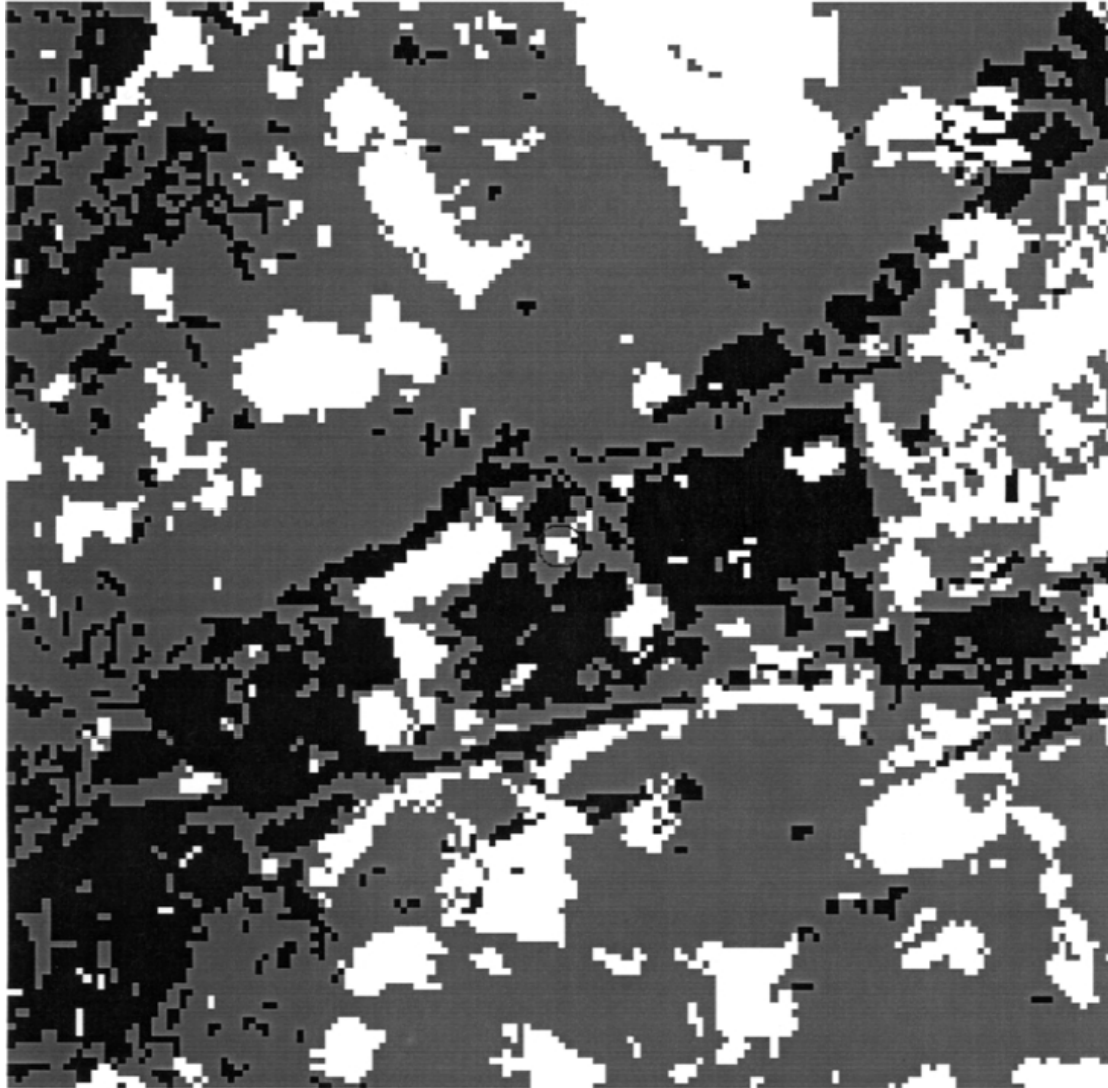


Figure 19: Urban (black) and suburban (grey) land use around the Birmingham experimental site, taken from the Centre for Ecology and Hydrology's 1990 land cover map (<http://www.ceh.ac.uk/sections/seo/lcm1990.html>). The areas left white are mainly parkland. The area shown is a square of side 4km centred on the experimental site, which is ringed in dark grey. Pixel resolution is 25m.

Calculating these quantities for a particular urban location is interesting in itself as a demonstration of their magnitudes. However this information becomes more useful when combined with geographical data on the composition of the *fetch* (or source-area) upwind. Figure 17 to Figure 20 show some of the many different ways in which urban topography may be characterised, each of which has important applications. Of these, the data in Figure 19 are arguably the most useful for providing the bottom boundary condition to a numerical model of the atmosphere. The data are spatially uniform and comprehensive, and have been pre-classified into a set of around 20 different types of land cover. For modelling the urban boundary layer, it would be beneficial to know to what degree data such as these could be relied upon as a proxy for z_0 etc., without having to resort to more labour-intensive methods such as the measurement of many individual buildings.



Figure 20: A plan aerial photograph of the setting of the Salford experiment. The position of the anemometry is marked with a white X. The region shown is 600m square. Cities Revealed® aerial photography copyright The Geoinformation® Group, 2000, and Crown Copyright.

The studies of Rooney (2001), Rooney et al. (2005) and Barlow et al. (2007) have examined this question with data from both experiments. The first two of these have demonstrated that the proportion in the upwind fetch of categories such as 'urban', 'suburban' etc does give some information as to the likely value of z_0 . The third study combines the sonic anemometry data with SODAR wind profiles to show how the wind profile reacts to the composition of the upwind fetch, in particular the approximate lengthscale of the 'patchiness' of different types of cover in the urban environment.

5.2.2 DAPPLE

5.2.2.1 Overview of DAPPLE

DAPPLE was a large research project designed to investigate pollutant dispersion processes in urban environments (Robins, 2003; Arnold et al, 2004; Dobre et al, 2005). The DAPPLE web site



can be found at <http://www.dapple.org.uk>. A series of field experiments were supported by complex numerical modelling (CFD) and by wind tunnel experiments. DAPPLE included studies of exposures of volunteers to pollutants, by carrying sampling equipment on their backs. Tracer compounds were released and a series of sampling bags used to measure concentrations at locations near the intersection. Turbulence as well as wind speeds were measured using a number of sonic anemometers, including some in streets.

5.2.2.2 Results from DAPPLE with Relevance to Wind Power

The novel focus of DAPPLE was its intensive study of flow and dispersion in and around a street intersection. Some additional studies were carried out, and those involving measurements of wind velocity from a point at 190 m altitude above the city (from the BT Tower) are of especial interest to wind power. It was shown by Dr Janet Barlow (personal communication) from Reading University that the wind on the BT tower (height ~190 m) closely matches the wind speed at the same height as inferred from the Met Office Unified Model. This is a much better characteristic than to try to define a roof top wind speed, as such measurements are much more susceptible to local influences. A roof top anemometer in a large city does not give a characteristic measure of the prevailing flow. Long term measurements from such a point over London could provide valuable data for the urban wind power community. Knowledge of the physics of the urban roughness sublayer and of the inertial sublayer above it may then be used to infer winds at altitudes below the top of the BT tower (see elsewhere in this report on the wind profiles over cities).

A striking observation from the DAPPLE dispersion and wind tunnel work, amply illustrated by CFD modelling, was the intermittent or fluctuating character of the flow – tracers can be moved alternately towards one side street and the other, and then wafted at intervals up over the buildings and away. Such fluctuating flows in all three dimensions demonstrate the complex nature of urban canopy wind speeds down amongst the buildings. In another attempt by DAPPLE to better characterise the wind profile over their test site in central London, a QinetiQ Lidar was deployed. This is a remote sensing instrument. It is designed to measure the horizontal component of the flow. It was demonstrated that the wind speed could be measured by this instrument at a series of heights between roof level and the top of the BT tower by placing this portable device on a roof and pointing it vertically upwards. The instrument uses a scanning mirror system to create a conical variable focal length beam and a telescope for sampling of the backscattered light from moving particles in the atmosphere. Such devices have been used elsewhere in the field of wind power to measure the approach flow to the blades of large wind turbines. However whilst valuable in demonstrating the usefulness of the lidar approach, the equipment was operated for too short a time for reliable statistics on the London wind profile to be garnered. Here is scope for future research.

In DAPPLE the ENFLO wind tunnel at Surrey University was used for scale modelling of the likely flow field over the model buildings representing the immediate surroundings of the DAPPLE test site. Professor Alan Robins summarised some DAPPLE wind tunnel studies at the DAPPLE Science Meeting in London on 30 November 2004. They studied street and roof level winds; horizontal advection and vertical mixing over the urban area. They measured vertical turbulent fluxes. Experiments measured the flow and its turbulent components, whilst visualisation experiments using laser sheet lighting revealed the nature of the flow in a visually fascinating way. In south-westerly winds the flow exhibited switching of the flow between the intersecting streets. As well as a simple time averaged picture of helical flow in street canyons, there was also intermittency – excursions in the flow velocity and direction (in 3-D) from the mean. Flow underwent switching at the intersection. This makes for a complex flow near the buildings that varies intermittently in time as well as in space. This would make siting of a wind power device at or above building/road intersections particularly challenging. In many ways the

real insights into the wind field around the intersection were clarified by these wind tunnel experiments.

Flow field measurements in the proximity of the street intersection of Marylebone Rd and Gloucester Place, in London U.K., formed part of the DAPPLE field study. Data from a 4 week period (29 April – 22 May 2003) were recorded by four 3-D ultrasonic anemometers and one propeller anemometer and wind vane from a nearby roof-top weather station. The flow field data are discussed by Dobre et al. (2005) and the experimental set up is described by Arnold et al. (2004). After summarising the main features of street canyon flow, with its vortex-like behaviour in ideal conditions, the paper then mentions the flow channelling and switching which occurs where two street canyons intersect. Here the flow is very sensitive to small changes in conditions, such as the roof-top wind. Time series data were analysed into spectra, showing a broad spectral maximum in the frequency range 3.3 mHz to 0.1 Hz, whose periods range from 10-300 s. After suitable scaling, they found that a 10-minute averaging period is suitable for analysing the main behaviours of the flow. These confirm the switching of the flow between streets at 90°. This leads them to derive a simple model for flow in the canyon as a superposition of two components, namely along-street channelling and across street circulation. This means the street flow direction may be estimated from the parallel and perpendicular roof top components of the wind. An averaging time of 10 minutes (or more) is needed for the underlying simple vortex circulation to become manifest. It is then seen as a basic feature of the flow, even as close as 30m to the intersection. Summarising, we see that Dobre et al. (2005) present a simple model for the wind direction in the canyon, and spectral analysis of the wind velocity.

5.2.3 The Mock Urban Setting Test (MUST) experiment

The Mock Urban Setting Test (MUST) experiment was a field trial of the flow and dispersion through an artificial urban environment at Dugway in the Utah desert (see Yee and Bilitoft, 2004). The urban environment was simulated with a nominally regular 12 by 10 array of shipping containers, each having a plan area of 12.2m by 2.42m and a height of 2.54m, with the overall array having both plan area density λ_p and frontal area density λ_f close to 0.1. The obstacle layout is illustrated in Figure 21. The site is locally flat with sparse vegetation consisting of sagebrush and greasewood reaching up to 0.75m. There are sand dunes about 5m high at a distance of 1km and mountains rising 600m above the site at a distance of 12km. Away from the urban array z_0 and d are estimated from the mean wind profile to be 0.045m and 0.37m. The experiments were conducted in stable conditions although for the bulk of the experiments the Obukhov length L was much greater than the obstacle height making the effective stability close to neutral.

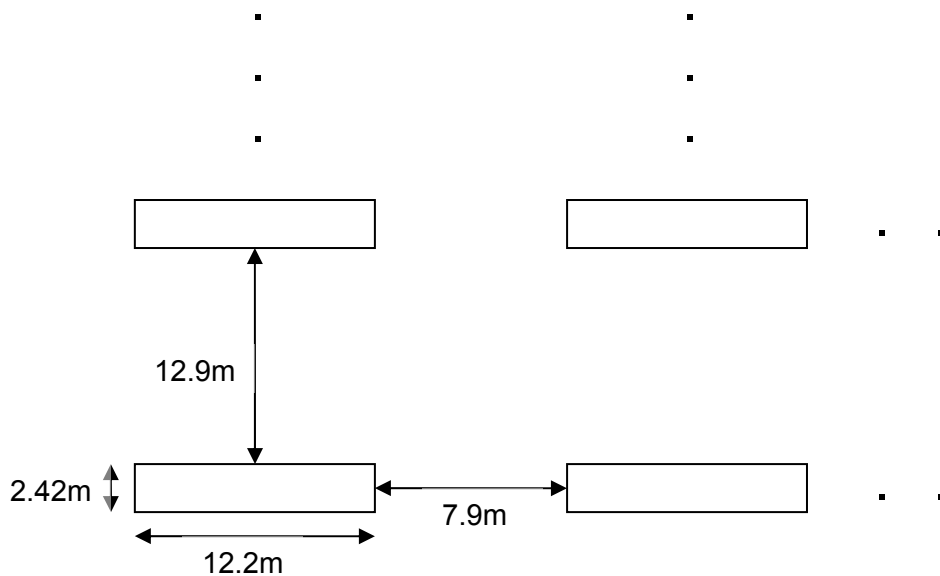


Figure 21: Illustration of the obstacle layout used in the Mock Urban Setting Test experiment

The emphasis of the experiments was on dispersion of contaminants within the mock urban area. However extensive measurements of wind and turbulence were made in support of this. These included masts upwind and downwind of the array, each with 2-D sonic anemometers (which measure the fluctuating horizontal wind components) at 4m, 8m and 16m above ground level. A mast near the centre of the array was used to mount 3-D sonics (which measure all three fluctuating wind components) at 4m, 8m, 16m and 32m and there were four smaller masts in the four quadrants of the array with 3-D sonics at 2.4m and 6m. These masts were all mounted on the ground between the obstacles rather than on top of the obstacles. Finally four 3-D sonics were positioned at 1.15m within the mock street canyons within the array, three sonics within a long 12.2m canyon and one in a short 2.42m canyon.

Yee and Biltoft (2004) present results for the mean wind and turbulence for two cases corresponding roughly to the wind being normal to the long side of the obstacles and being at 45 degrees to the obstacles. For normal incidence, the wind speed above the urban array at 4m and 8m (this is above the canopy) is reduced by 10-20% relative to that at the same height upwind of the array. Also the wind at canopy top and within the canopy is reduced substantially to between 10 and 30% of the upwind 4m wind (this is substantially slower than would be expected in the absence of the array using the values of z_0 and d given above). For oblique incidence, the reduction above the array is greater at between 20 and 40%, while the reduction within the array is less, with the wind speed being between 40 and 60% of the upwind 4m wind (this is still less than expected at the same height upwind of the array). For normal flow, the turbulent kinetic energy (TKE) is increased within the canopy and at 4m and 8m above the canopy, with the largest increases being more than a factor of 2. These largest increases occur at 4m and at the canopy top towards the downwind edge of the array. For the oblique flow, the increases in TKE are smaller with the largest increase being a factor of about 1.5.

The array is probably too short to estimate the effective roughness length of the array with confidence. However Yee and Biltoft make an indicative calculation based on the drag coefficient observed in near neutral conditions at 4m over the array (i.e. using wind speed and stress both measured at 4m). By assuming a displacement height d equal to 70% of the array height they

obtain a roughness length of 0.2m which is in line with the value to be expected from Figure 7 in Section 4.1 above.

The MUST experiment has been replicated in wind tunnel, water channel and numerical simulations and has been a focal point of the COST Action 723 on 'Quality assurance and improvement of micrometeorological models'. Wind tunnel and water channel experiments, with an emphasis on dispersion through the array rather than on the flow per se, were conducted by Gailis and Hill (2006), Yee et al (2006) and Gailis (2007). A simulation conducted in the University of Hamburg wind tunnel (Leitl et al, 2007) is noteworthy because of the precision with which they replicated the departures from perfect regularity in the layout of the shipping containers. The proceedings of a recent conference (Carruthers and McHugh, 2007) include 9 papers discussing numerical simulations of the experiment. MUST illustrates the power of combining field trials with wind tunnel experiments and numerical simulations. All three approaches complement each other and serve to give a better understanding of the flow. The wind tunnel and numerical simulations give reproducible results for detailed study and sensitivity tests, and the numerical simulations can give easy access to aspects of the flow that are very hard to measure. This complements the ground truth observed in the field.

5.3 Wind Tunnel Experiments

Wind tunnel modelling is used extensively to model flow in urban areas. Studies range from idealised studies of flow around single cubes, cube arrays and idealised street canyons to realistic urban configurations corresponding to real locations. They are often used in conjunction with numerical simulations or field experiments. The conditions can be controlled much more closely than in field experiments. This means that, like numerical simulations, they are much more suitable for systematic exploration of a range of conditions. However there are also some drawbacks. Reynolds numbers are much lower than in reality, and care needs to be taken to ensure that results are obtained in conditions where the turbulence is sufficiently fully developed for results to be insensitive to Reynolds number. Also the ratio of boundary layer depth to building height may be lower than in reality. This is a matter of choice and compromise in deciding on the building size – buildings that are small will reduce the building scale Reynolds number while large buildings will cause a mismatch in the building size to boundary layer depth ratio. Again this should not be a problem provided appropriate care is taken. Ideally the ratio should be sufficient to ensure that there is, at least approximately, an inertial sublayer. This is especially important if one wishes to use the experiment to relate the flow at the building scale to flows higher in the boundary layer. Both the Reynolds number and building to boundary layer scale ratio issues are improved by using large wind tunnels. In addition wind tunnel simulations cannot simulate the larger scales of motion in the atmosphere which lead, for example, to low frequency meandering of pollutant plumes. This is unlikely to be a problem however for wind energy applications. Finally, very few wind tunnels are capable of simulating thermal effects with most simulations being conducted in neutral stability. Again this is unlikely to be a problem because urban areas tend to be more neutral than other areas (due to increased roughness and, at night, the altered urban energy balance) and, in any case, thermal effects have their biggest impact in light wind conditions which are not of great interest for wind energy.

It is not feasible to summarise the enormous amount of wind tunnel work that has been conducted in connection with urban flows. Instead we have aimed to refer to specific wind tunnel (and water channel) studies in the other sections of the report where they relate to the issues being addressed. Examples are as follows:

- Idealised arrays of identical cuboids (Cheng and Castro, 2002; Davidson *et al.*, 1996; Hall *et al.*, 1996; Hall *et al.*, 1998; Macdonald *et al.*, 1998b – see sections 4.1 and 5.1.1)

- Street canyons (Pavageau *et al.*, 1997; Rafailidis, 1997; Rafailidis, 2001 – see sections 4.1, 5.1.1 and 5.1.2)
- Single buildings (Wilson, 1979 – see section 5.1.3)
- Replication of field experiments (Davidson *et al.*, 1996; Gailis and Hill, 2006; Gailis *et al.*, 2007; Leidl *et al.*, 2007; Yee *et al.*, 2006 – see sections 5.1.1 and 5.2.3)

5.4 Computational Fluid Dynamics (CFD)

CFD is a commonly used technique for numerical simulation of fluid flows based on the underlying governing equations, i.e. the Navier-Stokes equation, the equations governing the transport of heat and other scalars (e.g. moisture or pollutants), and the equation of state or some approximation to this such as the assumption of incompressibility. Usually the equations are solved using a spatial grid on which the values of the variables are stored. We will assume this in the following. Alternative numerical approaches such as finite element or spectral methods are possible but the differences are a matter of computational cost versus accuracy of the solution or the ease of treating complex geometries and they are not really essential from the purposes of this review.

As well as differences in the numerics, various approaches to the physics are possible. The approach that is most faithful to the physics is 'Direct Numerical Simulation' (DNS) where the governing equations themselves are simulated with no approximations (other than in the numerical schemes for approximating the equations). In this approach the grid needs to be fine enough to resolve all scales of motion down to the smallest eddies where energy is dissipated. This means the technique is restricted to low Reynolds number flows, although sometimes low Reynolds number simulations are used as approximations to high Reynolds number flows. When conducted with good numerics at the correct Reynolds number and with appropriate boundary conditions, DNS is reliable and accurate.

The next most faithful approach is 'Large-Eddy Simulation' (LES) where the larger eddies in the flow are simulated explicitly but the effect of the smaller eddies is parametrized. This is cheaper than DNS for the same flow because the grid does not have to be fine enough to resolve the smallest eddies. Also it is possible to simulate much higher Reynolds number flows. The approach is fairly reliable because most flows are insensitive to the behaviour of the smallest eddies. However there are potential inaccuracies near solid surfaces or in stable regions where all of the eddies may be small and so all are parametrized. In a sense the simulation ceases to be a 'large-eddy' simulation in such regions.

The third main category of simulation is 'Reynolds Averaged Navier-Stokes' (RANS). Here all the eddies are parametrized and only the average flow is simulated. This 'Reynolds' average can be regarded as the average over an ensemble of repetitions of the flow, or, for statistically steady flows, as a time average. Because the eddies are not explicitly represented and one may be looking for a steady solution, RANS approaches are cheaper than LES and DNS. Sometimes 'CFD' is used in a narrower sense than we've used it here to mean only RANS simulations. In RANS, equations for the average values of the fundamental quantities (e.g. of the velocity components u_i , $i = 1,2,3$) are derived from the basic equations, but these are not 'closed' as they involve the unknown correlations $\overline{u_i u_j}$, where the overbar denotes the average. Equations for these quantities can also be derived but they involve more unknowns, and this is repeated ad infinitum. Hence at some point approximations need to be made to obtain a closed set of equations. Common approximations are 'mixing-length' models, ' $k-\epsilon$ ' models, and 'second-order closure' models. In mixing-length models, the second-order correlations such as $\overline{u_i u_j}$ are approximated directly in terms of what is known using a 'mixing-length'. This is an estimate of

the eddy scale and often depends on the flow geometry (distances to the solid boundaries) and stability. In $k-\varepsilon$ models, equations for the turbulent energy k and rate of dissipation of turbulent energy ε are derived, the unknowns in these equations are approximated, and the second order correlations are approximated in terms of k , ε and the other known quantities. In second-order closure models, the equations for the second-order correlations and, commonly, for ε are used, and the unknowns in these equations are approximated as functions of what is known.

Generally one would expect second order closures to be a more faithful representation of the physics than $k-\varepsilon$ models (because an equation for $\overline{u_i u_j}$ is used, rather than simply estimating $\overline{u_i u_j}$ from other quantities), which in turn should be more faithful than mixing-length models. In practice this is probably true for flows that are well represented by these parametrizations. However the more sophisticated models also have more degrees of freedom to behave badly in flows that are hard to represent. This means that one needs a considerable degree of insight and experience in using these models to know what situations are likely to be well represented and which type of 'closure' is likely to perform best.

In addition to the above approaches, there is a hybrid approach called "Unsteady RANS" or URANS. This approach takes the RANS equations but applies them in situations where fluctuating eddies are produced by the equations, as in large-eddy simulation. Strictly speaking this is inconsistent because the turbulence closure is supposed to represent all turbulent fluctuations (if the flow is statistically steady, the turbulent fluctuations should include all unsteadiness). However the approach can sometimes give a more faithful representation of slowly varying aspects of the flow, such as oscillations caused by periodic shedding of vortices from opposite sides of an obstacle.

Conceptually CFD models are not unlike NWP models. The main differences are the range of scales treated, the importance of radiation and processes involving water and ice in NWP which are often absent from CFD, and the fact that NWP models usually use a regular grid whereas CFD models generally allow much more flexibility in grid design to fit complex geometries.

The number of choices which need to be made in designing and running CFD models is large and this can lead to considerable variability in results, as seen in the study by Ketzel *et al.* (2005) referred to in section 5.1.2 above. Here five different CFD simulations of a particular real street canyon are presented and significant differences are found. Significant differences occur even for the case where the same problem is solved using the same code by different groups (Cowan *et al.*, 1997; Castro *et al.*, 1999; Castro 2005b). This illustrates the importance of experience in running such models, and this sometimes need to be supplemented by wind tunnel or full scale experiments (perhaps for a limited subset of the conditions of interest) to add confidence to the results. This has led to a number of sets of guidelines being produced to help users and developers of CFD codes (see e.g. Hutton (2005), Castro (2005), Franke *et al.* (2007) and Britter and Schatzmann (2007a, 2007b)).

As in the section on wind tunnel experiments above, it is not feasible to summarise the enormous amount of CFD work that has been conducted in connection with urban flows. Instead we have referred to specific CFD studies in the other sections of the report where they relate to the issues being addressed. Examples are as follows:

- Idealised arrays of identical buildings (Coceal *et al.*, 2006; Heath *et al.*, 2007 – see sections 5.1.1 and 5.1.4)
- Street canyons (Ketzel *et al.*, 2005; Louka *et al.*, 2002; Sini *et al.*, 1996; Solazzo *et al.*, 2007; Xie *et al.*, 2006 – see section 5.1.2 and this section)
- Single buildings (Cowan *et al.*, 1997; Castro *et al.*, 1999; Castro, 2005b – this section)

- Replication of field experiments (Ketzler *et al.*, 2005 and 9 papers on the MUST experiment in Carruthers and McHugh (2007) – see sections 5.1.2, 5.2.3 and this section)

The main value of CFD in connection with small-scale urban wind power is the generic guidance it has given on aspects of the building-affected flow. CFD could conceivably also be used in connection with the siting of individual generators. However the cost of the computations involved mean that this would need to be done for a number of representative test locations. Even then it would probably not be practical to simulate a wide range of weather conditions. Instead, results for a limited set of conditions would need to be related to the large scale meteorology. The statistics on the large scale meteorology could then be used to extend the CFD results and give an assessment of the wind power potential of the site. The results for these locations, ideally combined with field measurements to give confidence in the results, could be used to provide more general guidance.

Commonly used commercial codes include CFX (Ansys Inc., <http://www.ansys.com/products/cfx.asp>), FLUENT (Ansys Inc., <http://www.fluent.com/>) and STAR-CD (CD-adapco, <http://www.cd-adapco.com/>). There are also numerous codes developed by a range of organisations initially for their own use, but subsequently used more widely. We note that the NWP model RAMS can, unlike most NWP models, be run at very high resolution with detailed building geometries (see e.g. Trini Castelli and Reisin (2007)).

6 Tools

6.1 Geostatistical Interpolation and Gridded Averages

One option for estimating the climatology at any arbitrary location is to take the available surface observations and interpolate them, typically onto a regular grid of points spanning the area of interest. This can be done using a variety of techniques such as kriging, thin plate splines and distance-weighted averaging. Such techniques make no attempt to model atmospheric processes – they exploit the information contained within the observations themselves (e.g. location, spatial correlation) and therefore require a sufficient density of stations to produce accurate results.

Spatial variations in climate data are known to depend on many factors. At short timescales the synoptic weather pattern (pressure systems, fronts etc) is dominant. However for longer timescales, such as monthly means and 30-year averages, there is often a strong correlation with a variety of geographic and topographic factors. For example, climatological averages of air temperature generally decrease with altitude but increase in urban areas. This means that to get good estimates of a climate variable at locations between the observing stations it is necessary to incorporate topographic information into the interpolation process. One fairly common approach is to use multiple linear regression analysis to model the dependency of the climate data on various topographic quantities and then apply the interpolation to the regression residuals (e.g. Agnew and Palutikof, 2000).

Interpolation techniques have been widely used for analysing daily, monthly and long-term average climate data. Many of the analyses are for temperature and rainfall and intercomparisons of various interpolation techniques have been published by a number of authors e.g. Nalder and Wein (1998), Vicente-Serrano et al (2003).

The interpolation of wind speed data has been much less studied. Mean wind speed is affected by a variety of topographic factors including location (latitude and longitude), altitude, terrain shape (at both the large scale and small scale), proximity to the coast and land use (i.e. surface roughness), as well as by local obstacles such as trees and buildings. Given the relationship between the local wind climatology and these various factors is complex, the creation of a gridded wind speed dataset from observations alone is a difficult task.

Possibly the only published example of a wind climatology for a large geographical area created by interpolating station data is described by Sokol and Stekl (1995). They produced a map of mean wind speed for the Czech Republic using data for 156 stations. The interpolation method is as follows. First the dependency of wind speed on altitude is determined for each observing site by fitting a polynomial equation to the data from the surrounding stations. This altitude dependency is then used to correct each station average to a common altitude. Both the altitude dependencies and the corrected station data are then interpolated onto a grid using a successive correction method (the text is unclear but this presumably means a technique in which the grid values are adjusted iteratively for differences between the grid and the observations). The grid of altitude dependencies is then used to transform the grid of mean speeds back to ground level. The accuracy of the interpolated data was found to be best in areas of intermediate elevation, with RMS errors of around 0.5 m/s (1 knot). Areas of lower and higher elevation had larger errors.

Palomino and Martin (1995) describe an analysis of hourly wind data collected at 6 towers in the Montesina Valley in southern Spain. They compare two interpolation methods based on

weighted averages i.e. where each value in the grid is a weighted average of the values at surrounding observing sites. They conclude that a weighting based on the inverse of the height difference (between each station and the grid point) gives superior results to conventional inverse-distance weighting (where more weight is given to stations that are closer horizontally). In addition the results are better in strong wind conditions (when the stability of the air is approximately neutral) than in light wind conditions (when thermal effects can become important).

Xia et al (1999) compared six techniques for interpolating monthly means of wind speed (as well as other climate variables) over an area of Bavarian forest. The techniques were two iterative, distance-weighted schemes (Barnes, Cressman), Optimal Interpolation (OI), a simple arithmetic mean of the five closest stations, an inverse-distance-squared weighted average of the five closest stations, and a multiple regression model against x, y and elevation. Four independent stations were used to verify the results. The technique with the lowest mean absolute error (MAE) varied according to the target station. For a low-level station the best results were obtained using OI (MAE = 1.05 m/s), for an intermediate station Barnes interpolation was the most accurate (MAE = 0.64 m/s) and for a high-level station Cressman interpolation was the best option (MAE = 0.28 m/s). These results are slightly counter-intuitive as it did not appear that any topographic data were used for the wind speed interpolation in the most accurate techniques.

The Met Office have been using geostatistical techniques to interpolate climate data for some years and have produced grids of 30-year averages (Perry and Hollis, 2005a) and monthly means (Perry and Hollis, 2005b) for a range of variables. Techniques for interpolating mean wind speed are currently under investigation and provisional grids of the 1961-90 and 1971-2000 averages have been produced from the 30-year station averages (described in §2). The analysis technique used so far is a combination of regression analysis and inverse-distance-weighted interpolation of the regression residuals. The independent variables used in the regression model comprise x, y, elevation, the proportion of sea within a 5km radius, and four terrain shape variables (the mean altitude over a circle of radius 5km offset by 10km to the north, south, east and west). Currently the effects of urban areas are not modelled.

Figure 22 shows a map of the provisional grid for the 1961-90 averaging period. Values for approximately 220 stations have been used to generate the grid. The resolution of the grid is 1km. Work is ongoing to look at how the analysis may be improved (e.g. to better capture surface roughness and terrain shape effects) and to assess the accuracy of the results.

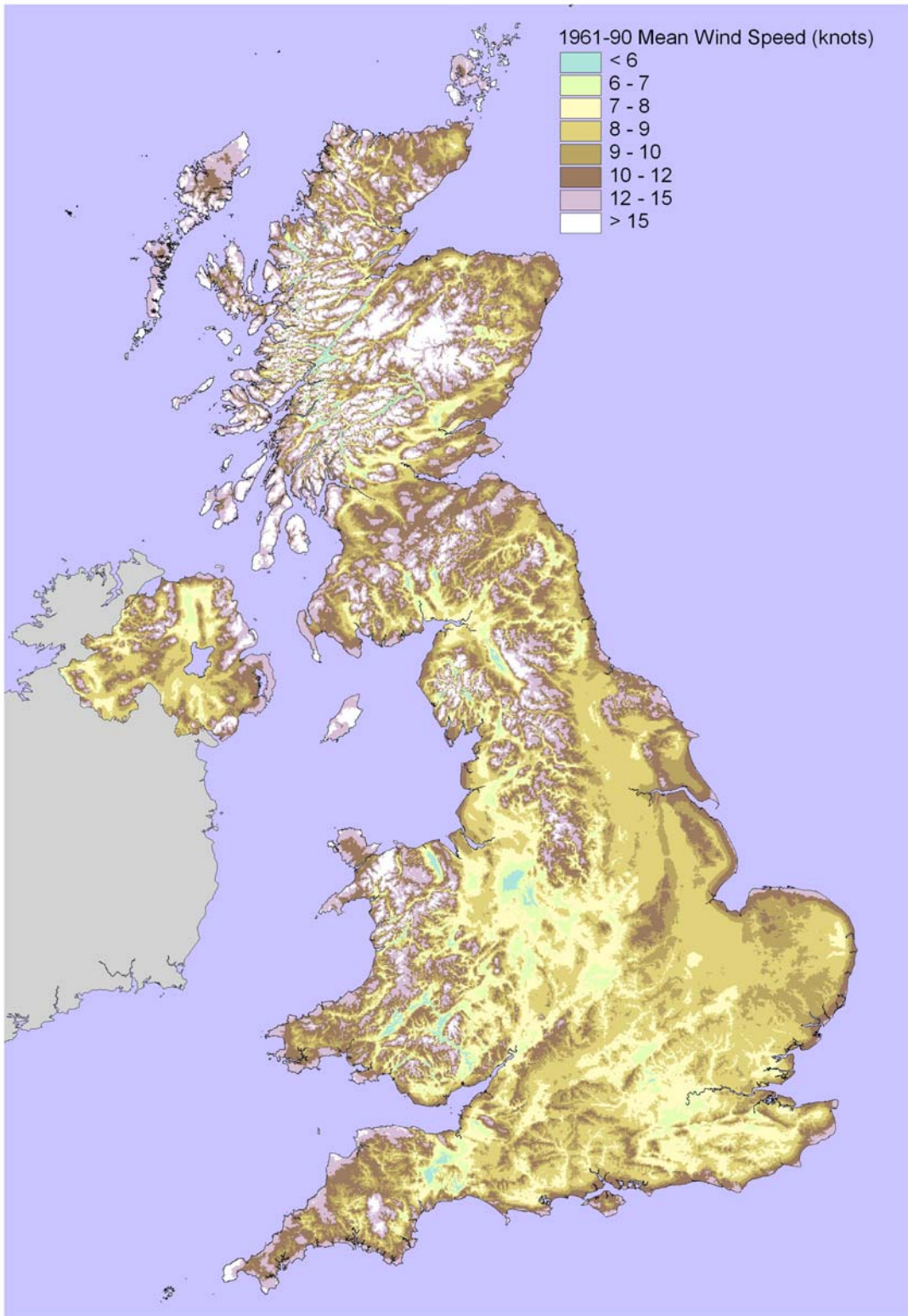


Figure 22: Map of mean wind speed obtained by geostatistical interpolation of surface anemometer data

6.2 Measure-Correlate-Predict

6.2.1 MCP Techniques

Measure-correlate-predict (MCP) is a purely statistical technique for estimating the wind climatology at a target site. The principles of the approach are:

- **Measurements** of wind speed and direction are made at the target site for a period typically between 3 months and 1 year
- These measurements are **correlated** with concurrent data from a reference station i.e. statistical techniques are used to establish the relationship between the observations at the two sites
- The statistical relationship is applied to a much longer period of data from the reference station to produce a **prediction** of the long-term climatology of the target site

Various approaches to characterising the relationship between the two sites have been used, of which perhaps the most common technique is some form of linear regression analysis. The following is a summary of the different methods in the literature:

Scalar wind speed regression – The most common approach is to use linear regression to relate the speed at the target site to the speed at the reference site i.e. $v = a + b u$ (where u and v are the wind speeds at the reference station and target site respectively). The data are usually grouped by the wind direction at the reference site and a separate regression equation is calculated for each direction sector e.g. Nygaard (1992), Achberger et al (2002). Various extensions of this approach have been tried, such as using either a polynomial relationship (e.g. $v = a u + b u^2$) or a power law ($\ln v = a + b \ln u$), or incorporating a variable to capture stability effects (e.g. $v = a + b u + c u \Delta T$, where ΔT is the difference between temperatures at two heights at the reference station) – see references in Rogers et al (2005). In all cases wind direction has to be treated separately, typically by calculating, for each direction sector at the reference station, the mean difference between the directions at the two sites. These mean differences are then used as fixed corrections to the long period data from the reference station.

Wind component regression – In this approach the speed and direction are converted into easterly and northerly components. A separate linear regression equation is derived for each component at the target site using the corresponding wind component at the reference station as the independent variable i.e. $v_x = a_1 + b_1 u_x$ and $v_y = a_2 + b_2 u_y$ (Achberger et al, 2002). Alternatively each component at the target site can be predicted from a linear combination of *both* components at the reference station i.e. $v_x = a_1 + b_1 u_x + c_1 u_y$ and $v_y = a_2 + b_2 u_x + c_2 u_y$. Multiple regression analysis is used to fit these equations to the data, separately for 12 wind direction sectors (see references in Rogers et al, 2005). A third option is to consider the easterly and northerly components as the real and imaginary parts of a complex number – a single linear regression equation, with complex coefficients, is used to relate the target and reference sites (Achberger et al, 2002). Wind direction is not treated separately as it can be derived from the values of the two components.

Matrix method – Woods and Watson (1997) describe a technique that aims to produce better estimates of the wind *direction* distribution than can be achieved using standard approaches (such as the mean direction difference). The concurrent data are used to obtain a joint frequency analysis of wind direction at the reference station and wind direction at the target site e.g. for 30° sectors the result is a 12x12 matrix of frequency counts. These counts are converted to percentage frequencies and then combined with the observed counts from the long period data at the reference station to produce estimates of the long-term wind direction distribution at the

target site. Linear regression is used to relate the wind speeds at the two locations, with a separate equation for each direction sector. The observed mean speed for each sector at the reference station is used with the relevant equation to produce a predicted mean speed for the target site. The mean speed for each sector at the target site is estimated by taking a weighted sum of these separate predictions, using the matrix of percentage frequencies to determine the weights. Note that this method only produces a prediction of the frequency and the mean speed for each direction sector at the target site – unlike most other MCP techniques, it does not produce a time series of predicted speeds and directions.

Binned Ratios method – In this approach the concurrent data are grouped into bins according to the speed and direction at the reference station (see references in Rogers et al, 2005). The ratio of the wind speeds at the target site and reference station is calculated from each pair of observations and then the mean and the standard deviation of this ratio are calculated for each speed/direction bin. The speed at the target site is predicted from the reference station value using the following equation:

$$v = (r_{\text{mean}} + e(s_r)) \cdot u$$

where r_{mean} and s_r are the mean and standard deviation of the wind speed ratio for the relevant speed/direction bin, and $e(s_r)$ is a random variable with a triangular distribution and a standard deviation equal to s_r .

Variance Ratio method – Rogers et al (2005) highlight a key deficiency of regression-based approaches i.e. that the variance of the predicted values from a regression analysis will be less than the variance of the observations by a factor of r^2 (where r is the correlation coefficient). They propose using the following alternative linear relationship:

$$v = \left(\bar{v} - \frac{s_v}{s_u} \bar{u} \right) + \frac{s_v}{s_u} u$$

where \bar{u}, \bar{v}, s_u and s_v are the mean and standard deviation of the concurrent data at the reference station and target site. This equation ensures that the predicted values have the same overall mean and variance as the observed values.

Kriging method – Zaphiropoulos et al (1999) use a kriging estimator to predict the speed at the target site from several neighbouring sites.

FFT method – Sreevalsan et al (2007) use a Fast Fourier Transform (FFT) to examine the power spectrums of the wind speed data at the target site and reference station. The results from the FFT analysis are used to apply a correction to a standard wind speed regression MCP analysis.

6.2.2 Comparisons of different MCP techniques

Several authors have compared more than one MCP technique:

Woods and Watson (1997) compare their matrix method with the scalar wind speed regression method. For the latter approach they look at two options: a) where the direction distribution at the target site is assumed to be the same as that at the reference station, and b) where the mean direction difference between the two locations is used to correct the observed directions from the reference station. The authors demonstrate that, for a target site with a direction distribution that is markedly different from that at the reference station, the matrix method can produce a

significant improvement in the representation of the sector frequencies, compared with the other two approaches. Even for a site that was more similar to the reference station they found improvements in the predictions of both sector frequencies and mean speeds.

Achberger et al (2002) compare scalar wind speed regression with two component regression methods, one that predicts each component from the corresponding component at the reference station, and one that treats the two components as parts of a complex number. They look at the performance of these techniques using three different reference 'stations' – a conventional surface anemometer, plus 10m and geostrophic winds from a mesoscale model. The target site is in open, uncomplicated terrain. The authors conclude that the 'complex component' technique produces the best predictions of the wind direction distribution and that with this approach the best results are obtained using the anemometer data. For both the mean wind speed and the wind speed distribution the best results were produced using anemometer data, followed by 10m model data and then geostrophic model data. The two component-based techniques tended to under-estimate the sector mean speeds, whereas the scalar wind speed regression was unbiased overall. All three techniques underestimated the frequency of speeds > 6m/s.

Rogers et al (2005) examine four techniques – scalar wind speed regression, a component regression method (in which each component at the target site is dependent on *both* components at the reference station), the binned ratios method, and their own variance ratio method. Their comparisons use data from eight stations with a variety of exposures – plains, ridge top, coastal and offshore. They assess the performance of each technique with regard to prediction of the overall mean speed, the wind speed distribution, the wind direction distribution and the annual energy production of a typical turbine. The authors conclude that only the variance ratio method seems to give consistently reliable predictions of all the metrics, although the binned ratio method also produces reliable results in most cases. The two regression methods both suffer from the problem that the variance of the predictions is too low. Only the component regression technique predicts the wind direction distribution, which it does relatively well. The authors also found that the accuracy of all the techniques improves as the period of concurrent data is increased up to 9 months, with little improvement for longer periods.

6.2.3 Limitations of MCP and Applicability to Urban Locations

MCP is based on the assumption that the wind speeds and directions at two sites have a simple deterministic relationship e.g. if it is 12 knots and 260° at Site A then it will always be 14 knots and 280° at Site B. Rogers et al (2005) point out that the relationship between two sites is made complicated by the following factors:

- stochastic variations in wind speed and direction over time and distance
- the effects of terrain on the flow
- time of flight delays
- large-scale and small-scale weather patterns
- local obstructions
- atmospheric stability

The result is that there is often a substantial amount of uncertainty in the statistical relationships (e.g. scatter about the regression line) and, therefore, the predicted values. In addition the relationships that have been established using data from one part of the year may not be applicable to other seasons. Possible enhancements to the technique include carrying out separate analyses for different seasons, introducing some degree of smoothing across wind direction sectors (e.g. by using data from adjacent sectors but with a lower weight) and excluding low wind speed data from the analysis (to improve the fit of the model to speeds that are of significance to wind energy generation). As with any statistical analysis, care has to be taken not



to split the data into so many classes that the uncertainties are increased due to the small sample sizes.

None of the papers considered in this study look at the performance of the MCP approach when the target site is in an urban area. However there is no theoretical or practical reason why it could not be applied to urban locations – the success of the MCP technique depends entirely on the strength of the correlations between the target site and reference station.

The Met Office's own MCP software has been used to produce a sample prediction for an urban location. The software uses linear regression to describe the relationship between the wind speeds at the target site and the reference station. A separate relationship is derived for each wind direction at the reference station (the observations have a resolution of 10° so there are 36 possible wind directions). In addition, for each wind direction and for 5 knot ranges at the reference station, the standard deviation of the target site wind speeds is calculated. For wind direction, the mean and standard deviation of the direction difference (reference station minus test site) is calculated for each wind direction at the reference station.

To produce a prediction of wind speed, first the relevant regression equation is applied to the speed from the reference station. Then a random number is drawn from a normal distribution with mean equal to the value given by the regression equation and with standard deviation equal to the value for the appropriate 5 knot bin. This random number is the predicted wind speed. For wind direction a random number is drawn from a normal distribution with parameters specified by the mean and standard deviation of direction difference for the relevant direction. The predicted direction is obtained by using this value to correct the observed direction at the reference station. This approach attempts to combine deterministic prediction (the regression equations and mean direction differences) with an element of natural variability (the use of random numbers drawn from a normal distribution) and thus produce results that have more realistic frequency distributions.

The target site for the analysis is Norwich Weather Centre (a city centre site) and the reference station is Coltishall (an airfield site 15km to the NNE of Norwich). The regression analysis is based on concurrent data for 1993. Over this period the mean speed at Coltishall was 8.4 knots and the mean speed at Norwich Weather Centre was 6.6 knots. The variation of mean speed with direction is shown in Figure 23, where the data have been grouped by the wind direction at Coltishall. The mean and variability of the direction difference between the two locations is shown in Figure 24.

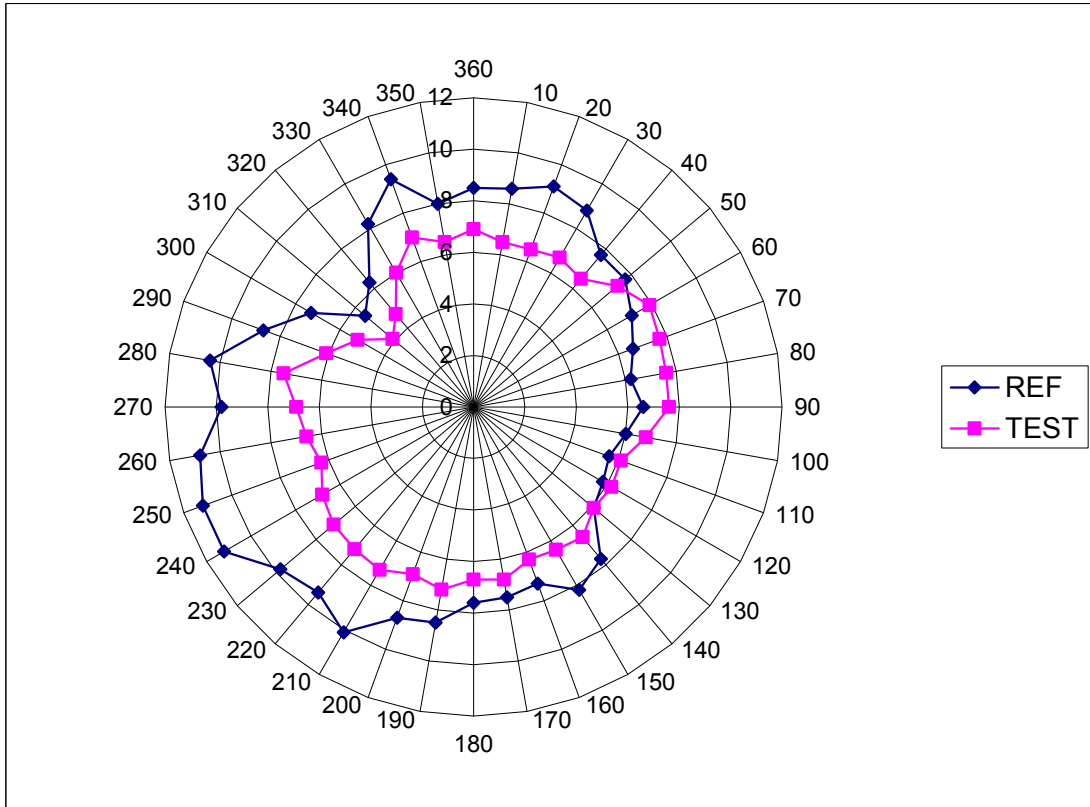


Figure 23: Observed variation of mean speed at Coltishall (REF) and Norwich Weather Centre (TEST) with wind direction at Coltishall during 1993. Speeds are in knots.

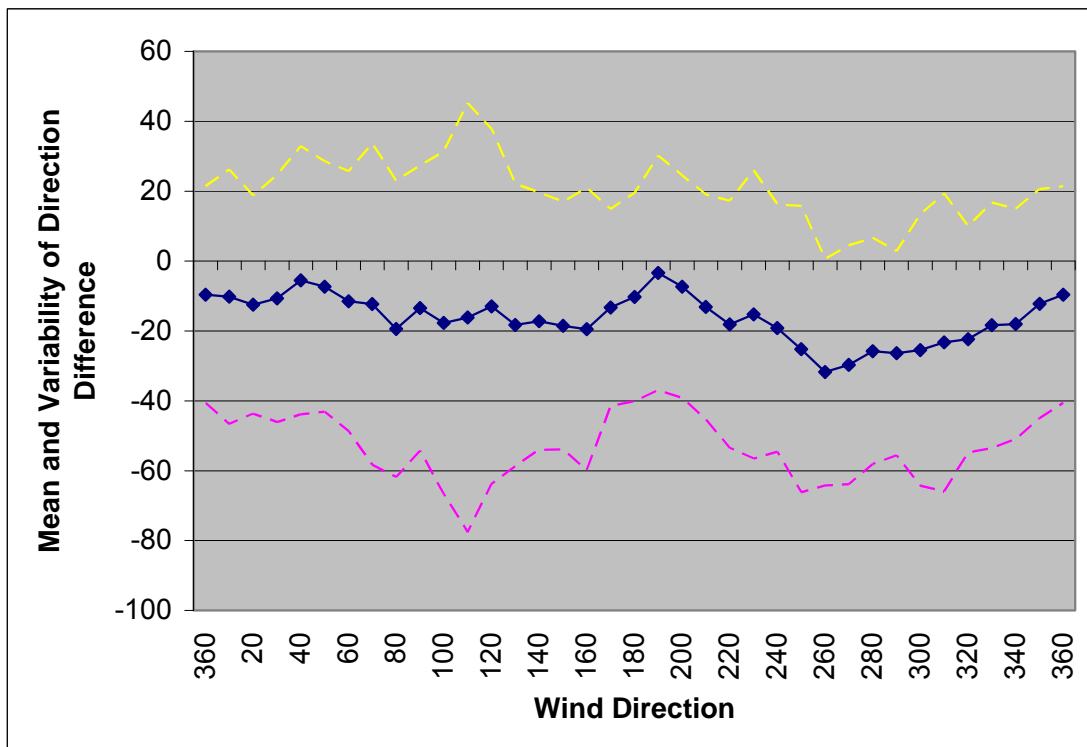


Figure 24: Observed variation of mean direction difference between Coltishall and Norwich Weather Centre (solid line) with wind direction at Coltishall during 1993. Differences are calculated as Coltishall minus Norwich. The variability is indicated by values of the mean +/- 2 standard deviations (dashed lines).

The regression relationships obtained from the 1993 data were applied to Coltishall data for 1994-1999 and the predictions compared with observations for the same six year period from Norwich Weather Centre. The mean speed at Coltishall during this period was 9.0 knots, the predicted speed for Norwich Weather Centre was 7.1 knots and the actual speed at Norwich Weather Centre was 6.9 knots. Figure 25 shows the results for the frequency distribution of wind direction and Figure 26 compares the sector mean speeds.

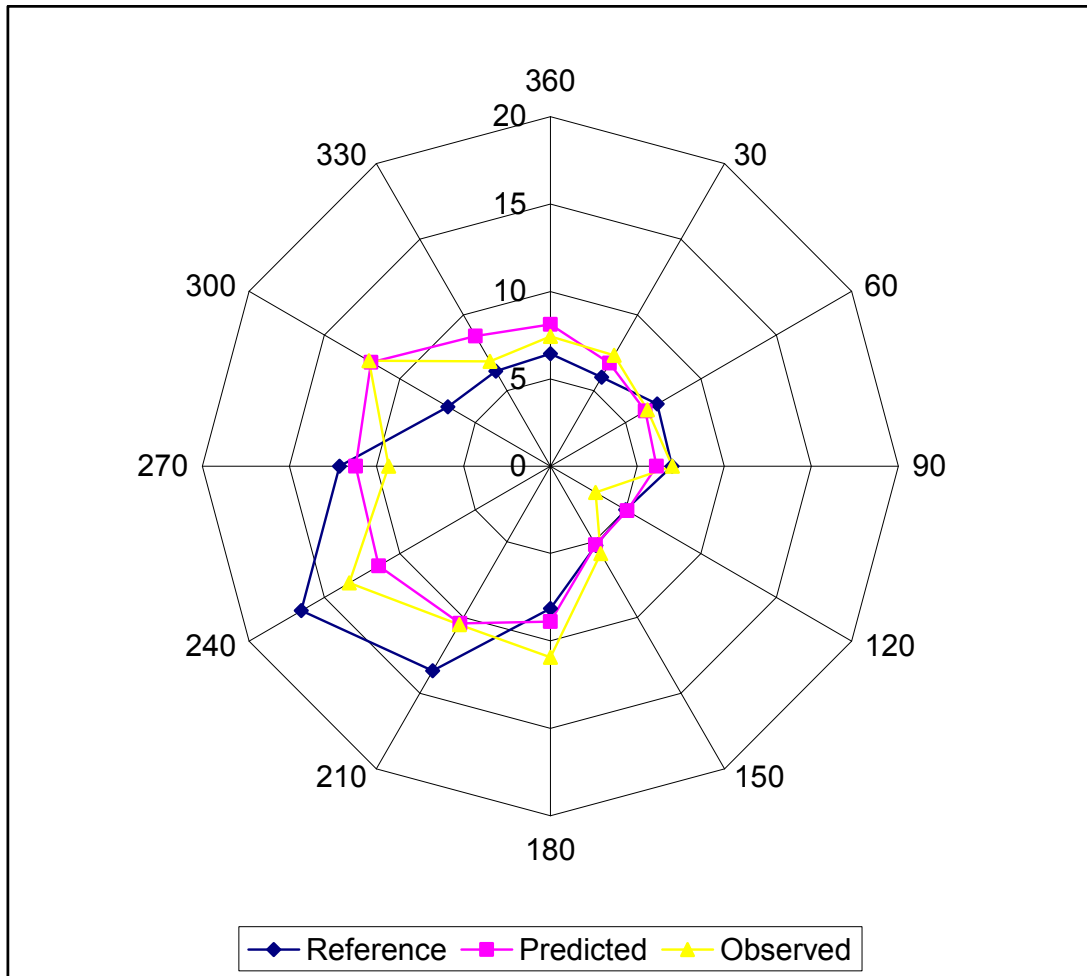


Figure 25: Frequency (%) of winds in 30° sectors during 1994-1999. Values are shown for a) Coltishall (Reference), b) the MCP prediction for Norwich Weather Centre from Coltishall data (Predicted) and c) the actual distribution at Norwich Weather Centre (Observed).

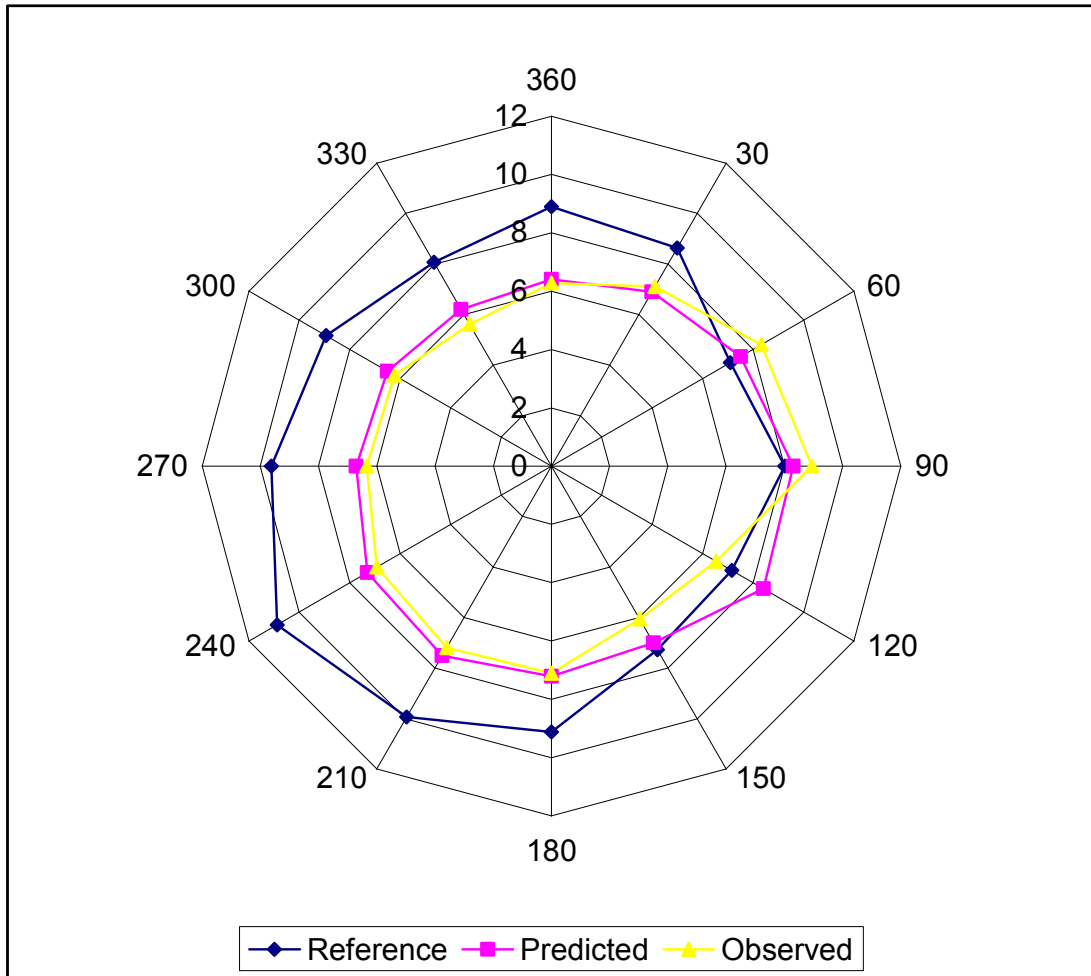


Figure 26: Mean wind speed (knots) by 30° sectors during 1994-1999. Values are shown for a) Coltishall (Reference), b) the MCP prediction for Norwich Weather Centre from Coltishall data (Predicted) and c) the actual distribution at Norwich Weather Centre (Observed).

It is not possible from this one example to state what sort of typical accuracy might be achievable using MCP techniques. However it seems likely that the correlations will be lower for locations closer to roof-top level (due to the greater influence of the local building geometry etc) and that therefore the predictive skill of the MCP approach will also be less compared with better exposed locations. Further work (and suitable data) would be required to test this hypothesis.

6.3 WAsP

6.3.1 Background

The Wind Atlas Analysis and Application Program (WAsP) is a PC software package for estimating the local wind climatology and predicting the energy resource at prospective wind farm sites. It was developed by the Wind Energy Department at Risø National Laboratory, Denmark and is a computer implementation of the methodology published in the European Wind Atlas (Troen and Petersen, 1989). The first version of WAsP was released in 1987 and the latest version (8.3) was released in April 2007.



An associated piece of software – WAsP Engineering – is available for the estimation of extreme wind speeds, wind shears, wind profiles and turbulence in complex (and simple) terrain. Version 1.0 was launched in July 2001 and the present version (2.0) was released in July 2005.

There are currently more than 1800 users in over 100 countries and territories (source – WAsP web site, <http://www.wasp.dk/index.htm>).

6.3.2 Methodology

WAsP employs a series of models to adjust observed wind speed data for the effects of surface roughness, near-by obstacles and variations in terrain elevation.

Roughness change model – The roughness change model uses equations for the growth of internal boundary layers and the logarithmic variation of wind speed with height to calculate a correction factor that relates the wind speed at the target site to the wind speed upstream of the specified roughness changes i.e. the wind speed that would occur in an area of homogeneous roughness typical of the region. The model superimposes the effects of multiple roughness changes, but with more weight given to roughness changes closer to the site.

Shelter model – The model uses expressions given by Perera (1981) for the sheltering effect of simple two-dimensional obstacles such as long rows of trees, walls or hedges. The sheltering effects are calculated for each of a number of radial lines, or rays. If a ray crosses more than one obstacle then the effects are combined. The total sheltering effect for a 30° sector is obtained by combining the results for eight rays.

Orographic model – WAsP uses the BZ model of Troen (1990) – this model is closely related to MS3DJH. The terrain is represented using a polar grid with a resolution that increases as you approach the target site e.g. for a domain of radius 10km the grid spacing varies from 2m near the site to around 300m on the edge of the domain. The model captures the climatological effects of the stably-stratified air above the boundary layer by specifying an inversion height and strength and then attenuating vertical motion on horizontal scales larger than this height.

The starting point of a WAsP analysis is a frequency analysis of wind speed and direction for a reference site with a long historical record. A typical analysis might use 10 years of hourly observations. The roughness, shelter and orographic models are used to correct the observed frequency distribution – the result is a frequency distribution that is representative of flat terrain without obstacles and for a roughness length characteristic of the upstream conditions. This adjustment process is carried out for each of 12 wind direction sectors.

The geostrophic drag law is then used with the upstream roughness length to produce a frequency distribution of geostrophic wind speeds and directions i.e. the wind climatology at the top of the boundary layer. This is followed by a downward transformation back to a height of 10m above ground level, but this time for four standard roughness lengths.

Next a two-parameter Weibull distribution is fitted to the wind speed distribution for each of the four roughness classes and 12 direction sectors. A moment fitting method is used which ensures that the total energy in the observed and fitted distributions are the same and that the probability of exceeding the observed mean speed is the same in both distributions. The method is designed to ensure a good fit to the higher (but not extreme) wind speeds as these are of most relevance to wind energy applications.

A logarithmic vertical profile is used to calculate the Weibull parameters for four additional heights (25, 50, 100 and 200 m). Finally a correction is applied to account for deviations from the standard logarithmic profile due to stability effects. This correction assumes these deviations are small (being a first order expansion in surface heat flux about a neutral basic state), and takes as inputs climatological estimates of mean and RMS surface heat fluxes. The end result is a set of 240 pairs of Weibull parameters i.e. a value of A (the scale parameter) and k (the shape parameter) for each of 4 roughness classes x 5 heights x 12 direction sectors.

To generate a wind climatology for a target site WAsP takes the results from a reference site (i.e. the Weibull parameters for standard roughness classes and heights, as described above) and modifies them to reflect the characteristics of the target site. The first step is to extract, for each wind direction sector, the Weibull parameters corresponding to the upstream roughness length at the target site and then interpolate them to the required height above ground level. A correction for stability effects is applied at this point. The roughness change, shelter and orographic models are then used to derive correction factors from details of the terrain and obstacles around the target site. These factors are applied to the Weibull parameters to obtain the required wind climatology.

The WAsP software makes use of a number of parameters to control how the models function e.g. the extent of the zone of coastal influence, the height of the inversion, various factors determining the perturbations to the flow due to roughness changes and orography, the mean and RMS heat fluxes etc. These can be modified from their default values by the user.

6.3.3 Published Literature

WAsP has been applied to a wide variety of situations including flat, open terrain (Achberger et al, 2002), offshore locations (Barthelmie et al, 1996; Lange & Hojstrup, 2001), coastal locations (Romeo & Magri, 1994), mountainous terrain (Botta et al, 1992; Reid, 1997), forested terrain (Suarez et al, 1999), extreme winds (Abild, 1994; Kristensen et al, 2000) and short-range weather forecasting (Landberg & Watson, 1994). None of these studies relate directly to the problem of wind flow in urban areas, nor do there appear to be any investigations focussing directly on the shelter model used in WAsP. Amongst these studies there are big differences in the choice of reference data, both in terms of record length (anything from a few months to many years) and type e.g. surface observations from anemometers, surface and geostrophic winds from numerical models, upper-level wind data from radiosondes.

Although it is difficult to draw any general conclusions, the various studies do highlight some interesting points:

Achberger et al (2002) compared WAsP predictions of mean speed and the probability of speeds greater than 6m/s obtained from three types of reference data. For a site in flat, open terrain they found the best results were obtained using data from a nearby anemometer (located 25km southwest of the target site). Using 10m winds from a mesoscale numerical model gave less accurate results and geostrophic model winds gave the poorest results.

Landberg and Watson (1994) looked at using WAsP to apply corrections to individual wind speed values from the HIRLAM numerical model. They found that the best results were obtained using the actual model wind at around 150m above ground level as the starting point (rather than the geostrophic model wind at a higher level, as might have been expected).

Reid (1997) investigated the ability of WAsP to model the wind climatology in areas where there was significant channelling of the wind. The study area was the southern end of North Island,

New Zealand (although the topography of the UK is less extreme, channelling is nevertheless observed in many areas e.g. Cheshire Gap, Vale of York, Bristol Channel, the Central Lowlands of Scotland). Using the default setup, WAsP was found to under-predict both the mean speed and the frequency of winds in the channelled direction. By empirically altering some of the model parameters (specifically the inversion height and 'softness') it was possible to obtain results that were significantly more accurate. It was not clear how values for these parameters should be selected in advance of an analysis. By varying the size of the analysis domain from 3km to 500km across, Reid also demonstrated the importance of ensuring the height data cover a sufficiently large area to capture the dominant orographic features.

Suarez et al (1999) studied an area of mountainous, forested terrain in western Scotland. Using an anemometer on an exposed ridge as their reference site, they found that WAsP produced an accurate estimate of the mean speed at another nearby hill-top site (7.5km to the east-southeast). However for two valley locations in the same area the mean speed was underestimated by around 15%, and for a site in a saddle and a site on the side of a valley the WAsP estimates were too high by 15-20%.

Botta et al (1992) compared WAsP and AVENU (a boundary layer flow model developed in the US). Their analysis, which was for a mountainous area in Italy, found that predictions of the annual energy resource can be out by 30-40%.

Romeo & Magri (1994) found that WAsP produced good estimates of the mean speed for a coastal site in southeast Sicily. They used data from a numerical model as the starting point for the analysis.

Barthelmie et al (1996) found that for offshore locations WAsP tended to over-predict the mean speed. The differences were thought to be due to the incorrect assignment of roughness lengths, but could also be due to stability effects.

Lange and Hojstrup (2001) found generally good agreement between observed and predicted values for offshore locations. Differences were attributed to differences in the length of the sea fetch at each target site. The authors also looked at the vertical profile of wind speed and found some differences from the observed profile. Various possible causes were identified – the lack of wind-speed dependent sea surface roughness, atmospheric stability effects, and incorrect modelling of internal boundary layers due to roughness changes.

Nygaard (1992) used WAsP to correct anemometer data prior to an MCP analysis but only achieved minor improvements in accuracy.

6.3.4 Applicability of WAsP to Urban Environments

There are a number of aspects of WAsP that have a bearing on its ability to predict wind speeds in urban areas. These are discussed below, with the more important factors listed first:

WAsP can model the effects of urban areas, but only as regions of homogeneous surface roughness. It does not explicitly model the roughness sublayer i.e. the region within a few building heights of the top of the urban canopy.

The shelter model only captures reductions in wind speed well away from simple two-dimensional obstacles. It is not valid close to an obstacle where flow separation, interference with wakes from other obstacles and the detailed geometry of the obstacles themselves are all important.



The BZ model can describe the effects of small hills with modest slopes with reasonable accuracy. However it does not represent mesoscale effects, such as the channelling of winds by wide valleys (Frank and Landberg, 1997 – see also the discussion of linear models in §4.4.4). Such effects could be important for some cities in the UK e.g. Glasgow and Edinburgh.

WAsP is also unable to represent thermally induced circulations (e.g. seas breezes) or mountain-valley wind systems (e.g. katabatic and anabatic winds) (Frank and Landberg, 1997). Such winds may be important components of the climatology of towns in coastal and upland regions. However they tend to be relatively light and therefore do not contribute greatly to the total wind energy resource.

The stability correction used in WAsP makes use of fixed (i.e. climatological) values of the mean and RMS heat flux over land and sea. The default values can be changed by the user e.g. to values more representative of urban areas. It is not known how sensitive the results would be to such changes.

6.4 Other Wind Farm Applications Software

There are a number of proprietary systems used by the wind energy industry for planning and designing new wind farm installations. The authors do not have any direct experience of using these systems. However, so far as it is possible to determine from the associated web sites, all of these systems make use of analysis techniques that are described elsewhere in this report. Three of these systems are summarised in the following sections.

6.4.1 WindFarmer

The WindFarmer software can:

- Calculate the wind energy resource directly from on-site observations
- Import wind resource data from WAsP and other wind flow modelling software (WindSim, meteodyn, METRAS)
- Perform an MCP analysis using concurrent measurements from the target site and a reference station

6.4.2 WindFarm

The WindFarm software can:

- Calculate wind flow using the MS-Micro/3 model (which is integrated into WindFarm)
- Import wind resource data from WAsP
- Produce a long-term wind climatology using MCP. The approach involves a separate analysis for each of a number of wind direction sectors.
- Calculate vertical wind profiles

In addition the web site makes reference to an 'alternate roughness change model', although it is not clear what this might entail.

6.4.3 WindPRO

The WindPRO software can:

- Calculate the wind energy resource using a simplified version of the WASP model that is integrated into the software. The model is stated to be suitable for rolling terrain with height differences of less than 50m and only a few, large obstacles.
- Calculate the vertical wind profile
- Calculate the wind energy resource from on-site wind data, either directly or by first fitting a Weibull distribution to the data. In both cases the data are corrected from the measurement height to the hub height using a Hellmann exponential profile
- Calculate the wind energy resource by calling the WASP program (which must be installed on the user's computer)
- Produce a long-term wind climatology using MCP. Four options are supported – a) linear regression, b) a matrix method that uses the joint distribution of wind speed and wind direction, c) scaling of the parameters of Weibull distributions that have been fitted to the data, and d) correlation of monthly averages of the energy yield (derived from either a real or generic power curve)
- Generate files of wind data, orography and roughness in a format suitable for use in WindSim, a CFD software package

6.5 NOABL and the DTI Wind Speed Database

A good example of a mass-consistent model (Section 4.4.6) is the NOABL model, originally developed by Science Applications Inc., USA (Traci *et al*, 1978). Though the authors do not formulate the model using the variational approach, Homicz (2002) points out that their resulting equations are equivalent.

NOABL has been used in a very wide variety of applications. The version used by ETSU to estimate UK wind (Burch and Ravenscroft, 1992) has been heavily modified but the fundamental starting point is a mass-consistent model run over overlapping regions of the UK, each 100x100 km. Given the size of these areas, each region typically only contained one or two observation sites, so most of the spatial variation comes from the mass-consistent model. The most important modifications are first, an attempt at normalisation of input station data to '10 m above short grass' roughness and, second, application of a correction downstream of the coast for roughness changes (see above discussion of internal boundary layers). Though each region was combined to produce a near-seamless map, the authors had to scale individual regions in order to achieve this, using scaling factors varying between 0.726 and 1.321, with standard deviation 0.11. This indicates a level of reliability of the scaling of each region (though not an overall accuracy).

The ETSU analysis used observations for the 10-year period 1975-84 for 56 stations to create grids of mean wind speed covering the UK (Burch and Ravenscroft, 1992). The resultant estimates of mean wind speed are available at a horizontal resolution of 1km and at heights of 10m, 25m and 45m above ground level. These data are collectively known as the DTI Wind Speed Database and can be accessed from the British Wind Energy Association web site (<http://www.britishwindenergy.co.uk/noabl/index.html>).

Figure 27 shows a map of the 10m wind speed from the DTI Wind Speed Database.

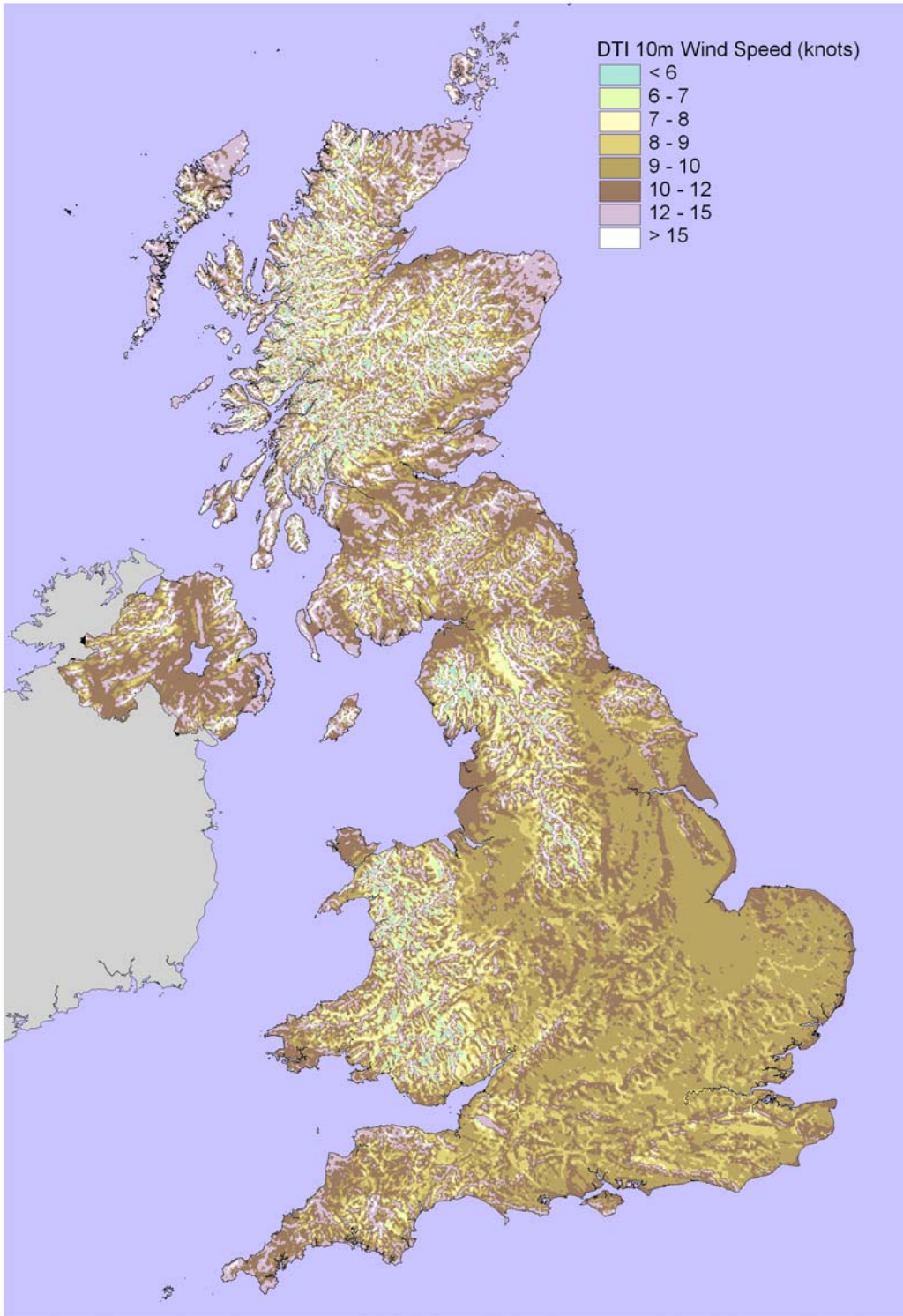


Figure 27: Mean wind speed at 10m above ground level from the DTI Wind Speed Database

Figure 28 compares values from the DTI Wind Speed Database with Met Office long-term averages for the period 1961-90. Points are plotted for all stations with at least 10 years of data during the 30-year averaging period (109 stations). The method used to calculate the station averages is described in section 2.2.1. The station with a mean speed of 21 knots is Great Dun Fell, which is located in the Pennines at an altitude of 847m above sea level. The DTI values have been obtained from the database using bi-linear interpolation of the values for the four 1km

squares surrounding each station. Also shown are the line of equality (pink line) and linear trend line (thick black line).

The average wind speed across all 109 stations is 10.1 knots for the Met Office station averages and 10.6 knots for the DTI database. This bias may be due in part to the different data periods used in the two analyses (1961-90 for the Met Office station averages vs. 1975-84 for the DTI database).

The DTI values also exhibit less variability than the Met Office averages, with standard deviations of 1.9 knots and 2.5 knots respectively. This difference in variability can be seen in Figure 28 which shows that the DTI database tends to over-estimate the mean value at sites with low observed speeds and that for windier sites (observed mean > 12 knots) the database tends to produce under-estimates.

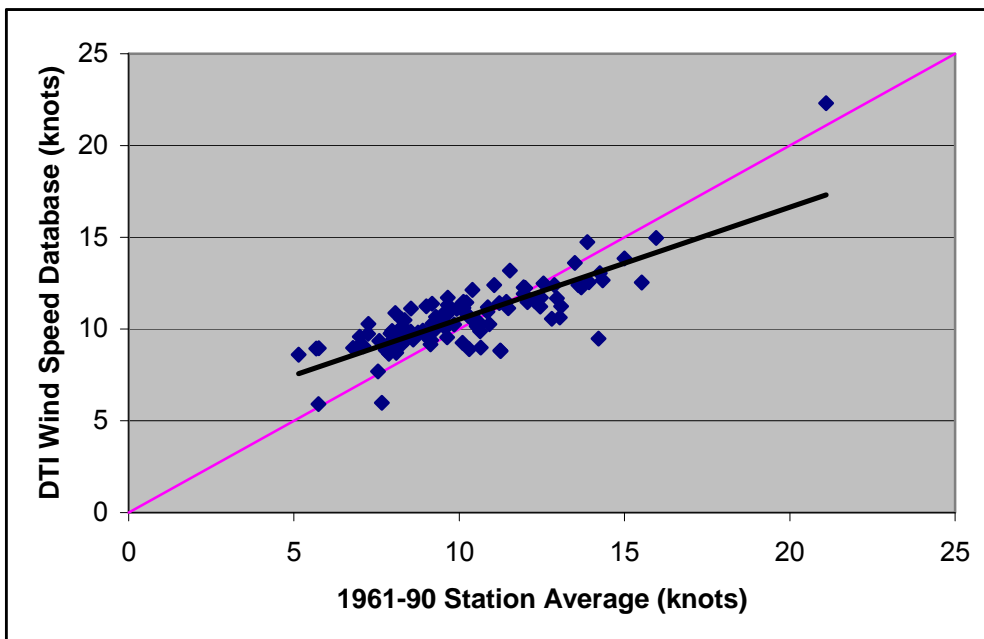


Figure 28: Comparison of mean wind speeds from the DTI database with observed mean speeds from Met Office anemometer stations

6.6 ADMS

Although aimed primarily at dispersion prediction, models such as ADMS (Carruthers et al, 1994; CERC, 2005), AERMOD (Cimorelli et al, 1998) and NAME (Jones et al, 2007; Hort et al, 2002) contain approaches that could be applied to assessing the wind energy resource. The discussion here will focus on ADMS, although we will comment briefly on the similarities and differences between ADMS and the approaches in AERMOD and NAME.

ADMS (Atmospheric Dispersion Modelling System) is a PC-based model for calculating concentrations of pollutants dispersing over short distances, up to say 30km from their source. There are three aspects of ADMS that are relevant here, namely the boundary layer profiles assumed, the treatment of terrain effects, and the treatment of the effect of a single dominant building. In the treatment of boundary layer profiles, ADMS, AERMOD and NAME are very similar, especially in near neutral conditions which are the conditions likely to be of most interest

for wind power generation. For terrain, although AERMOD does model the effect of terrain on dispersion, it does not do this via a model that describes the flow field over the terrain. Hence the terrain aspects of AERMOD are unlikely to be useful for wind power applications. ADMS and NAME have options to make use of the conceptually similar linear terrain models FLOWSTAR and LINCOM respectively. For building effects, AERMOD makes use of the ‘PRIME’ building model (Schulman et al 2000) which is very similar to the ADMS building model, at least at a conceptual level. NAME uses a somewhat different approach for building effects, constructing a mass consistent flow with the right general characteristics around the building (Hort et al, 2002).

The ADMS boundary layer profiles are an example of the idealised analytic semi-empirical profiles which are often used for describing idealised boundary layers (see e.g. Panofsky and Dutton, 1984). They describe the variation with height over ideal homogeneous surfaces of various wind statistics as a function of the friction velocity u_* , roughness length z_0 , surface sensible heat flux H_s and boundary layer depth h_{BL} . The wind statistics in question are (i) the mean wind speed u , (ii) the turbulent velocity standard deviations σ_u , σ_v and σ_w in the along-wind, across-wind and vertical directions, (iii) the turbulent energy dissipation rate, and (iv) the eddy length and time scales. Here ‘mean wind’ means the wind averaged over, say, 30 minutes to smooth out the turbulent fluctuations but to retain lower frequency fluctuations caused by changes in meteorology. In neutral conditions the wind speed and turbulent velocity standard deviation profiles take the form

$$u = \frac{u_*}{\kappa} \ln \frac{z + z_0}{z_0}$$

$$\sigma_u = 2.5u_*(1 - 0.8z/h_{BL})$$

$$\sigma_v = 2.0u_*(1 - 0.8z/h_{BL})$$

$$\sigma_w = 1.3u_*(1 - 0.8z/h_{BL})$$

with $\kappa = 0.4$. These formulae are very similar to other semi-empirical formulae in the literature based on theoretical scalings combined with experimental measurements made over homogeneous surfaces (see e.g. Panofsky and Dutton, 1984). The formulae are not appropriate for heights comparable to the height of the roughness elements of the underlying surface, i.e., in urban areas, they are not applicable at heights below, say, twice the height of the buildings. Also the wind speed profile is based on inertial sublayer theory (the inertial sublayer being the range of heights that are significantly above the roughness elements but still much less than the boundary layer top) and so is not strictly applicable at heights comparable to h_{BL} . However it is used in ADMS right up to the top of the boundary layer. This seems a reasonable approximation given that the wind shear decreases in the upper part of the boundary layer. The use of $z + z_0$ instead of $z - d$ in the wind profile is slightly unconventional, but simply reflects the fact that the profile is intended for use well above the roughness elements where the difference is small. With this choice the wind speed tends to zero at $z = 0$. For comparison we note the neutral wind speed profile assumed in AERMOD is virtually the same, but without the “+ z_0 ” and with the profile replaced below $7z_0$ by a linear interpolation to zero at the surface. The turbulence profiles are also similar. ADMS also contains a parametrization for the relation between the geostrophic wind and the friction velocity in terms of roughness length and stability. Again this is in broad agreement with other such semi-empirical parametrizations in the literature. In addition ADMS makes use of these profiles and the geostrophic wind versus friction velocity parametrization to provide a means to convert winds from one roughness to another. This conversion method is similar to those discussed in sections 4.2.3 to 4.2.5, although in ADMS the whole boundary layer is assumed to have come into equilibrium with the underlying surface.

The effect of terrain on the wind flow is modelled in ADMS using the model FLOWSTAR (Carruthers et al, 2004). The effects of changes in both terrain height and in roughness length are represented. Both the mean wind and the turbulent velocity standard deviations are

diagnosed. The model assumes that an input wind is available which is upwind of and unaffected by the terrain and roughness changes. The model is essentially a linear flow model following the approach described by Hunt et al (1988a, 1988b) for hills and Belcher et al (1990) for roughness changes, although with one extension beyond the linear flow approach. This concerns stable conditions where the 'dividing streamline' concept (Sheppard, 1956) is used to represent the fact that air approaching below a certain height will flow round instead of over the hill. This extension is however unlikely to be relevant to estimating wind energy resource which is dominated by strong wind conditions where stability is relatively unimportant.

ADMS, AERMOD and NAME (Jones et al, 2007; Hort et al, 2002) provide a quantitative description of some aspects of the flow around a single building or a single effective building. Such approaches are designed more for industrial buildings with flat roofs than for residential houses. None-the-less the methods used can give guidance on the extent and general nature of building effects for other types of building. In ADMS and AERMOD there is provision for computing the dimensions of a single effective building from information on a group of buildings. However the model physics only treats a single building and so this will only be appropriate to the extent that the actual flow is approximately like that round a single building. The approaches used in ADMS and AERMOD are very similar conceptually and a detailed comparison is presented by Robins (2001). Here we give a brief summary of the approach used in ADMS (Robins and Apsley (2005), Robins et al (1997)). The building is approximated by a cuboid aligned with the wind direction. The cuboid length (in the along-wind direction), width (across-wind) and height will be denoted by L_B , W_B and H_B . Upstream of the building the flow is not affected. This is clearly an oversimplification but is consistent with the fact that the upstream extent of disturbances is small compared to the downstream extent. There is also no effect at heights above $\min(3 H_B, H_B + 2 W_B)$ which serves as a measure of the vertical extent of building effects. Downstream of the building there is a recirculation region followed by a wake region with reduced wind speed, enhanced turbulence levels, and streamline deflection giving a downward flow.

The recirculation region is represented as a region of strongly enhanced mixing but without any explicit description of the flow being given. The downwind extent of the region from the rear of the building is modelled using an empirically derived formula:

$$\frac{1.8AW_B}{1 + 0.24W_B / H_B}$$

Here $A = (H_B/L_B)^{0.3}$ but with the value of A limited by the values at $H_B/L_B = 1/3$ and $10/3$. For $L_B \geq \min(H_B, W_B/2)$ it is assumed that the separation from the leading edge of the roof reattaches and so the main recirculation region starts at the rear edge of the roof. Otherwise the recirculation region starts from the leading edge of the roof. The recirculation region is taken to be bounded above by the arc of an ellipse in the downwind-vertical plane. If the true building is at 45 degrees to the flow then a strong downwash is created due to vortices shed from the roof. Here the flow above the recirculation is modelled as following the edge of the recirculation region, with this deflection decaying linearly with height to the top of the region affected by the building. The deflection is reduced for other building orientations (it is zero for a building aligned with the flow) and is also reduced for tall buildings ($H_B > (L_B + W_B)/2$). Clearly the details of this downwash model are only directly applicable to buildings that are actually roughly cuboidal.

The wake is represented using a three-dimensional version of the two-dimensional wake theory of Counihan et al (1974). This predicts a wind speed on the centre line behind the building given by

$$u = U_H \left(1 - \frac{0.8 W_B}{2\pi 2\lambda_y} \left(\frac{H_B}{2\lambda_z} \right)^2 \frac{z}{2\lambda_z} \exp\left(-\frac{z^2}{4\lambda_z^2} \right) \right)$$

where U_H is the upstream flow at roof level, λ_y and λ_z are scales for the wake size, z is height above ground and the 0.8 is a semi-empirical constant. λ_y and λ_z are given by

$$\lambda_y^2 = ku_* H_B (x - x_0) / U_H \quad \lambda_z^2 = 2ku_* H_B (x - x_0) / U_H$$

where x_0 is chosen so that $u = 0$ at the rear of the building and u_* is the friction velocity in the undisturbed flow. This is modified a little for the case of very wide buildings ($W_B > 5 H_B$). As the wind speed in the wake recovers, mass conservation implies that there is inflow from the sides and from above. The turbulent velocity variances are enhanced in the wake by a fraction

$$\frac{U_H \Delta u}{u_*} \frac{2\sqrt{2}\lambda_z}{x - x_0}$$

where Δu is a measure of the cross-wake averaged velocity deficit.

6.7 Intercomparisons

A number of papers have been published that compare different methods of estimating the mean wind speed or the wind energy resource. None relate specifically to urban areas. The following is a summary of the key findings:

Guo & Palutikof (1990) compared three mass-consistent models (NOABL, COMPLEX and MC-3) with a potential flow model (CONFORM) and a model based on Jackson and Hunt theory (MS3DJH). For a hill-top site in the Northern Pennines they obtained good estimates of the seasonal mean speed using MC-3, CONFORM and MS3DJH., whereas COMPLEX and NOABL produced underestimates.

Walmsley et al (1990) compared three models based on the linear theory of Jackson and Hunt (Mason-King Model D, MS-Micro/2 and WAsP) with one mass-consistent model (NOABL). Their focus was on the effects of orography – the four models were compared with field observations from Blashaval Hill, North Uist, Scotland. The models gave results that were in good agreement with each other and generally within the range of variation in the observations. Overall the three Jackson and Hunt models performed slightly better than NOABL. For some wind directions the predictions of all four models were outside the range of observed variation, probably because the assumptions on which the models were based were not valid for these directions. Increasing the size of the domain to include hills upwind and downwind of the test site helped to reduce the errors.

Barnard (1991) compared the performance of two models based on Jackson and Hunt theory (MS3DJH/3R and WAsP) and one mass-consistent model (NOABL) for two areas of complex terrain – Askervein Hill in Scotland and the Altamont Pass area of California. Overall they conclude that the performance of all three models is about the same. For Askervein Hill (an isolated hill of moderate slope) the RMS errors in predicted mean speed are 8-10%. Altamont Pass is an area of very complex terrain with many hills and some steep slopes and all three models over-estimate the wind speed in this area. RMS errors are around 25% but these can be substantially reduced (to 9-10%) by incorporating data from more stations into the analysis (either as input to NOABL or for post-processing the output from the linear flow models).

Finardi et al (1993) and Homicz (2002) also compared mass consistent and linear flow models. The performance of mass consistent models was found to deteriorate significantly if there was not sufficient resolution of input data over the topography of interest.

Landberg & Mortensen (1993) compare WAsP and MCP using data from six stations in complex terrain in northern Portugal. They demonstrate that WAsP will produce poor results if the reference station and target site are in different climatic zones. They also show that if low wind

speeds are excluded from the MCP analysis (to improve the fit to the higher wind speeds of interest to wind energy studies) then the technique can produce biased predictions. Errors in the MCP predictions decrease as the monitoring period increases, but there still remains quite a lot of uncertainty in the results (demonstrated by using several different data periods of the same length). The authors conclude that both techniques are capable of making useful predictions, although in complex terrain the uncertainties can be quite large, especially for MCP.

Frank & Landberg (1997) compare values from WAsP with results obtained by down-scaling data from a mesoscale model (see §3.2.2 for more details of this technique). Given that the mesoscale model cannot capture sub-grid scale effects, the comparison is made with WAsP predictions for flat terrain and uniform roughness. The study area is the whole of Ireland. The authors find that the range of values in the mesoscale model predictions is less than that in the WAsP data. Reasonable agreement is obtained for windier sites but for sites with lower mean speeds the mesoscale model tends to over-predict the available wind energy. The likely explanation for these differences is that the down-scaling process does not allow for situations when the surface wind flow is decoupled from the free atmosphere above e.g. due to a temperature inversion.

Suarez et al (1999) compare WAsP and MS-Micro/3 with a scoring system known as DAMS. DAMS was developed for forestry applications to allow the relative windiness of different sites to be compared. It involves assigning a score to each of a number of geographic factors (climatic zone, aspect, elevation, exposure, terrain shape and orientation). An overall windiness score is determined by combining these individual scores together, based on their relative importance as determined from field experiments). The DAMS scores were converted to wind speeds by scaling them by the ratio of the observed mean speed and DAMS score at one particular location in the study area (an area of complex forested terrain in Scotland). The authors found that all three approaches produced variable results. The two linear models were most accurate on exposed hill tops whereas DAMS was more accurate in valleys and on lower slopes. Overall the DAMS system was found to perform as well as the terrain flow models, despite a number of limitations (no surface roughness dependency or wind direction dependency). The DAMS windiness scores have subsequently been calculated for the whole of the country. The authors suggest that DAMS could potentially be used to correct the output from linear flow models.

Achberger et al (2002) compare the WAsP model with three versions of the MCP technique (see previous discussion in §6.2 and §6.3). The target site is a location in southern Sweden in flat, open terrain. They compare results from three different reference datasets – anemometer data from a nearby observing station, plus 10m and geostrophic winds from a mesoscale model. In terms of mean wind speed and the probability of speeds > 6 m/s, the best results were obtained with the WAsP model in combination with the anemometer data.

Landberg et al (2003) summarise eight methods for generating estimates of wind resources: folklore; the use of unadjusted measurements only; MCP; global re-analyses of NWP data (adjusted to the surface using the geostrophic drag law); the wind atlas methodology (i.e. the use of terrain flow models, such as WAsP, or even CFD, to correct surface observations for local effects); the use of on-site measurements to drive terrain flow and CFD models; statistical-dynamical down-scaling of mesoscale model data; the use of terrain flow models to adjust the output from a mesoscale model. They do not consider geostatistical interpolation techniques. The authors identify four areas where estimation techniques need to be improved: in complex terrain; at offshore locations; for large heights above ground level; for sites in forest clearings. For sites in forested areas (arguably the most similar to urban locations, which are not mentioned) they note the need to take into account the displacement height, as well as speed-up and separation effects at clearing boundaries.

7 Siting Guidelines

In this section we consider the relative suitability of different possible small scale turbine locations from the range of choices that would typically be available to a potential turbine purchaser. In contrast to the situation for large turbine arrays, for small scale generation the purchaser is not so much interested in where the best locations in the country are but where the best locations are in the locality of his home. To assess the absolute suitability one would need also to take account of wind strengths in the area using a method like that proposed in part two of this report (Urban Wind Energy Research Project, Part 2: Estimating the Wind Energy Resource). We consider both urban and rural situations, although the main interest here is for urban wind power generation.

From a meteorological perspective, there are two main issues to bear in mind in siting a wind turbine. These are that wind speed generally increases with height and that upwind obstructions tend to reduce wind speed and increase turbulence levels. High turbulence levels can reduce the effectiveness of wind turbines. There are also some other meteorological issues which arise if one has a large area to choose from in siting the turbine and there are significant differences in the character of the terrain across the area. In practice there will of course also be other non-meteorological issues to consider, such as the cost and safety of erecting and connecting the turbine, the ease and safety of maintenance, the noise and vibration from the turbine, and planning permission. However we are not concerned with such issues here. Some of these issues are discussed by BRE Certification Limited (2007) and Gipe (2004).

Turbine Height: We consider first the question of height. All else being equal, the turbine should be mounted as high as possible. Wind speed generally increases with height according to the log law:

$$u = \frac{u_*}{\kappa} \ln \frac{z-d}{z_0}$$

(see section 4.1). As a result, the fractional increase in wind speed $\Delta u/u$ for a given fractional increase in height $\Delta z/z$ is given by:

$$\frac{\Delta u}{u} \approx \frac{\Delta z}{z} \times \frac{1}{\left(1 - \frac{d}{z}\right) \ln \frac{z-d}{z_0}}$$

This means that the advantages of increasing the height are larger over rough surfaces (such as urban areas and forests where z_0 and d are large) than they are over smoother areas. Note that the equation is only formally justified at heights well above the roughness elements (buildings, trees etc). However there is some evidence that in urban areas it works reasonably well in practice down to near the top of the building “canopy”, although with somewhat more scatter and variability from one location (in the horizontal) to another. The equation also assumes neutral conditions, but these are the most important when considering wind energy as the stability is normally close to neutral in strong winds. The factor on the right hand side of the equation can be estimated using typical values of z_0 and d as given, for built-up areas, in Table 4 in section 4.1. For rural (non-built-up) conditions there are numerous tables of values available, especially for z_0 . The following values of z_0 are based on those used in the Met Office Unified Model and the Met Office Surface Exchange Scheme II (MOSES II) (see Essery *et al.* 2001):

	Forests	Shrubs	Open country/Grass	Water
z_0	$h / 20 \approx 1 \text{ m}$	$h/10 \approx 0.18 \text{ m}$	0.14 m	0.0003 m

Here h is the height of the trees or shrubs. The true roughness for short grass itself is rather smaller than given here, say about 0.03 m, but it is rare to have extensive grassland uninterrupted by hedges, bushes etc, so the value given in the table is generally more appropriate in practice (and is the value currently used in the Met Office Unified Model). The displacement height d can be neglected in rural settings except for forests where it can be estimated as 2/3 of the height of the trees (Oke 1987, p116).

At heights below the top of the roughness elements the wind decreases rapidly with height and becomes more turbulent (relative to the mean wind speed) and harder to predict. As a result such locations should be avoided if possible. The estimates given in the second half of this report (Urban Wind Energy Research Project, Part 2: Estimating the Wind Energy Resource) show generally poor turbine performance is expected at heights just above the canopy top; within the canopy the results will be worse.

Note that, when we refer to roughness elements in the above, we have in mind the general character of the neighbourhood. For an isolated house in an open rural setting, the house would not be included in the roughness elements but would be regarded as an “isolated obstruction”.

Obstructions: The second key issue to consider is obstructions to the wind flow. Obstructions fall into two main types (with some overlap): those that form part of the general surrounding roughness (e.g. a house in an estate of similar houses) and those that protrude above the general roughness and form more isolated obstructions (e.g. a tower block in an area of one or two storey housing). The obstructions which form part of the general roughness act collectively to slow the flow, but the effect of any one element is not very large. This is especially true as regards the flow above the roughness canopy where, for reasonably dense canopies, the flow tends to skim over the top of the canopy. In contrast the obstructions which protrude above the general roughness generally have a much larger effect, especially in the case of buildings. They can cause substantial vertical motions up and down the front face of the building, large separation and wake regions, and downwash behind the building (see section 5.1.3). The reason for the difference is primarily because in the former case the flow is already substantially slowed within the canopy by the other roughness elements. Hence the energy and momentum of the flow within the canopy is low and, even when deflected by obstacles, is insufficient to substantially affect the flow above the canopy. The CFD study by Heath *et al.* (2007 – see especially figures 9 and 10) shows clearly the different character of the flow around a building in the two cases.

Of course in reality obstructions form a continuum between those which are clearly embedded within a canopy and those that are more isolated. At one extreme we have, for example, a low density rural environment where the spacing between buildings may be large enough that the flow, after being disturbed by one building, has time to reach equilibrium with the ground before encountering another building. At the other extreme we have the narrow street canyon where the size of the recirculation behind one row of buildings is constrained in size by a second row. In between we have situations where the separated flow behind a building reattaches, but where the next building lies within the low velocity wake of the first building.

As a rough rule of thumb we regard an obstruction as being part of the general canopy if there are a number of other obstacles of similar or greater height nearby with at least one within a horizontal distance of 5-10 times the obstacle height. A certain amount of judgment and common sense is needed in applying this, e.g. one might in the case of trees, regard a small clump of trees as a single obstacle. The basis for this criterion is as follows. The typical length of the recirculation region behind an isolated building (see section 5.1.3) is between 3 and 12 times the building height. Also the street canyon results of Sini *et al.* (1996) show that the street canyon vortex splits into two and eventually reattaches as the street width increases from 5 to 9 times

the building height. The length of the wake region behind an obstacle can of course be much longer than the recirculation region, but that length is more relevant as a criterion for there to be some influence of one building on the next rather than for the obstacles to form a canopy. Oke (1987, p266) gives a somewhat lower spacing of about 3 times the building height for the recirculation regions behind and in front of buildings to collide (he calls separations greater than this “isolated roughness flow”, although this does not mean that there is no interaction between the far wake beyond the recirculation region and the next building).

Obstructions forming part of the canopy: We consider obstructions which form part of the general canopy first. Because the flow tends to skim over the top of the canopy the effect, on a turbine mounted above the roof tops, of any individual roughness element is likely to be small. There is no particular reason to take such obstacles into account in siting the turbine, although there will of course be a general reduction in wind speed from their collective effect. This conclusion will be less reliable the closer one is to the canopy top. However even here there is little likelihood of being able to predict departures from the horizontally averaged wind without a detailed site-specific study, for example in a wind tunnel or through wind speed measurements at possible siting locations. This is because the effects will depend on the detailed geometry of a number of the obstructions. Also the results will vary with wind direction and in general we would expect there to be no location at the height of interest which is preferred for all wind directions.

If the location is below the height of the obstacles then the situation is different. The wind speed in general at such heights will be reduced and the effects of the roughness elements will vary as the turbine location varies in the horizontal plane at the height of interest. In particular there is a danger of encountering recirculating flows. The primary advice must be to mount the turbine higher if at all possible. However if this is not possible then one should choose a location with as much unobstructed view as possible in the direction from which the prevailing wind blows. As in the case of locations close to the top of the canopy, the results will in general be hard to predict without detailed study. However unlike the former situation, the effects of the precise siting will be more important.

The CFD study of Heath *et al.* (2007) shows examples where the ‘maximum unobstructed view’ approach is not optimal for a turbine at or below the canopy top. This illustrates the difficulty of making reliable general rules for such situations. They consider possible mounting locations on a detached pitched roof house in an array of similar houses. When considering mounting below the maximum roof height they find that for some wind directions the optimal location is at the downwind corner. Unfortunately they only give the wind speed at the optimal location so it is not possible to compare with that at other locations. However in such locations the performance may be compromised by turbulence and we would not recommend such locations without detailed site-specific study.

Isolated obstructions: We now consider isolated obstacles. These can produce effects over large areas. In the case of buildings the effects can extend up to 2-3 times the obstacle height above the ground (more for buildings with width much greater than height) and up to 30 times the building height in the downwind direction, although for buildings with strong roof top generated vortices the wake can persist further downwind (see sections 5.1.3 and 6.6). The upwind extent of the influence is generally small.

We note also the guidance for making meteorological wind observations given by the Met Office (2000). These say the ideal is open terrain with no obstructions within 300m. However if there are significant obstructions they recommend raising the anemometer to at least the height of the obstacle and sometimes more, depending on the size and distance of the obstacle. If the wind is measured by a mast on a roof top, they recommend a measurement height of at least half and ideally three-quarters of the building height above the roof. In practice it may be impossible to meet these high standards in siting turbines and avoid any influence from such obstructions.

However it should be remembered that even small effects on wind speed can have a significant effect on power output. Isolated trees or groups of trees and hedges are likely to have effects on the flow which are similar to but somewhat smaller than buildings of the same size (see section 5.1.3).

As a result of the above, the primary guidance must be to put the turbine as far away from such obstacles as is practical, especially when the obstacle is in the upwind direction relative to the prevailing wind direction. This should ideally be either 30 obstacle heights downwind or 2-3 obstacle heights above ground. In many cases this will be impractical and compromises will be required. However, if this is the case, one should try to ensure that one is well outside any recirculation region behind the obstacle, at least for obstacles which are upwind for the prevailing wind. This region can be regarded as extending to typically 3-10 building heights downwind, with the larger values being applicable to obstacles for which the width is large compared to the height (see section 5.1.3). The height of the recirculation is more complex to assess. It is at least equal to the height of the obstacle, but may be deeper, say 1.5 times the building height, for buildings that have pitched roofs (see simulations in Heath *et al.* (2007)) or whose along wind dimension is short enough for roof top reattachment not to occur (see section 5.1.3).

Separate considerations are needed if the turbine is to be mounted directly on a building which constitutes an isolated obstruction. For flat roofed buildings, the height above the roof should exceed the height of any roof top recirculation region or wake region. This can be estimated as $0.28 \min(W_B^{7/9} H_B^{2/9}, W_B^{5/9} H_B^{4/9})$ using the results of Wilson (1979) – see section 5.1.3. Here W_B is the maximum of the length and width of the building and H_B is the height of the building. For pitched roof buildings, one should again aim to keep the turbine out of the recirculation region. We do not have a lot of evidence to say what this requires in terms of mounting position. However, based on the isolated building simulation by Heath *et al.* (2007), we propose the following. The turbine should be mounted at least half the height of the roof (i.e. half the vertical distance from the roof base to peak) above the peak, or should be mounted at or in front of the peak from the perspective of the prevailing wind direction (and ideally both).

In some situations the wind speed can be enhanced by flow over buildings. However it is difficult to exploit this without a detailed site-specific study. The speed up is likely to be restricted to a certain range of wind directions and may be associated with significant vertical motions or increased turbulence which may reduce or eliminate the benefit, even for the directions which do yield a speed up.

Larger scale terrain variations: If there is a wide area over which the turbine could be located, such as may be the case on farms or large estates or where someone is fine tuning their choice of where to live based on the potential for wind power, then there are additional considerations that arise. For example it is appropriate to choose areas where the general character of the area is as smooth as possible, preferring e.g. open grassland to forested areas.

This is not just a question of obstructions – an unobstructed location above a rough area such as a forest will generally experience substantially lower wind speeds than are found at the same height over a smooth surface such as grass. In principle there is an exception where the rougher area is too small to affect the wind at the turbine height. However unless the turbine is especially high or the rough area very small (in which case it may be better regarded as an obstruction) this is unlikely to be relevant in practice (see Figure 9 and note that, for the relevant part of the graph near the origin, the growth of the internal boundary layer is rapid; in addition there is considerable uncertainty in the initial growth with complications due to displacement heights and vertical motions generated as the flow decelerates).

In general one should regard a region as rougher if the roughness elements are taller or more densely packed. However this is not universally true. If the roughness elements are all of a

similar height – e.g. a collection of similar houses – then the roughness can decrease as the housing density increases due to the tendency for the flow to ‘skim’ over the top of the buildings (see discussion in section 4.1). If one has to locate the turbine over a rougher area, it is appropriate to prefer locations where the distance to a smoother area is small and where the shortest distance to the smooth area is in the direction of the prevailing wind.

For example one would prefer locations near the south-west edge of a town (where that’s the prevailing wind direction) to those elsewhere (even if the south-west wasn’t substantially less urban). It’s harder to compare the centre and the north-east edge - the north-east will be better for north-easterlies but worse for south-westerlies than the centre (assuming similar urban density at the two locations) and so the net effect will depend on the relative frequencies of different wind directions and the size of the urban area.

There are also benefits in siting turbines on the tops of hills. Here the speed up can be substantial (see section 4.4.1). However if the hill is not smoothly varying in height (an extreme case would be at the edge of a cliff top) then the turbulence may be excessive. Also, if the terrain is steep, greater than something in the range 1 in 5 to 1 in 2 (the value depends on the ratio of the hill length scale to the roughness length – see Wood 1995, figure 11), one should be right at the top to avoid being in a region of separated flow behind the hill, or at least one should be on the upwind side of the top from the point of view of the prevailing wind direction.

Mast versus building mounting: The question of whether one should mount the turbine on a mast or on a building is a significant issue. A mast can enable one to mount the turbine at a higher height or further from obstacles and so better meet the above criteria for siting. However we are not aware of any purely meteorological reason why a mast is intrinsically superior if the above guidelines can be met in another way. Of course the non-meteorological reasons may also have a role to play in deciding whether to use a mast (see discussion in Gipe (2004)).

Non-optimal siting: In situations where the power requirement is low or where the wind is sufficiently strong, there is more scope for siting the turbine in a position which is non-optimal from a meteorological perspective. One could even conceive of choosing such a site deliberately to keep the winds more within the optimal range of a turbine. However it should be kept in mind that if a turbine is in a location where there are significant effects from obstructions to the flow, then the results will be less predictable.

Summary: The main issues for the optimal siting of a small scale wind turbine can be summarised as follows.

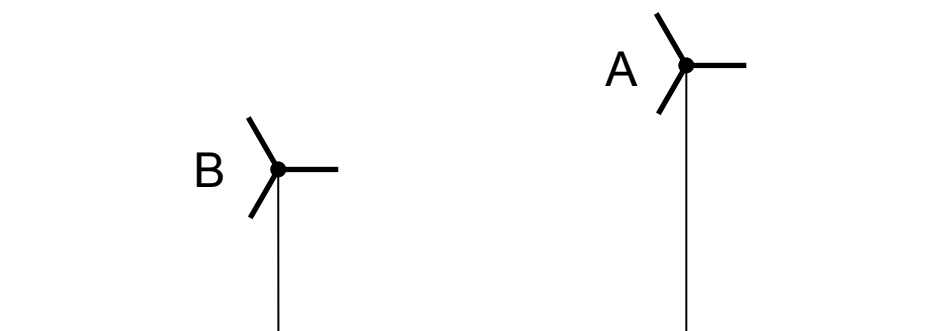
- Locate the turbine as high as practical
- Locate the turbine above the general level of the roughness elements (buildings, trees etc) if at all possible
- If, despite the above, the turbine is to be below the general level of the roughness elements, ensure the view in the direction of the prevailing wind is as unobstructed as possible
- For each obstacle that protrudes above the general level of the roughness elements (e.g. a tower block within an area of generally one or two storey housing) which one is not trying to fix the turbine to:
 - Try to ensure that the turbine is located **either** further away than 3 to 10 times the obstacle height, with the larger factors applying to obstacles with a large width to height ratio as seen from the turbine location, and further still if possible up to 30 obstacle heights, **or** higher than 1 to 1½ times the obstacle height, with the larger factors applying when the obstacle is a pitched roof building or a building with an along-sight length viewed from the turbine location which is less than the height, and higher still if possible up to 1¾ to 2 obstacle heights
 - If this is impossible, try to do it for such obstacles in the prevailing wind direction

- For a turbine mounted on a flat roof building that protrudes above the general level of the roughness elements:
 - Try to ensure that the turbine height above the roof is at least $0.28 \min(W_B^{7/9} H_B^{2/9}, W_B^{5/9} H_B^{4/9})$ where W_B is the maximum of the length and width of the building and H_B is the height of the building
- For a turbine mounted on a pitched roof building that protrudes above the general level of the roughness elements:
 - Try to ensure that **either** the turbine height above the roof peak is at least half the vertical depth of the roof (base to peak) **or** the turbine is mounted at or in front of the peak from the perspective of the prevailing wind direction (and ideally both)
- Locate the turbine over a rural, non-forested area in preference to built up or forested areas
- If in a built up or forested area, locate the turbine near the edge of the area and near the point on the edge of the area that is upwind of the area from the perspective of the prevailing wind
- Locate the turbine near the top of smoothly varying hills, but be cautious about sharply varying terrain (e.g. cliff tops may be very turbulent; also if the terrain is steep one should be right at the top or, if this is impossible, on the upwind side of the top from the point of view of the prevailing wind direction).

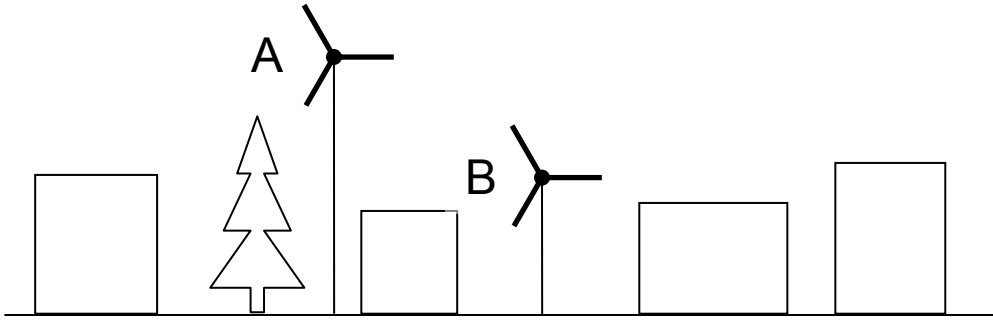
These guidelines are illustrated in somewhat simplified form in Figure 29. We note that it is impossible for these guidelines to cover all possibilities and that, to interpret the guidelines appropriately in a complex situation, it is useful to understand the motivation for the guidelines. Also, especially when there are obstructions to the flow, results may not be very predictable without a detailed site-specific study, for example in a wind tunnel or through wind speed measurements at possible siting locations.

Figure 29: Illustration of the siting guidelines in simplified form. In each case, location A is preferred to B and, if C is present, B is preferred to C. Except where stated otherwise, the arrow indicates the prevailing wind. The figures illustrate the effect of (i) height, (ii) being above or within the canopy layer, (iii) having an unobstructed view for the prevailing wind, (iv) obstacles which are taller than the general urban canopy height, (v) obstacles which are taller than the general rural canopy, (vi) recirculation and wake above flat roof building (here the arrow is just an example wind direction), (vii) roof effects on pitched roof buildings, (viii) open country, forested and urban terrain, (ix) upwind edge of urban area (from prevailing wind perspective) versus centre and downwind edge, (x) hills. The figures should be regarded as simplified mnemonics for the guidelines but not as substitutes for them.

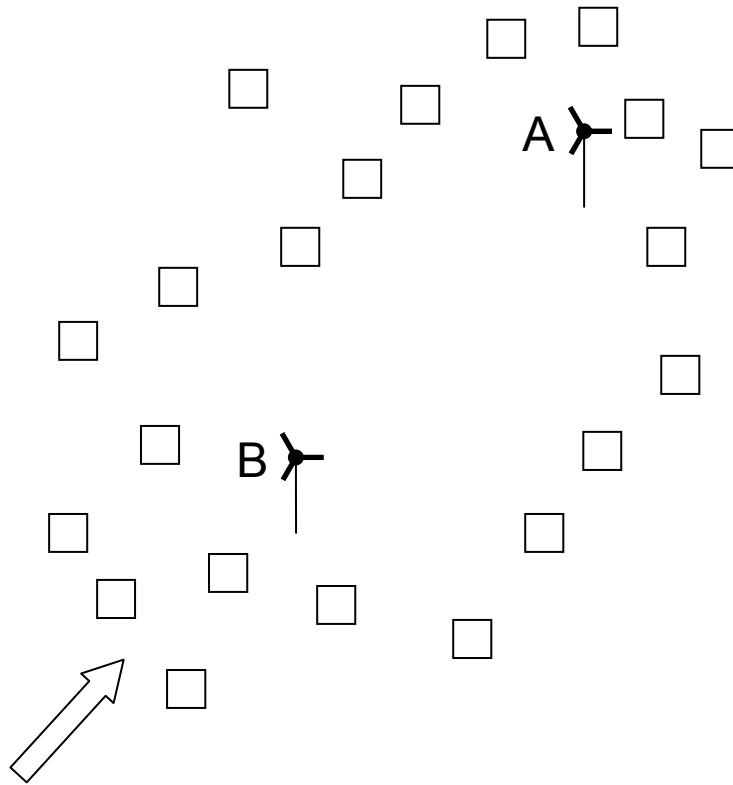
(i)



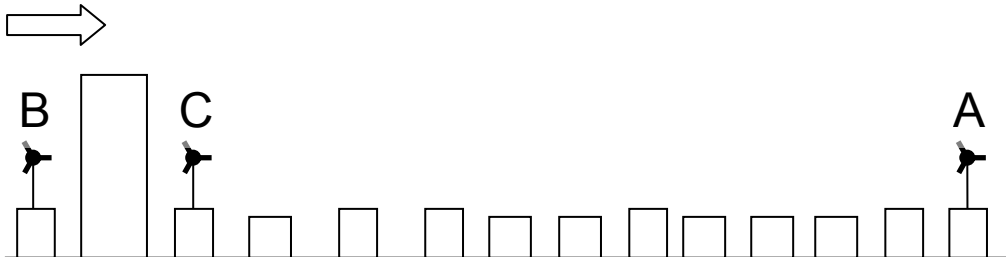
(ii)



(iii)



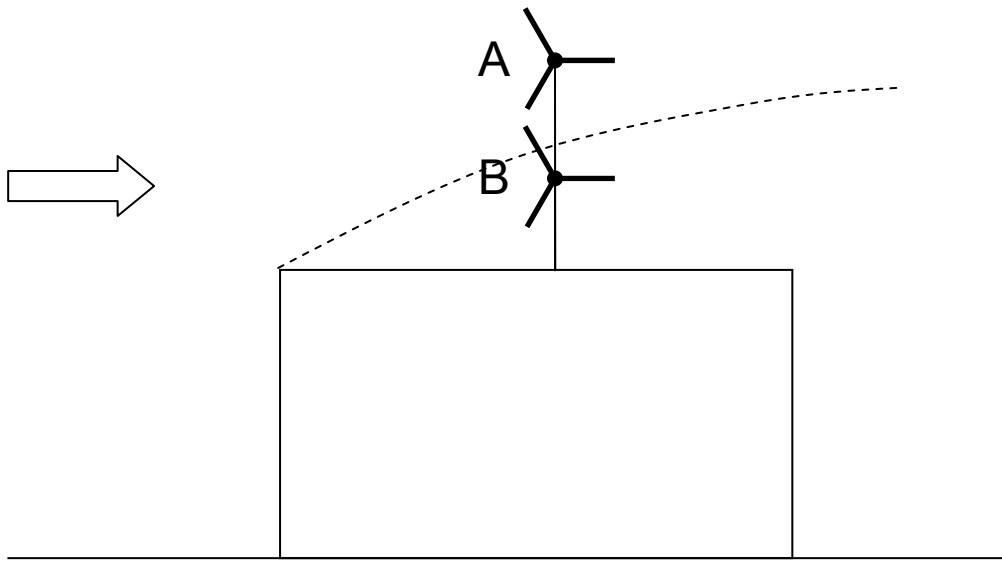
(iv)



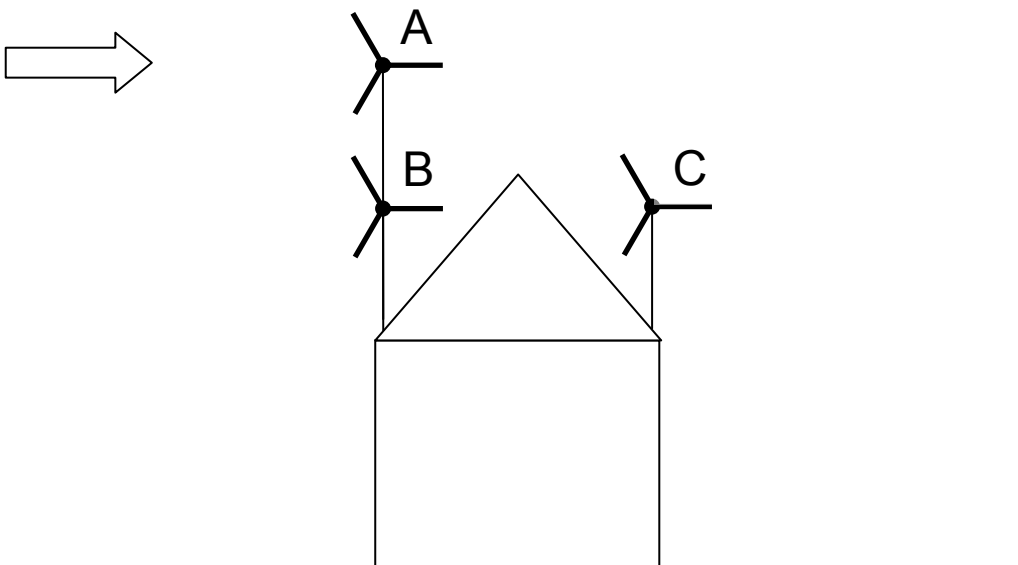
(v)



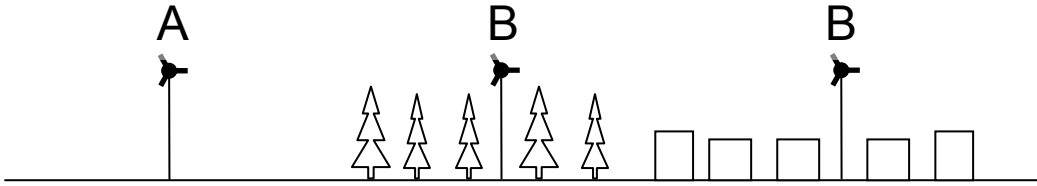
(vi)



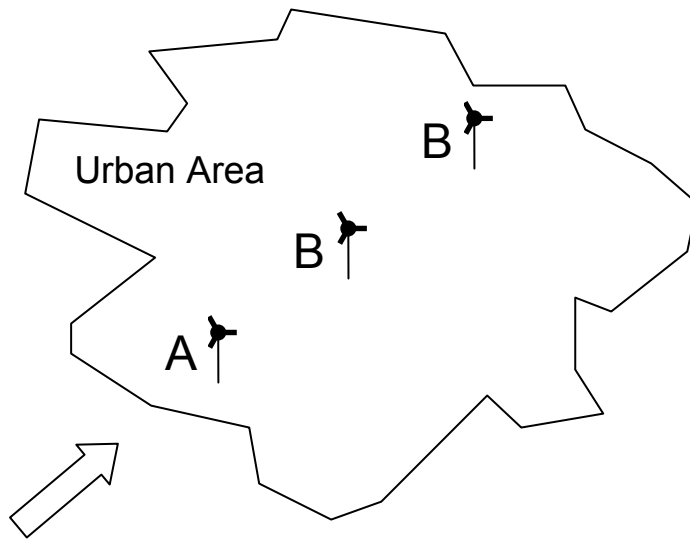
(vii)



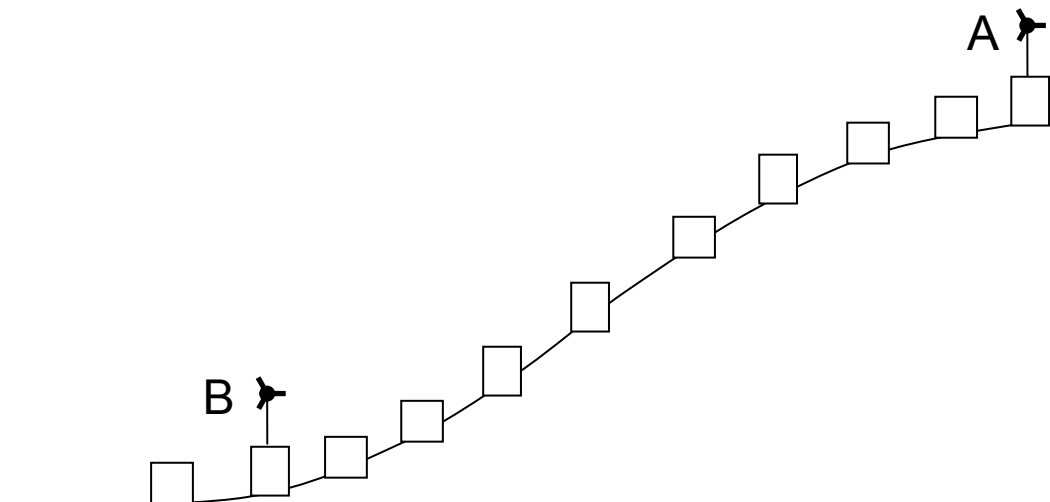
(viii)



(ix)



(x)



8 Summary

Chapter 2 – Conventional Surface Observations

The Met Office anemometer network includes a number of sites in urban areas. However few, if any, have exposures that are typical of urban wind turbines.

Long-term averages of wind speed have been calculated for 1961-1990 and 1971-2000 for the sites in the Met Office observing network.

The 2-parameter Weibull distribution is widely used for modelling the wind speed frequency distribution. The acceptance of this as the only distribution to use is questioned by some researchers.

Chapter 3 – Atmospheric Models

Conceptually the atmosphere can be represented by a number of layers i.e. free atmosphere, boundary layer, inertial sublayer, roughness sublayer, canopy layer. Different processes dominate in each layer, but the layers are nevertheless interdependent i.e. each layer influences, and is influenced by, the adjacent layers. The urban boundary layer has a particularly complex structure involving wide variations in time and space.

The wind speed in the free atmosphere is proportional to the horizontal pressure gradient. Climatologies of wind speed at levels above the boundary layer can be obtained in a number of ways e.g. from surface pressure data, from radiosonde data, or by correcting surface wind data.

The winds nearer the surface are driven by, and vary with, the wind in the free atmosphere. In strong wind conditions the effects of heating and cooling of the atmosphere are not significant and over uniform terrain the vertical profile of wind speed has a logarithmic shape. However the relationship in general is complex and time-varying. Even in simple situations (neutral stability and open terrain) it is difficult to predict the surface wind to within 10% purely from the wind speed in the free atmosphere.

Operational weather forecast models (NWP) and reanalyses are important sources for the derivation of climatologies of wind speed and direction at heights above the boundary layer. The major drawback of reanalyses is the relatively coarse horizontal resolution of 100-200km currently available. Finer scale (~10km) climatologies have been derived by a variety of methods: statistical, statistical-dynamical and dynamical adaptation, which are increasingly expensive in computation and processing. To reduce costs a smaller set of finer-scale model simulations are performed based on a classification of the reanalyses into classes.

Operational NWP limited area models offer a more direct approach by forming means of the past weather forecasts of wind. These are currently available at ~10km resolution. The advantages are that the computing cost of dedicated simulations is saved and potentially all weather regimes and transitions may be sampled to produce a consistent and comprehensive climatology. A possible disadvantage is that the models have evolved over time and so the accuracy of the data is not uniform over long periods.

Chapter 4 – Boundary Layer Models

Urban areas are represented in numerical models at various levels of complexity. The simplest models characterise urban areas as homogeneous regions. Others resolve detail within built-up

areas, distinguishing between, say, urban areas, suburban areas and open spaces (parks etc). The most sophisticated models can resolve street canyons, or describe the flow around individual buildings. The level of detail depends on the scale (global, regional or local) and purpose (operational weather forecasting or scientific research) of the model.

The drag exerted on the wind at the surface is parametrized in large-scale modelling through a lengthscale called the roughness length. The roughness length is greater over urban surfaces than many other types of surface. Values are difficult to determine accurately even for homogeneous urban areas, and a variety of methods have been proposed for estimating both the roughness length and a related parameter known as the displacement height, which quantifies flow-blocking effects.

Urban areas alter the rate at which heat energy is exchanged between the surface and the air above and they also affect the dissipation of that energy into the lower layers of the atmosphere. This affects the stability of the air and hence has an impact on the wind flow through and immediately above the buildings.

Linear flow models (e.g. MS3DJH, BZ, FLOWSTAR) are often used to represent the effects of hills. Although there are differences in the details of their formulations, they fundamentally share the same strengths and weaknesses. In general, they are probably adequate for representing the effects of small-scale hills in the vicinity of the majority of urban areas in the UK, with the errors introduced through the assumption of linearity being smaller than those associated with other uncertainties (e.g. the representation of the effects of the urban areas themselves on the wind). Representation of the effects of larger-scale hill ranges (such as the Pennines) through linear models is likely to be less successful as channelling effects will not be well modelled, and the idea of a single 'undisturbed' profile becomes more problematical. For these larger scales, non-linear models (such as those used in NWP) will perform better.

Mass consistent models can produce a reasonable wind field given sufficient input data. However, they have only limited predictive skill in representing the effects of small-scale hills that the input observational data do not resolve.

Chapter 5 – Urban Roughness Sublayer

The effect of the urban area on the atmospheric boundary layer above say 2 to 3 times the building heights can be represented by a roughness length and a displacement height. In this region the usual logarithmic wind profile (or the stability corrected logarithmic wind profile) holds. However below this height, in the "roughness sublayer", the flow is more complex. It is more complex still within the "urban canopy sublayer" which is the bottom part of the roughness sublayer extending up to the top of the urban "canopy". The horizontally averaged wind profile in the roughness sublayer tends to have a maximum in the wind shear (i.e. an inflection point in the wind profile) at the canopy top, with a quasi exponential decay of wind speed with height towards the ground. This horizontally averaged flow can be modelled by mixing length models. However, although these models have led to an understanding of the basic physics, accurate predictions are difficult, especially near the top of the canopy where the wind speed varies rapidly with height.

The flow in certain idealised building configurations is also quite well understood. Particular configurations discussed include the idealised "street canyon" and the isolated building. The latter is probably not of wide interest for urban flows, but is relevant towards the edge of urban areas as the building density decreases or for particularly large buildings which have a dominant effect over that of the surrounding buildings.



In more complex situations with many buildings, wind tunnel experiments or numerical simulations offer a tool to understand the flow in detail. However there is still a need to test such approaches against full scale measurements.

There are a number of full scale field studies that have been conducted to help understand urban flows. Results from DAPPLE (Marylebone Road), Salford, Birmingham and MUST experiments have been discussed. The last of these is a field trial, although not full scale, consisting of a mock urban setting constructed from shipping containers. Field experiments in Birmingham and Salford showed that wind speeds at 15m above ground in a built-up area can be 20% less than those at 10m above ground in open terrain. Also the variations of wind speed with height above ground level can be approximated by a simple power law. The experiments also showed that estimates of surface roughness can be derived from land use data together with estimates of the upwind fetch over which the surface influences a given measurement.

Chapter 6 – Applied Tools

Geostatistical interpolation techniques have been used to interpolate station long-term averages onto a 1km grid. However these grids do not attempt to capture the effects of urban areas on the mean wind speed.

The measure-correlate-predict (MCP) technique estimates the wind climatology of a target site by using the statistical relationship between concurrent observations from the target site and a nearby reference site to correct the reference site climatology. There is no practical reason why the MCP method could not be applied to urban locations – a sample calculation for a site in the centre of Norwich suggested that satisfactory results can be obtained. However the skill of the technique depends on the statistical correlation between the target site and reference station and it seems likely that this will be lower for typical turbine locations than for more exposed sites.

WAsP can model the effects of urban areas, but only as regions of homogeneous surface roughness. The shelter model treats obstacles in a fairly simple way and is only applicable at some distance from the obstacle (at least five times the obstacle height). WAsP is unable to model the details of the wind flow close to buildings and other obstacles. The WAsP software has been used to estimate the wind climatology in a wide range of situations including offshore locations and complex terrain. There do not appear to be any published studies relating directly to the wind climatology of urban areas.

Proprietary software packages used by the wind energy industry (e.g. WindFarmer, WindFarm and WindPRO) make direct or indirect use of several techniques for modelling the wind climate. These include boundary layer flow models (WAsP, MS-Micro/3), MCP and CFD.

The 1961-1990 station averages have been used to assess the 10m data from the DTI Wind Speed Database. The DTI Database tends to over-estimate the mean wind speed at sites with low observed averages and under-estimate the mean at sites with higher observed averages.

Models for the dispersion of pollutants such as ADMS, AERMOD and NAME contain algorithms for describing the flow which have potential for application to wind energy problems. For example, ADMS includes (i) parametrizations of boundary layer wind and turbulence profiles over homogeneous terrain above the roughness sublayer, (ii) a linear flow model for predicting terrain effects on the flow, and (iii) a model which predicts aspects of the flow around isolated buildings (although this does not provide a complete flow field).

Various inter-comparisons of WAsP, MCP, NOABL and down-scaling of NWP models have been published. These shed some light on the relative strengths and weaknesses of the different



approaches, however none of the studies relate specifically to the problem of predicting wind speeds in urban areas.

Chapter 7 – Siting Guidelines

Drawing on the information contained in the preceding chapters, an assessment has been made of the relative suitability of different locations for small-scale wind turbines. Consideration has been given to positioning both pole-mounted and roof-mounted turbines. The key factors to consider are the height of the turbine and the influence of upwind obstacles. Guidelines have been produced covering a variety of common situations.

9 Conclusions

The aim of this first phase of the project has been to examine the range of existing data sources, analysis techniques and tools that might be used to a) clarify the performance of small-scale wind turbines in urban areas, and b) clarify how turbines should be sited for maximum carbon savings. The following conclusions are drawn:

The extent of data available to describe wind conditions in urban areas:

- There are a variety of sources of wind speed and direction data available, including anemometer data (both routine measurements and from field trials), NWP data and reanalysis data.
- All of these data types have limitations, either in terms of their temporal or spatial extent, or in terms of their representativity of urban areas.
- Any of these data sources could, in principle, be used to estimate wind conditions in urban areas if combined with appropriate interpolation, correction or downscaling techniques.
- There are no existing datasets from which it would be possible to estimate directly the total UK wind energy resource from micro-generation.

The state of the art in predicting wind conditions in urban areas:

- There are a range of techniques available for predicting wind conditions near the surface, including NWP models (with or without downscaling), linear flow models (e.g. WAsP), simple analytic models of fetch effects and roughness changes, MCP, geostatistical interpolation, mass consistent models (e.g. NOABL) and CFD.
- These techniques have applications in a wide variety of situations e.g. weather forecasting (NWP models), climate monitoring (geostatistical interpolation), pollutant dispersion modelling (linear flow models), wind farm siting (linear flow models, MCP, mass consistent models), modelling fluid flow (CFD).
- None of these techniques have been developed specifically for predicting wind conditions in urban areas.
- Through the use of appropriate input data, combination of techniques, model tuning and calibration, any of these techniques could be used to predict urban wind conditions.
- Note that there are practical limitations associated with using some of these techniques to generate predictions over a large area such as the UK e.g. the amount of data processing that would be required, issues associated with ensuring the predictions vary smoothly and consistently over the analysis area etc.

Applicability of techniques developed for large-scale wind farms:

- None of the principal data sources or analysis techniques used for siting large-scale wind farms was developed with urban wind energy generation in mind.
- The DTI Wind Speed Database (created using the NOABL model) does not reflect the effects of urban areas (the wind speed values are representative of open, level terrain).
- The WAsP model can describe the large-scale effects of areas of high surface roughness (such as urban areas) but is not designed to model the wind flow close to buildings.

- The MCP technique *can* be applied to urban locations although the quality of the predictions depends on the level of correlation with the reference site. However, given the need to gather data from the target site (and that in urban areas these data will be representative of a very limited area), this is not a practical technique for estimating wind conditions over large areas.
- Tools such as WindFarmer, WindFarm and WindPRO do not include any functionality designed specifically for siting turbines in urban areas.

Siting of turbines:

- For maximum efficiency, turbines should be sited as high as possible and away from any obstructions (particularly in the prevailing wind direction).
- General guidelines on siting have been given for a number of idealised situations (including some specific recommendations for how high, or how far from an obstacle, a turbine should be sited).
- However, in many real situations (particularly in urban areas) there will be several competing factors to consider and/or the exposure of the site will be very complex. For such locations it is likely that a detailed site-specific study will be required to determine the optimal position for a turbine.

The second part of this report (Urban Wind Energy Research Project, Part 2: Estimating the Wind Energy Resource) will examine how estimates of the UK energy resource from small-scale turbines can be derived using the available analysis techniques and data sources.

10 Glossary

Boundary layer – That part of the atmosphere that is adjacent to the Earth's surface and which is affected by the properties of that surface.

Canopy layer or *sublayer* – The part of the atmospheric boundary layer occupied by the roughness elements (buildings in the urban case).

Fetch – The area upwind of a site, over which the air has travelled.

Flow separation – The process by which an eddy forms on the windward or leeward sides of bluff objects or steeply rising hillsides.

Flux – Rate of transport.

Hydrostatic equilibrium – The state of balance between the force of gravity and the vertical component of the pressure gradient force. It is a state of the atmosphere in which there is no vertical acceleration of the air.

Inertial sublayer – The part of the atmospheric boundary layer that is much lower than the boundary layer depth but much higher than the surface roughness elements.

Morphometric – Based on the form of the surface i.e. based on the dimensions and distribution of roughness elements.

Obukhov length – A quantity that characterises the relative importance of mechanically and thermally produced turbulence.

Roughness layer or *sublayer* – The part of the atmospheric boundary layer that is not much higher than the surface roughness elements.

Surface layer – For the large scale meteorological community, this is synonymous with *inertial sublayer*. However the urban meteorological community often uses the term to mean the *inertial sublayer* and *roughness sublayer* combined.

11 List of Symbols

LATIN

a	Constant
a, b, c	Empirical constants in linear regression equations (MCP analysis)
a_1, b_1, c_1	
a_2, b_2, c_2	
a	Decay constant for exponential canopy wind profile
A	Weibull scale parameter
A, B, C	Empirical constants (different in different equations).
A_F	Frontal area of roughness element
A_P	Plan area of roughness element
A_T	Total plan area of roughness element and surrounding space
b	Constant
B_T	turbulent buoyancy flux
c	Empirical constant in IBL relationship.
C_d	Bulk building drag coefficient.
c_d	Sectional building drag coefficient.
C_n	Wind speed, height n metres, Coleshill site, $n=10, 15, 30, 45$
D_i	Canopy drag.
D_y, D_z	Crosswind and vertical source weight distributions.
D_n	Wind speed, height n metres, Dunlop Tyres Ltd site, $n=10, 15, 30, 45$
d	Zero plane displacement height.
$E_1()$	First E_n
f	Coriolis parameter.
G	Geostrophic wind.
g	Acceleration due to gravity.
H	equilibrium boundary layer depth according to Rossby similarity theory.
H_B	Building or street canyon height
H_h	Hill height.
H_δ	Sensible heat flux at the top of the internal boundary layer.
H_s	Surface sensible heat flux.
h	Mean building height (or canopy height).
h_{BL}	Height of boundary layer
k	Wavenumber (of surface heterogeneity) = $2\pi/\lambda$.
k	Turbulent kinetic energy per unit mass (used mainly in the phrase “ $k - \varepsilon$ model”)
k	Weibull shape parameter
L	Obukhov length.
L_B	Building length
L_h	Hill width at half height.
L_R	Length scale of each region of roughness for heterogeneous surface.
L_c	Canopy-drag length scale.
ℓ	Turbulent length scale.

ℓ_b	Blending height.
l_c	Mixing length
ℓ_d	Diffusion height.
l_i	Inner region depth.
l_0	Internal boundary layer depth scale.
M	Roughness change parameter, $M = \ln(z_{02}/z_{01})$.
N_c	Canopy adjustment number.
P_x	Magnitude of horizontal pressure gradient
p	Constant in source area model.
P	Power (exponent) in simple wind profile power law
r	Correlation coefficient
r_{mean}	Mean value of the ratio of the concurrent wind speeds at a reference station and a target site in an MCP analysis
s	Constant in source area model
s_r	Standard deviation of the ratio of the concurrent wind speeds at a reference station and a target site in an MCP analysis
s_u, s_v	Standard deviations of the concurrent data at a reference station and a target site in an MCP analysis
T	Temperature.
ΔT	Urban-rural temperature difference.
ΔT	Difference between the air temperatures at two heights at a reference station (MCP analysis)
t	Time.
U_A	'Large scale' or 'Rural' wind speed at reference height z_A .
U_c	Representative wind speed within the urban canopy
U_H	Wind speed at building height
U_i	In-canopy wind speed.
U, V	Wind speed
$u(z)$	Wind speed profile.
$u_{\text{ref}}(z)$	Reference wind speed profile.
$u'(z)$	Perturbation wind speed profile.
u_0	Internal boundary layer velocity scale.
u_1	Wind speed at height z_1
u_2	Wind speed at height z_2
u_*	Friction velocity.
u_{*1}, u_{*2}	Friction velocity upstream (1) and downstream (2) of a roughness change.
u_i	The i th component of the velocity
u, v	Wind speeds at a reference station and a target site (MCP analysis)
u_x, v_x	Easterly component of wind speed at a reference station and a target site
u_y, v_y	Northerly component of wind speed at a reference station and a target site
\bar{u}, \bar{v}	Mean values of the concurrent data at a reference station and a target site in an MCP analysis
x	Distance along wind direction (e.g. from edge of urban area).
y	Distance perpendicular to wind direction
W_B	Building width
W_S	Street canyon width



z	Height (above ground).
$\bar{z}(x)$	Mean plume height.
z_A	Reference height for 'large scale' or 'rural' wind.
z_0	Roughness length.
z_{01}, z_{02}	Roughness length upstream (1) and downstream (2) of a roughness change.
z_{0A}	Roughness length for 'Large scale' or 'Rural' wind U_A .
z_{0eff}	Effective roughness length of aggregated surface.
z^*	Height of the urban roughness sub-layer
z_H	Average height of buildings and other roughness elements
Z	Non-dimensional height (within urban roughness sub-layer)

GREEK

α	The angle between the top-of-boundary layer wind and surface stress.
β	Drag coefficient modification parameter for building arrangement.
β_v	Volume of canopy occupied by buildings.
γ	Euler's constant, 0.577216.
δ	Internal boundary layer depth.
Δu	Cross-wake averaged velocity deficit behind a building
ε	Rate of dissipation of turbulent kinetic energy per unit mass (used mainly in the phrase " $k - \varepsilon$ model")
κ	Von Karman's constant (0.4).
λ	Wavelength (of surface heterogeneity).
λ_{eq}	Roughness density AND plan-area density, when these are assumed to be equal
λ_f	Roughness density, i.e. total frontal area of buildings per unit ground area.
λ_p	Plan-area density.
λ_s	Mean building height to street width aspect ratio.
ν	Kinematic viscosity.
ρ	Air density.
$\sigma_u, \sigma_v, \sigma_w$	Standard deviation of the turbulent velocity fluctuations in the along wind, across wind and vertical directions
σ_y	Gaussian plume width.
τ	Turbulent stress; local Reynolds stress.
τ_{adv}	Advection timescale.
Φ	Latitude
$\Phi_h(z/L)$	Monin-Obukhov stability function for heat
$\Phi_m(z/L)$	Monin-Obukhov stability function for momentum
$\Psi(z/L)$	Monin-Obukhov stability function.
Ω	Rate of rotation of Earth.

12 References

- Abild, J, Application of the wind atlas method to extremes of wind climatology, Riso-R, NO. 722, Roskilde, Riso Natl.Lab. (1994)
- Abramowitz, M. and Stegun, I. A. (Eds.). "Exponential Integral and Related Functions." Ch. 5 in Handbook of Mathematical Functions with Formulas, Graphs, and Mathematical Tables, 9th printing. New York: Dover, pp. 227-233, 1972.
- Achberger, C, Ekstrom, M and Barring, L, Estimation of local near-surface wind conditions - a comparison of WASP and regression based techniques, *Meteorological Applications*, **9** (2), 211-221 (2002).
- Agnew, M.D., Palutikof, J.P., GIS-based construction of baseline climatologies for the Mediterranean using terrain variables., *Climate Research*, **14** (2), 115-127 (2000)
- S.Arnold, H.ApSimon, J.Barlow, S.Belcher, M.Bell, D.Boddy, R.Britter, H.Cheng, R.Clark, R.Colvile, S.Dimitroulopoulou, A.Dobre, B.Greally, S.Kaur, A.Knights, T.Lawton, A.Makepeace, D.Martin, M.Neophytou, S. Neville, M.Nieuwenhuijsen, G.Nickless, C.Price, A.Robins, D.Shallcross, P.Simmonds, R.Smalley, J.Tate, A.Tomlin, H.Wang, P.Walsh, Dispersion of Air Pollution & Penetration into the Local Environment – DAPPLE, *Science of the Total Environment*, **332**, 139-153 (2004)
- Arya S.P.S. and Wyngaard, J.C., Effect of baroclinicity on wind profiles and the geostrophic drag law for the convective planetary boundary layer, *J. Atmos. Sci.*, **32**, 767-778 (1975)
- Ayotte, K.W. and Taylor, P.A., A mixed spectral finite-difference 3D model of neutral planetary boundary-layer flow over topography. *J. Atmos. Sci.*, **52**, 3523-3537 (1995)
- Ayotte, K.W., Xu, D. and Taylor, P.A., The impact of turbulence closure schemes on the predictions of the mixed spectral finite-difference model for flow over topography, *Bound.-Layer Met.*, **68**, 1-33 (1994)
- Belcher, S. E., Jerram, N. and Hunt, J. C. R., Adjustment of a turbulent boundary layer to a canopy of roughness elements, *J. Fluid Mech.*, **488**, 369-398 (2003)
- Barlow, J. F. and Belcher, S. E., A wind tunnel model quantifying fluxes in the urban boundary layer, *Boundary-Layer Meteorol.*, **104**, 131-150 (2002)
- Barlow, J. F., Harman, I. N. and Belcher, S. E., Scalar fluxes from urban street canyons. Part I. Laboratory simulations. Part II. Model, *Boundary-Layer Meteorol.*, **113**, 369-410 (2004)
- Barlow, J.F., Rooney, G.G., von Hunerbein, S. & Bradley, S.G., Relating urban boundary layer structure to upwind terrain for the SALFEX campaign, *Boundary-Layer Meteorol.*, in submission (2007)
- Barnard, J.C., An evaluation of three models designed for siting wind turbines in areas of complex terrain, *Solar Energy*, **46** (5) , 283-294 (1991)



- Barthelmie, R.J., Courtney, M.S., Hojstrup, J., Larsen, S.E., Meteorological aspects of offshore wind energy: observations from the Vindeby wind farm, *Journal of Wind Engineering and Industrial Aerodynamics*, **62** (2-3), 191-211 (1996)
- Basumatary, H., Sreevalsan, E., Sasi, K.K., Weibull parameter estimation: a comparison of different measures, *Wind Engineering*, **29** (3), 309-315 (2005)
- Belcher, S.E., Xu, D.P. and Hunt, J.C.R., The response of the turbulent boundary layer to arbitrarily distributed roughness changes, *Q. J. R. Meteorol. Soc.*, **116**, 611-635 (1990)
- Beljaars, A.C.M., Walmsley, J.L. and Taylor, P.A., A mixed spectral finite-difference model for neutrally stratified boundary-layer flow over roughness changes flow over topography, *Bound.-Layer Met.*, **38**, 273-303 (1987)
- Bentham, T. and Britter, R., Spatially averaged flow within obstacle arrays, *Atmos. Environ.*, **37**, 2037-2043 (2003)
- Best, M. J., Representing urban areas within operational numerical weather prediction models, *Boundary-Layer Meteorol.*, **114**, 91-109 (2005)
- Best, M. J., Grimmond, C. S. B. and Villani, M. G., Evaluation of the urban tile in MOSES using surface energy balance observations, *Boundary-Layer Meteorol.*, **118**, 503-525 (2006)
- Bornstein, R. and Lin, Q., Urban Heat Islands and Summertime Convective Thunderstorms in Atlanta: Three Case Studies, *Atmos. Environ.*, **34**, 507-516 (2000)
- Borresen, J.A., Wind atlas for the North Sea and the Norwegian Sea, Norwegian Met. Inst. (Norw.Univ.Press), Oslo, 8200352765 (1987)
- Botta, G., Castagna, R., Borghetti, M., Mantegna, D., Wind analysis on complex terrain - The case of Acqua Spruzza, *Journal of Wind Engineering and Industrial Aerodynamics*, **39** (1-3), 357-366 (1992)
- BRE Certification Limited, Requirements for contractors undertaking the supply, design, installation, set to work commissioning and handover of micro and small wind turbine systems, Draft 3 of Report MIS 3003 (2007)
- Britter, R. and Schatzmann, M. (editors), Model evaluation guide and protocol document. COST 732 report, COST Office, Brussels (2007)
- Britter, R. and Schatzmann, M. (editors), Background and justification document to support the model evaluation guidance and protocol. COST 732 report, COST Office, Brussels (2007)
- Brower, M, Ewing, G and McCullen, P, Project Report, Republic of Ireland – Wind Atlas 2003 (2003)
<http://www.sei.ie/uploadedfiles/RenewableEnergy/IrelandWindAtlas2003.pdf>
- Brown, A.R., Large-eddy simulation and parametrization of the baroclinic atmospheric boundary layer. *Quart. J. Roy. Meteorol. Soc.*, **122**, 1779-1798 (1996)
- Burch, S.F. and Ravenscroft, F., Computer Modelling of the UK Wind Energy Resource: Overview Report, ETSU WN7055 (1992)



- Ca, V. T., Ashie, Y. and Asaeda, T., A k- ϵ turbulence closure model for the atmospheric boundary layer including urban, *Boundary-Layer Meteorol.*, **102**, 459-490 (2002)
- Carruthers, D.J., Holroyd, R.J., Hunt, J.C.R., Weng, W.-S., Robins, A.G., Apsley, D.D., Thomson, D.J. and Smith, F.B., UK-ADMS: A new approach to modelling dispersion in the earth's atmospheric boundary layer, *J. Wind Eng. Ind. Aerodyn.*, **52**, 139-153 (1994)
- Carruthers, D.J. and McHugh, C.A. (editors), Proceedings of the 11th International Conference on Harmonisation within Atmospheric Dispersion Modelling for Regulatory Purposes, Cambridge Environmental Research Consultants (2007)
- Carruthers, D.J., Weng, W.-S., Dyster, S.J., Singles, R. and Hlgson, H., Complex terrain module. ADMS 3 Technical Specification (2004). Available from <http://www.cerc.co.uk>
- Castro, I.P., The QNET-CFD knowledge base, Proceedings of the International Workshop on Quality Assurance of Microscale Meteorological Models, edited by M. Schatzmann and R. Britter, COST 732 report, European Science Foundation (2005)
- Castro, I.P., The EMU model comparison study, Proceedings of the International Workshop on Quality Assurance of Microscale Meteorological Models, edited by M. Schatzmann and R. Britter, COST 732 report, European Science Foundation (2005b)
- Castro, I.P., Cowan, I.R. and Robins, A.G., Simulations of flow and dispersion around buildings, *J. Aerospace Eng.*, **12**, 145-160 (1999)
- CERC, ADMS 3 Technical Specification (2005). Available from <http://www.cerc.co.uk>.
- Chadee, J.C., Sharma, C., Wind speed distributions: a new catalogue of defined models, *Wind Engineering*, **25** (6), 319-337 (2001)
- Cheng, H. and Castro, I.P., Near wall flow over urban-like roughness, *Boundary-Layer Meteorol.*, **104**, 229-259 (2002)
- Cimorelli, A.J., Perry, S.G., Venkatram, A., Weil, J.C., Paine, R.J., Wilson, R.B., Lee, R.F. and Peters, W.D., AERMOD – Description of model formulation, US Environmental Protection Agency Support Centre for Regulatory Air Models (1998). www.epa.gov/scram001
- Clark, P.A., Development of an automated site specific forecast model, 3rd European conference on applications of meteorology, 23-26 September 1997, Lindau, Germany (1997)
- Coccal, O. & Belcher, S.E., A canopy model of mean winds through urban areas, *Q. J. Royal Meteorol. Soc.*, **130**, 1349-1372 (2004)
- Coccal, O. and Belcher, S. E., Mean Winds Through An Inhomogeneous Urban Canopy, *Boundary-Layer Meteorology*, **115**, 47-68 (2005)
- Coccal, O., Thomas, T.G., Castro, I.P. and Belcher, S. E., Mean flow and turbulence statistics over groups of urban-like cubical obstacles, *Boundary-Layer Meteorology*, **121**, 491-519 (2006)
- Cooper, W. S., Hinton, C. L., Ashton, N., Saulter, A., Morgan, C., Proctor, R., Bell, C., Hugget, Q., An introduction to the UK marine renewable atlas, *Maritime Engineering*, **159**, MAI, 1-7 (2006)

Counihan, J., Hunt, J.C.R. and Jackson, P.S., Wakes behind two-dimensional surface obstacles in turbulent boundary layers, *J. Fluid Mech.*, **64**, 529-563 (1974)

Cowan, I.R., Castro, I.P. and Robins, A.G., Numerical considerations for simulations of flow and dispersion around buildings, *J. Wind Eng. Ind. Aerodyn.*, **67 & 68**, 535-545 (1997)

Davenport, A.G., Grimmond, C.S.B., Oke, T.R. & Wieringa, J., Estimating the roughness of cities and scattered country, 12th Conference on Applied Climatology, Asheville NC, American Meteorological Society (2000)

Davidson, M.J., Mylne, K.R., Jones, C.D., Phillips, J.C., Perkins, R.J., Fung, J.C.H. and Hunt, J.C.R., Plume dispersion through large groups of obstacles – a field investigation, *Atmos. Environ.*, **29**, 3245-3256 (1995)

Davidson, M.J., Snyder, W.H., Lawson, R.E. and Hunt, J.C.R., Wind tunnel simulations of plume dispersion through groups of obstacles, *Atmos. Environ.*, **30**, 3715-3731 (1996)

Dobre, A., Arnold, S.J., Smalley, R.J., Boddy, J.W.D., Barlow, J.F., Tomlin A.S. and Belcher, S.E., Flow field measurements in the proximity of an urban intersection in London, UK, *Atmos. Environ.*, **39**, 4647-4657 (2005)

Dupont, S., Otte, T. L. And Ching, J. K. S., Simulations of meteorological fields within and above urban and rural canopies with a mesoscale model, *Boundary-Layer Meteorol.*, **113**, 111-158 (2004)

Dupont, S. and Mestayer, P. G., Parameterisation of the urban energy budget with the submesoscale soil model, *J. Applied Meteorol. And Clim.*, **45**, 1744-1765 (2006)

Elliott, W.P., The Growth of the Atmospheric Internal Boundary Layer, *Trans. Amer. Geophys. Union*, **39**, 1048-1054 (1958)

Ellis, N.L. and Middleton, D.R., Field measurements and modelling of urban meteorology in Birmingham, UK. Met Office Turbulence and Diffusion Note 268 (2000)

Ellis, N.L. and Middleton, D.R., Field measurements and modelling of surface fluxes in Birmingham, UK. COST Action 715 – Surface energy balance in urban areas – Extended abstracts of an expert meeting, Antwerp, Belgium, 12 April 2000, edited by M. Piringer, Office for Official Publications of the European Communities, EUR 19447 (2001)

Essery, R., Best, M. and Cox, P., MOSES II technical documentation, Hadley Centre Technical Note 30, available from www.metoffice.gov.uk (2001)

Finardi, S., Brusasca, G., Morselli, M.G., Trombetti, F. and Tampieri, F., Boundary-layer flow over analytical two-dimensional hills: a systematic comparison of different models with wind tunnel data, *Bound.-Layer Met.*, **63**, 259-291 (1993)

Finnigan, J.J., Turbulence in plant canopies, *Ann. Rev. Fluid. Mech.*, **32**, 519-572 (2000)

Fisher, B.E.A., Joffre, S., Kukkonen, J., Piringer, M., Rotach, M. and Schatzmann, M., Meteorology Applied to Urban Air Pollution Problems. Final Report of COST Action 715. Demetra Ltd Publishers, 276 pp., ISBN 954-9526-30-5 (2005)

Frank, H. P., and Landberg, L., Modelling the wind climate of Ireland, *Boundary-Layer Meteorol.*, **85**, 359-378 (1997)

- Franke, J., Hellsten, A., Schlünzen, H. and Carissimo, B. (editors), Best practice guideline for the CFD simulation of flows in the urban environment. COST 732 report, COST Office, Brussels (2007)
- Frey-Buness, F., Heimann, D., and Sausen, R., Statistical-dynamical downscaling procedure for global climate simulations, *Theor. Appl. Climatol.*, **50**, 117-131 (1997)
- Fuentes, U., Heimann, D., An improved statistical-dynamical downscaling scheme and its application to the alpine precipitation climatology, *Theor. Appl. Climatol.*, **65**, 119-135 (2000)
- Gailis, R.M. and Hill, A., A wind-tunnel simulation of plume dispersion within a large array of obstacles, *Boundary-Layer Meteorol.*, **119**, 289-338 (2006)
- Gailis, R.M., Hill, A., Yee, E. and Hilderman, T., Extension of a fluctuating plume model of tracer dispersion to a sheared boundary layer and to a large array of obstacles, *Boundary-Layer Meteorol.*, **122**, 577-607 (2007)
- Gandemer, J., Wind shelters, *J. Ind. Aerodyn.*, **4**, 371-389 (1979)
- Garratt, J. R., The Internal Boundary Layer – A Review, *Boundary-Layer Meteorol.*, **50**, 171-203 (1990)
- Garratt, J.R., The atmospheric boundary layer, Cambridge University Press (1992)
- Gibson, J.K. and Kållberg, P. and Uppala, S. and Hernandez, A. and Nomura, A. and Serrano, E., ERA Description, ERA-15 Project Report Series No. 1, from www.ecmwf.int/publications (1997)
- Gipe, P., Wind Power: Renewable Energy for Home, Farm, and Business (completely revised and expanded edition). Chelsea Green Publisher (2004)
- Girard, C., R. Benoit and M. Desgagné, Finescale Topography and the MC2 Dynamics Kernel, *Mon. Wea. Rev.*, **133**, 1463-1477 (2005)
- Glazer, A., Benoit, R., Yu, W., Numerical wind energy atlas for Canada, Geophysical Research Abstracts, **7** (2005)
- Grant, A.L.M. and Whiteford, J., Aircraft estimates of the geostrophic drag coefficient and the Rossby similarity function A and B over the sea, *Bound.-Layer Meteorol.*, **39**, 219-231 (1987)
- Goode, K. & Belcher, S.E., On the parameterisation of the effective roughness length for momentum transfer over heterogeneous terrain, *Boundary-Layer Meteorol.*, **93**, 133-154 (1999)
- Grimmond, C.S.B. & Oke, T.R., Aerodynamic properties of urban areas derived from analysis of surface form, *J. Applied Meteorol.*, **38**, 1262-1292 (1999)
(see also Grimmond, C.S.B. & Oke, T.R., Corrigendum, *J. Applied Meteorol.*, **39**, 2494 (2000))
- Gryning, Sven-Erik, and Batchvarova, Ekaterina, Analytical model for the growth of the coastal internal boundary layer during onshore flow, *Q. J. R. Meteorol. Soc.*, **116**, 187-203 (1990)
- Guo, X and Palutikof, JP, Wind speed prediction methods in complex terrain with a low computing requirement, Fifth Conference on Mountain Meteorology, June 25-29, 1990, Boulder, Colorado (1990)

Hall, D.J., Macdonald, R.W., Walker, S. and Spanton, A.M., Measurements of dispersion within simulated urban arrays – a small scale wind tunnel study, BRE Client Report CR 178/96, Building Research Establishment (1996)

Hall, D.J., Macdonald, R.W., Walker, S. and Spanton, A.M., Measurements of dispersion within simulated urban arrays – a small scale wind tunnel study, BRE Client Report CR 244/98, Building Research Establishment (1998)

Hanna, S.R. & Britter, R.E., Wind flow and vapour cloud dispersion at industrial and urban sites, Center for Chemical Process Safety, American Institute of Chemical Engineers, NY (2002)

Harman, I. N., The energy balance of urban areas, PhD thesis, University of Reading (2003)

Harman, I. N., Best, M. J. and Belcher, S. E., Radiative exchange in an urban street canyon, *Boundary-Layer Meteorol.*, **110**, 301-316 (2004)

Heath, M.A., Walshe, J.D. and Watson S.J., Estimating the potential yield of small building-mounted wind turbines, *Wind Energy*, **10**, 271-287 (2007)

Heimann, D., A model-based wind climatology of the eastern Adriatic coast, *Meteorologische Zeitschrift*, **10**, 5-16 (2001)

Hinneburg, D. and Tetzlaff, G., Calculated wind climatology of the south-Saxonian/north-Czech mountain topography including improved resolution of mountains, *Annales Geophysicae*, **14**, 767-772 (1996)

Homicz, Gregory F., Three-Dimensional Wind Field Modeling: A Review, SAND Report SAND2002-2597, Sandia National Laboratories, Albuquerque, New Mexico 87185 and Livermore, California 94550 (2002)

Hopwood, W. Phillip, Source Area Modelling of Surface Fluxes: Part I - Theory and Implementation in the Site Specific Forecast Model, Forecasting Research Technical Report 237 (1998)

http://www.metoffice.gov.uk/research/nwp/publications/papers/technical_reports/index.html

Hort, M.C., Devenish, B.J. and Thomson, D.J., Building affected dispersion: development and initial performance of a new Lagrangian particle model, 15th Symposium on Boundary Layers and Turbulence, American Meteorological Society (2002)

Hosker, R.P., Flow and diffusion near obstacles, Atmospheric Science and Power Production, edited by D. Randerson, US Dept of Energy (1984)

Howard T. and Clark, P., Correction and downscaling of NWP wind speed forecasts, *Meteorol. Appl.*, **14**, 105-116 (2007)

Hunt, J.C.R., Abel, C.J., Peterka, J.A. and Woo H., Kinematical studies of the flows around free or surface mounted obstacles; applying topology to flow visualisation, *J. Fluid Mech.*, **86**, 179-200 (1978)

Hunt, J.C.R., Richards, K.J. and Brighton, P.W.M., Stably stratified flow over low hills, *Q. J. R. Meteorol. Soc.*, **114**, 859-886 (1988a)



- Hunt, J.C.R., Leibovich, S. and Richards, K.J., Turbulent shear flow over hills, *Q. J. R. Meteorol. Soc.*, **114**, 1435-1470 (1988b)
- Hutton, A.G., Evaluation of CFD codes – The European project QNET-CFD. Proceedings of the International Workshop on Quality Assurance of Microscale Meteorological Models, edited by M. Schatzmann and R. Britter, COST 732 report, European Science Foundation (2005)
- Jackson, P.S. and Hunt, J.C.R., Turbulent wind flow over a low hill, *Quart. J. Roy. Meteorol. Soc.*, **101**, 929-955 (1975)
- James, P. M., An objective classification method for Hess and Brezowsky Grosswetterlagen over Europe, *Theoretical and Applied Climatology*, **88**, 17-42 (2007)
- Jones, A.R., Thomson, D.J., Hort, M.C. and Devenish, B.J., The U.K. Met Office's next-generation atmospheric dispersion model, NAME III. Air pollution modeling and its application XVII, edited by C. Borrego and A.-L. Norman, Springer (2007)
- Kaimal, J.C. and Finnigan, J.J., Atmospheric Boundary Layer Flows, Their Structure and Measurement, O.U.P., ISBN 0-19-506239-6 (1994)
- Kalnay, E., Kanamitsu, M., Kistler, R., Collins, W., Deaven, D., Gandin, L., Iredell, M., Saha, S., White, G., Woollen, J., Zhu, Y., Leetmaa, A., Reynolds, B., Chelliah, M., Ebisuzaki, W., Higgins, W., Janowiak, J., Mo, K.C., Ropelewski, C., Wang, J., Jenne, R., Joseph, D., The NCEP/NCAR 40-Year Reanalysis Project, *Bull. Amer. Meteorol. Soc.*, **77**, 437-471 (1997)
- Karppinen, A. and Robins, A., Summary of WG2 activities – inventory of databases. Proceedings of the International Workshop on Quality Assurance of Microscale Meteorological Models, edited by M. Schatzmann and R. Britter, COST 732 report, European Science Foundation (2005)
- Kastner-Klein O and Rotach M W, Mean flow and turbulence characteristics in an urban roughness sublayer, *Boundary Layer Meteorology*, **111**, 55-84 (2004)
- Ketzel, M., Louka, P., Sahm, P., Guilloteau, E. and Sini, J.-F., TRAPOS model comparison study. Proceedings of the International Workshop on Quality Assurance of Microscale Meteorological Models, edited by M. Schatzmann and R. Britter, COST 732 report, European Science Foundation (2005)
- Khurshudyan, L. H., Snyder, W. H. and Nekrasov, I. V., Flow and dispersion of pollutants over two-dimensional hills, U.S. Envir. Prot. Agcy. Rpt. No. EPA-6000/4-81-067. Res. Tri. Pk., NC (1981)
- King, J.C., Anderson, P.S., Vaughan, D.G., Mann, G.W., Mobbs, S.D. and Vosper, S.B., Wind-borne redistribution of snow across an Antarctic ice rise, *J. Geophys. Res.*, **109**, No. D11, D11104 (2004)
- Kistler, R., Kalnay, E., Collins, W., Saha, S., White, G., Woollen, J., Chelliah, M., Ebisuzaki, W., Kanamitsu, M., Kousky, V., van den Dool, H., Jenne, R. and Fiorino, M., The NCEP–NCAR 50-year reanalysis: Monthly means CD-Rom and documentation, *Bull. Am. Meteorol. Soc.*, **82**, 247–267 (2001)
- Kondo, H., Genchi, Y., Kikegawa, Y., Ohashi, Y., Yoshikado, H. and Komiyama, H., Development of a multi-layer urban canopy model for the analysis of energy consumption in a big city: Structure of the urban canopy model and its basic performance, *Boundary-Layer Meteorol.*, **116**, 395-421 (2005)

- Krayenhoff, E. S. and Voogt, J. A., A microscale three-dimensional urban energy balance model for studying surface temperatures, *Boundary-Layer Meteorol.*, **123**, 433-461 (2007)
- Kristensen, L, Rathmann, O, Hansen, SO, Extreme wind in Denmark, *Journal of Wind Engineering and Industrial Aerodynamics*, **87** (2-3), 147-166 (2000)
- Landberg, L and Mortensen, NG, A comparison of physical and statistical methods for estimating the wind resource at a site, In Proceedings of the Fifteenth BWEA Wind Energy Conference, Pitcher, KF (ed.), BWEA, London, 119-125 (1994)
- Landberg, L, Myllerup, L, Rathmann, O, Petersen, EL, Jorgensen, BH, Badger, J and Mortensen, NG, Wind resource estimation: an overview, *Wind Energy*, **6** (3), 261-271 (2003)
- Landberg, L, Watson, SJ, Short-term prediction of local wind conditions, *Boundary Layer Meteorology*, **70**, 171-195 (1994)
- Lange, B, Hojstrup, J, Evaluation of the wind-resource estimation program WAsP for offshore applications, *Journal of Wind Engineering and Industrial Aerodynamics*, **89** (3-4), 271-291 (2001)
- Leitl, B., Bezpalcova, K. and Harms, F., Wind tunnel modelling of the MUST experiment, Proceedings of the 11th International Conference on Harmonisation within Atmospheric Dispersion Modelling for Regulatory Purposes, edited by D.J. Carruthers and C.A. McHugh, Cambridge Environmental Research Consultants (2007)
- Lemonsu, Aude and Masson, Valéry, Simulation Of A Summer Urban Breeze Over Paris, *Boundary-Layer Meteorology*, **104**, 463-490 (2002)
- Lettau, H., Note on aerodynamic roughness-parameter estimation on the basis of roughness element description, *J. Appl. Met.*, **8**, 828-832 (1969)
- Louka, P., Vachon, G., Sini, J.-F., Mestayer, P.G. and Rosant, J.-M., Thermal effects on the airflow in a street canyon – Nantes '99 experimental results and model simulations, *Water Air Soil Pollution Focus*, **2**, 351-364 (2002)
- Lyons, T.J., Mesoscale contribution to available wind power potential, *Solar Energy*, **42**, 483-485 (1989)
- Macdonald, R. W., Modelling the Mean Velocity Profile in the Urban Canopy Layer, *Boundary-Layer Meteorol.*, **97**, 25-45 (2000)
- Macdonald, R.W., Griffiths, R.F. & Hall, D.J., An improved method for the estimation of surface roughness of obstacle arrays, *Atmos. Environment*, **32**, 1857-1864 (1998)
- Macdonald, R.W., Hall, D.J. and Walker, S., Wind tunnel measurements of wind speed within simulated urban arrays, BRE Client Report CR 243/98, Building Research Establishment (1998b)
- Martilli, Alberto, Clappier, Alain and Rotach, Mathias W., An Urban Surface Exchange Parameterisation for Mesoscale Models, *Boundary-Layer Meteorol.*, **104**, 261-2002 (2002)
- Martilli, A., Numerical study of urban impact on boundary layer structure: sensitivity to wind speed, urban morphology, and rural soil moisture, *Journal of Applied Meteorology*, **41**, 1247-1266 (2002a)

- Mascart, P., Noilhan, J., and HGiordani, H., A modified parameterization of flux-profile relationship in the surface layer using different roughness length values for heat and momentum, *Boundary-Layer Meteorol.*, **72**, 331-344 (1995)
- Mason, P.J., The formation of areally-averaged roughness lengths, *Q. J. Royal Meteorol. Soc.*, **114**, 399-420 (1988)
- Mason, P.J. and King, J.C., Measurements and predictions of flow and turbulence over an isolated hill of moderate slope, *Quart. J. Roy. Meteorol. Soc.*, **111**, 617-640 (1985)
- Masson, V., A physically-based scheme for the urban energy budget in atmospheric models, *Boundary-Layer Meteorol.*, **94**, 357-397 (2000)
- Mengelkamp, H.-T., Kapitza, H., Pfluger, U., Statistical-dynamical downscaling of wind climatologies, *Journal of Wind Engineering and Industrial Aerodynamics*, **67-68**, 449-457 (1997)
- Meroney, R.N., Turbulent diffusion near buildings. Engineering Meteorology, edited by E.J. Plate, Elsevier (1982)
- Met Office, Observer's Handbook, fourth edition, ISBN 0 86180 353 1 (2000)
- Mikhail, A.S. and Justus, C.G., Comparison of height extrapolation models and sensitivity analysis, pp377-397 in Physical Climatology for Solar and Wind Energy, Miramare – Trieste – Italy, 21 April – 16 May 1986, edited by Guzzi R. and Justus C.G., World Scientific (1988)
- Monin, A.S. and Yaglom, A.M., Statistical fluid mechanics, Vol. 1, MIT Press (1971)
- Morrison, N.L. and Webster, H.N., An assessment of turbulence profiles in rural and urban environments using local measurements and numerical weather prediction results, *Boundary-Layer Meteorology*, **115**, 223-239 (2005)
- Mulhearn, P.J., Relations between Surface Fluxes and Mean Profiles of Velocity, Temperature and Concentration, Downwind of a Change in Surface Roughness, *Quart. J. Roy. Meteorol. Soc.*, **103**, 785-802 (1977)
- Nakamura, Y. and Oke, T.R., Wind, temperature and stability conditions in an east-west orientated urban canyon, *Atmos. Environ.*, **22**, 2691-2700 (1988)
- Nalder, I.A., Wein, R.W., Spatial interpolation of climatic normals: test of a new method in the Canadian boreal forest, *Agricultural and Forest Meteorology*, **92** (4), 211-225 (1998)
- Nygaard, TA, Estimating expected energy capture at potential wind turbine sites in Norway, *Journal of Wind Engineering and Industrial Aerodynamics*, **39** (1-3), 385-393 (1992)
- Offerle, B., Grimmond, C.S.B. and Fortuniak, K., Heat storage and anthropogenic heat flux in relation to the energy balance of a central European city centre, *Int. J. of Climatol.*, **25**, 1405-1419 (2005)
- Oke, T.R., Boundary layer climates, 2nd edition, Routledge (1987)
- Oke, TR, Initial Guidance to Obtain Representative Meteorological Observations at Urban Sites, IOM Report No.81, WMO/TD. No. 1250. World Meteorological Organization, Geneva (2006)



- Otte, T. L., Lacser, A., Dupont, S. and Ching, J. K. S., Implementation of an urban canopy parameterisation in a mesoscale meteorological model, *J. Appl. Meteorol.*, **43**, 1648-1665 (2004)
- Palomino, I., Martin, F., A simple method for spatial interpolation of the wind in complex terrain, *Journal of Applied Meteorology*, **34** (7), 678-1693 (1995)
- Palutikof, J.P., Guo, X. and Halliday, J.A., Climate variability and the UK wind resource, *Journal of Wind Engineering and Industrial Aerodynamics*, **39**, 243-249 (1992)
- Panofsky, H.A. and Dutton, J.A., Atmospheric Turbulence: Models and Methods for Engineering Applications, John Wiley and Sons, New York, 397pp (1984)
- Panofsky, H.A. and Townsend, A.A., Change in Terrain Roughness and the Wind Profile, *Quart. J. Roy. Meteorol. Soc.*, **90**, 147-155 (1964)
- Pavageau, M., Rafailidis, S. and Schatzmann, M., A comprehensive experimental databank for the verification of urban car emission dispersion models, *Int. J. Environment and Pollution*, **8**, 738-746 (1997)
- Perera, M.D.A.E.S., Shelter behind two-dimensional solid and porous fences, *Journal of Wind Engineering and Industrial Aerodynamics*, **8**, 93-104 (1981)
- Perry, M., Hollis, D., The development of a new set of long-term climate averages for the UK, *International Journal of Climatology*, **25** (8), 1023-1039 (2005a)
- Perry, M., Hollis, D., The generation of monthly gridded datasets for a range of climatic variables over the UK, *International Journal of Climatology*, **25** (8), 1041-1054 (2005b)
- Rafailidis, S., Influence of building areal density and roof shape on the wind characteristics above a town, *Boundary-Layer Meteorol.*, **85**, 255-271 (1997)
- Rafailidis, S., Influence of stable atmospheric thermal stratification on urban street-canyon re-aeration, *Int. J. Environment and Pollution*, **16**, 393-403 (2001)
- Raupach, M.R., Antonia, R.A., Rajagopalan, S., Rough-wall turbulent boundary layers, *Appl. Mech. Rev.*, **44**, 1-25 (1991)
- Raupach, M. R., Simplified expressions for vegetation roughness length and zero-plane displacement as functions of canopy height and area index, *Boundary-Layer Meteorol.*, **71**, 211-216 (1994)
- Raupach, M. R., Corrigenda, *Boundary-Layer Meteorol.*, **76**, 303-304 (1995)
- Reid, S, Modelling of channelled winds in high wind areas of New Zealand, *Weather and Climate*, **17** (1), 3-21 (1997)
- Robins, A.G., McHugh, C.A. and Carruthers D.J., Testing and evaluating the ADMS building effects module, *Int. J. Environment and Pollution*, **8**, 708-717 (1997)
- Robins, A.G., Comparison of ADMS-BUILD and PRIME, Environmental Flow Research Centre Paper ME-FD/01.110, University of Surrey (2001)
- Robins, A.G., Wind tunnel dispersion modelling - some recent and not so recent achievements, *J. Wind Eng.*, **91**, 1777-1790 (2003)

- Robins, A.G. and Apsley, D.D., Modelling of building effects in ADMS, ADMS 3 Technical Specification (2005). Available from <http://www.cerc.co.uk>
- Rogers, A.L., Rogers, J.W., Manwell, J.F., Comparison of the performance of four measure-correlate-predict algorithms, *Journal of Wind Engineering and Industrial Aerodynamics*, **93** (3), 243-264 (2005)
- Romeo, R, Magri, S, Wind energy evaluation for breakwater plants, *Wind Engineering*, **18** (4), 199-206 (1994)
- Rooney, G.G., Comparison of upwind land use and roughness length measured in the urban boundary layer, *Boundary-Layer Meteorol.*, **100**, 469-486 (2001)
- Rooney, G.G., Longley, I.D. & Barlow, J.F., Variation of urban momentum roughness length with land use in the upwind source area, as observed in two U.K. cities, *Boundary-Layer Meteorol.*, **115**, 69-84 (2005)
- Rotach, M.W., Turbulence close to a rough urban surface, Part II: variances and gradients, *Boundary-Layer Meteorol.*, **66**, 75-92 (1993)
- Rotach, M W, On the influence of the urban roughness sublayer on turbulence and dispersion, *Atmospheric Environment*, **33**, 4001-4008 (1999)
- Roth M, Review of atmospheric turbulence over cities, *Q J Roy Met Soc*, **126**, 1941-1990 (2000)
- Sasaki, Y., An Objective Analysis Based on the Variational Method, *Journal of the Meteorological Society of Japan*, **36**, 77-88 (1958)
- Sander J. and Chun S., Validated Digital Wind Atlas for Poland, *Wind Engineering*, **28**, 129-138 (2004)
- Savelyev, S. A. and Taylor, P. A., Notes on Internal Boundary-Layer Height Formula, *Boundary-Layer Meteorol.*, **101**, 293-301 (2001)
- Savelyev, Sergiy A. and Taylor, Peter A., Internal Boundary Layers: I. Height Formulae for Neutral and Diabatic Flows, *Boundary-Layer Meteorology*, **115**, 1-25 (2005)
- Schatzmann, M., Grawe, D. and Leitl, B., Strengths/weaknesses of laboratory and field data, Proceedings of the International Workshop on Quality Assurance of Microscale Meteorological Models, edited by M. Schatzmann and R. Britter, COST 732 report, European Science Foundation (2005)
- Schmid, H. P. and Oke, T. R., A model to estimate the source area contributing to turbulent exchange in the surface layer over patchy terrain, *Q. J. R. Meteorol. Soc.*, **116**, 965-988 (1990)
- Schmid, H.P., Cleugh, H.A., Grimmond, C.S.B. & Oke, T.R., Spatial variability of energy fluxes in suburban terrain, *Boundary-Layer Meteorol.*, **54**, 249-276 (1991)
- Schulman, L.L., Stirmaitis, D.G. and Scire, J.S., Development and evaluation of the PRIME plume rise and building downwash model, *J. Air & Waste Management Assoc.*, **50**, 378-390 (2000)



- Sempreviva, Anna Maria, Larsen, S. E., Mortensen, N. G. and Troen, I., Response of neutral boundary layers to changes of roughness, *Boundary-Layer Meteorol.*, **50**, 205-225 (1990)
- Sheppard, P.A., Airflow over mountains, *Q. J. R. Meteorol. Soc.*, **82**, 528-529 (1956)
- Sherman, C. A., A Mass-Consistent Model for Wind Fields over Complex Terrain, *Journal of Applied Meteorology*, **17**, 312-319 (1978)
- Simmons, A., Uppala, S., Dee, D., Kobayashi, S., ERA-Interim: New ECMWF reanalysis products from 1989 onwards, ECMWF Newsletter No. 110 – Winter 2006/07 (2007)
- Simpson, J.E., Sea Breeze and Local Winds, C.U.P, 234pp (1994)
- Sini, J.-F., Anquetin, S. and Mestayer, P.G., Pollutant dispersion and thermal effects in urban street canyons, *Atmos. Environ.*, **30**, 2659-2677 (1996)
- Sokol, Z., Stekl, J., Estimation of annual mean ground wind speed over the territory of the Czech Republic, *Meteorologische Zeitschrift, Neue Folge*, **4** (5), 218-222 (1995)
- Solazzo, E., Cai, X. and Vardoulakis, S., Evaluation of the traffic producing turbulence within a modelled street canyon using computational fluid dynamics calculations, Proceedings of the 11th International Conference on Harmonisation within Atmospheric Dispersion Modelling for Regulatory Purposes, edited by D.J. Carruthers and C.A. McHugh, Cambridge Environmental Research Consultants (2007)
- Solazzo, E., Di Sabatino, S. and Britter, R., Modelling the flow within and above the urban canopy layer, Proceedings of the 11th International Conference on Harmonisation within Atmospheric Dispersion Modelling for Regulatory Purposes, edited by D.J. Carruthers and C.A. McHugh, Cambridge Environmental Research Consultants (2007b)
- Sreevalsan, E., Das, S.S., Sasikumar, R. and Ramesh, M.P., Wind farm site assessment using Measure-Relate-Predict (MCP) analysis, *Wind Engineering*, **31** (2), 111-116 (2007)
- Suarez, JC, Gardiner, B.A, Quine, CP, A comparison of three methods for predicting wind speeds in complex forested terrain, *Meteorological Applications*, **6** (4), 329-342 (1999)
- Szepesi, D.J., Buki, R., Fekete, K.E., Preparation of regional scale wind climatologies, *Idojaras*, **104**, 197-211 (2000)
- Taylor, P.A., Mason, P.J. and Bradley, E.F., Boundary-layer flow over low hills, *Bound.-Layer Met.*, **39**, 107-132 (1987)
- Taylor, P.A. and Teunissen, H.W., The Askervein Hill project: overview and background data, *Bound.-Layer Met.*, **39**, 15-39 (1987)
- Taylor, P.A., Walmsley, J.L. and Salmon, J.R., A simple model of neutrally stratified boundary layer flow over real terrain incorporating wavenumber-dependent scaling, *Bound.-Layer Met.*, **26**, 169-189 (1983)
- Traci, R. M., Phillips, G. T. and Patnaik, P. C., Developing a Site Selection Methodology for Wind Energy Conversion Systems, DOE/ET/20280-3, prepared for the U. S. Department of Energy by Science Applications Incorporated, La Jolla, CA (1978)

Troen, I and Petersen, E, European Wind Atlas, Risø National Laboratory, Roskilde, Denmark, 656pp (1989)

Troen, I., A high resolution spectral model for flow in complex terrain., Ninth symposium on turbulence and diffusion, April 30 - May 3 1990, Roskilde, Denmark. Preprints, pp.417-420 (1990)

Uppala, S. M., KÅllberg, P. W., Simmons, A. J., Andrae, U., Da Costa, Bechtold V. , Fiorino, M., Gibson, J. K., Haseler, J , Hernandez, A., Kelly, G. A, Li, X., Onogi, K., Saarinen, S., Sokka, N., Allan, R. P., Andersson, E., Arpe, K., Balmaseda, M. A., Beljaars, A. C. M., Van De Berg, L., Bidlot, J., Bormann, N., Caires, S., Chevallier, F., Dethof, A., Dragosavac, M., Fisher, M., Fuentes, M., Hagemann, S., Hólm, E., Hoskins, B. J., Isaksen, L., Janssen, P. A. E. M., Jenne, R., McNally, A. P. , Mahfouf, J.-F. , Morcrette, J.-J. , Rayner, N. A., Saunders, R. W., Simon, P., Sterl, A., Trenberth, K. E. , Untch, A., Vasiljevic, D., Viterbo, P., Woollen, J., The ERA-40 re-analysis, *Quart. J Roy. Met. Soc.*, **131**, 2961-3211 (2006)

Trini Castelli, S. and Reisin, T.G., Application of a modified version of RAMS model to simulate the flow and turbulence in presence of buildings: the MUST COST 732 exercise, Proceedings of the 11th International Conference on Harmonisation within Atmospheric Dispersion Modelling for Regulatory Purposes, edited by D.J. Carruthers and C.A. McHugh, Cambridge Environmental Research Consultants (2007)

Vachon, G., Louka, P., Rosant, J.-M., Mestayer, P.G. and Sini, J.-F., Measurements of traffic-induced turbulence within a street canyon during the Nantes '99 experiment, *Water Air Soil Pollution Focus*, **2**, 127-140 (2002)

Vicente-Serrano, S.M., Saz-Sanchez, M.A., Cuadrat, J.M., Comparative analysis of interpolation methods in the middle Ebro Valley (Spain): application to annual precipitation and temperature, *Climate Research*, **24** (2), 161-180 (2003)

Vosper, S., Development and testing of a high resolution mountain-wave forecasting system, *Meteorol. Appl.*, **10**, 75-86 (2003)

Walmsley, J.L., Taylor, P.A. and Keith, T., A simple model of neutrally stratified boundary-layer flow over complex terrain and surface roughness modulations (MS3DJH/3R), *Bound.-Layer Met.*, **36**, 157-186 (1986)

Walmsley, J.L., Internal Boundary-Layer Height Formulae – A Comparison with Atmospheric Data, *Boundary-Layer Meteorol.*, **47**, 251-262 (1989)

Walmsley, J.L., Troen, I., Lalas, D.P. and Mason, P.J., Surface-layer flow in complex terrain: comparison of models and full-scale observations, *Boundary Layer Meteorology*, **52** (3), 259-281 (1990)

Weibull, W., A statistical distribution function of wide applicability, *Journal of Applied Mechanics*, **18**, 293-297 (1951)

Wieringa, J., Roughness-dependent geographical interpolation of surface wind speed averages, *Quart. J. R. Met. Soc.*, **112**, 867-889 (1986)

Wilson, D.J., Flow patterns over flat-roofed buildings and application to exhaust stack design, *ASHRAE Trans.*, **85**, 284-295 (1979)



- Wilson, J. D., Numerical studies of flow through a windbreak, *J. Wind Eng. Ind. Aerodyn.*, **21**, 119-154 (1985)
- Wilson, J.D., On the choice of a windbreak porosity profile, *Boundary-Layer Meteorol.*, **38**, 37-49 (1987)
- Wong, K. and Dirks, R., Mesoscale Perturbations on Airflow in the Urban Mixing Layer, *J. Appl. Meteorol.*, **17**, 677-688 (1978)
- Wood, N., The onset of separation in neutral, turbulent flow over hills, *Bound.-Layer Met.*, **76**, 137-164 (1995)
- Wood, N. and Mason, P.J., The pressure force induced by neutral, turbulent flow over hills, *Quart. J. Roy. Meteorol. Soc.*, **119**, 1233-1267 (1993)
- Woods, J.C., Watson, S.J., A new matrix method of predicting long-term wind roses with MCP, *Journal of Wind Engineering and Industrial Aerodynamics*, **66** (2), 85-94 (1997)
- World Meteorological Organization, Guide to Meteorological Instruments and Methods of Observation, WMO-No. 8, Geneva (1996)
- Xia, Y., Winterhalter, M., Fabian, P., A model to interpolate monthly mean climatological data at Bavarian forest climate stations, *Theoretical and Applied Climatology*, **64** (1-2), 27-38 (1999)
- Xie, X., Liu, C.-H., Leung, D.Y.C. and Leung, M.K.H., Characteristics of air exchange in a street canyon with ground heating, *Atmos. Environ.*, **40**, 6396-6409 (2006)
- Xu, D., Ayotte, K.W. and Taylor, P.A., Development of a non-linear mixed spectral finite-difference model for turbulent boundary layer flow over topography, *Bound.-Layer Met.*, **70**, 341-367 (1994)
- Yee, E. and Biltoft, C.A., Concentration fluctuation measurements in a plume dispersing through a regular array of obstacles, *Boundary-Layer Meteorol.*, **111**, 363-415 (2004)
- Yee, E., Gailis, R.M., Hill, A., Hilderman, T., and Kiel, D., Comparison of wind-tunnel and water-channel simulations of plume dispersion through a large array of obstacles with a scaled field experiment, *Boundary-Layer Meteorol.*, **121**, 389-432 (2007)
- Ying R. and Canuto, V.M., Turbulence modelling over two-dimensional hills using an algebraic Reynolds stress expression, *Bound.-Layer Met.*, **77**, 69-99 (1996)
- Yu, W., Benoit, R., Girard, C., Glazer, A., Lemarquis, D., Salmon, J. R., Pinard, J.-P., Wind Energy Simulation Toolkit (WEST): A Wind Mapping System for Use by the Wind Energy Industry, *Wind Engineering*, **30**, 15-33 (2006)
- Žagar, N., Žagar, M., Cedilnik, J., Gregorič, G., Rakovec, J., Validation of mesoscale low-level winds obtained by dynamical downscaling of ERA40 over complex terrain, *Tellus, Series A*, **58A**, 445-455 (2006)
- Žagar, M., Žagar, N., Cedilnik, J., Gregorič, G., Rakovec, J., High-resolution wind climatology from ERA-40 (2005). www.cnrm.meteo.fr/aladin/newsletters/news28/PAPERS/ZAGAR.pdf
- Zaphiropoulos, Y., Dellaportas, P., Morfiadakis, E., Glinou, G., Prediction of wind speed and direction at a potential site, *Wind Engineering*, **23** (3), 167-175 (1999)



Small-scale Wind Energy – Technical Report

Urban Wind Energy Research Project

Part 2 - Estimating the Wind Energy Resource

Prepared for the Carbon Trust

by

Peter Clark, Mark Gallani, Dan Hollis,
Dave Thomson and Clive Wilson

Reviewed by: Brian Golding

Authorised for issue by: Ross Lothingland

August 2008

The information in this report is provided in good faith and is believed to be correct, but the Met. Office can accept no responsibility for any consequential loss or damage arising from any use that is made of it.

Met Office FitzRoy Road Exeter Devon EX1 3PB
Tel: 0870 900 0100 consulting@metoffice.gov.uk

www.metoffice.gov.uk

© Crown Copyright 2008

Contents

1	Introduction	3
2	A Generic Methodology for Estimating Urban Wind Energy.....	4
2.1	Large-scale reference wind climatology	4
2.2	Adaptation and down-scaling to local surface and orography.	4
2.2.1	Orography.....	4
2.2.2	Inertial sub-layer	5
2.2.3	Roughness and canopy sub-layers.....	5
2.2.4	Building-scale flow	5
2.3	Local wind energy resource	5
2.4	UK wind energy resource	6
3	Evaluation of available methods	7
3.1	Large-scale reference wind climatology	7
3.2	Orography	9
3.3	Correction to inertial sub-layer (local roughness)	11
3.4	Correction to mean profile in the roughness sublayer (including within the urban canopy)	12
3.5	Correction for the specific local building geometry	14
4	Calculation Methodologies	16
4.1	Previous Work.....	16
4.1.1	Paper by Heath et al (2007).....	16
4.2	UK Energy Resource	19
4.2.1	Outline method	19
4.2.2	Estimating the Wind Speed	19
4.2.3	Estimating the Energy Resource	26
4.2.4	Sensitivity Analyses	35
4.2.5	Critique of the Methodology	37
4.2.6	Outline of Possible Improvements	39
5	Predicted changes in UK wind climate due to climate change	44
5.1	Changes in mean speed	44
5.2	Wind speed frequency distribution	45
5.3	Wind direction distribution	46
5.4	Extremes	46
5.5	Summary of relevant on-going research	47
6	Summary.....	49
7	Conclusions	52
8	Appendix A.....	53
9	References.....	58

1 Introduction

This is the second part of the report describing the findings of a study to clarify the performance of small-scale wind turbines in urban areas.

The first half of this report (Urban Wind Energy Research Project, Part 1: A Review of Existing Knowledge) summarised the extent of available data and the analysis techniques and tools that could be used for determining wind conditions in urban areas.

In this part of the report the practical problem of estimating the total UK wind energy resource available from micro-generation is considered. In Section 2 a generic methodology for estimating wind conditions in urban areas is described. This involves applying a series of corrections to a large-scale reference wind climatology. The options available for generating the reference climatology and the required corrections are evaluated in Section 3. In Section 4 a detailed description is given of the method that has been used to estimate a) the surface wind climatology, and b) the available wind energy, at any given location within the UK. The latter is obtained by combining the former with a turbine power curve. This section also gives some figures for the total UK energy resource, provides a critique of the method and outlines how the chosen approach could be improved or extended. Finally, Section 5 describes current predictions for how anthropogenic climate change might alter the wind climatology of the UK.

Note that the estimates of total UK energy resource given in Section 4 are quoted separately for each of seven turbine types and assume a uniform market penetration of 1%. These figures have been generated by combining estimates of the energy generated by a single turbine with UK population statistics. To make an estimate of the overall UK energy resource from micro-wind generation requires an assessment of the generation costs and the likely market penetration of each turbine type. Consideration of these factors is beyond the scope of this study and they are not discussed in this report.

2 A Generic Methodology for Estimating Urban Wind Energy

A number of approaches may be conceived to estimate urban wind energy. Many of these may be thought of as following a similar methodology. This methodology comprises a number of steps, and at each step different choices may be made. In this section we outline this methodology and evaluate a number of available approaches to each step. The evaluation will cover a number of aspects, including cost, simplicity, accuracy and consistency with approaches in other steps.

The generic methodology is summarised in Fig. 1 and summarised as follows:

2.1 *Large-scale reference wind climatology*

The starting point is a 'large-scale reference' wind climatology. By 'large-scale reference' we mean a climatology that has uniform validity across the country, at a specified reference height and over a standard surface (usually short grass, as this is the specified surface over which standard meteorological measurements are made). Exactly what scale orography this climatology is consistent with depends on the climatology, but it is generally the case that orography at relatively small or local scale is not included explicitly. Since the impact of the local surface diminishes with height, it is common to consider the idea of 'large-scale' as being in some way equivalent to 'top of boundary layer' or around 500-1000 m. This may be direct, in that the climatology may be genuinely derived from elevated winds or geostrophic winds, which ignore surface friction. Alternatively, the climatology may be relevant to some near-surface level such as 10 m or 45 m, in which case, when applying to a different surface it is necessary first to use an appropriate wind profile to correct upwards to some appropriate height then use a different profile over the new surface to correct downwards to the new surface.

Note that deriving the large-scale reference climatology itself may not be a straightforward process and may involve using some of the stages that follow backwards to remove the effects of local conditions from available data.

The large-scale reference climatology may exist in a number of forms, such as a time series of gridded data covering a long period at intervals of a few hours, statistical summaries such as wind roses (probabilities of experiencing given 'bins' of wind speed and direction) or an intermediate form (such as sets of representative wind-fields and their probabilities). Since the climatology varies in space it is generally derived at a representative set of points (such as a regular grid) sufficiently close together that it may be assumed that the climatology at intermediate points may be derived by a simple method such as linear interpolation.

2.2 *Adaptation and down-scaling to local surface and orography.*

Given the large scale climatology, the next step is to adapt this to local conditions. Though some methods (such as use of fine-resolution mesoscale models) may combine several steps, it is not possible, with current technology, to cover all steps in one go, so a certain amount of sequential processing, using different techniques, is inevitable. Many techniques assume that different processes operate independently, so the process may be thought of as a succession of corrections. An essential feature of each step is that new information is introduced about the local conditions which is at successively finer scale.

2.2.1 *Orography*

The impact of local orography is often regarded as being independent of local land-cover. This is not strictly true, but may be a useful, and even necessary, approximation. Many major UK urban areas are built on only gentle orography and simple correction techniques may be applicable.

However, some towns (such as Edinburgh or Lincoln) present a challenge even to sophisticated high-resolution models.

Whatever method is applied, input orographic height is required. This is readily available at 100 m resolution, and, if necessary, and at some cost, at higher resolution.

2.2.2 Inertial sub-layer

The first step 'downwards' is to the inertial sub-layer. Surface characteristics may be described by a small number of parameters (at its simplest, the roughness length) which are representative of areas of at least a few 100 m across. Though local equilibrium may be assumed near the surface it is necessary to at least consider the nature of the upwind fetch when deriving the inertial sub-layer wind profile. This may be by using internal boundary layer ideas where transitions from one surface to another are clear (and in one definable place) or by successively applying inertial sub-layer theory to an aggregated surface then to a more local surface using blending-height ideas where the fetch is made up of successive patches of different land-use.

2.2.3 Roughness and canopy sub-layers

The majority of small turbines will not be mounted in the inertial sub-layer but lower in the roughness sub-layer or even in the canopy itself. A mean wind profile may be applied, driven by the inertial sub-layer wind. Furthermore, we may be able to say something about the temporal (turbulent) variation. More local canopy characteristics may be used, and it may be possible to consider transition effects on the scale of a few streets, but it is important that the roughness sub-layer and inertial sub-layer are considered together in order to maintain some consistency in description of the overall surface. In general, more information regarding building characteristics and morphology will be required to predict the canopy flow than the inertial sub-layer flow.

2.2.4 Building-scale flow

The canopy flow represents an average over a number of buildings – the flow round each building varies both in the mean and in its turbulent component. If we wish to identify the best place on or near a building to mount a turbine, and wish to know the advantage gained through this choice, we need to know about this building-scale flow. A certain amount of information may be generic (i.e. be insensitive to the precise locality) but it must be recognised that the flow round buildings interacts in potentially complex ways.

It is also important to remember that some buildings (such as the BT Tower, in London) will not fit well into this scheme, as they are sufficiently different from their neighbourhood that techniques based on averaging concepts cannot work. In such cases the best approach may be to assume that the building scale is embedded not in the canopy flow but in the inertial sub-layer flow.

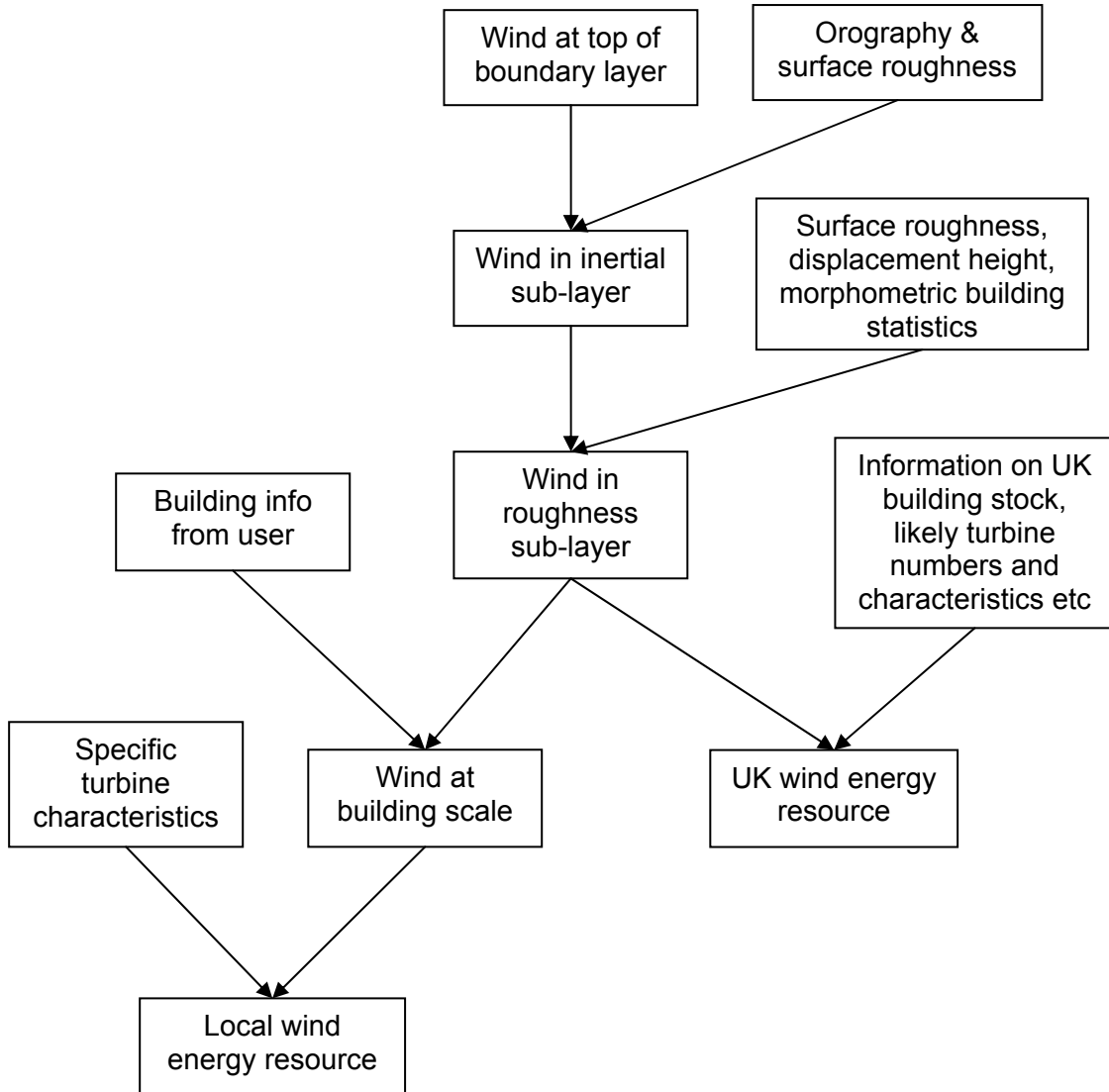
2.3 Local wind energy resource

The above down-scaling process will need to be followed to provide a wind climatology for optimal mounting of a wind turbine on a given building. Information about the turbine will be required at two stages; first, to apply any limitations on mounting, such as height or roof vs tower mounting and second, to convert the climatology to statistics of power generation given the turbine characteristics.

A great deal of information is required to follow this process. In practice, it is unlikely that we will have available (or wish to use) information about every building. Instead it may be most practicable to separate the process at the building scale, i.e. to make an overall calculation of roughness-sublayer or even inertial sub-layer flow and to supplement this with a building scale correction using user-supplied information about individual buildings and their surroundings at the site of interest. This would then be combined with information on the particular turbine to be used.

2.4 UK wind energy resource

While it is desirable to maintain consistency with the building-scale estimation above as far as possible, it is unrealistic to suppose that the national resource will be estimated by summing over all buildings. Instead, roughness-sublayer wind climatology will be combined with scenarios describing likely installation of turbines (number, type) and assumptions about optimality of installation. The roughness-sublayer climatology may be derived using as detailed information regarding building characteristics as feasible, but it is likely that many errors will average out; the main value of detail will be in capturing the impact of correlations between data (e.g. between take-up scenarios and building characteristics) which may be poorly understood in any case.



3 Evaluation of available methods

The methods listed below are evaluated within the context of the generic methodology described in Section 2.

3.1 Large-scale reference wind climatology

Method	Source Data	Cost	Accuracy	Strengths	Weaknesses
WAsP	Nearest surface observation.	Medium for individual site evaluation. High for whole UK.	Implicitly relies on inverse correction for orography. Errors may cancel if target site similar to observation site in character.	Uses local observations directly. Physically sound inverse orography correction based on linear flow. (See comments under orography)	Method designed for single-site evaluation. Method may break down in very complex terrain. Does not automatically result in consistent fields everywhere where regions influenced by different stations overlap.
Geostatistical Interpolation (Met Office approach)	All available surface observations are used to model relationship with topography. Final estimate depends on a distance-weighted average of nearby observations.	Low	Estimated RMS error is 1.3 knots (0.7 m/s)	Already exists. Able to include all scales of orographic effect (assuming these are reflected in the source data).	Only provides mean wind speed. No attempt to homogenise source data. Treatment of orography is statistically rather than physically based.

Method	Source Data	Cost	Accuracy	Strengths	Weaknesses
NOABL	Surface observations within local 'tile' (100x100 km)	Relatively inexpensive	Implicitly relies on inverse correction for orography. Unlikely to be high as orography correction generally only works well for dense data. Accuracy reflected in the need for a consistency correction (~20%) for overlapping tiles	Very cheap to produce (given software) and freely available. 'Uniform' (after consistency correction) UK coverage.	Poor physical basis. Only provides mean wind speed (though method could be extended)
NWP Re-analysis	Mainly upper-air, satellite.	Very expensive to produce (but already produced). Expensive to use as large amounts of data to handle.	Represents best available large-scale climatology, but scale is coarse and small, extreme events may be absent.	Definitive, flexible (i.e. statistics can be tailored to application). Consistent over wide area. Long time series (40-45+ years)	Unwieldy. Bridge between well-represented scales and local scale may be too large to bridge well using simple techniques.
NWP Operational	Mainly upper-air, satellite. More use of surface observations in smaller scale models.	Very expensive to produce (but already produced). Expensive to use as large amounts of data to handle.	Finer scale than re-analysis but smallest scales still not fully represented.	Flexible (i.e. statistics can be tailored to application), Consistent over wide area. Finer scale than standard surface observation network density	Unwieldy. Model changes over long time-series. Only relatively short time-series available for finest resolutions. Downscaling may be made more complex by impact of sub-grid parametrization schemes.

3.2 Orography

Method	Method	Cost	Accuracy	Strengths	Weaknesses
WAsP	Analytical linear flow model, with higher accuracy closest to analysis site.	Medium for individual site evaluation. High for whole UK.	Reasonably good for relatively gentle terrain, neutral flow. Errors may cancel if target site similar to input observation site in character.	Uses local observations directly. Physically sound orography correction based on linear flow. However, mainly useful for neutral atmosphere and gentle terrain.	Method designed for small site evaluation. Method may break down in very complex terrain. Does not automatically result in consistent fields everywhere where regions influenced by different stations overlap.
MS3DJH	Analytical linear flow model similar to WAsP but more suited to general application over grid.	Medium for individual site evaluation. Medium/high for whole UK.	Reasonably good for relatively gentle terrain, neutral flow.	Could be used with a variety of input climatologies, including NWP.	Method may break down in very complex terrain. Cannot be applied to whole UK at once – needs ‘tiled’ approach.
3dVOM and MSFD	Numerical solution of linear flow equations	Medium/high for whole of UK	Similar to MS3DJH, but better for stability effects	As MS3DJH	As MS3DJH
Potential flow (in linear flow model context)	Simplified form of MS3DJH.	Low-medium	May compete with other linear approaches, but does not capture near-surface subtleties.	Physically sound orography correction based on linear flow. However, mainly useful for neutral atmosphere and gentle terrain. Correction factors can be computed for all conditions using two runs of the model.	Method may break down in very complex terrain. Cannot be applied to whole UK at once – needs ‘tiled’ approach.

Method	Method	Cost	Accuracy	Strengths	Weaknesses
Mass consistent (NOABL)	Enforce consistency with mass conservation.	Low.	Unlikely to be high as mass consistent approach generally only works well for dense data.	Very cheap to produce (given software) and freely available. 'Uniform' (after consistency correction) UK coverage.	Poor physical basis. Only provides mean wind speed (though method could be extended). Cannot be applied to whole UK at once – needs 'tiled' approach.
'Howard and Clark' NWP correction.	Local roughness correction (see below) and simple height-dependent wind speed correction based on linear flow with many simplifications.	Very low, but designed for use with NWP data.	Works reasonably well for hill-top speedup, not so well for valleys.	Extremely cheap addition to NWP data – needs some further work on consistent application over low hills. Main use is in local roughness correction.	Uses single, representative, orography wavelength so should be less accurate than other linear approaches.
High-resolution mesoscale model	Full fluid dynamical model, driven by real case data or 'uniform flow' from climatology statistics	Very expensive to produce and to use as large amounts of data to handle.	Should out-perform linear approaches when applied in similar way.	Definitive, flexible. Consistent over wide area. Can handle more complex orography (but maybe not very steep terrain) and simultaneously deals with surface characteristics.	Unwieldy. Benefits may be lost by need to run for 'representative' events or uniform flow in order to reduce cost.

3.3 Correction to inertial sub-layer (local roughness)

Method	Method	Cost	Accuracy	Strengths	Weaknesses
WAsP	Uses a perturbed IBL wind profile to calculate the effect of multiple roughness changes	Medium for individual site evaluation. High for whole UK.	Reasonable	Simple and scientifically sound	
3dVOM and MSFD	Numerical solution of linear flow equations	Medium/high for whole of UK (but no additional cost if same method is used for orography)	Reasonable for moderate roughness changes	Simple and scientifically sound	Linear approach less accurate for dramatic roughness changes
Neutral IBL	Calculates wind profile for local roughness based on estimated height of IBL	Low.		Simple and scientifically sound for neutral flow.	May be very difficult to accurately identify urban/rural boundary.
'Howard and Clark' NWP correction.	Local roughness correction	Very low, but designed for use with NWP data.			
High-resolution mesoscale model	Full fluid dynamical model, driven by real case data or 'uniform flow' from climatology statistics	Very expensive to produce and to use as large amounts of data to handle.	Should out-perform other approaches when applied in similar way.	Definitive, flexible. Consistent over wide area. Can handle more complex land-use and simultaneously deals with orography.	Unwieldy. Benefits may be lost by need to run for 'representative' events or uniform flow in order to reduce cost.

3.4 Correction to mean profile in the roughness sublayer (including within the urban canopy)

Method	Method	Cost	Accuracy	Strengths	Weaknesses
Analytic profile	Use of the standard log law above the canopy matched to an exponential decay within the canopy.	Very low.	Medium (i.e. typical of the methods available for representing the roughness sublayer).	Simple to apply. Uses a small number of statistical properties of the canopy.	Invalid when the character of the canopy is rapidly changing. Limited validation.
COST-715 method	Integration of the inertial sublayer form of the flux-gradient relation using the local flux at each height together with an analytic description of the flux profile.	Low, but not trivial.	Probably medium, but hard to judge.	Uses a small number of statistical properties of the canopy.	The local scaling idea lacks a strong theoretical basis and there is not much empirical validation data. Inapplicable below displacement height.
1-D mixing length model	Numerical solution of 1-D mixing length model.	Low, but not trivial.	Medium.	Uses a small number of statistical properties of the canopy.	Invalid when the character of the canopy is rapidly changing. Limited validation.
2-D mixing length model	Numerical solution of mixing length model in wind-aligned vertical plane.	Medium.	Medium.	Can account for changes in the character of the canopy. Useful for studying theoretical aspects of canopy flow.	Requires more detailed information on statistical properties of the canopy as the canopy changes in space. Difficult to know what scale to compute canopy properties over. In practice the improved accuracy in most situations is likely to be small and unlikely to justify the extra effort.

Method	Method	Cost	Accuracy	Strengths	Weaknesses
CFD model (treats 3.4 and 3.5 issues in one go)	Solution of the 3-D flow field through an explicitly described building geometry.	Very high, prohibitively so for more than a few locations.	Should outperform other methods when applied appropriately.	Can account for the actual building geometry.	Requires detailed descriptions of the buildings to get the best results. Requires substantial expertise and judgement in setting up models to get the best results.
MCP (see note)	Uses statistical correlations between a target site and a reference station	Low computational cost for an individual site. High data collection cost (would need to collect data at neighbourhood scale for whole UK).	Can be high for well observed / well correlated sites.	Uses observations from the target site	Requires complete time series (not just frequency distribution). Difficult to generalise results to other locations. Only gives results for the monitoring height – still need to assume a form for the vertical profile.

Note: MCP could be used to estimate the wind climatology at the top of the roughness sublayer either from data for a well-exposed anemometer or from NWP data for higher up in the boundary layer. Used in this way the MCP method effectively short-circuits some of the preceding stages in the generic methodology.

3.5 Correction for the specific local building geometry

Method	Method	Cost	Accuracy	Strengths	Weaknesses
Ignore local effects	Ignore local effects.	Zero.	None for the extra local effect. However such effects are not predictable with great accuracy in any case (except with great cost) and the effects are likely to be unimportant for estimating total energy resource (as opposed to that at particular locations).	Simple.	Local effects can be important for assessing particular locations or making siting decisions.
Rules of thumb	Rules of thumb based on nature and location of upwind obstacles.	Low (at least for one site; data may not be available to cover many different sites in an automated way).	Not great, but likely to give a worthwhile improvement over ignoring local effects.	Simple to apply (at a single location).	We are not aware of any rules of this type, much less well tested rules. However it seems likely that such rules could be developed.
CFD model (treats 3.4 and 3.5 issues in one go)	Solution of the 3-D flow field through an explicitly described building geometry.	Very high, prohibitively so for more than a few locations.	Should outperform other methods when applied appropriately.	Can account for the actual building geometry.	Requires detailed descriptions of the buildings to get the best results. Requires substantial expertise and judgement in setting up models to get the best results.



Met Office

Method	Method	Cost	Accuracy	Strengths	Weaknesses
MCP (see note)	Uses statistical correlations between a target site and a reference station	Low computational cost for an individual site. High data collection cost. Prohibitive to apply it to all properties in the UK.	Can be high for well observed / well correlated sites.	Uses observations from the target site	Requires complete time series (not just frequency distribution). Very difficult to generalise results to other locations.

Note: MCP could be used to estimate the wind climatology in the vicinity of an individual building either from data for a well-exposed anemometer or from NWP data for higher up in the boundary layer. Used in this way the MCP method effectively short-circuits some of the preceding stages in the generic methodology.

4 Calculation Methodologies

4.1 Previous Work

4.1.1 Paper by Heath et al (2007)

Summary of Heath methodology:

Published formulae (Macdonald *et al.*, 1998) are used for calculating z_0 and d from building morphology i.e. frontal and plan area densities, the drag coefficient of the buildings, a constant determined by the building arrangement and a correction factor for building drag.

The vertical wind speed profile in an urban area is assumed to be logarithmic above the mean building height and exponential below the mean building height.

The methodology uses 10m wind speed data from the DTI Wind Speed Database (NOABL model) as its starting point – these are assumed to relate to a roughness length of $z_0 = 0.03$ m.

The wind speed in a rural location is related to the wind speed in an urban location by matching the log profiles at the height of the internal boundary layer (IBL).

The IBL depth is calculated from the urban roughness length and the distance from the roughness change i.e. from the edge of the urban area.

CFD studies were used to determine local building effects, as follows:

- Buildings are modelled as 10m cubes with a 45° pitched roof
- These buildings are arranged as a staggered array – 4 rows of 6 houses. The street width (i.e. distance between rows) was 20m and the distance between buildings within a row was 5m. The roughness length of the ground between the buildings was assumed to be 0.001m (typical of well-mown grass, concrete or tarmac).
- For this arrangement of buildings the plan and frontal area densities are both 22%. Using published values for a staggered array of cubes for the other quantities (drag coefficient etc) gives $z_0 = 0.8$ m and $d = 4.3$ m.
- The inflow wind to the CFD model follows the log/exp profile (this point is not absolutely clear – the text refers to a “semi-log” wind profile).
- The results are taken from the building in the middle of the most downwind row of houses. It is assumed that the flow is fully adjusted by the time it reaches the fourth row of houses.
- A ‘local effect coefficient’ is calculated for four different turbine mounting points – front, corner, gable and centre. This coefficient is the ratio of the wind speed at the specified point to the upstream velocity at mean building height – it varies with the wind direction (relative to the building orientation) and height (i.e. turbine hub height).

To estimate the energy yield for a specific house:

- Use the local effect coefficients and the prevailing wind direction (not the full wind direction frequency distribution) to estimate the optimum mounting position for the intended turbine hub height
- Extract the 10m NOABL wind speed from the DTI database
- Calculate z_0 and d from suitable morphometric data
- For each wind direction:
 - o Calculate the distance to the edge of the city
 - o Calculate the IBL height from this distance and z_0
 - o Calculate the mean speed at mean building height from the rural and urban roughness lengths, IBL height and mean building height
 - o Adjust the mean speed using the appropriate local effect coefficient
 - o Combine a Rayleigh frequency distribution with the appropriate mean with the power curve for the selected turbine to get mean energy yield
 - o Multiply the energy yield by the frequency of winds from that direction to get the yield for that direction
- Sum over all wind directions

Example Calculation:

Scenario: installation of a 1.5kW turbine on a 3m mast above a house in west London. The environment is assumed to be homogeneous and similar to that used in the CFD studies i.e. plan and frontal area densities of 22%, mean building height of 10m etc. The house is orientated so that the ridge line runs north-south.

Observations from Heathrow show the prevailing wind direction is southwest. For this wind direction the optimum mounting position is 3m above the north gable end.

The 10m NOABL wind speed for the location is 4.9m/s.

The roughness length is 0.8m and the displacement height is 4.3m (calculated from the morphometric data).

For a northerly wind direction:

- the distance to the edge of the city is 28km
- this gives an IBL height of 2591m at the location of the house
- the mean speed at mean building height in the vicinity of the house is estimated to be 2.3m/s (obtained from the NOABL value by matching the log profiles at the IBL height)
- the local effect coefficient (from the CFD studies) for the north gable end for a northerly wind is 1.2
- the local mean wind speed is therefore $2.3 \times 1.2 = 2.8$ m/s
- combining a Rayleigh distribution with a mean of 2.8 m/s with the power curve for the selected turbine and adjusting for the frequency of northerly winds (10%, as observed at Heathrow) gives an energy yield for this wind direction of 79 kWh/yr

This calculation process is repeated for each of the other seven wind direction sectors. The results are added up to give a total energy yield of 520 kWh/yr. This corresponds to a capacity factor of 4% i.e. the predicted energy yield is 4% of the maximum possible yield (1.5 kW x 8760 hours = 13,140 kWh/yr).

Notes:

The authors note the following limitations of the methodology:

- No allowance was made for vegetation in urban areas i.e. trees, hedges and bushes. As the space between buildings is often filled with plants and trees this means the roughness length is likely to have been underestimated.
- No allowance was made for yaw error i.e. the speed of the air passing through the turbine is likely to be less than the actual wind speed due to the turbine's inability to follow changes in wind direction exactly. This will lead to an overestimation of energy yield.
- The roughness length and displacement height are estimated from building densities, drag coefficients etc for simple arrays of cubes. Methods need to be developed for estimating these quantities for more realistic/complicated building arrangements.
- There is no assessment of the impact of turbulence on turbine performance.
- There is a lack of measurements from real urban environments for validating the predictions.

Additional comments:

It appears that there is no limit on the calculated depth of the internal boundary layer. In practice the boundary layer does not extend beyond around 1km from the surface. Once the internal boundary layer (generated by a change in surface roughness) reaches this height then it may be considered that the whole of the boundary layer has come into equilibrium with the new surface i.e. it is not meaningful to have an IBL depth greater than about 1km. If the IBL depth in the example calculation is set to 1000m (instead of 2591m) then the mean speed at building height increases slightly to 2.4m/s (from 2.3m/s).

Regarding the CFD results, the authors note that there is a general decrease in velocity as the wind crosses the rows of houses and that this suggests the inflow wind profile is not consistent with the assumed building canopy properties. The plot shown in Figure 8 of the paper is for a level equal to half the building height so it is difficult to judge the impact this might have on the 'local effect coefficient' for heights above roof level. The use of a revised inflow profile or periodic boundary conditions may help to reduce uncertainties in the calculated coefficients due to this feature of the analysis.

4.2 UK Energy Resource

4.2.1 Outline method

Here we present a relatively simple approach to estimating the total UK small scale wind energy resource. This follows the broad structure outlined in section 2. More sophisticated approaches are possible. However the approach adopted here does, we believe, provide a reasonable balance between the need to produce an estimate quickly and the accuracy of the results. Some tests of sensitivity to the assumptions made are presented. Comments are made at each stage to highlight the simplifications made and summarised in an overall critique of the approach. An outline of possible improvements is then given. The use of these more sophisticated methods and/or of further tests of sensitivity to the assumptions made would add confidence to the results.

The method can be summarised as:

- 1) From large-scale mean wind speed at a reference height above the surface layer compute grid-box average mean wind speed at a blending height representative of grid-box averaged roughness.
- 2) Using a local wind profile calculate the mean wind speed at the turbine hub height.
- 3) Using a typical wind speed distribution and the turbine power curve compute the annual total energy generated by a turbine.
- 4) Combine the annual total energy generated by a turbine with the population distribution to estimate the total energy that could be generated, assuming a fraction of the population install turbines.

4.2.2 Estimating the Wind Speed

4.2.2.1 Large-scale wind climatology

We have assumed neutral equilibrium profiles in inertial sublayers. Directional effects (i.e. upwind distance to the edge of an urban area) have been ignored to simplify the computational approach. This enables a single wind speed distribution to be used, and, with the further simplification of modelling the distribution with a function that requires only one parameter, a single large-scale mean wind speed (varying spatially) is all that is required. This needs to be representative of the wind near the top of the boundary layer. However, since most of the wind-shear occurs in the inertial sub-layer, and wind speed profiles are less well defined outside this layer, we have chosen a reference height, z_{ref} , of 200 m. This is similar in magnitude to the diffusion height¹ over an urban surface (based on typical urban heterogeneity scales) and also close to the top of the inertial sub-layer. It also corresponds to the internal boundary layer depth about 2 km downwind of a typical rural/urban transition.

We have used the large scale 30-year mean wind climatology from 1971-2000 produced by the Met Office's National Climate Information Centre (NCIC) (see Figure 1). This uses geostatistical techniques to interpolate available wind data (at 10 m) and takes orography into account through this method. No additional correction for orography has been applied. This is available on a 1 km grid, and this grid has been used for subsequent calculations as it is a reasonable scale at which to apply the surface heterogeneity methods used. See section 6.1 of the preceding report (Urban Wind Energy Research Project, Part 1: A Review of Existing Knowledge) for a more detailed description of this data set.

¹ The diffusion height is the height above a heterogeneous surface at which the mean wind speed is spatially uniform.

The 10 m wind has been scaled up to z_{ref} using a reference rural roughness length of $z_{0ref} = 0.14$ m, representative of ‘open country’ (including isolated trees and hedges) rather than uniform grass. Thus:

$$u_{ref}(z_{ref}) = u(10) \ln(z_{ref}/z_{0ref}) / \ln(10/z_{0ref}) \quad (1)$$

Comments:

1. For a large city, it could be argued that a greater reference height should be used. However, provided the value is reasonably large, the result is quite insensitive. For example, the wind speed at 400 m is only 9% larger than that at 200 m assuming a logarithmic profile, and much of this difference cancels when the wind at blending height is computed.
2. We have not used the DTI wind speed database (based on the NOABL model) as it covers fewer years, we are not confident that the method used to allow for orography is appropriate or effective and (we believe) it uses fewer input stations. However, the effect of using it is considered in the sensitivity study in Sec. 4.2.4. The NOABL data (see Figure 1(c)) has a slightly higher mean (5.4 rather than 5.1 $m\ s^{-1}$) but emphasises smaller scales of variability due to orography than the NCIC data. Speeds over most of the areas containing large conurbations are higher by 10-30% in the NOABL data.
3. Other authors have referenced to $z_{0ref} = 0.03$ m (see e.g. section **Error! Reference source not found.**). This would reduce the reference wind speed by about 12%.

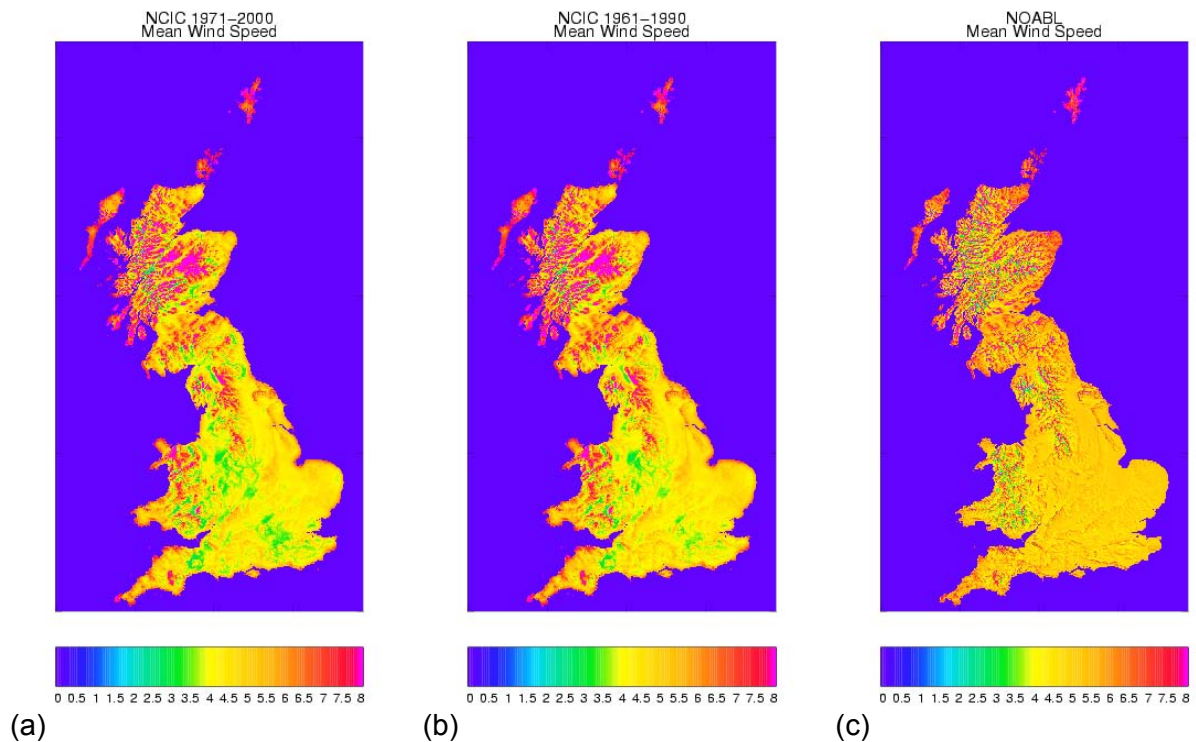


Figure 1 Annual mean wind speed at 10 m (a) NCIC 1971-2000 (b) NCIC 1961-1990 (c) NOABL

4.2.2.2 Blending-height wind speed

The grid box-averaged wind speed at the blending height², l_b , is computed using the effective grid box-averaged roughness length, z_{0eff} , and zero-plane displacement height, d_{eff} , thus:

$$u(l_b) = u(z_{ref}) \ln\left(\frac{(l_b - d_{eff})}{z_{0eff}}\right) / \ln\left(\frac{(z_{ref} - d_{eff})}{z_{0eff}}\right) \quad (2)$$

The grid box-averaged parameters and the grid box blending height are obtained below.

Comments:

1. Blending height theory does not usually take into account the zero-plane displacement height. However, the formulation can be extended quite readily. The main issue is that the theory does not give us a method of estimating the grid box averaged zero-plane displacement height.

4.2.2.3 Grid box-average surface parameters

The grid-box average roughness and displacement height are central to converting the 'regional' wind speed to something representative of the neighbourhood on the scale of the 1 km grid box.

To derive grid box-average surface parameters we have used a methodology similar to that used in the Met Office's UK forecast model. Land use data from the Centre for Ecology and Hydrology (CEH) at 25 m resolution covering 25 categories of surface cover has been aggregated to the proportion of each of 8 surface types in each 1 km square. The two 'urban' categories, essentially suburban and dense urban, have been retained but the vegetation categories simplified. Note that the CEH data gives us the area of these categories, but tells us nothing more about them (such as building height). The types and their assumed properties are summarised in the table below and the proportions of land occupied by the most important types are shown in Figure 2.

Parameter	Surface type							
	Broad-leaved trees	Needle-leaved trees	Grass/Crops	Shrubs	Water	Soil	Sub-urban (See below)	Urban (See below)
Roughness length z_0 (m)	0.95	1.075	0.14	0.18	3×10^{-4}	3×10^{-4}	0.70	1.60
Canopy Height, h , (m)	19	20	1.4	1.8	0	0	6.00	12.00
Displacement height, d , (m)	$19 * 2/3$	$20 * 2/3$	0	0	0	0	3.10	7.00

² The blending height is the height below which the local wind profile can be treated as being in equilibrium with the local surface roughness, and above which the *area-average* profile is in equilibrium with the effective *area-average* surface roughness.

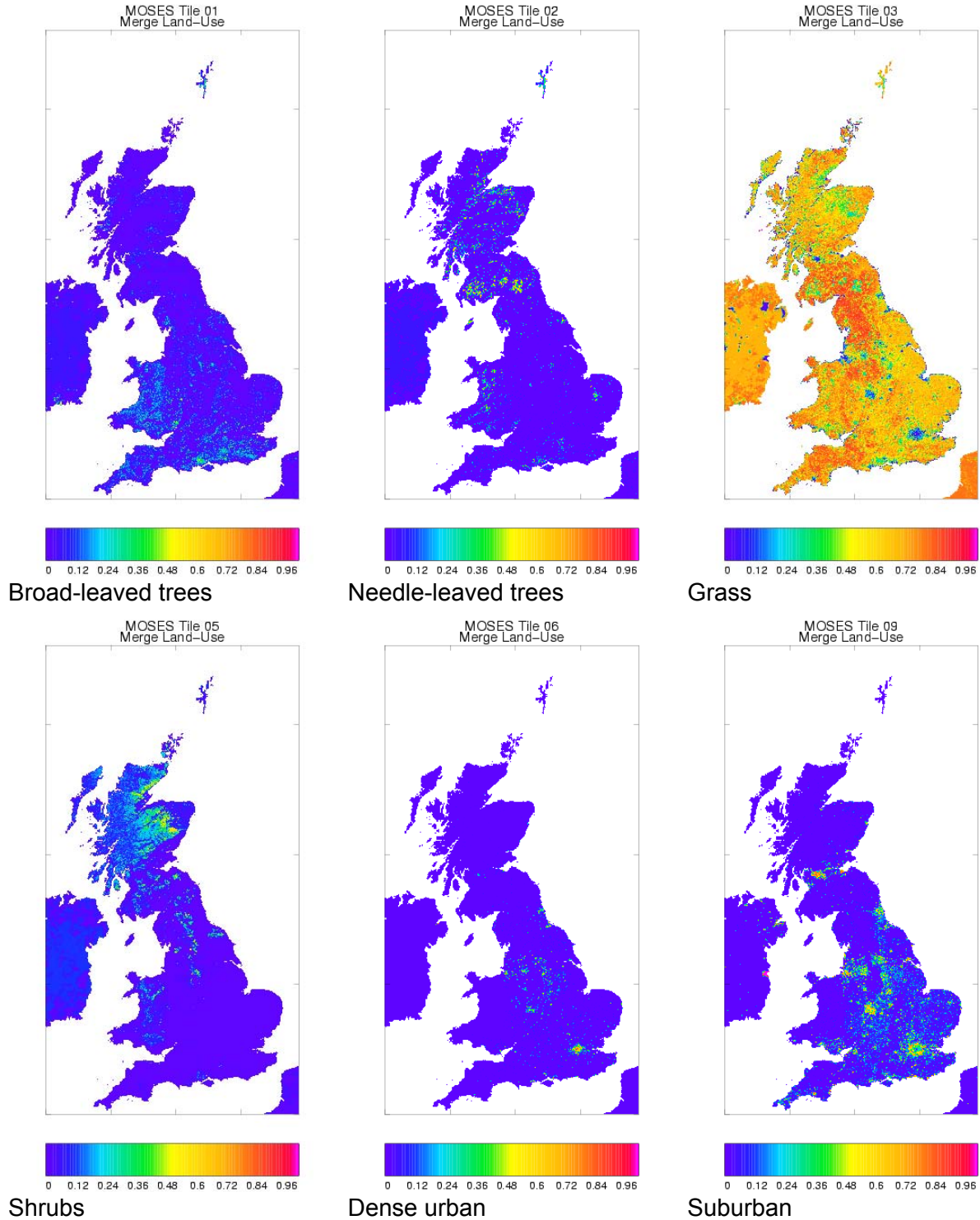


Figure 2 Proportions of different land-use derived from CEH data (supplemented by IGBP over Ireland) for various surface types. Remaining proportions are bare soil and lakes.

Note that the 1990 land cover map has been used (see <http://www.ceh.ac.uk/sections/seo/lcm1990.html>, supplemented by International Geophysical Biosphere Programme (IGBP) data over Northern Ireland, as this data set has been purchased by the Met Office. Ideally, the more recent 2000 dataset would be used (see http://www.ceh.ac.uk/sections/seo/lcm2000_home.html) but this is not readily available to the

Met Office. Consistency checks were performed between UK census population data and land-use data and it is believed that the impact of changes in land-use are very small between these datasets.

We characterise the urban surfaces in terms of mean canopy height h , plan area index λ_p and frontal area index λ_f . In fact λ_p is not required for our approach but is included because some discussion of it is useful in choosing a value for λ_f . We choose the following values:

	Assumed values			Derived parameters			
	h	λ_p	λ_f	d/h	z_0/h	d	z_0
Suburban	6 m	0.4	0.2	0.525	0.117	3.1 m	0.70 m
Urban	12 m	0.6	0.3	0.585	0.133	7.0 m	1.6 m

The values for h and λ_p have been selected based on our general impressions of UK cities. More precise values would be possible using detailed survey information but this is not readily available in a form which can be applied to the whole of the UK. We note the h values roughly correspond to the 'low height' category and the boundary between the 'medium height' and 'tall' categories in Grimmond and Oke's (1999) table 6. The urban λ_p value corresponds to the 'high density' category in Grimmond and Oke's Table 7 and the suburban λ_p values falls into the overlap between their 'low density' and 'medium density' categories. Values of λ_f are generally lower than λ_p and, although there is a lot of scatter, $\lambda_f = \lambda_p/2$ runs roughly through the middle of the data points in figure A1(f) in Grimmond and Oke (1999). In the absence of more detailed survey information we have adopted $\lambda_f = \lambda_p/2$. For estimating d and z_0 we have used the formulae of Raupach (1994, 1995) with $\kappa = 0.4$ rather than those of Macdonald *et al.* (1998) as used by Heath *et al.* (2007). This is based on the recommendations of Grimmond and Oke (1999), who found that, while Macdonald's formulae work well in many situations, they tend to under-predict roughness when $\lambda_p > 0.4$.

Land-use fractions less than 0.01 have been ignored; otherwise they can, in our approach, dominate the displacement height estimate. The area-averaged displacement height is taken to be the maximum of that of the non-zero fraction land-use types. The blending height is taken to be the larger of 10 m or twice the maximum canopy height of any land use with non-zero fraction. In practice, this means that the blending height is somewhere between 10 m and 40 m. The sensitivity to this has not been tested but experience suggests that over this range results are quite insensitive. The area-averaged roughness is then taken to be given by:

$$\left(\ln\left(\frac{l_b - d_{eff}}{z_{0eff}}\right)\right)^{-2} = \sum_{i=\text{Land use types}} F_i \left(\ln\left(\frac{l_b - d_i}{z_{0i}}\right)\right)^{-2} \quad (3)$$

where F_i denotes the fraction of land use for the i th land use type. The result is shown in Figure 3.

Comments:

1. The derived urban parameters are important in determining the urban wind speed at a given height (above ground or roof level). The sensitivity to the assumed urban canopy height h will be investigated below.

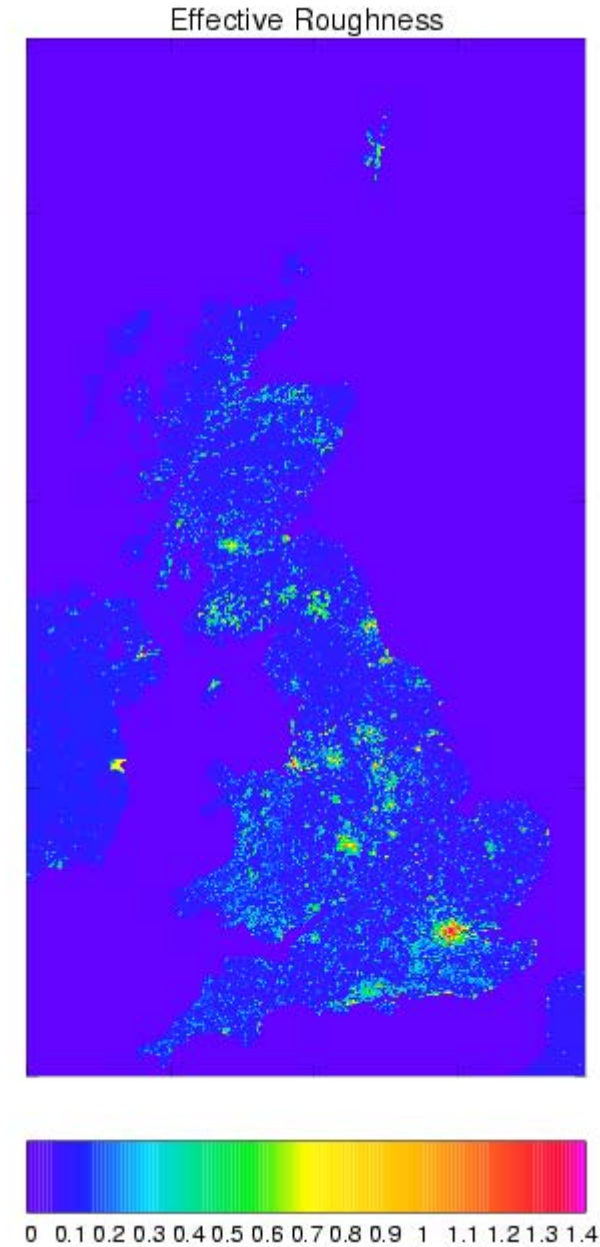


Figure 3 Overall effective roughness length (m) generated from land-use and blending.

4.2.2.4 Wind at turbine hub height

The wind at hub height is calculated using a local wind profile appropriate for the local roughness. Three local environments are considered, rural, sub-urban and urban, on the basis of the CEH classification (and the assumption that most rural dwellers live in ‘open countryside’ rather than forest). This could easily be extended if more information were available on building morphology.

For the rural environment, a well-exposed site is assumed and the roughness length assumed to be z_{0ref} . The wind speed at hub height, z_{hub} , is thus:

$$u(z_{hub}) = u(l_b) \ln(z_{hub}/z_{0ref}) / \ln(l_b/z_{0ref}) \quad (4)$$

Note that if $z_{hub} = 10$ m this will not exactly recover the input 10 m wind as we assume that the latter has been standardised to the basis that everywhere has the reference roughness, while this ‘rural’ wind speed still takes into account the impact of nearby enhanced roughness (through the impact of grid box-averaged roughness length z_{0eff} on $u(l_b)$).

For the urban and suburban environments, once the inertial sublayer wind profile has been characterised (in terms of l_b , $u(l_b)$, z_0 , and d), we need to estimate the (neighbourhood averaged) profile in the roughness sublayer. We believe that there is little evidence of superior performance in practice from more complicated approaches that have been proposed in the literature and so we recommend a simple analytic profile. In the region between the canopy top and the inertial sublayer this is simply a downward extension of the log law which is valid in the inertial sublayer above (Cheng and Castro, 2002; Coceal and Belcher, 2004). Hence, for $z_{hub} \geq h$ we have

$$u(z_{hub}) = u(l_b) \ln\left(\frac{z_{hub} - d_{(sub)urban}}{z_{0(sub)urban}}\right) / \ln\left(\frac{l_b - d_{(sub)urban}}{z_{0(sub)urban}}\right) \quad (5)$$

Below the canopy top we assume an exponential decay with decay constant a given by Macdonald’s (2000) empirical estimate $a = 9.6\lambda_f$. This leads to

$$u(z_{hub}) = u_h \exp\left(-9.6\lambda_f \frac{h - z_{hub}}{h}\right) \quad (6)$$

where u_h is the wind speed at height h derived from equation (5).

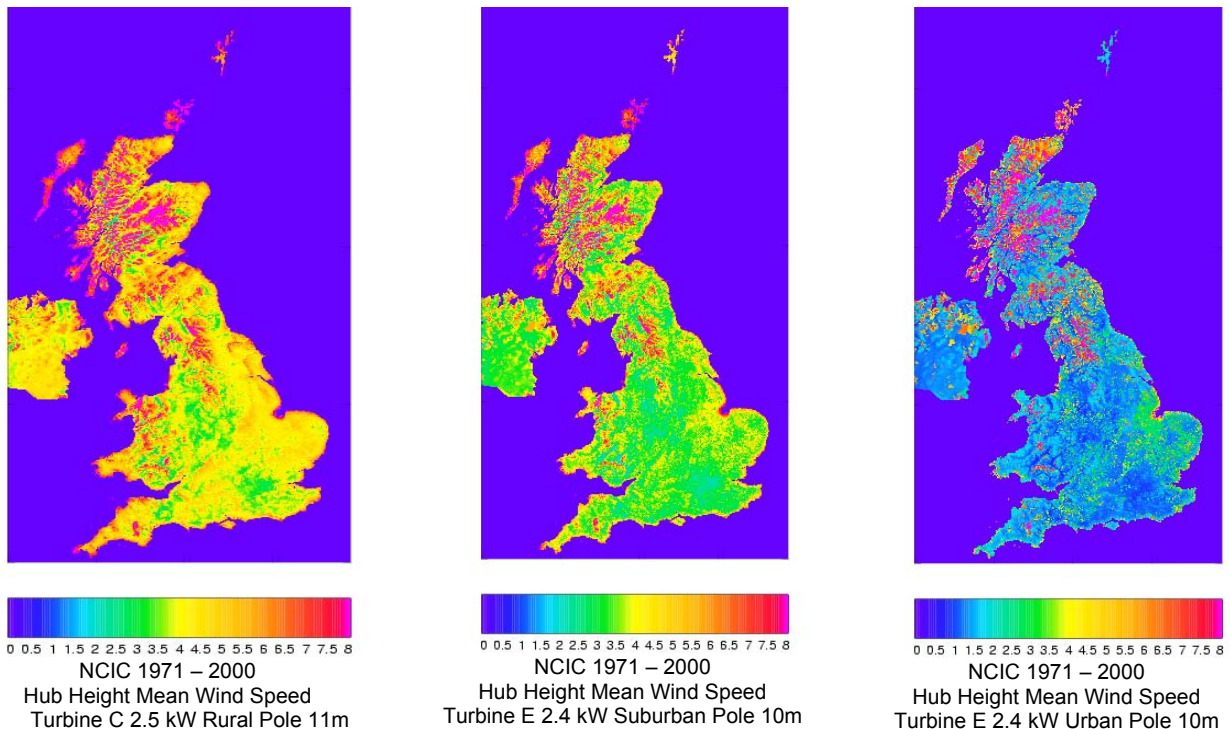


Figure 4 Examples of annual mean wind speed calculated for different local environments and similar heights representative of pole-mounted turbines.

Note that this results in different wind speeds in each grid box depending on the assumed *local* environment.

As examples, the mean wind speeds for pole-mounted turbines at similar heights are shown in

Figure 4 for rural, suburban and urban environments.

Note that these data do not necessarily represent wind speeds that could be measured in reality; if, for example, there were to be an urban area on the top of Cairngorm then the wind speed for a turbine mounted on a 10 m pole would be estimated by the value in the appropriate grid box in

Figure 4(c), but, since in fact, there is no significant urban area there, the wind-speed shown is too high (because z_{0eff} is too low). However, if a small village were to be built large enough to have a well defined ‘roughness’, but small enough to have negligible impact on the overall roughness (about 100-200 m across), this would be the wind speed likely at the centre. The rural wind speed is similar (but not identical) to Figure 1(a), the source data, but does show the impact of urban roughness in the major conurbations. The suburban speed is significantly lower, while the urban speed is very low, reflecting the fact that the height of the wind (10m) is below the assumed building height.

Comments:

1. Extending the log law into the roughness sub-layer appears to work reasonably well, but should not be regarded as scientifically justified by inertial sublayer scaling, as this should not apply so close to the displacement height.
2. The exponential form in eq. 6 is only used when the hub height is below roof level. Given the choice of turbines considered in this study (see section 4.2.3.1) this means the exponential form is used only for the urban pole-mounted turbines (the roof-mounted turbines and the suburban pole-mounted turbines are all above roof level). This exponential decay emphasises the very substantial reduction in power generation that results from mounting below roof level.

4.2.3 Estimating the Energy Resource

4.2.3.1 Choice of turbines

In order to estimate the overall energy resource, we have to make decisions about the actual turbines used and their likely mounting. The turbines shown in the following table have been used as models. In the case of roof-mounted turbines it is assumed that there is a limit on the height above roof level of the highest part of the device. For a horizontal axis device the highest point is reached by the tips of the blades, so the hub height is determined from the limiting height and the rotor diameter. Three maximum heights have been chosen – 3, 4 and 10 m. The 10 m height is unlikely to be practicable, but has been used to illustrate the benefit to be gained from use of a very tall mounting.

Turbine	Mounting	Hub Height	Application
Turbine A 15kW	Pole	15 m	Rural
Turbine B 6kW	Pole	15 m	Rural
Turbine C 2.5kW	Pole	11 m	Rural
Turbine D 80W	Pole	6 m	Rural
Turbine E 2.4kW	Pole	10 m	Urban
Turbine F 1.5kW	Roof	1.95 m 2.95 m 8.95 m	Urban

Turbine G	1kW	Roof	2.125 m 3.125 m 9.125 m	Urban
-----------	-----	------	-------------------------------	-------

The hub heights given for the pole-mounted turbines are height above ground level. The hub heights for the Turbine F and Turbine G are height above roof level and are based on rotor diameters for these devices of 2.1m and 1.75m respectively.

4.2.3.2 Weibull Distribution

The mean wind speed computed above has been converted into a distribution by assuming a Weibull distribution. This is characterised by a scale parameter, A, and a shape parameter, k, thus

$$f(u) = \frac{k}{A} \left(\frac{u}{A}\right)^{k-1} \exp\left(-\left(\frac{u}{A}\right)^k\right) \quad (7)$$

$$F(u) = 1 - \exp\left(-\left(\frac{u}{A}\right)^k\right) \quad (8)$$

$$\bar{u} = A \Gamma\left(1 + \frac{1}{k}\right) \quad (9)$$

Here, $f(u)$ is the distribution function, $F(u)$ the cumulative distribution function and \bar{u} the mean speed. Values of k obtained by fitting a Weibull distribution to hourly mean speed data vary between 1.5 and 2.1 (based on figures in the European Wind Atlas). Values of $1/\Gamma(1+1/k)$ are tabulated in the European Wind Atlas (Troen and Petersen, 1989):

k	A
1.6	1.115 \bar{u}
1.8	1.124 \bar{u}
2.0	1.128 \bar{u}

We have assumed $k = 1.8$. Note $k = 2.0$ gives a Rayleigh distribution.

Comments:

1. The parameter k determines the relative frequencies of the different wind speed ranges and so can have a significant impact on power once combined with the power curves. It determines how long a "tail" exists at high wind speeds which is likely to be especially important. The sensitivity to k is evaluated below.

4.2.3.3 Mean Power Calculation

Assuming the power curve is defined at 1 m/s intervals and that the wind speed, u , is in m/s then:

$$\text{Mean Power} = \sum_u P(u) \times (F(u+0.5) - F(u-0.5)) \quad (10)$$

where $P(u)$ is the power generated at wind speed u . This form is chosen to ensure that the total wind-speed probability sums to 1. The power curves for the turbines considered here are shown in Figure 5.

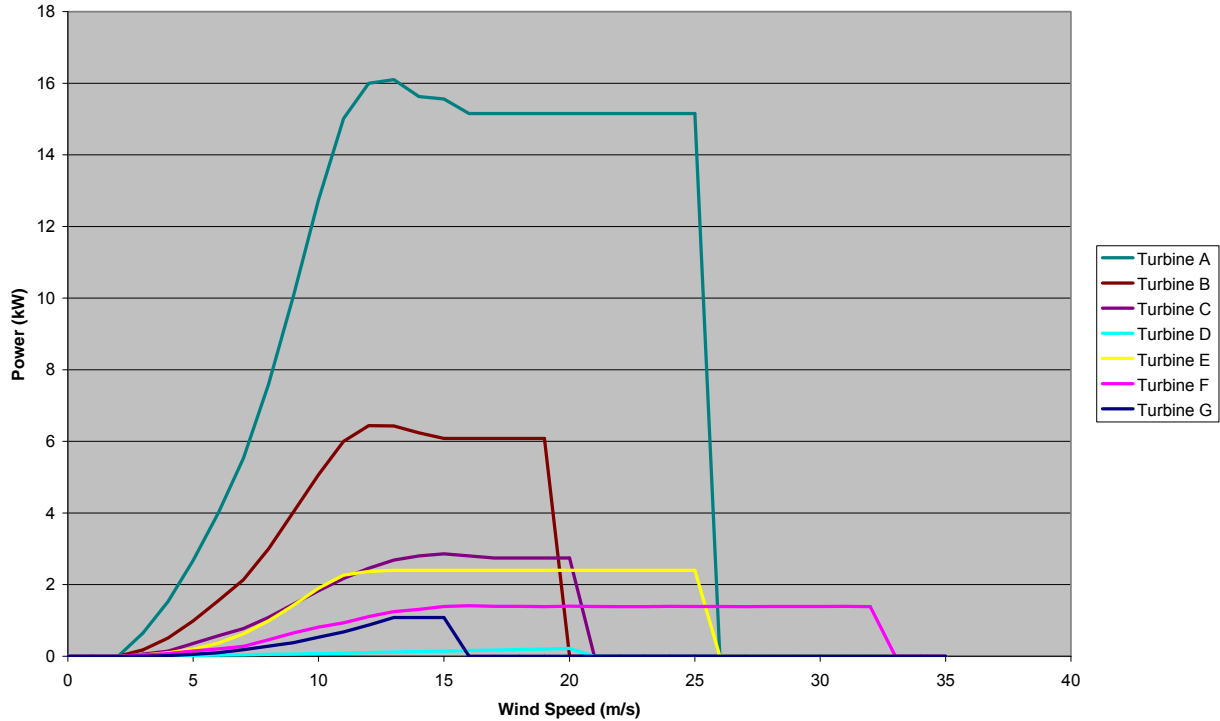


Figure 5 Assumed power curves for selected turbines.

The annual energy production can be obtained by multiplying the annual mean power by the number of hours in one year (i.e. $365.25 \times 24 = 8766$):

$$E = 8766 \sum_u P(u) \times (F(u+0.5) - F(u-0.5)) \quad (11)$$

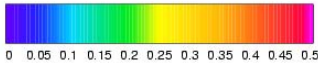
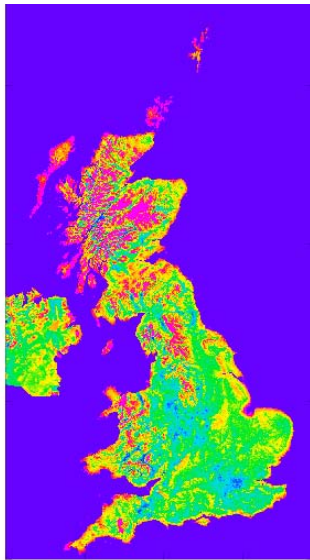
The total energy per year generated by a single turbine is thus calculated by first calculating the annual mean wind speed at turbine height (Section 4.2.2.4) then combining the published power curve for the turbine with the Weibull Distribution based on the annual mean speed.

The combination of turbines, environments and heights leads to a total of 18 different maps of energy generated by a turbine in a year. These have been used below to estimate the total resource. However, to facilitate inter-comparison, it is also useful to consider the capacity factor, defined as the energy generated divided by the energy that would be generated if the turbine produced its nominal or rated output continuously. These are shown in Figure 6.

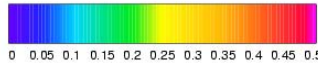
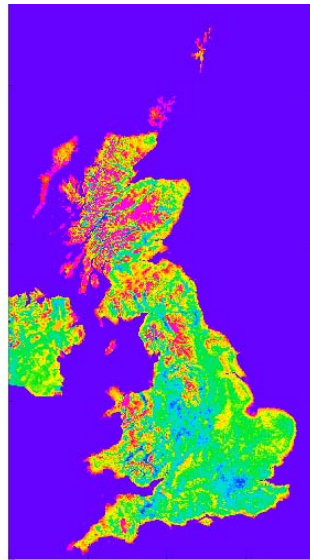
A number of conclusions can be drawn from these figures:

- 1) A rural turbine may achieve a capacity factor of 15-20% in the English countryside. This may be substantially exceeded if mounted near hilltops in hilly terrain, or near the coast. On the other hand, it is likely that small turbines will be mounted near houses which are more likely to be in valleys than on hilltops, so 15-20% may be a realistic typical figure.

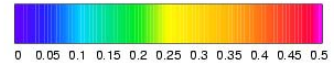
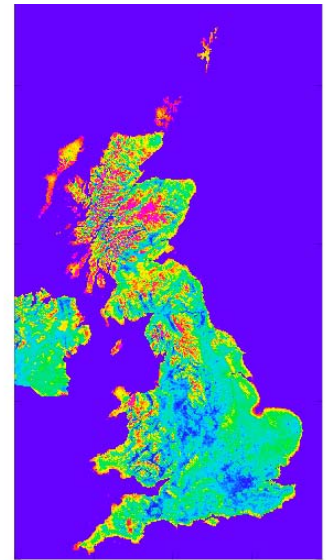
- 2) Suburban turbines achieve capacity factors substantially less than this, with less than 10% being common, while urban turbines may achieve capacity factors of only a few percent.
- 3) Rural turbines are thus generally likely to produce a much higher proportion of their nominal output than suburban, which themselves are likely to perform better than urban turbines.
- 4) Comparing different turbine makes, the individual power curves have much less impact on the capacity factor than mounting height and environment.
- 5) Urban and suburban turbines need to be mounted as high as possible above the mean building height.



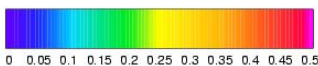
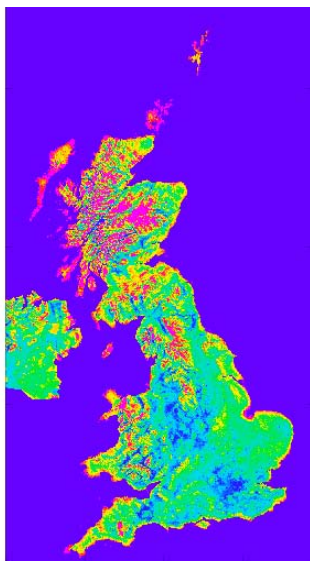
NCIC 1971 – 2000 Capacity Factor
Turbine A 15 kW Suburban Pole 15m



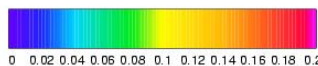
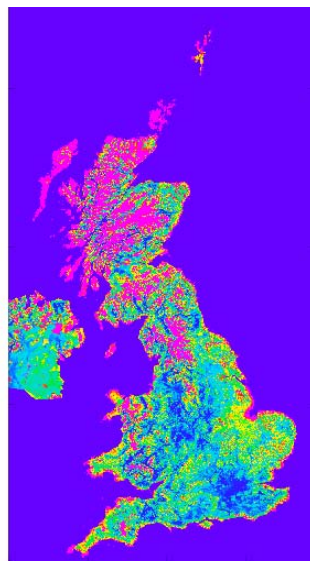
NCIC 1971 – 2000 Capacity Factor
Turbine B 6 kW Rural Pole 15m



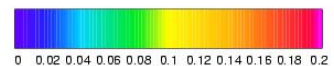
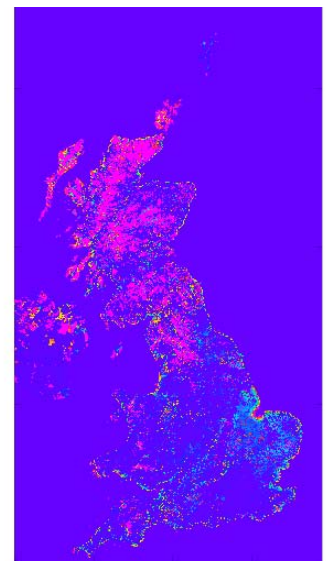
NCIC 1971 – 2000 Capacity Factor
Turbine C 2.5 kW Rural Pole 11m



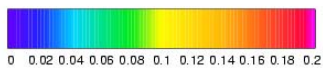
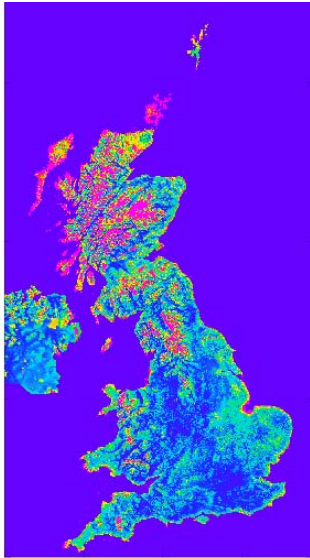
NCIC 1971 – 2000 Capacity Factor
Turbine D 0.08 kW Rural Pole 6m



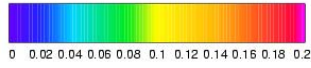
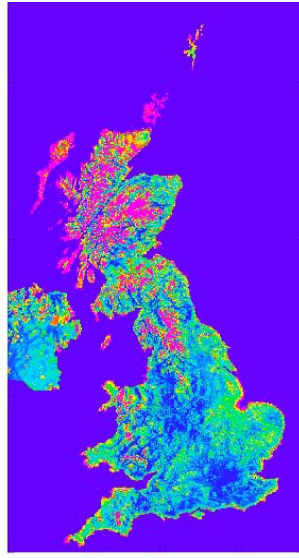
NCIC 1971 – 2000 Capacity Factor
Turbine E 2.4 kW Suburban Pole 10m



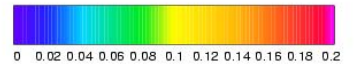
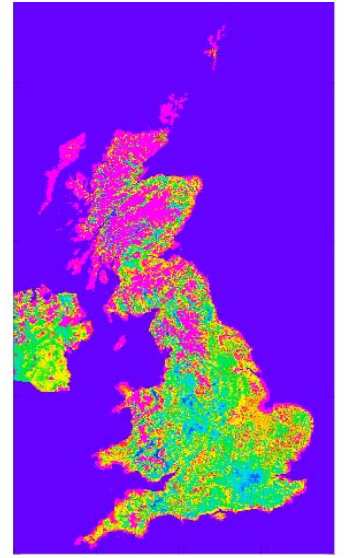
NCIC 1971 – 2000 Capacity Factor
Turbine E 2.4 kW Urban Pole 10m



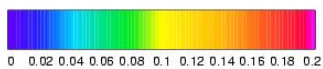
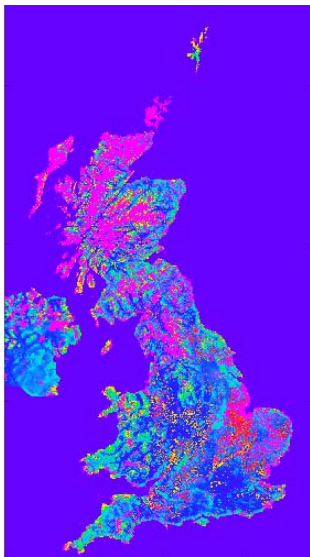
NCIC 1971 – 2000 Capacity Factor
Turbine F 1.5 kW Suburban Roof 1.95m



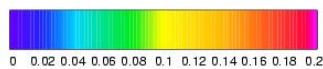
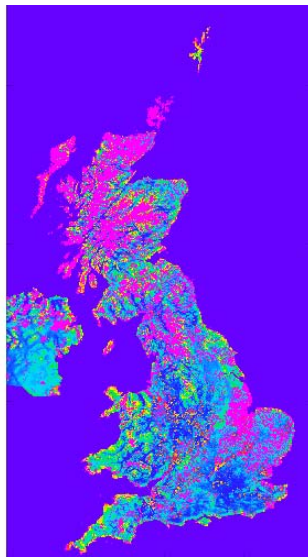
NCIC 1971 – 2000 Capacity Factor
Turbine F 1.5 kW Suburban Roof 2.95m



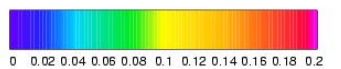
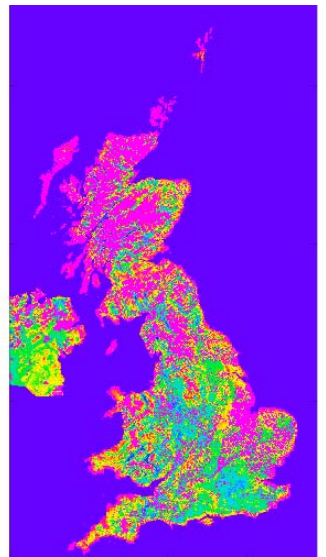
NCIC 1971 – 2000 Capacity Factor
Turbine F 1.5 kW Suburban Roof 8.95m



NCIC 1971 – 2000 Capacity Factor
Turbine F 1.5 kW Urban Roof 1.95m



NCIC 1971 – 2000 Capacity Factor
Turbine F 1.5 kW Urban Roof 2.95m



NCIC 1971 – 2000 Capacity Factor
Turbine F 1.5 kW Urban Roof 8.95m

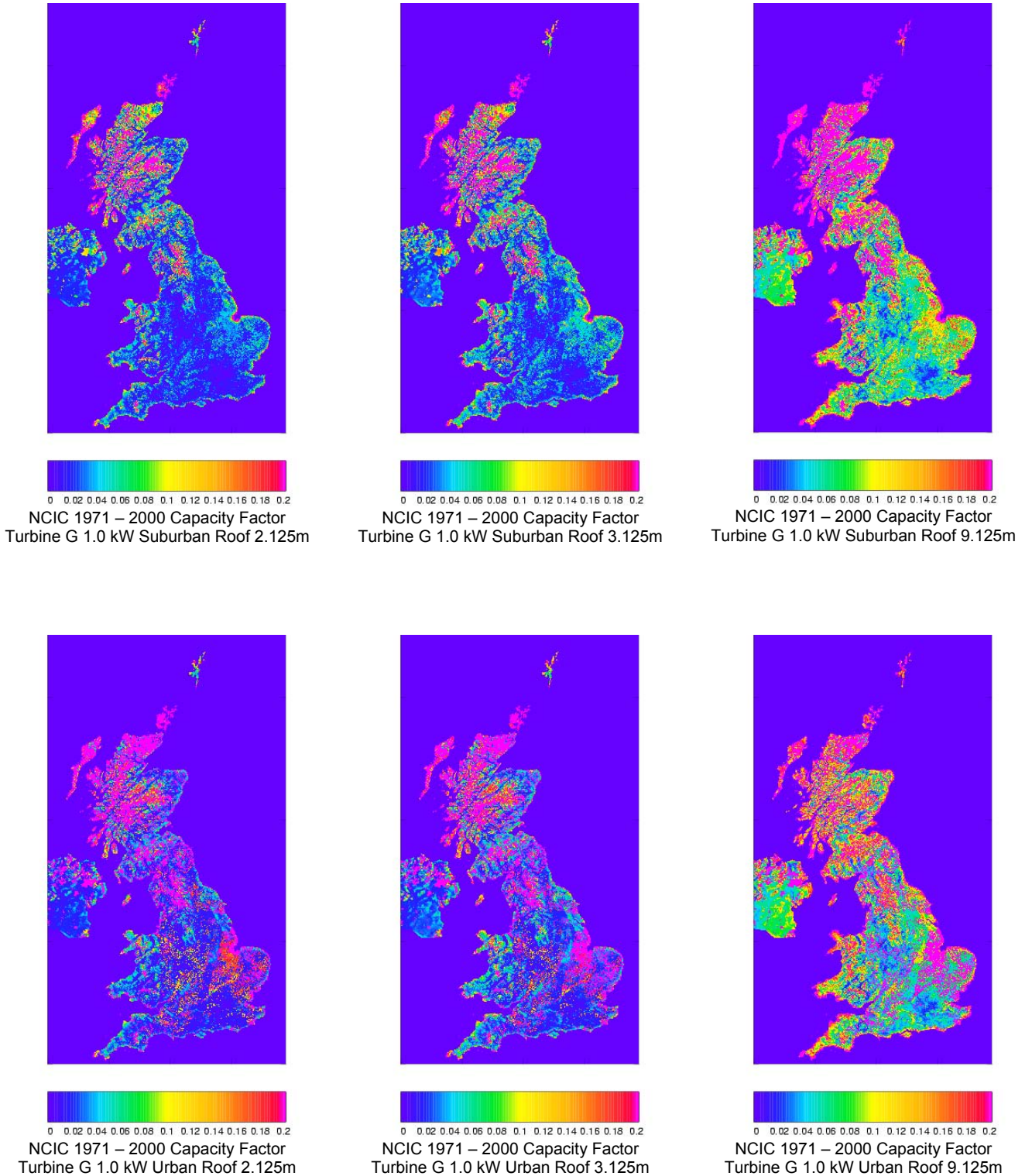


Figure 6 Annual mean capacity factors for selected turbines, environments and mounting heights. Note the different scales for rural and urban/suburban.

4.2.3.4 Total Energy Calculation

We have assumed three different environments for the turbines. ‘Rural’ turbines are assumed to be used in a rural environment. ‘Urban’ turbines are assumed to be used in either a suburban or urban environment. The maximum energy, M , generated by each turbine type in each 1km cell is given by

$$M = \frac{N}{n_h} E \quad (12)$$

This is the energy that would be generated if every household installed each turbine. Here, N is the number of people within each grid box that live in the given environment, n_h is the average number of people per household (taken to be 2.35, the same), so N/n_h is the number of households in the grid box.

The value of N has been determined for the rural and built-up environments by transferring 2001 census data onto the 1km grid. Use has been made of census data for both the ‘Super Output Areas’ of the census (which cover the entire land area of the UK) and urban areas/settlements (which only cover built-up areas).

The census data are initially mapped onto a 100m grid. The boundaries of the urban areas/settlements are used to determine which 100m grid boxes are classified as ‘built-up’ and which are classified as ‘rural’. For the purposes of this analysis only built-up areas with a population of 1000 people or more have been used – there are 3019 such areas.

The UK is divided into 9319 Super Output Areas (SOAs). The SOAs are defined such that they each contain a similar population, which means that in densely populated parts of the UK the SOAs are very small. It is therefore possible to determine spatial variations in population density across large built-up areas from the SOA census figures. In such regions the population of each SOA is assumed to be distributed uniformly across the 100m grid boxes that lie within its boundaries.

In less densely populated regions of the UK the SOAs are much larger and may encompass one or more smaller settlements. In these regions the population of each settlement is distributed uniformly across the 100m grid boxes within its boundaries. The remaining population in each SOA (i.e. after subtracting the population of the built-up areas) is distributed uniformly across the 100m grid boxes that lie within the SOA but outside the built-up areas.

A few SOAs do not contain any built-up areas and are thus entirely ‘rural’. The population of the SOA is distributed uniformly across all 100m grid boxes within its boundaries.

The final step is to aggregate the 100m population data to 1km resolution to match the grid used for the wind speed analysis. The result is a value for the rural population, N_{rural} , and a value for the built-up area population, $N_{built-up}$, for each 1km grid box. Because of the way in which the population mapping has been done it is possible for 1km grid boxes around the fringes of built-up areas to contain both a rural population and an urban population.

The rural population is identified as living in the rural environment. We have split the number of people living in built-up areas, $N_{built-up}$, into suburban and urban populations according to the proportions of suburban and urban land use (and assumed suburban for the small number of

cells with no suburban or urban land use). The numbers of households in each category obtained by this method are: 2.373 million rural, 4.365 million urban, 18.177 million suburban.

In practice, some cells generate more energy per turbine than others. We have ordered the grid boxes by descending power generated per turbine and plotted three graphs:

- 1) Total energy, i.e. the cumulative sum of M
- 2) The average capacity factor, given by the cumulative sum of M divided by both the cumulative sum of households and by the rated energy per year (i.e. the rated power times number of hours per year). This represents a measure of the return in terms of power generated compared with that obtained if the turbine generates at its rated value all the time.
- 3) Average cost factor given by 1000 times the inverse total energy. This is a relative measure of the cost per unit of energy generated. It needs to be multiplied by actual annual cost to get a unit energy cost. The factor 1000 is used merely to scale the output to a more easily plotted value (noting that annual costs are likely to be of order £100-1000). Thus, for example, if a 1 kW generator ran constantly (with capacity factor 1) it would provide 8766 kWh per year. If the running cost was £1000 (obviously rather high!) the cost factor would be $1000/8766=0.114$.

Each is plotted against the cumulative sum of households. The plots for each combination of turbine, environment and height are shown in Appendix A.

In practice, not all households will install a turbine. If f is a factor to allow for market penetration, energy losses, etc., we may estimate the total energy generated two ways. If no account is taken of the return (i.e. a random proportion, f , install turbines) then the total energy generated is just f times the total energy generated if all households install a turbine (i.e. the maximum value in the first graph). Alternatively, an optimal set of users are that portion f of households closest to the left of the first graph. If we take $f = 0.01$, we obtain the following:

Table 1 Annual energy generation from various turbine/mounting choices.

Rating (kW)	Environment	Mounting	Height (above roof for roof mounted)	Maximum Energy Generated (TWh/year)	Energy Generated 1% Random Penetration (TWh/year)	Energy Generated 1% Optimal Penetration (TWh/year)
15.000	Rural	Pole	15.000	70.73254	0.70733	1.87917
6.000	Rural	Pole	15.000	27.09664	0.27097	0.67802
2.500	Rural	Pole	11.000	8.60518	0.08605	0.26643
0.080	Rural	Pole	6.000	0.30142	0.00301	0.01107
2.400	Urban	Pole	10.000	0.11891	0.00119	0.03148
2.400	Suburban	Pole	10.000	17.15543	0.17155	0.85889
1.500	Urban	Roof	1.950	1.41376	0.01414	0.10424
1.500	Suburban	Roof	1.950	6.36949	0.06369	0.28891
1.500	Urban	Roof	2.950	1.81141	0.01811	0.12269
1.500	Suburban	Roof	2.950	8.3071	0.08307	0.35881
1.500	Urban	Roof	8.950	3.9884	0.03988	0.19737
1.500	Suburban	Roof	8.950	17.8332	0.17833	0.64281
1.000	Urban	Roof	2.125	0.50902	0.00509	0.05953
1.000	Suburban	Roof	2.125	2.35314	0.02353	0.16947
1.000	Urban	Roof	3.125	0.70633	0.00706	0.06967

1.000	Suburban	Roof	3.125	3.35195	0.03352	0.21584
1.000	Urban	Roof	9.125	1.95827	0.01958	0.10396
1.000	Suburban	Roof	9.125	8.98625	0.08986	0.38461

Note: Each row in the table gives an estimate of the energy that would be generated if 1% of households in the specified environment install the specified turbine at the specified height. An estimate of the total UK energy resource from a 1% take up can be obtained by taking a weighted average of the four rural values (based on the expected distribution of turbine choices), doing the same for suburban and urban, and then adding the three amounts together. Note also that the number of significant figures in the table does not imply accuracy - these have been retained only to facilitate onward calculations.

The conclusions drawn in Section 4.2.3.3 are supported by the graphs in Appendix A and the numbers derived in the table above. In addition, we may conclude that:

- 1) Height above roof level is a critical parameter. For random market penetration changing the limit on the height of the highest point of the turbine from 3 m to 4 m is estimated to increase power output by a factor of around 1.3 to 1.4, and by a factor of 3 to 4 if the height limit is increased to 10m. The increase is less for optimal sites, with factors of 1.2 and 2 for height limits of 4m and 10m respectively (compared with a height limit of 3m).
- 2) The capacity factor plots shown in Appendix A show that some households are better located than others – in the urban and suburban context these are generally in small towns and villages so that they benefit from generally stronger local winds, though larger scale geographical variation is also a factor. However, the achievable energy generation per household changes quite slowly once penetration exceeds a few percent.
- 3) At the 1% market penetration level, rural energy generation can be improved by factors typically of 2.5-3 by targeting the optimal households. In suburban areas, this factor is higher, ranging from 4 to 7. However, this primarily reflects the low capacity factor (less than 5%) achieved at most locations. Even higher factors can occur in urban areas (reflecting even lower capacity factors).
- 4) Even though the suburban households outnumber the rural households by roughly 8 to 1, the rural resource is potentially larger (at the same level of penetration) because capacity factors are larger and pole-mounting enables use of larger turbines.
- 5) Put simply, the more rural a location, the more potential for energy generation there is; urban dwellers in villages will achieve more return than those in towns, those at the edges of towns will be favoured over those at the centre, and those in small towns will be favoured over those in large towns or cities. For the majority of households, these factors outweigh regional (non-urban) differences in wind climatology (see Figure 6).

4.2.4 Sensitivity Analyses

Sensitivity experiments, re-computing according to the above procedure, have been carried out as follows:

Table 2 Key to sensitivity experiments.

Experiment ID	Description
NL	Using NOABL data
ZR	Reference height $z_{ref} = 400$ m
TB	Assuming taller buildings in urban roughness calculation. h=8 m for suburban, 16 m for dense urban.
RA	Weibull shape parameter=2.

In each case, for each turbine/height combination, the results are summarised in terms of the percentage change in annual energy for 1% penetration with random take-up or optimal take-up.

Table 3 Percentage change in total annual energy generated for 1% random penetration (Table 1) by various turbine/mounting choices for changes in input assumptions (see Table 2 for key).

Turbine	Rating (kW)	Environment	Mounting	Height (above roof for roof mounted) (m)	NL	ZR	TB	RA
Turbine A	15	Rural	Pole	15	24.1	-0.4	-0.7	-2.5
Turbine B	6	Rural	Pole	15	25.1	-0.4	-0.7	-2.5
Turbine C	2.5	Rural	Pole	11	27.4	-0.4	-0.8	-4.1
Turbine D	0.08	Rural	Pole	6	27.9	-0.3	-0.7	-4.3
Turbine E	2.4	Urban	Pole	10	73.1	-7.6	-95.8	-24.4
Turbine E	2.4	Suburban	Pole	10	52.2	-4.2	-41.2	-11.7
Turbine F	1.5	Urban	Roof	1.95	48.2	-6.4	5.4	-8.9
Turbine F	1.5	Suburban	Roof	1.95	46.2	-3.8	1.3	-8.9
Turbine F	1.5	Urban	Roof	2.95	46.6	-6.2	2.0	-8.2
Turbine F	1.5	Suburban	Roof	2.95	44.5	-3.7	-1.3	-8.3
Turbine F	1.5	Urban	Roof	8.95	42.8	-5.7	-3.2	-6.6
Turbine F	1.5	Suburban	Roof	8.95	40.8	-3.4	-3.9	-6.7
Turbine G	1	Urban	Roof	2.125	66.2	-8.3	6.5	-17.7
Turbine G	1	Suburban	Roof	2.125	65.3	-4.9	1.1	-18.3
Turbine G	1	Urban	Roof	3.125	63.9	-7.9	2.1	-16.1
Turbine G	1	Suburban	Roof	3.125	62.1	-4.8	-2.1	-16.4
Turbine G	1	Urban	Roof	9.125	55.7	-7.3	-3.9	-11.2
Turbine G	1	Suburban	Roof	9.125	53.0	-4.3	-5.0	-11.2

Table 4 Percentage change in total annual energy generated for 1% optimal penetration (Table 1) by various turbine/mounting choices for changes in input assumptions (see Table 2 for key).

Turbine	Rating (kW)	Environment	Mounting	Height (above roof for roof mounted) (m)	NL	ZR	TB	RA
Turbine A	15	Rural	Pole	15	-0.9	0.3	-0.1	4.4
Turbine B	6	Rural	Pole	15	-0.3	0.2	-0.1	6.6
Turbine C	2.5	Rural	Pole	11	-0.9	0.3	-0.1	5.1
Turbine D	0.08	Rural	Pole	6	-2.0	0.5	-0.1	1.4
Turbine E	2.4	Urban	Pole	10	31.3	2.4	-90.1	-10.6
Turbine E	2.4	Suburban	Pole	10	2.2	0.9	-28.6	-3.9
Turbine F	1.5	Urban	Roof	1.95	20.5	0.9	-7.5	-2.8
Turbine F	1.5	Suburban	Roof	1.95	2.4	1	5.8	-5.9
Turbine F	1.5	Urban	Roof	2.95	19.3	0.8	-8.6	-2.0
Turbine F	1.5	Suburban	Roof	2.95	2.3	1	3.3	-4.9
Turbine F	1.5	Urban	Roof	8.95	14.2	0.5	-8.1	0.8
Turbine F	1.5	Suburban	Roof	8.95	1.8	0.7	0.5	-1.4
Turbine G	1	Urban	Roof	2.125	22.1	0.6	-5.3	-2.4
Turbine G	1	Suburban	Roof	2.125	2.8	1.2	6.2	-8.6
Turbine G	1	Urban	Roof	3.125	19.5	0.5	-6.0	-1.0
Turbine G	1	Suburban	Roof	3.125	2.5	1.0	3.2	-6.4
Turbine G	1	Urban	Roof	9.125	8.9	-0.1	-4.1	4.3
Turbine G	1	Suburban	Roof	9.125	1.6	0.5	0.0	1.9

The following conclusions may be drawn from these sensitivity tests:

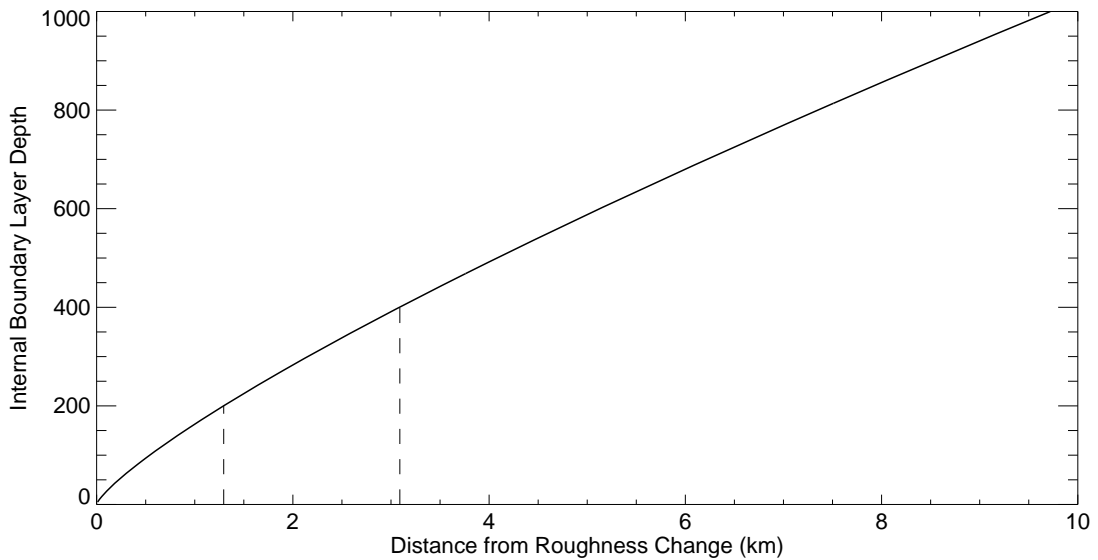
- 1) The choice of reference height, z_{ref} , has only minor impact on the results.
- 2) The building height assumption generally has an impact of less than 10%, and may be of either sign for roof-mounted turbines (tall buildings tending to increase the power in suburban areas, and decrease power in dense urban areas, presumably because of competing factors of increasing overall roughness (and so decreasing wind speed) and lifting the turbine higher in the wind profile. On the other hand, the pole-mounted urban/suburban turbine is extremely sensitive to building height, as an increase in building height moves it closer to roof top in the suburban case (where it is mounted above roof top height) and further into the urban canopy in the urban case. As a result, the Turbine E results must be regarded as much more uncertain and, in practice, sensitive to the precise local building heights.
- 3) The Weibull shape parameter also generally has an impact of less than 10% except for the Turbine E and Turbine G with random penetration, where the impact can be closer to 20%. This presumably reflects sensitivity to the frequency of wind around their lower cut-in limit (about 4 m s^{-1}) which changes significantly with the shape of the wind-speed distribution.
- 4) The choice of annual mean wind speed has the largest impact with random penetration, as much as 73% (although this applies to a turbine generating very little energy). Certainly, 50-60% change is plausible. This reflects the different spatial patterns, as the overall average wind speed is very comparable. It is clear from Figure 1 that the NOABL data shows much less variability on large scales but much more on small scales.

Relative to NCIC, the overall wind-speed around the main population centres tends to be significantly higher, while that over remote highland areas (with generally higher wind speeds) tends to be lower. Interestingly, since the 'optimal' households in each environment (urban, suburban and rural) are, by definition, in the more windy locations, there is much less sensitivity to the choice of large-scale wind if the market penetration is optimal (because the NCIC and NOABL wind speeds are more similar in the windier areas).

4.2.5 Critique of the Methodology

The approach taken here is very simplistic, and it is probably realistic to assume that overall energy generation estimates are accurate to about a factor of 2, given knowledge of both market penetration (the largest uncertainty) and turbine height (the major planning constraint). It is, perhaps, reassuring that the major uncertainty actually arises from the uncertain knowledge of the large-scale wind climatology. Most of this uncertainty arises from the method used to interpolate between observation sites and to correct for orography and proximity to the sea.

(a)



(b)

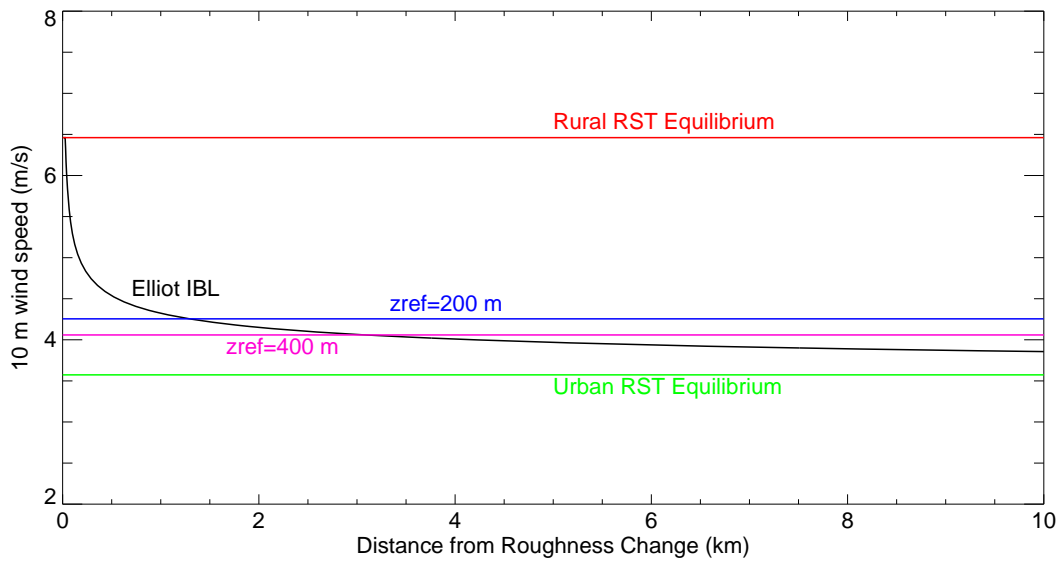


Figure 7 Idealised profiles of (a) internal boundary-layer height and (b) wind speed 10 m above the displacement height using the Elliot Internal Boundary Layer formulation for a 10 m s^{-1} geostrophic wind. In (b) the uniform wind speed assuming Rossby Similarity Theory (RST) over the rural and urban areas is shown along with the wind speed derived using reference heights of 200 m and 400 m.

A second major deficiency is neglect of edge or directional effects. Buildings on the ‘upstream’ edge of a city will experience stronger winds than implied by the ‘equilibrium’ approach adopted. This is allowed for to a small extent by using a relatively low reference height. This is illustrated in Figure 7. Note that even this picture is idealised – real rural/urban transitions are complicated by stability effects. This figure shows that the method used is likely to substantially underestimate the wind over the first 500 m or so from the edge of the city, and slightly over-estimate (by, perhaps 0.5 m s^{-1}) elsewhere. Clearly, the overall error depends on the size of the city. With a uniform distribution of wind direction, buildings in the transition zone will experience enhanced speed half the time (though the depth of the zone at a particular part of the city edge will vary with wind direction).

It is possible to roughly estimate the proportion of buildings that could be affected by this boundary zone. Using the land-use data we can estimate the area of contiguous regions of urban area (defined as urban+suburban fraction greater than some threshold). If we assume that these contiguous regions are circular and the depth of the boundary region is 0.5 km, with a threshold of 50% urban cover we estimate that about 6% of buildings are in the boundary region (and so, allowing for variation of wind direction, experience more rural wind-speeds about 32 % of the time). This effect could therefore be very crudely allowed for by re-allocating about 2% of the suburban population to rural, an increase of rural households by about 15%. This is well within the overall uncertainty of the method.

The other area of obvious weakness is the crude assumptions made concerning morphology of buildings in urban areas. Obtaining detailed information concerning building heights and areas is difficult and, generally, the data are proprietary and expensive. The above sensitivity study suggests the results are not extremely sensitive for roof-mounted turbines (mounted above roof level), but much more so for fixed-height pole-mounted turbines. This sensitivity could be explored further using, for example, distributions of parameters rather than constant values, and, perhaps, using census data on detached, semi-detached etc. houses, but assumptions would still be required about morphology and distribution.

Related to this is the assumption of a uniform number of people per household. In practice, this varies with location and housing type, and the influence of this could be taken into account. It is difficult, however, to separate this from more socio-economic studies of the likely uptake of turbines. In practice, it is unlikely that uptake will be random – presumably turbines are more likely to be installed by those with more disposable income. Fortuitously, this may bias uptake towards the more optimal locations, but estimating the extent of this bias is beyond the scope of this study.

4.2.6 Outline of Possible Improvements

The analysis methodology described in the preceding sections has been constrained in part by the specific aims and scope of the current project. There are various aspects of the approach that could potentially be improved and these are discussed below:

a) Large-scale climatology

Given the large sensitivity of the overall UK energy resource to the mean large scale wind speed, alternative approaches to determining this should be investigated. A convenient and comprehensive data source is the Met Office archive of operational NWP analyses and forecasts. Winds from relatively fine resolution NWP models (with horizontal grid of 12km) are available from the last 10 years. Data from a finer resolution 4km model for a shorter recent period of 15 months can also be used. These have the advantage that model winds are sampled at a finer scale than the conventional wind observations, which form the basic input to both the NCIC and NOABL data. The NWP models carry forward the observational data from previous times and adjust winds dynamically to the finer scales. The NWP winds can be processed to form annual mean wind speed estimates, as for the NCIC and NOABL data used above, combined with a Weibull distribution. Rather than assumed parameters for the distribution, these could be fitted by also calculating the mean cubed wind. However there is scope for more aspects to be investigated. A frequency of wind speeds by directional sectors (wind rose) could be employed, using the analyses (4 per day) and short period hourly forecasts. This may be applied either directly or by fitting to intermediate Weibull distributions in each sector. The sensitivity of power generation to diurnal and seasonal variations in wind speeds could also be investigated with NWP data.

Whilst NWP data provides greater opportunity to look at these directional, seasonal and other influences, the processing is necessarily more extensive and costly.

b) Modelling of Orography

The NCIC and NOABL data both take into account orography at fine scale, though using very different methods and obtaining very different results. It is likely that both suffer from errors at intermediate scales (10-50 km) which are likely to be affected by non-linear processes and stability effects. These scales should be better handled by the NWP data (especially at 4 km resolution), but the finer scales are not treated. Linear models could be used to downscale NWP data to fine-scale orography, using a linear flow model such as MS3DJH or the potential flow part of such a model for gridded data, or using WASP where individual site studies are required.

c) *Edge Effects*

In the present analysis the reference height, z_{ref} , has been fixed at a value of 200m. In Section 4.2.5 it was shown that this has the effect of underestimating the wind speeds in the fringes of urban areas and overestimating the wind in areas further towards the centre. Although the sensitivity tests indicate that changing this value does not have a large impact, one option would be to allow the reference height value to vary across the UK, in accordance with the scale of heterogeneity in the surface roughness. A finer classification of urban area may be achievable, including 'distance from edge of town' to enable a different reference height to be used close to the edge of towns. If directionally dependent wind data are used, the direction to the edge could also be employed to enable a reference height based on the internal boundary layer depth to be used. Such an approach may need to be fine-tuned by comparison with more detailed models (for a small selection of conditions). A particular issue is the precise definition of town edge. In many cases there is a clear demarcation, but in others the rate of change of effective surface roughness may be quite slow and an accurate approach may be difficult to define.

Such an approach may not be justified for estimation of overall resource because, as discussed above, other factors dominate uncertainty. However, in selecting locations for individual turbines (or advising an installer on likely output) these effects may be very important, as the optimal locations for urban installation will lie close to the edge of towns.

d) *Directional Dependencies / Fetch Effects*

There is no allowance for wind direction in the current analysis. Clearly the wind does not blow from all directions with equal frequency, nor, in general, is the upwind roughness length the same in all directions. Use of directionally-dependent data (such as mean wind speed and Weibull parameter for different wind sectors, where a wind sector might cover 30°) would facilitate a directionally dependent interaction with orography and a more accurate treatment of edge effects as discussed above.

e) *Blending Height and related parameters*

Further work is required to test the sensitivity of the results to the algorithm used to determine the blending height and parameters related to it. Blending heights are theoretically well defined where the characteristic length scale for variability of surface is well defined. This is very difficult to establish in practice, but better classification of surface parameters and analysis of scales of variability (e.g. through wavelet analysis of roughness) might enable a more scientifically rigorous blending height to be defined.

In addition, the effective displacement height is poorly defined and there is very little literature on the subject. Alternative approaches should be considered, based on alternative weightings of the individual surface type displacement height, and sensitivity tests conducted.

f) *Stability Effects*

The calculations currently assume that the stability of the atmosphere is neutral. NWP data do include a measure of surface stability, and this could be incorporated by using Monin Obukhov Similarity Theory to replace the logarithmic profiles used with stability-dependent profiles.

g) Building Morphology

The values of mean building height, h , plan area density, λ_p , and frontal area density, λ_f , have been assigned fixed values for the urban and suburban environments. Consequently the roughness length, z_0 , and displacement height, d , also have fixed values. In reality these values would vary from one urban area to another and between different neighbourhoods within a single urban area. This is likely to be more important in estimating the energy from a single turbine than in estimating the overall UK resource.

A possible alternative approach would be to use housing stock information to estimate spatially-varying values for the building height and densities. Potentially suitable data can be obtained from census information. This includes the numbers of detached, semi-detached and terraced properties, and the number of flats or apartments, in each urban area/settlement. However this would have to be supplemented by information or assumptions on the non-residential buildings.

h) Market Size

To calculate the total UK wind energy resource it is necessary to estimate the size of the market for small-scale wind turbines. This is currently done by calculating the number of households in each part of the country by scaling the population by the average number of people per household (assumed to be 2.35). A potential improvement would be to use the actual number of households in each area, as recorded in the census data.

i) Weibull Shape Parameter

The frequency distribution of wind speed is modelled using a Weibull distribution with a fixed shape parameter of 1.8. The sensitivity tests show that changing this value does have an impact on the estimated resource, particularly if the take-up of turbines is not optimal.

Given that the impact is non-linear, it may be worth examining how the shape parameter varies from place to place across the UK. This could be done from existing archives of hourly mean wind speed data.

j) Short-duration Fluctuations

Variations in wind speed and direction over short time-scales (seconds to minutes) are not addressed in the current analysis procedure. Small turbines can respond fairly rapidly to changes in wind speed. Given the non-linear relationship between wind power and wind speed, ignoring these fluctuations (by using hourly mean speeds) may lead to an underestimate of the available wind power. Conversely, variations in speed around the cut-in and cut-out speeds could lead to a reduction in energy generation due to the turbine becoming disconnected from the power distribution network. Fluctuations in wind direction will always tend to reduce the turbine efficiency, so ignoring these could result in an overestimate of the energy resource.

To determine whether these are significant effects, an assessment could be carried out of any differences that may be observed between the frequency distributions of hourly means and 1-minute means obtained from surface anemometer data. If higher frequency data is needed a stochastic model of the sub 1 minute fluctuations could be used to supplement the data. However for accurate results (and to take any account for the reduction in turbine efficiency due to wind direction fluctuations) it would be necessary to combine this with a model for the turbine response.

k) Local Effects / Micro-siting

In assessing the UK wind energy resource no attempt has been made to model the impacts of either nearby obstacles or the topography of the immediate area (e.g. trees, hedges, banks, surrounding houses), nor has any account been taken of the effect on roof-mounted turbines of the building itself.

It would not be practical to include such effects in an assessment of the total UK resource, especially as the precise locations where turbines will be installed are not known. However, if an estimate is required for a specific location then it should be possible to extend the basic approach to give a more site-specific result. Examples of how this could be achieved include:

- The values of mean building height and plan and frontal area densities could be obtained by inspection of the neighbourhood surrounding the target site or from aerial photographs.
- For a rural location the roughness length could be estimated from an inspection of the surrounding area.
- A site inspection could be used to identify sectors where there are obstacles that could have a significant impact on the local wind flow. The assessment would need to consider the properties of the surrounding obstacles (tall, thin buildings have a different impact to low, wide buildings) and the conclusions would be dependent on whether the turbine is to be located above or below the mean building height.
- For roof-mounted turbines it would also be necessary to consider the height above roof level. The impact will differ for flat-roofed and pitched-roofed buildings, and will depend on the position of the turbine on the roof relative to prevailing wind direction.

The effects of local building geometry are complicated and difficult to predict – consequently it is not anticipated that definitive ‘correction factors’ could be determined that would have general applicability. Instead the assessment process described above would identify energy that was ‘at risk’. To find out how much energy is actually lost in practice would require a more detailed site assessment, perhaps including wind measurements at the proposed turbine location.

Note that to allow properly for local obstacles and building geometry it is necessary to retain information on the distribution of wind directions, rather than simply working in terms of wind speeds.

l) Calibration and Verification

Ideally the estimates produced in this study would be compared with observations in order to assess objectively their accuracy and/or calibrate the output. Given the number of turbines installed in the UK is still quite small, verification of the total UK wind energy resource is clearly impractical. However it may be possible to test some aspects of the calculations, for example:

- Roughness lengths and displacement heights for some limited urban areas could be computed using real building data and compared with the values obtained using assumed values for mean building height and density. There are a number of potential sources of suitable building data, including block models and digital surface models from Getmapping.com and the Virtual London project run by University College London.
- The predicted wind at blending height could be compared with observations from roof-mounted anemometers in urban areas (e.g. London Weather Centre).

- Additional CFD studies (similar to those done by Heath et al, 2007) could be carried out with a) periodic boundary conditions, and b) real building data.
- A high-resolution (e.g. 500m) mesoscale model could be run over the London area for a windy day and the results compared with surface observations and with output from coarser models. (Such a model would, itself, need data on building morphology to define surface roughness and other parameters, and would not provide data at the neighbourhood scale.)
- Tatter flags could be used as an inexpensive way to assess the relative windiness of urban areas and compared with model predictions.
- A windiness index derived from tatter flag data has already been developed for the forestry industry and could be compared with the results obtained in this study.

5 Predicted changes in UK wind climate due to climate change

5.1 Changes in mean speed

The UKCIP02 report (Hulme, Jenkins et al., 2002), based on results from the Met Office's Regional Climate Model (RCM), provides a range of scenarios of climate change (for temperature, precipitation, wind and many other parameters) up to the 2080s based on a range of possible emissions scenarios, covering low, medium-low, medium-high and high greenhouse gas emissions. Although the magnitude of the changes by the 2080s depends strongly on future greenhouse gas emissions, the changes predicted for the 2050s and especially the 2020s depend largely on past and present-day emissions, due to the long lifetime of carbon dioxide in the atmosphere. Due to the large natural variability of wind speeds, the report's predictions for wind speed are stated as having less certainty than its predictions for temperature and precipitation changes. The higher the emissions scenario, and the further ahead one looks, the greater the predicted change in the wind (and other parameters), and the more likely it is that the magnitude of the change will be greater than that which could be explained by natural variability. However, even by the 2080s for the high emissions scenario, there are still some areas of the UK where no change is given in the report because the change predicted by the RCM is within the range expected due to natural variability. This occurs mainly in autumn and even more so in winter, as those seasons have the greatest natural variability in the wind.

The UKCIP02 report says that by the 2080s, the winter seasonal average mean wind speeds over the UK are predicted to increase by between 3 and 5% over most of southern and central Britain even in a low emissions scenario. In a high emissions scenario, they are predicted to increase by between 5 and 9% over most of southern and central Britain, with increases of between 3 and 5% over northern England. Over most of Scotland the changes are within the range of natural variability even in the high emissions scenario, but over the northern tip of Scotland the average winter wind speed is predicted to decrease by up to 3%. The report says that in summer, the seasonal average wind speeds over the UK are predicted to decrease slightly in most eastern and western coastal areas of Britain, mainly by up to 3% even in the high scenario, but by more than 7% in some parts of Northern Ireland. Summer mean wind speeds are predicted to increase slightly by up to 3% in most southern and central parts of England, as well as northern Scotland. In spring, average wind speeds are predicted to increase over most of the UK, although generally by less than 3% even in the high scenario. In autumn, average wind speeds are predicted to decrease over the southern half of the UK as well as eastern Scotland, whilst in other parts of the UK the changes are within the range of natural variability. The autumn decreases are generally between 3 and 5% in the high and medium-high scenarios, and between 0 and 3% in the low and medium-low scenarios. Over the year as a whole, the increases in some seasons and decreases in others combine so that even in the high scenario by the 2080s, most of the UK sees annual mean wind speed increases of less than 3%. In the low scenario, by the 2080s the annual mean wind speed changes are within the range of natural variability over almost the whole of the UK.

Harrison et al. (2007) looked at the effect on wind energy production of the changes predicted by the Met Office climate model, and said "Monthly production in early summer in Northern Scotland could rise by up to 19% while that in Northern Ireland would experience decreases of up to 33%. The increases in winter production for the locations in England and Wales are of the order of 9 to 13% with late summer decreases of 5 to 14%." They conclude "The UK Climate Impacts Programme regional climate change scenarios for the 2080s suggest a slight overall

increase in annual mean wind speeds of 0.5% averaged across the UK. This disguises significant trends in seasonal wind speeds and energy production: winter production rising by up to 15% in the south and falling in the north; summer production would tend to fall by up to 10% although some areas would experience more severe reductions.”

The latest UN IPCC report (Christensen et al., 2007) says in its “Regional Climate Projections” chapter that confidence in future changes in windiness in Europe remains relatively low, and that although several model studies have suggested increased average and/or extreme wind speeds in northern and/or central Europe, some studies point in the opposite direction. It also says that models suggest a general similarity between the changes in average and extreme wind speeds, even though extreme wind speeds in Europe are mostly associated with strong winter cyclones, the occurrence of which is only indirectly related to the time-mean circulation.

5.2 Wind speed frequency distribution

Harrison et al. (2007) say that wind speed tends to have a highly-skewed distribution and note that it is common practice in climate change studies to describe this using a Rayleigh distribution. In the Rayleigh distribution the peak probability occurs below the mean wind speed: see Figure 8 below for an illustration of the way Rayleigh distributions change as the mean changes.

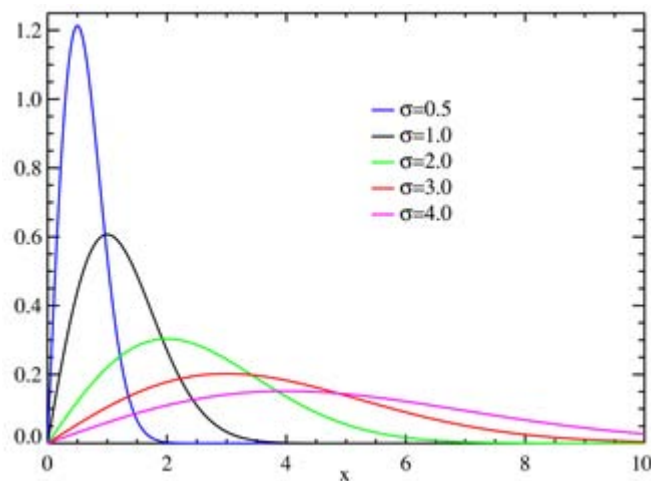


Figure 8 Rayleigh distributions for different values of sigma (standard deviation). For wind speeds, probability would be shown on the y-axis and wind speed would be shown on the x-axis.

As noted in the previous section, the Met Office’s climate models predict that in spring and winter most of the UK will experience higher mean wind speeds, and most of the UK will also experience increases in the annual mean wind speed. Given the speed at which a turbine cuts in is fixed, these changes should mean that a turbine will be generating power for a greater proportion of time. The flatter distribution should also mean that the turbine is operating at or near its rated output for substantially more of the time.

Table 5 shows the estimated increase in output that would result from a 1% increase in the mean wind speed from 4 m/s to 4.04 m/s. These values were calculated using a Weibull frequency distribution with a shape parameter of 1.8.

Table 5 Percentage Increase in Energy Output for a 1% Increase in the Mean Wind Speed

<i>Turbine</i>		<i>Increase in Output (%)</i>
Turbine A	15kW	2.3
Turbine B	6kW	2.4
Turbine C	2.5 kW	2.6
Turbine D	80W	2.3
Turbine E	2.4kW	3.0
Turbine F	1.5kW	2.6
Turbine G	1kW	3.4

5.3 Wind direction distribution

The UKCIP02 report gives very little information on possible changes to the wind direction distribution due to climate change, and the IPCC 2007 report says nothing about possible changes to wind directions over the UK or even northern Europe. The UKCIP02 report only gives information about possible wind direction changes in the “uncertainties and wider issues” chapter, instead of the main chapters on predicted climate changes. It says that in winter for the 2080s, the RCM used in the UKCIP02 report simulates small increases in westerly winds in the south, and reduced south-westerlies in the north. It also says that in summer in the 2080s the RCM shows a weak increase in north-westerly flow over Scotland and a weakening of the summer south-westerly flow over southern England. The report makes it clear that there is low confidence in the modelled changes in wind direction, as the generation of the Met Office RCM previous to the one used in the UKCIP02 report predicted quite different changes in wind direction in all seasons, except for the changes predicted over Scotland in summer.

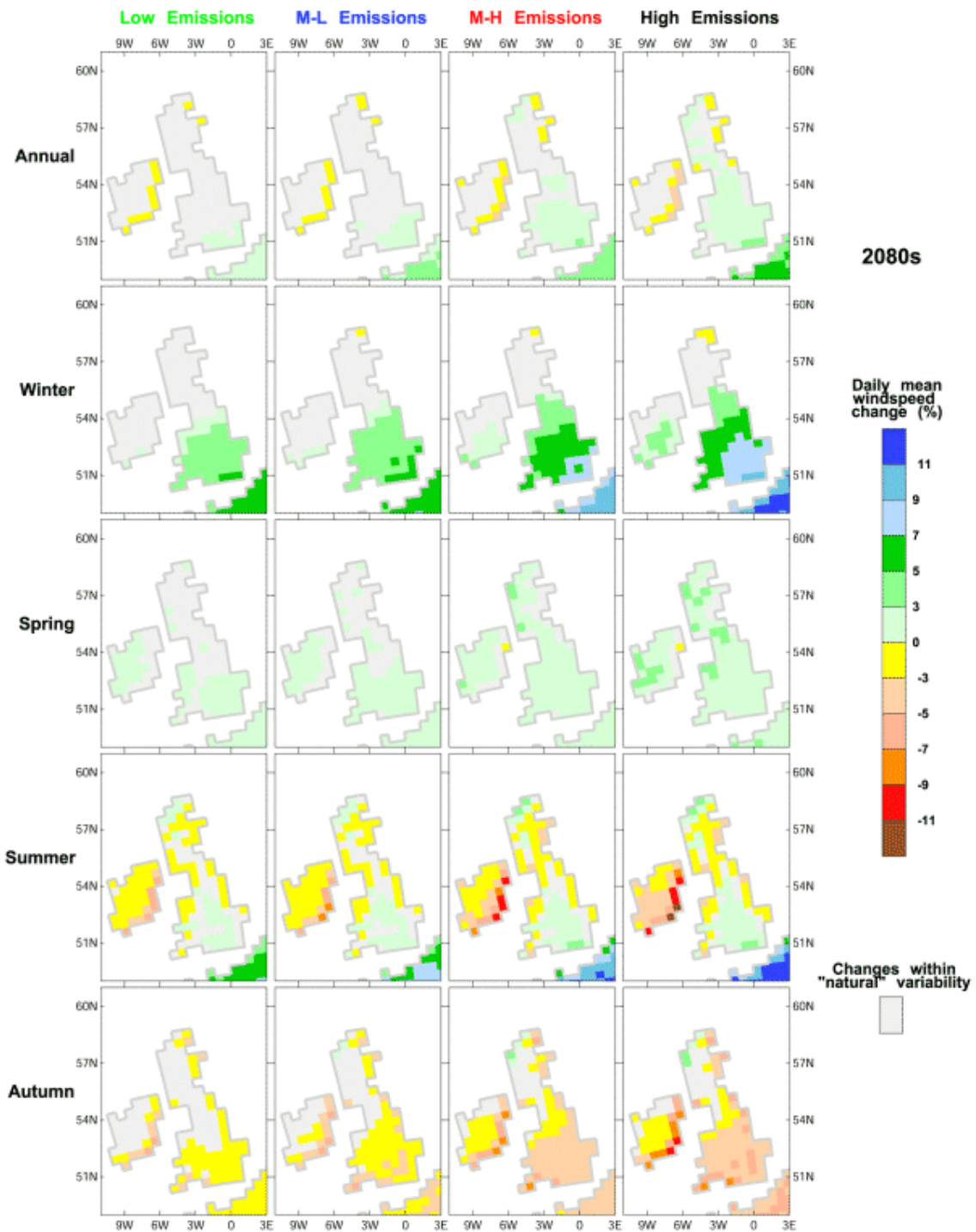
5.4 Extremes

The UKCIP02 report provides some information on changes to extreme winds e.g. the change in the daily mean wind speed that is exceeded on average once every N years (also referred to as the N-year return period value). These are given for future climate scenarios from the 2020s to the 2080s, and for return periods from 2 to 20 years. The changes in return periods are less reliable as the return period increases, so the UKCIP02 report concentrates on the changes in 2-year return period (RP) events. It says that by the 2080s, the 2-year RP daily mean wind speed increases in most parts of the UK in winter, especially in the south of the UK, where it is predicted to increase by between 4% and 6% (for the high scenario) in many parts. In summer by the 2080s, the 2-year RP daily mean wind speed is predicted to decrease by between 2% and 6% in most parts of the UK in the high scenario, although northern Scotland and the south east of England are predicted to see little change or slight increases of less than 4%. For the year as a whole the changes in the 2-year RP daily mean wind speed by the 2080s are predicted to be quite small over most of the UK, even in the high scenario, although in that case some parts of northern England and the far south of England are predicted to see increases of between 4% and 6%. The changes for other scenarios and for the 2050s and 2020s are similar, but of smaller magnitude. It says that the changes in seasonal-average and extreme wind speeds seem to be partly driven in the climate model by a southward movement across the UK of the average winter depression tracks. However, it also cautions that “climate models remain rather poor at simulating small-scale and high intensity wind speeds..., and relatively low confidence should be attached to these results.”

Alexander, Tett & Jonsson (2005) examined changes in severe storms (defined as 3-hourly pressure changes exceeding an extreme magnitude) over the UK over the past several decades. They found that the UK regions have tended towards larger magnitude events in recent decades, particularly in the more southerly regions, and that there has been a significant increase in the number of severe storms over the UK as a whole since the 1950s providing some evidence for a shift in the North Atlantic storm track.

5.5 Summary of relevant on-going research

A new UKCIP report (UKCIP08) is due for release in the second half of 2008. Like the previous report, it is again based on data from the Met Office's RCM. The most important difference will be that it will use an ensemble of simulations of future global climate, created by varying certain model parameters within physically realistic ranges. The results of each model version will be weighted according to how well it represents the current climate and its recent evolution, and as a result probabilistic climate projections will be produced for the UK for each of three future scenarios of greenhouse gas emissions (Low, Medium and High). These should better support a risk-based assessment of impacts and adaptations associated with a changing climate.



Source: UKCIP02 Climate Change Scenarios (funded by DEFRA, produced by Tyndall and Hadley Centres for UKCIP)

Figure 9 Percentage change in average annual and seasonal wind speed (with respect to 1961 – 1990) for four emissions scenarios for the 2080s

6 Summary

This second phase of the project has examined how the total UK wind energy resource from small-scale generation may be estimated. A generic approach has been identified in which a series of correction factors are applied to a large-scale reference wind climatology. These correction factors modify the reference climatology for the effects of local orography, surface roughness and building geometry.

A number of options for generating the reference climatology and the correction factors have been evaluated. It is not possible to give a definitive recommendation for the best methods to use without further investigation, especially as the optimal approach will depend on the available resources, timescales and desired accuracy.

For the purposes of this study a simplified method has been used to generate estimates of UK wind energy resource given various assumptions about turbine characteristics, mounting height and market penetration. More sophisticated approaches are possible. However the approach adopted here does, we believe, provide a reasonable balance between the need to produce an estimate quickly and the accuracy of the results. The sensitivity of the results to various parameters and assumptions has been tested.

The approach can be summarised as follows:

- The chosen reference climatology is a 1km grid of the mean wind speed at 10m above open, level terrain, obtained by geostatistical interpolation of surface observations.
- The reference wind speed is transformed up to a reference height of 200m above ground level using a roughness length representative of 'open country'.
- The wind speed at 200m is transformed down to an intermediate blending height using an area-averaged surface roughness length
- The wind speed at blending height is transformed down to turbine hub height using a roughness length appropriate to the local environment. Three environments relevant to small-scale wind turbines are considered – urban, suburban and rural.
- The mean wind speed at hub height is used to define a wind speed frequency distribution using a Weibull distribution with a fixed shaped parameter of 1.8.
- The wind speed frequency distribution is combined with a turbine power curve to obtain an estimate of the annual energy production from a single turbine. Calculations have been done for seven different turbine models, including two roof-mounted systems.
- Grids of 'energy per turbine' have been combined with grids of population data. The results have been accumulated to obtain estimates of the total energy, average capacity factor and average cost factor for the UK for each turbine system. Figures have been calculated assuming a market penetration of 1%.

In this study we have chosen to use the NCIC wind speed dataset as our reference climatology rather than the long-established NOABL dataset. The two datasets may be compared, as follows:

- Both datasets describe the effects of orography
- Neither dataset allows for variations in surface roughness – the wind speed values represent open, level terrain in a rural environment
- NOABL is a 10-year climatology based on 56 stations, whereas the NCIC dataset is a 30-year climatology based on approximately 220 stations

- NOABL was constructed from over-lapping 100x100km tiles, scaled to produce a near-seamless map. The NCIC dataset was generated by fitting a single wind speed model across the entire area of the UK.
- In NOABL most of the spatial variation comes from the mass consistent model (because each tile typically contained only one or two observation sites). In the NCIC dataset the spatial variations are inferred empirically from the observations (through a regression relationship with terrain elevation, terrain shape etc).

Ultimately wind speed is a complex quantity to interpolate and neither dataset can be expected to model the true wind climatology perfectly. The comparison of NOABL with long-term station averages suggests that this dataset underestimates slightly for higher wind speed sites and overestimates for lower wind speed ones. On balance, the larger amount of data used, the greater homogeneity of the analysis method and the empirical approach to characterising the spatial variations were considered sufficient reasons to prefer the NCIC dataset as the basis for the calculations in this report.

The main findings of this study are:

- 1) Rural turbines are generally likely to produce a much higher proportion of their nominal output than suburban, which themselves are likely to perform better than urban turbines. A rural turbine may achieve a capacity factor of 15-20% in the English countryside. This may be substantially exceeded if mounted near hilltops in hilly terrain, or near the coast. Suburban turbines achieve capacity factors substantially less than this, with less than 10% being common, while urban turbines may achieve capacity factors of only a few percent.
- 2) Comparing different turbine makes, the individual power curves have much less impact on capacity factors than mounting height and environment.
- 3) Some households are better located than others – in the urban and suburban context these are generally in small towns and villages so that they benefit from generally stronger local winds, though larger scale geographical variation is also a factor. However, the achievable energy generation per household changes quite slowly once penetration exceeds a few percent.
- 4) Urban turbines need to be mounted as high as possible above the mean building height. Height above roof level is a critical parameter – for random market penetration changing the limit on the height of the highest point of the turbine from 3 m to 4 m is estimated to increase power output by 30 to 40%, and increasing the limit to 10 m can increase power by a factor of 3 to 4 compared with a 3 m height limit (the increases are less for optimal sites). Turbines mounted below roof height, as may be the case for pole-mounted turbines in dense urban areas, on average experience very low wind speeds and so generate little power.
- 5) At the 1% market penetration level, rural energy generation can be improved by factors typically of 2.5-3 by targeting the optimal households. In suburban areas, this factor is higher, ranging from 4 to 7. However, this primarily reflects the low capacity factor (less than 5%) achieved at most locations. Even higher factors can occur in urban areas (reflecting even lower capacity factors).
- 6) Even though the suburban households outnumber the rural households by roughly 8 to 1, the rural resource is potentially larger (at the same level of penetration) because capacity factors are larger and pole-mounting enables use of larger turbines.

- 7) Put simply, the more rural a location, the more potential for energy generation there is; urban dwellers in villages will achieve more return than those in towns, those at the edges of towns will be favoured over those at the centre, and those in small towns will be favoured over those in large towns or cities. For the majority of households, these factors outweigh regional (non-urban) differences in wind climatology.
- 8) The uncertainty in overall estimates of mean generation arising from meteorological assumptions (as opposed to assumption about market penetration and mounting height) is about a factor of two. The dominant source of this uncertainty is the choice of wind climatology used in the computation (including methods used to interpolate and allow for orography). Here we have used the Met Office 1971-2000 climatology generated by geostatistical interpolation of surface data. It is clear from Figure 1 that the NOABL data shows much less variability on large scales but much more on small scales. The overall wind-speed around the main population centres tends to be significantly higher, while that over remote, highland areas, tends to be lower. The choice of annual mean wind speed has the largest impact with random penetration. Interestingly, since the 'optimal' households in each environment (urban, suburban and rural) are, by definition, in the more windy locations, there is much less sensitivity to choice of large-scale wind if the market penetration is optimal (because the NCIC and NOABL wind speeds are more similar in the windier areas).

A number of potential improvements to the analysis method have been identified. Of these the ones most likely to deliver significant benefit in terms of improved accuracy are:

- 1) Use of a directionally dependent wind climatology, preferably taking into account spatial and directional variation in the shape of the wind speed distribution (as well as in the mean wind speed).
- 2) Incorporation of edge and fetch effects and the influence of small scale orography (using directionally-dependent data).
- 3) Incorporation of better knowledge of building characteristics (height, area etc.).

7 Conclusions

In the Introduction to Part 1: A Review of Existing Knowledge we began by setting out the following two key questions:

- a) What is the total potential wind energy resource in the UK from small-scale turbines?
- b) What is the potential wind energy resource at any given location?

In this report we have described a methodology for estimating the mean wind speed at turbine hub height for a number of different environments (urban, suburban and rural). We have used this methodology to generate grids of wind speed data for the UK and we have demonstrated how these data can be combined with turbine power curves and population data to obtain an estimate of the total small-scale wind energy resource.

The main conclusions from this analysis are:

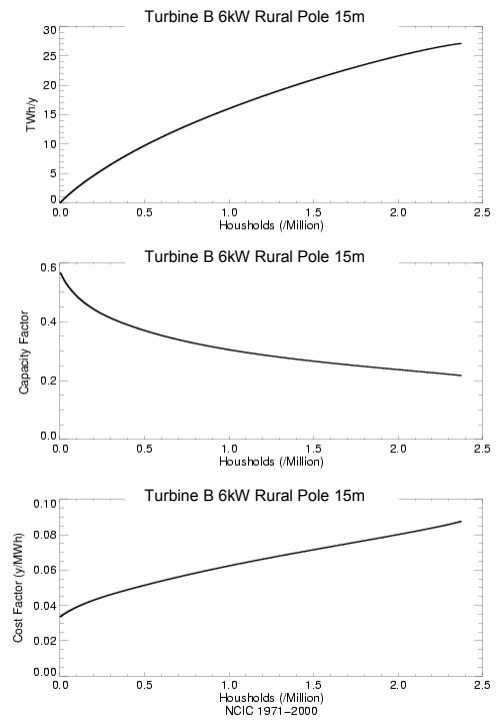
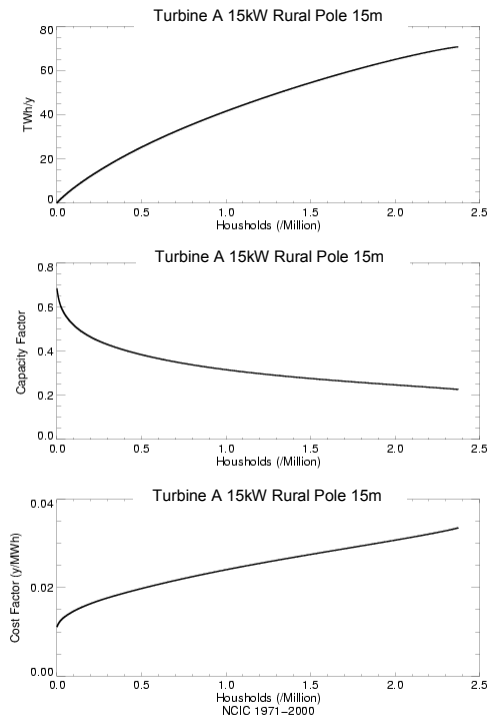
- 1) The urban environment has a dramatic impact on wind speed and wind power generation capacity.
- 2) This impact varies considerably with height relative to roof-top. The sheltering effect due to surrounding buildings means that turbines mounted below rooftop are unlikely to generate, on average, capacity factors of more than a few percent. Significant improvements can be gained by mounting above rooftop, but heights several metres above rooftop are likely to be required.
- 3) Rural turbines typically have higher capacity factors, with 15%-20% being typical and more being achievable at some locations.
- 4) To maximise return from investment and carbon savings, turbines should be installed in locations as rural as feasible, i.e. hill-top sites rather than valleys, open countryside rather than forested, isolated buildings rather than villages rather than towns, edges (within a few 100 m) of towns rather than in the centre.

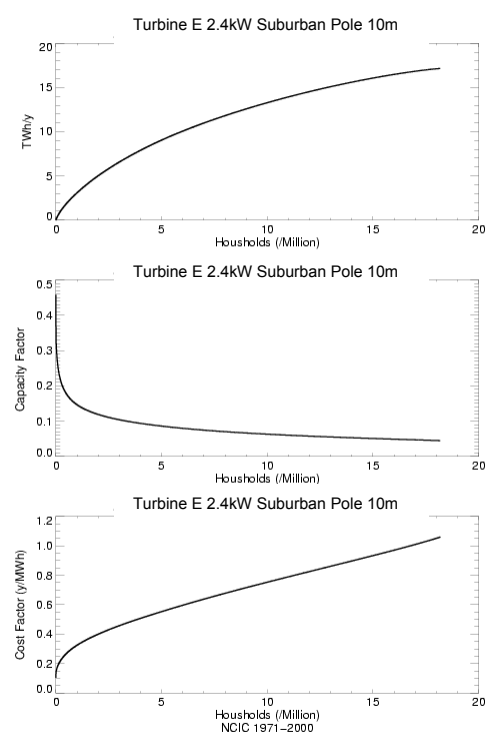
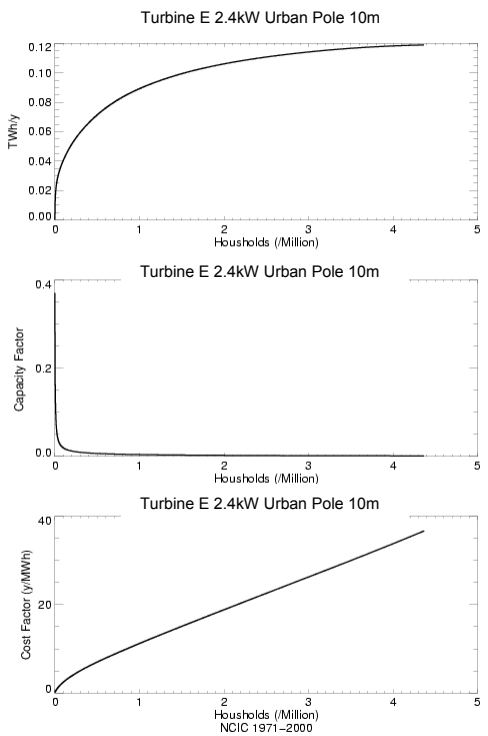
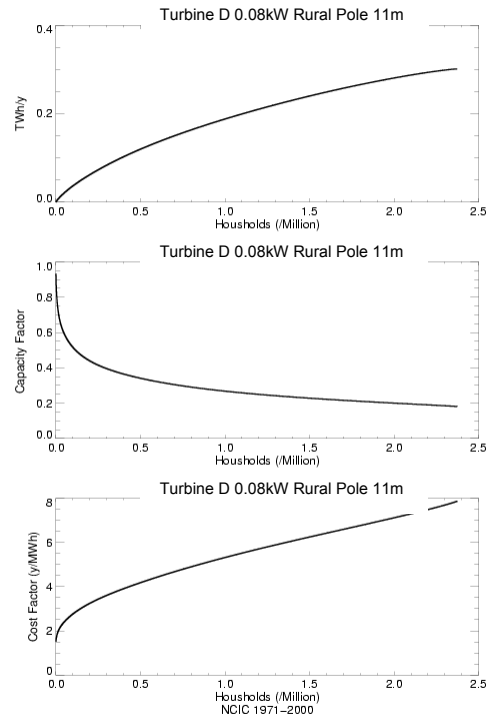
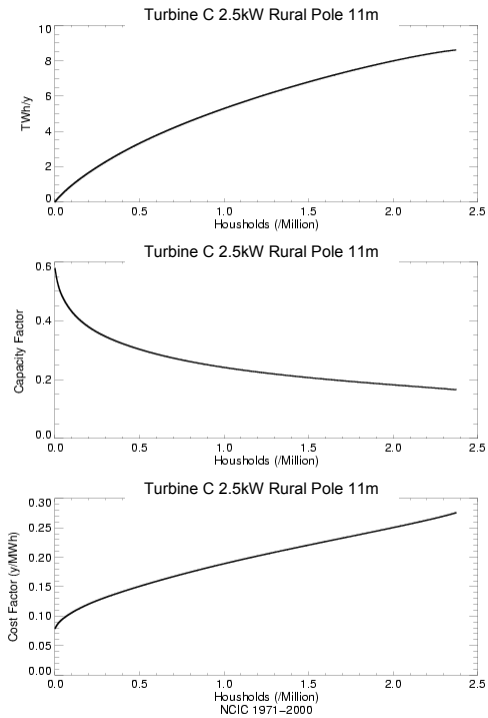
As well as estimating the UK resource, the approach described in this report could, in principle, be used to compute an estimate of the resource at an individual location. Although such estimates would give a useful guide to the wind energy potential at the neighbourhood scale, they would not allow for detailed local effects such as sheltering by individual buildings or trees, very local variations in surface roughness or small-scale terrain effects. The importance of these factors in determining turbine yields was highlighted in the siting guidelines set out in section 7 of Part 1: A Review of Existing Knowledge.

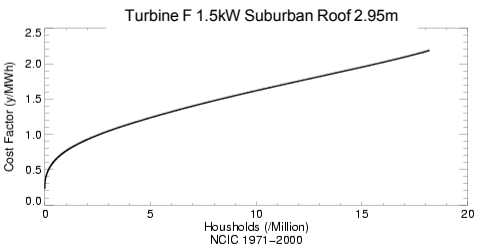
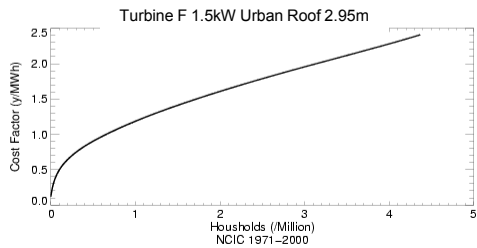
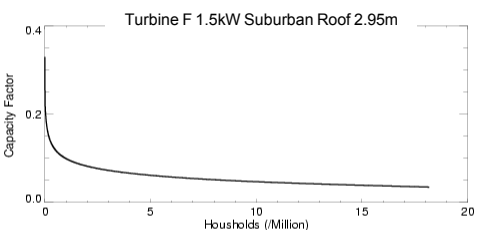
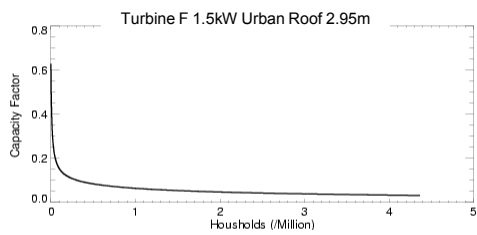
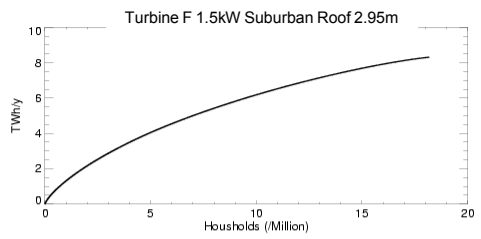
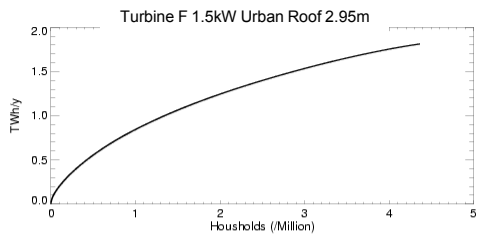
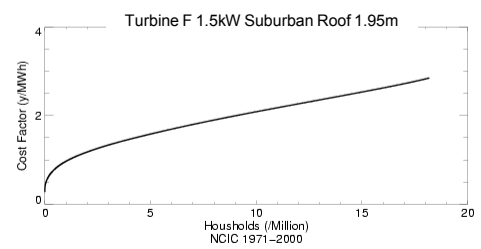
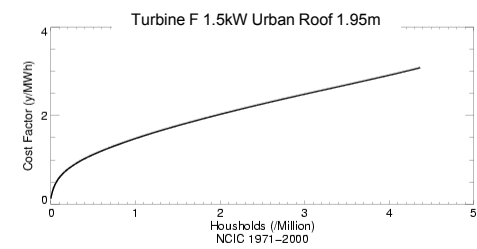
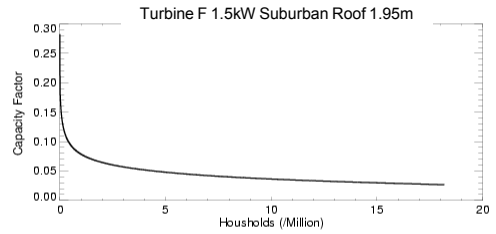
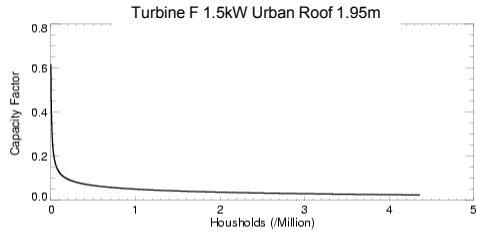
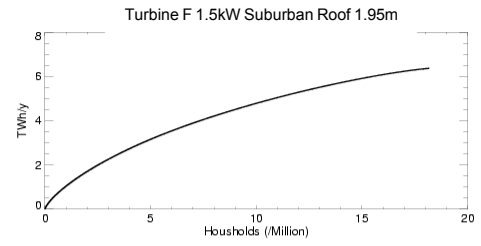
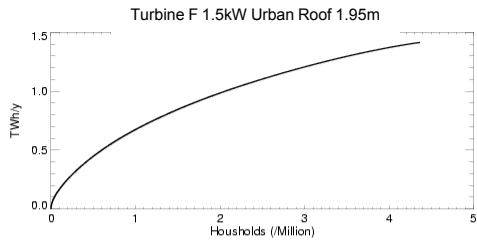
We recommend that if the techniques described here are to be used to provide individual householders with an evaluation of their site then any energy estimates must be accompanied by clear guidance on the limitations of the methodology and the importance of good micro-siting for optimum turbine performance.

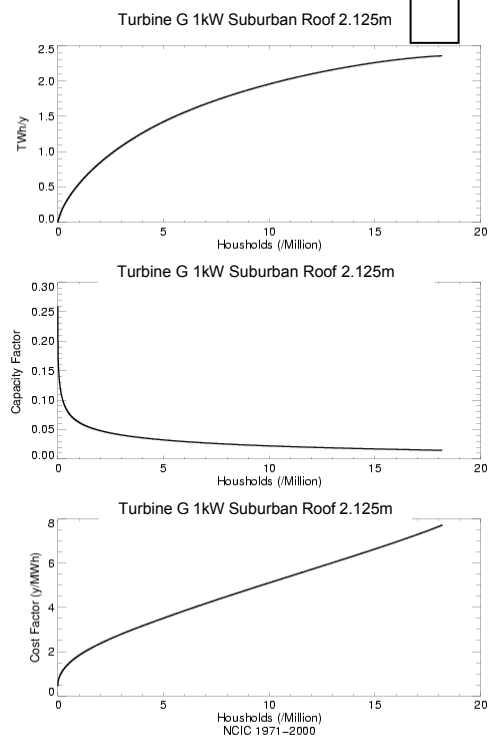
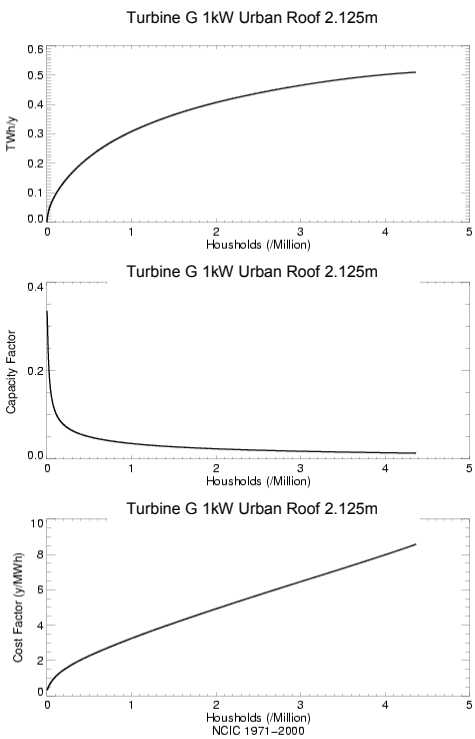
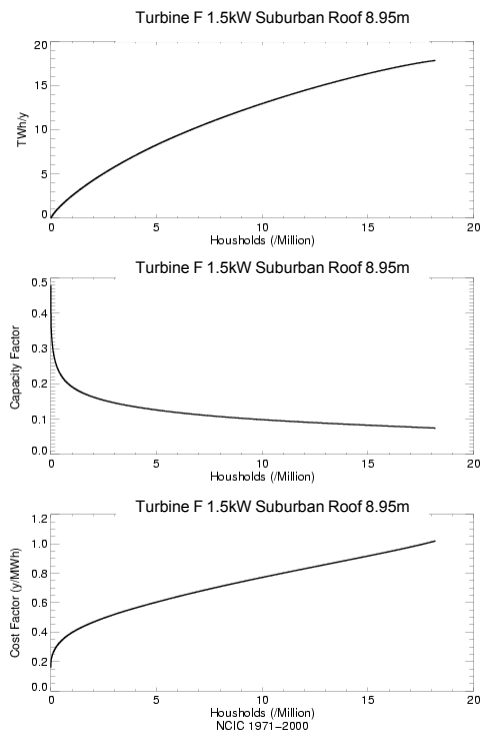
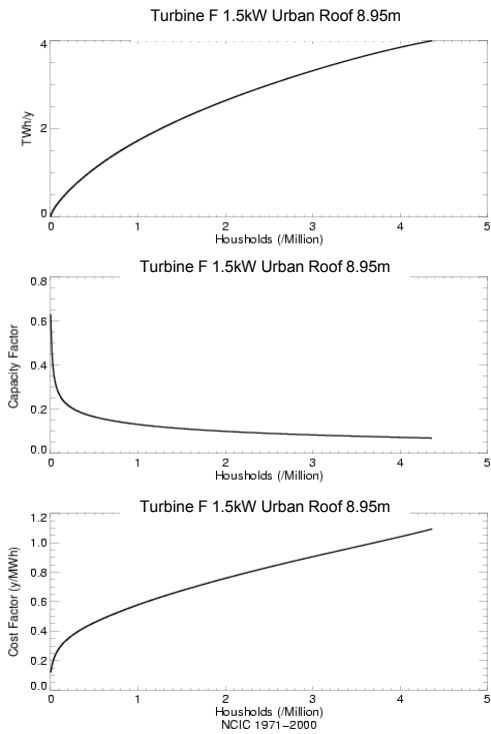
8 Appendix A

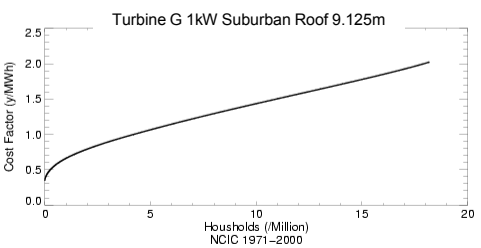
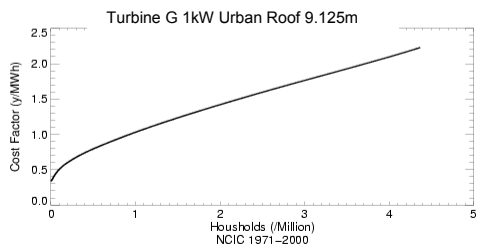
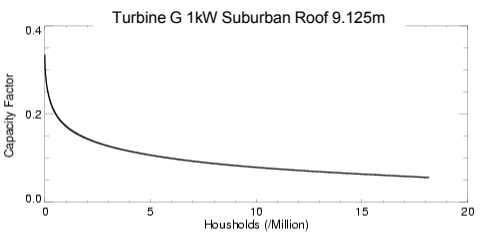
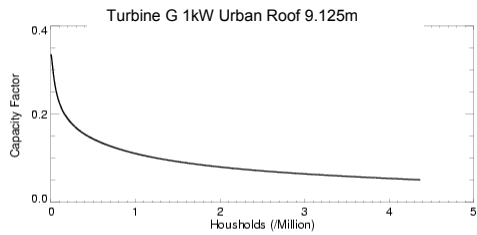
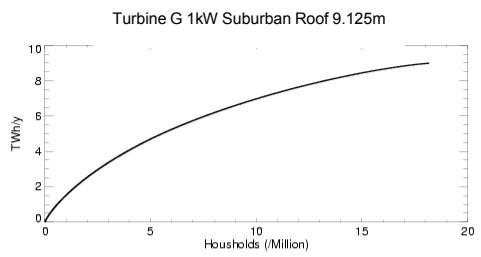
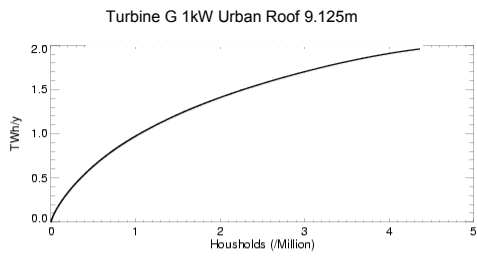
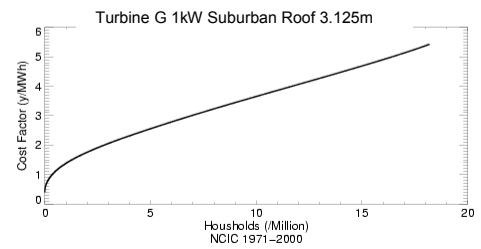
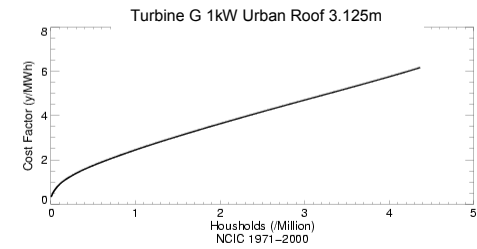
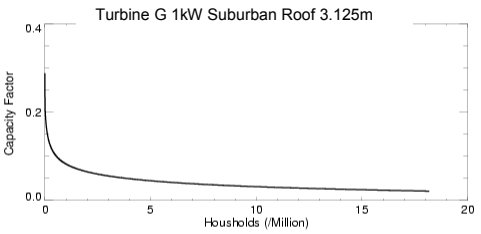
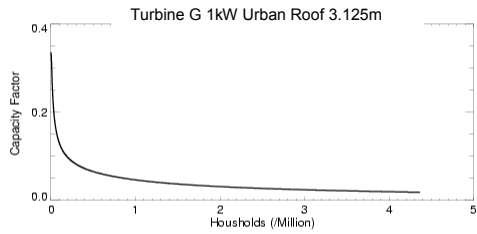
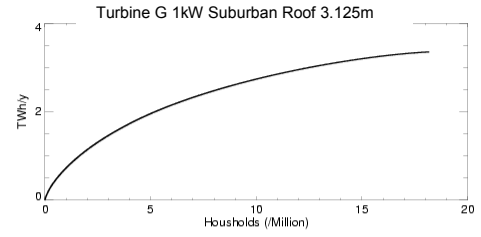
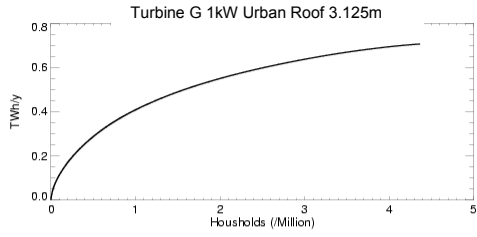
Cumulative distributions of annual energy generated, average capacity factor and cost factor are shown for the chosen turbine/environment/height combinations in the following charts.











9 References

- Alexander, L., Tett, S. & Jonsson, T. (2005): Recent observed changes in severe storms over the United Kingdom and Iceland. *Geophys Res Lett*, **32**, L13704. doi:10.1029/2005GL022371
- Christensen, J.H., B. Hewitson, A. Busuioc, A. Chen, X. Gao, I. Held, R. Jones, R.K. Kolli, W.-T. Kwon, R. Laprise, V. Magaña Rueda, L. Mearns, C.G. Menéndez, J. Räisänen, A. Rinke, A. Sarr and P. Whetton, 2007: Regional Climate Projections. In: *Climate Change 2007: The Physical Science Basis. Contribution of Working Group I to the Fourth Assessment Report of the Intergovernmental Panel on Climate Change* [Solomon, S., D. Qin, M. Manning, Z. Chen, M. Marquis, K.B. Averyt, M. Tignor and H.L. Miller (eds.)]. Cambridge University Press, Cambridge, United Kingdom and New York, NY, USA.
- Grimmond, C.S.B. & Oke, T.R., Aerodynamic properties of urban areas derived from analysis of surface form, *J. Applied Meteorol.*, **38**, 1262-1292 (1999)
(see also Grimmond, C.S.B. & Oke, T.R., Corrigendum, *J. Applied Meteorol.*, **39**, 2494 (2000))
- Harrison, G.P., Cradden, L.C., Chick, J.P., Preliminary assessment of climate change impacts on the UK onshore wind energy resource, Invited paper for Special Issue of "Energy Sources" on Global Climate Change and Sustainable Energy Development, 2007 Available at <http://www.see.ed.ac.uk/~gph/publications/EnergySourcesDraft.pdf>
- Heath, M.A., Walshe, J.D. and Watson S.J., Estimating the potential yield of small building-mounted wind turbines, *Wind Energy*, **10**, 271-287 (2007)
- Hulme, M., Jenkins, G.J., Lu, X., Turnpenny, J.R., Mitchell, T.D., Jones, R.G., Lowe, J., Murphy, J.M., Hassell, D., Boorman, P., McDonald, R. and Hill, S. (2002) *Climate Change Scenarios for the United Kingdom: The UKCIP02 Scientific Report*, Tyndall Centre for Climate Change Research, University of East Anglia, Norwich, UK. 120pp.
- Macdonald, R.W., Griffiths, R.F. & Hall, D.J., An improved method for the estimation of surface roughness of obstacle arrays, *Atmos. Environment*, **32**, 1857-1864 (1998)
- Raupach, M. R., Simplified expressions for vegetation roughness length and zero-plane displacement as functions of canopy height and area index, *Boundary-Layer Meteorol.*, **71**, 211-216 (1994)
- Raupach, M. R., Corrigenda, *Boundary-Layer Meteorol.*, **76**, 303-304 (1995)
- Troen, I and Petersen, E, *European Wind Atlas*, Risø National Laboratory, Roskilde, Denmark, 656pp (1989)



Met Office
FitzRoy Road, Exeter
Devon, EX1 3PB
UK

Tel: 0870 900 0100
Fax: 0870 900 5050
consulting@metoffice.gov.uk
www.metoffice.gov.uk/consulting